ABC Cardiol
Arquivos Brasileiros de Cardiologia

Volume 117 | Number 6
December 2020

Brazilian Society of Cardiology
ISSN-0066-782X

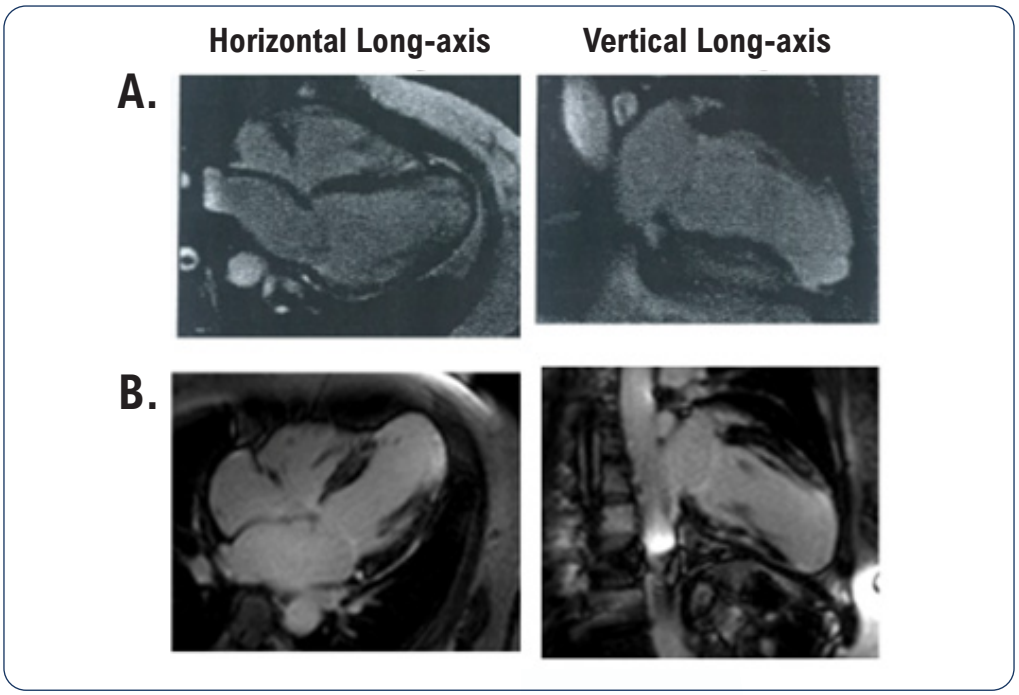

Figure 2, page 1086

ABC Cardiol
Arquivos Brasileiros de Cardiologia
JOURNAL OF BRAZILIAN SOCIETY OF CARDIOLOGY - Published since 1943

Contents

ABC Cardiol
Arquivos Brasileiros de Cardiologia
JOURNAL OF BRAZILIAN SOCIETY OF CARDIOLOGY - Published since 1943

Editorial Board

Sociedade Brasileira de Cardiologia

President (Leave of absence)
Marcelo Antônio Cartaxo Queiroga Lopes

President
Celso Amodeo

Financial Director
Ricardo Mourilhe Rocha

Scientific Director
Fernando Bacal

Managing Director
Olga Ferreira de Souza

Service Quality Director
Sílvio Henrique Barberato

Communication Director
Harry Corrêa Filho

Information Technology Director
Leandro Ioschpe Zimerman

Governmental Relations Director
Nasser Sarkis Simão

State and Regional Relations Director
João David de Souza Neto

Cardiovascular Health Promotion Director – SBC/Funcor
José Francisco Kerr Saraiva

Director of Specialized Departments
Andréa Araujo Brandão

Research Director
David de Pádua Brasil

Coordinator of Science, Technology and Innovation
Ludhmila Abrahão Hajjar

Coordinator of Continued Medical Education
Brivaldo Markman Filho

Coordinator of Management Supervision and Internal Control
Gláucia Maria Moraes de Oliveira

Coordinator of Compliance and Transparency
Marcelo Matos Cascudo

Coordinator of Strategic Affairs
Hélio Roque Figueira

Editor-in-Chief of the Arquivos Brasileiros de Cardiologia
Carlos Eduardo Rochitte

Editor-in-Chief of the IJCS
Claudio Tinoco Mesquita

Coordinator of the University of the Heart
Evandro Tinoco Mesquita

Coordinator of Standards and Guidelines
Brivaldo Markman Filho

Presidents of State and Regional Brazilian Societies of Cardiology:
SBC/AL – Carlos Romerio Costa Ferro

SBC/AM – Kátia do Nascimento Couceiro

SBC/BA – Gilson Soares Feitosa Filho

SBC/CE – Gentil Barreira de Aguiar Filho

SBC/DF – Alexandra Oliveira de Mesquita

SBC/ES – Tatiane Mascarenhas Santiago Emerich

SBC/GO – Leonardo Sara da Silva

SBC/MA – Mauro José Mello Fonseca

SBC/MG – Henrique Patrus Mundim Pena

SBC/MS – Gabriel Doreto Rodrigues

SBC/MT – Marcos de Thadeu Tenuta Junior

SBC/NNE – Nivaldo Menezes Filgueiras Filho

SBC/PA – Dilma do Socorro Moraes de Souza

SBC/PB – Lenine Angelo Alves Silva

SBC/PE – Fernando Ribeiro de Moraes Neto

SBC/PI – Luiz Bezerra Neto

SBC/PR – Raul DAurea Mora Junior

SOCERJ – Wolney de Andrade Martins

SBC/RN – Maria Sanali Moura de Oliveira Paiva

SOCERON – Daniel Ferreira Mugrabi

SOCERGS – Mario Wiehe

SBC/SC – Amberson Vieira de Assis

SBC/SE – Eryca Vanessa Santos de Jesus

SOCESP – João Fernando Monteiro Ferreira

Presidents of the Specialized Departaments and Study Groups

SBC/DA – Antonio Carlos Palandri Chagas

SBC/DCC – Bruno Caramelli

SBC/DCC/CP – Klebia Magalhães Pereira Castello Branco

SBC/DCM – Celi Marques Santos

SBC/DECAGE – Izo Helber

SBC/DEIC – Evandro Tinoco Mesquita

SBC/DERC – Gabriel Leo Blacher Grossman

SBC/DFCVR – Antoinette Oliveira Blackman

SBC/DHA – Audes Diógenes de Magalhães Feitosa

SBC/DIC – Carlos Eduardo Rochitte

SBCCV – Eduardo Augusto Victor Rocha

SOBRAC – Ricardo Alkmim Teixeira

SBHCI – Ricardo Alves da Costa

DCC/GAPO – Danielle Menosi Gualandro

DCC/GECETI – Luiz Bezerra Neto

DCC/GECO – Roberto Kalil Filho

DCC/GEMCA – Roberto Esporcatte

DCC/GERTC – Adriano Camargo de Castro Carneiro

DEIC/GEICPED – Estela Azeka

DEIC/GEMIC – Marcus Vinicius Simões

DERC/GECESP – Clea Simone Sabino de Souza Colombo

DERC/GECN – Lara Cristiane Terra Ferreira Carreira

DERC/GERCPM – Carlos Alberto Cordeiro Hossri

GECIP – Marcelo Luiz da Silva Bandeira

GEECG – Carlos Alberto Pastore

DCC/GETA – Carlos Vicente Serrano Junior

DCC/GECRA – Sandra Marques e Silva

Arquivos Brasileiros de Cardiologia

Volume 117, Nº 6, December 2021

Indexing: ISI (Thomson Scientific), Cumulated Index Medicus (NLM), SCOPUS, MEDLINE, EMBASE, LILACS, SciELO, PubMed

Address: Av. Marechal Câmara, 160 - 3º andar - Sala 330
20020-907 • Centro • Rio de Janeiro, RJ • Brasil
Phone.: (21) 3478-2700
E-mail: arquivos@cardiol.br
http://abccardiol.org/
SciELO: www.scielo.br

Commercial Department
Phone: (11) 3411-5500
E-mail: comercialsp@cardiol.br

Editorial Production
SBC - Scientific Department

Graphic Design and Diagramming
SBC - Communication and Events Department

Validation of an Artificial Intelligence Algorithm for Diagnostic Prediction of Coronary Disease: Comparison with a Traditional Statistical Model

Luis Correia,[1,2] Daniel Lopes,[1] João Vítor Porto,[1] Yasmin F. Lacerda,[1] Vitor C. A. Correia,[1] Gabriela O. Bagano,[1] Bruna S. B. Pontes,[1] Milton Henrique Vitoria de Melo,[1] Thomaz E. A. Silva,[1] André C Meireles,[1]

Escola Bahiana de Medicina e Saúde Pública,[1] Salvador, BA – Brazil

Hospital São Rafael,[2] Salvador, BA – Brazil

Abstract

Background: Multivariate prognostic analysis has been traditionally performed by regression models. However, many algorithms capable of translating an infinity of patterns into probabilities have emerged. The comparative accuracy of artificial intelligence and traditional statistical models has not been established in the medical field.

Objective: To test the artificial intelligence as an accurate algorithm for predicting coronary disease in the scenario of acute chest pain and evaluate whether its performance is superior to traditional statistical model.

Methods: A consecutive sample of 962 patients admitted with chest pain was analyzed. Two probabilistic models of coronary disease were built using the first two-thirds of patients: a machine learning algorithm and a traditional logistic model. The performance of these two predictive strategies were evaluated in the remaining third of patients. The final logistic regression model had significant variables only, at the 5% significance level.

Results: The training sample had an average age of 59 ± 15 years, 58% males, and a 52% prevalence of coronary disease. The logistic model was composed of nine independent predictors. The machine learning algorithm was composed of all candidates for predictors. In the test sample, the area under the ROC curve for prediction of coronary disease was 0.81 (95% CI = 0.77 - 0.86) for the machine learning algorithm, similar to that obtained in logistic model (0.82; 95% CI = 0.77 - 0.87), p = 0.68.

Conclusion: The present study suggests that an accurate machine learning prediction tool did not prove to be superior to the statistical model of logistic regression.

Keywords: Validation Studies; Artificial Intelligence; Coronary Artery Disease/diagnostic; Data Interpretacion, Statistical.

Introduction

In the last decades, computers' ability to generate and store data has improved substantially, leading to highly complex and large datasets. Traditional statistical modeling has the advantage of simplicity, as it fits the relationship between predictors and outcomes into a regression formula. However, these models have many assumptions that are difficult to be satisfied in complex sets of information: limited number of variables, adequate distribution, independence of observations, no multicollinearity, and concerns with interactions. In contrast, the prediction mechanism of artificial intelligence is algorithm-based, with no assumptions or limit of variables. Therefore, different from statistical modelling, prediction algorithms do not become less accurate as data get complex. In these scenarios of "big data", artificial intelligence becomes more accurate than traditional statistics.[1,2]

Medical data can suffer from bias if not collected under a pre-established protocol. For this reason, the traditional epidemiological approach of small sets of data, prospectively collected, is the most appropriate choice in medical research.[3] Therefore, it is important to explore whether artificial intelligence remains superior to statistical modelling if exposed to samples of moderate size and limited number of variables, as in most epidemiological studies.

Prediction of coronary artery disease (CAD) in patients with acute chest pain is a major challenge for the emergency physician who has to decide whether to discharge the patient, proceed with further non-invasive tests or go directly to invasive angiography. Discharging a patient with unstable coronary disease may be devastating, but admitting anybody with chest pain could have unintentional consequences.[4] In this process, the probability of obstructive CAD should drive medical decision-making.[5]

In the present study, we utilized data from a prospective registry of chest pain[5] to build a machine learning model to predict obstructive coronary disease. We aimed to evaluate

Mailing Address: Luis Correia •
Escola Bahiana de Medicina e Saúde Pública – A. Princesa Leopoldina, 19/402. Postal Code 40050-420, Salvador, BA – Brazil
E-mail: luis.correia@bahiana.edu.br
Manuscript received July 09, 2020, revised manuscript November 09, 2020, accepted December 02, 2020

DOI: https://doi.org/10.36660/abc.20200302

whether an artificial intelligence algorithm is a better predictor than logistic regression in a traditional set of simple epidemiological data, considering both discrimination and calibration properties.

Methods

Sample selection

From September 2011 to November 2017, all patients admitted with chest pain and clinical suspicion of CAD (regardless of electrocardiogram or troponin results) to the coronary care unit of our hospital were included in the study. Exclusion criterion was patient's refusal to participate. As defined *a priori,* a total of 962 patients were divided into the derivation sample (first two-thirds, n=641) and validation sample (last third, n= 321). The study was approved by an institutional review committee and that the subjects gave informed consent.

Predictors of obstructive CAD

At admission (baseline), three sets of variables were recorded as candidates for prediction of obstructive CAD. First, 13 variables related to medical history and clinical presentation; second, 14 characteristics of chest discomfort; third, 11 variables related to abnormalities in imaging or laboratory tests at admission: ischemic changes on electrocardiogram (T wave inversion ≥ 1 mm or dynamic ST deviation ≥ 0.5 mm), positive troponin (> 99th percentile for the general population; Ortho-Clinical Diagnostics, Rochester, NY, USA), N-terminal pro-B-type natriuretic peptide (NT-proBNP, enzyme-linked fluorescent assay, Biomérieux, France), high-sensitivity C-reactive protein (CRP, nephelometry, Dade-Behring, USA), D-Dimer (immunoenzymatic essay, Biomérieux, France), low-density lipoprotein (LDL)-cholesterol (Friedwald equation), creatinine, white cell count, platelets, plasma glucose, and hemoglobin. Laboratory tests were performed in plasma material collected at presentation to the emergency department. Medical history and chest pain characteristics were recorded by three investigators (M.C., A.M.C., R.B.), trained to interview participants in a standardized manner to minimize bias and improve reproducibility. Radiologic signs of ventricular failure and the electrocardiogram were interpreted by the same investigator (L.C.).

Outcomes

The primary outcome to be predicted by the model was diagnosis of obstructive CAD, defined by subsequent tests performed during hospital stay. Outcome data was collected by three investigators (M.C., A.M.C., R.B.) and confirmed by a fourth investigator (L.C.). For diagnostic evaluation, patients underwent invasive coronary angiography or a provocation test (perfusion magnetic resonance imaging, single-photon emission computed tomography or dobutamine stress echocardiogram), at the discretion of the assistant cardiologist. In case of a positive non-invasive test, patients had angiography for confirmation. Based on this diagnostic algorithm, obstructive CAD was defined as a stenosis ≥ 70% by angiography. A normal non-invasive test indicated absence of obstructive CAD and no further test was required. Regardless of coronary tests, patients were classified as "no obstructive CAD" if one of the following conditions was diagnosed by imaging test – pericarditis, pulmonary embolism, aortic dissection, or pneumonia.

Statistical analysis

Shapiro-Wilk test was used to assess whether the data was normally distributed. For descriptive analysis, we used mean and standard deviation for continuous variables with normal distribution, and median and interquartile range for continuous variables without normal distribution. Category variables were described as frequencies. In the derivation sample, we first used unpaired Student's *t* test for normally distributed continuous variables and Pearson's chi-square test for univariate analysis of categorical variables. Numeric variables without normal distribution were analyzed by the non-parametric Mann-Whitney test. Then, variables with a p-value < 0.20 in the univariate analysis were included in the multivariate logistic regression analysis for prediction of obstructive CAD.

Multivariate models were developed by the stepwise method; all variables were fitted into a logistic regression model by using the forced entry and, at each step, the least significant stepwise term was removed from the model, using the Wald test. Initially, three intermediate models were built, according to the type of predictive variables (medical history, chest pain characteristics or physical exam/laboratory tests). Independent predictors ($p < 0.10$) in each intermediate model were included as covariates in the final model, constructed by including significant variables only, at the 5% significance level.

The machine learning algorithm recognizes patterns of clinical characteristics associated with outcome probabilities. Fisher discriminant analysis was used to generate dendrograms, which were combined repeatedly until the error ratio indicated optimal performance. The derivation sample was used for building the machine learning algorithm. Different from logistic regression, there was no preselection of variables and all 55 parameters were included with no further elimination. The influence of each variable on the probability calculation was defined by the purity of nodes and the percentage increase of associated error. As the result of the graphical analysis, we made 8,000 combination interactions.

The two models were compared in the validation sample. Area under the receiver operating characteristic (ROC) curves were used to test discrimination and compared between the models by DeLong's test. Calibration was evaluated by the Hosmer-Lemeshow test (applied to the probabilities generated by the models), and by calculating the calibration slope and intercept of the linear plot of mean predicted probability against observed incidence of events per deciles of prediction (a perfectly calibrated model has an intercept of 0 and slope of 1). Before performing linear regression, the following assumptions had to be verified: linear relationship, independence of observations, normality of residuals, homoscedasticity of residuals.

Statistical significance was defined as $p < 0.05$. The SPSS software was used for data analysis.

Determination of sample size

Machine learning does not have sample size assumptions. For logistic regression, the derivation set was planned to allow inclusion of at least 15 covariates in logistic regression model. Calculation was based on the following assumptions: 50% prevalence of obstructive CAD and the need for 10 events for each covariate in the logistic regression model.[6,7] Therefore, a minimum of 300 patients would be required in the derivation sample. The validation sample was set to test the discriminatory accuracy by the ROC curve analysis. Based on the assumption of an AUC of 0.70, to provide 90% power to reject the null hypothesis of AUC equal 0.50, with an alpha of 5%, a minimum of 85 patients was required. Therefore, a minimum of 100 patients would be required in the validation group. These assumptions were satisfied. The analysis of this sample was performed and completed in January 2018 to avoid multiple testing.

Results

Characteristics of the derivation sample

Six hundred forty-one patients were studied, aged 59 ± 15 years, 58% males, 30% with previous history of coronary disease. Median time elapsed between the onset of symptoms and first clinical evaluation in the hospital was 4.2 hours (interquartile range 1.9 - 14 hours). By using the study protocol, we identified 330 patients with obstructive CAD, a prevalence of 52%. All these cases had the diagnosis confirmed by invasive coronary angiography. Regarding the 311 patients without CAD, 93 were classified by a negative angiography, 169 by a negative noninvasive test and 52 had other dominant diagnosis (14 pulmonary embolism, five aortic dissection, 28 pericarditis, two pneumonia).

Characteristics of the validation sample

Three hundred twenty-one patients were studied, with some characteristics similar to the derivation group, age of 59 ± 16 years, 58% males, 22% with previous history of coronary disease. Time elapsed between onset of symptoms and first clinical evaluation in the hospital had a median of 7.0 hours (interquartile range = 2.4 - 23 hours). Using the study protocol, we identified 163 patients with obstructive CAD, a prevalence of 51%. All these cases had the diagnosis confirmed by invasive coronary angiography. Regarding the 158 patients without CAD, 88 were classified by a negative angiography, 13 by a negative non-invasive test and 57 had another dominant diagnosis (25 pulmonary embolism, two aortic dissection, 25 pericarditis, five pneumonia).

Development of the logistic model

Among the 13 variables related to medical history and clinical presentation, seven were positively associated with obstructive CAD at a significance level < 10%: age, male gender, acute left ventricular dysfunction, previous history of CAD, diabetes, smoking, and symptoms triggered by exercise – Table 1. When these seven variables were included in the logistic regression, previous history of CAD lost significance and all others remained significant at a level < 5% - (Intermediate Model 1, Table 2).

Regarding chest pain characteristics, among 14 variables, six had positive association with CAD: oppressive nature, irradiation to left arm, severe intensity, duration in minutes, relief with nitrates, similarity to previous infarction; and three had negative association with CAD: worsening with compression, arm movement and deep breath (Table 1). When these nine variables were added to the logistic regression, only three remained significant at a level < 5 – worsening with compression, deep breath and severe intensity (intermediate model 2, Table 2).

Among 11 laboratory tests, seven were positively associated with CAD: ischemic electrocardiogram, positive troponin, creatinine, glycaemia, NT-pro-BNP, CRP, white cell count (Table 1). When these seven variables were included in the logistic regression, only ischemic electrocardiogram and positive troponin remained significant at a level < 5% (intermediate model 3, Table 2).

The 11 significant variables in the intermediate model were included in the final logistic regression analysis, generating a final model with nine significant variables to predict the presence of CAD: age, male gender, ischemic electrocardiogram, positive troponin, left ventricular dysfunction, exercise induction, smoking, diabetes, and worsening with deep breath as the only "protective variable". Regression coefficients and odds ratios are depicted in Table 3.

Development of the machine learning model

All 55 variables related to medical history, clinical presentation, chest pain characteristics and laboratory tests were included in the machine learning model. Performance of each variable in the model is depicted in Table 4 by the parameters of node purity and percentage increase in associated error.

Machine Learning versus Logistic Regression (validation sample)

Regarding discrimination, the area under the ROC curve of the machine learning probabilities was 0.81 (95% CI = 0.77 – 0.86), very similar to the area under the curve of logistic regression model 0.82 (95% CI = 0.78 – 0.87), p = 0.68 (Figure 1).

Regarding calibration, both models were validated by the Hosmer-Lemeshow test, but the logistic model showed lower level of significance of the difference between predicted and observed values (chi-square = 6.2; p = 0.62), as compared with the machine learning (chi-square = 12.9; p = 0.11), suggesting a better calibration of the first model.

Accordingly, linear regression between mean predictive probability and observed incidence of events per deciles of prediction showed an intercept of 0.010 (95% CI = -0.083 – 0.103) and slope of 1.004 (95% CI = 0.840 – 0.168) for logistic regression (r = 0.981). For machine learning, an intercept = -0.119 (95% CI = -0.296 – 0.059) and slope = 1.228 (95% CI = 0.909 – 1.547; r = 0.953) were found (Figure 2).

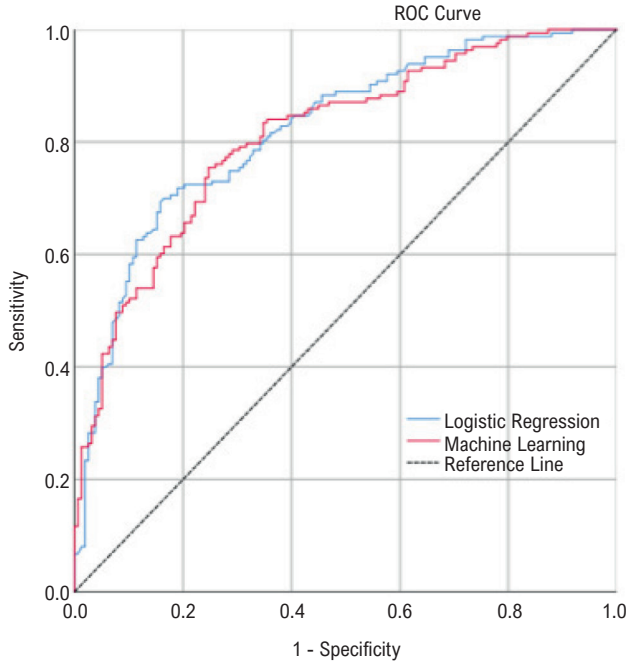

Figure 2 – *Area under the ROC curves of probabilities by the machine learning model and logistic regression model, respectively 0.81 (95% CI = 0.77 – 0.86) and 0.82 (95% CI = 0.78 – 0.87).*

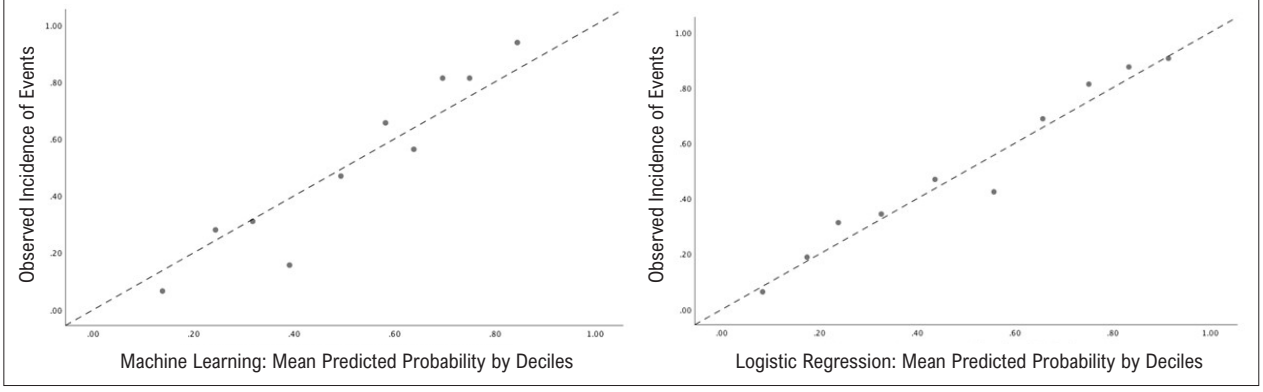

Figure 1 – *Scatter plot for linear regression analyses between mean predictive values per deciles and observed incidences. Panel A indicates calibration of machine learning model (intercept = -0.119, slope = 1.228, r = 0.953). Panel B shows calibration of logistic regression model (intercept = 0.010, slope = 1.004, r = 0.981).*

Table 1 – Comparison of medical history, chest pain characteristics and laboratory tests between patients with and without obstructive coronary artery disease in the derivation sample

	Obstructive CAD		p-value
	Yes (N = 330)	No (N = 311)	
Medical History			
Age (years)	63 ± 13	56 ± 16	< 0.001
Male gender	226 (69%)	148 (48%)	< 0.001
Body Mass Index (Kg/m^2)	28 ± 4.8	28 ± 5.9	0.86
Systolic Blood Pressure (mmHg)	154 ± 32	152 ± 30	0.55
Heart rate (bpm)	78.7 ± 19	79.4 ± 19	0.63
X-ray and clinical signs of LVF	41 (13%)	6 (2.0%)	< 0.001
History of CAD	113 (34%)	77 (25%)	0.01
Diabetes	122 (37%)	74 (24%)	< 0.001
Systemic hypertension	236 (72%)	210 (68%)	0.27
Current smoking	44 (13%)	26 (8.4%)	0.04
Family history of CAD	87 (26%)	79 (25%)	0.78
Exercise induction	50 (15%)	22 (7.1%)	0.001
Emotional induction	8 (2.4%)	15 (4.8%)	0.10
Chest pain characteristics			
Anterior left side location	268 (81%)	261 (84%)	0.37
Oppressive nature	189 (57%)	157 (51%)	0.09
Irradiation to neck	82 (25%)	74 (24%)	0.76
Irradiation to left arm	120 (36%)	93 (30%)	0.08
Vagal symptoms	146 (44%)	132 (42%)	0.65
Severe intensity	185 (56%)	150 (48%)	0.05
Number of episodes	1 (1 – 2)	1 (1 – 3)	0.14
Duration (minutes)	75 (20 – 129)	60 (11 – 214)	0.07
Intensity (1 – 10 scale)	7.7 ± 2.4	7.3 ± 2.4	0.03
Relief with nitrate	134 (41%)	98 (32%)	0.02
Similar to previous infarction	105 (32%)	76 (24%)	0.04
Worsening with compression	19 (5.8%)	43 (14%)	0.001
Worsening with position change	53 (16%)	60 (19%)	0.28
Worsening with arm movement	19 (5.8%)	31 (10%)	0.05
Worsening with deep breath	34 (10%)	68 (22%)	< 0.001
Laboratory tests at admission			
Ischemic changes on ECG	219 (66%)	119 (38%)	< 0.001
Positive troponin	215 (65%)	102 (33%)	< 0.001
NT-proBNP (pg/ml)	432 (155 – 1212)	73 (24 – 301)	< 0.001
Plasma creatinine (mg/dl)	0.90 (0.80 – 1.20)	0.80 (0.70 – 1.1)	< 0.001
LDL-cholesterol (mg/dl)	104 ± 53	108 ± 74	0.46
Plasma glucose (mg/dl)	130 (99 – 160)	107 (90 – 145)	0.009
C-reactive protein (mg/L)	7.4 (2.4 – 15)	6.3 (1.6 – 15)	0.003
White cell count	7.600 (6.050 – 10.100)	7.200 (5.700 – 9.550)	0.04
Platelets	232 (192 – 290)	232 (197 – 274)	0.83
D-Dimer (ng/ml)	474 (279 – 981)	424 (278 – 913)	0.43
Hemoglobin (g/dl)	14.1 ± 1.9	13.7 ± 1.7	0.11

CAD: coronary artery disease; Family history of CAD implies a first-degree female relative with disease before 55 years of age or first-degree male relative before 45 years of age; LVF: left ventricular failure; NT-pro-BNP: N-terminal pro b-type natriuretic peptide; ECG: electrocardiogram; LDL: low-density lipoprotein.

Table 2 – Intermediate logistic regression models of medical history (Model 1), chest pain characteristics (Model 2) and laboratory tests (Model 3)

Variables	Multivariate significance level
Model 1 (medical history)	
Age (years)	< 0.001
Male gender	< 0.001
X-ray or clinical signs of LVF	< 0.001
Exercise trigger	0.005
Diabetes	0.009
Smoking	0.02
Previous CAD	0.32
Model 2 (pain characteristics)	
Worsening with deep breath	0.001
Worsening with compression	0.01
Severe intensity	0.01
Oppressive nature	0.06
Similar to previous infarction	0.08
Irradiation to left arm	0.16
Relief with nitrate	0.25
Duration (minutes)	0.32
Worsening with arm movement	0.67
Model 3 (laboratory tests)	
Ischemic changes on ECG	< 0.001
Positive troponin	< 0.001
NT-proBNP (pg/ml)	0.89
Plasma creatinine (mg/dl)	0.17
Plasma glucose (mg/dl)	0.12
C-reactive protein (mg/L)	0.58
White cell count	0.80

CAD: coronary artery disease; LVF: left ventricular failure; NT-pro-BNP: N-terminal pro b-type natriuretic peptide; ECG: electrocardiogram; LDL: low-density lipoprotein.

Table 3 – Final model of logistic regression defining the independent predictors of obstructive coronary artery disease

Variables	βeta	Odds Ratio (95% IC)	p Value
Age (each year)	0.032	1.03 (1.02 – 1.05)	< 0.001
Male gender	1.04	2.8 (1.9 – 4.2)	< 0.001
Ischemic changes on ECG	1.05	3.0 (1.96 – 4.2)	< 0.001
Positive troponin	1.03	2.8 (1.9 – 4.1)	< 0.001
Signs of LVF	1.49	4.4 (1.7 – 12)	0.002
Exercise induction	0.93	2.5 (1.4 – 4.7)	0.003
Smoking	0.63	1.9 (1.5 – 3.4)	0.03
Diabetes	0.53	1.7 (1.1 – 2.6)	0.01
Worsening with deep breath	- 0.93	0.39 (0.23 – 0.68)	0.001
Constant	-3.70	----	----
Excluded Variables			
Severe Intensity	----	----	0.06
Worsening with compression	----	----	0.20

Hosmer-Lemeshow test = 4.1; p = 0.85; Area under the ROC curve of the model = 0.81; 95%CI = 0.77 – 0.84; p < 0.001. ECG: electrocardiogram; LVF: left ventricular failure.

Table 4 – Model of machine learning showing the weight of each variable in defining probability, according to the parameters of nodes purity and percentage increase of associated error

	Parameters	
	Node purity	Error increase (%)
Age (years)	9.966665	0.015613620
Male gender	2.8464500	0.007500700
Weight (kg)	4.1309610	0.001209398
Height (cm)	3.4111841	0.001045826
Systolic blood pressure (mmHg)	4.9687120	0.001186313
Diastolic blood pressure (mmHg)	3.8970542	0.000573540
Heart rate (bpm)	4.8355910	0.001049536
X-ray and clinical signs of LVF	1.5479285	0.002145387
History of CAD	0.774541	0.000883823
History of angioplasty	0.809141	0.000852728
Past surgical revascularization	0.407289	0.000246474
History of stroke	0.502479	0.000155925
Carotid disease	0.352677	0.000111797
Peripheral artery disease	0.237674	0.000046758
Diabetes	0.606332	0.00041533
Systemic hypertension	0.680378	0.00059024
Current smoking	0.515775	0.00027025
Family history of CAD	0.471644	0.00002877
Statin therapy	0.496937	0.00023743
Aspirin therapy	1.004764	0.00120421
Chronic renal failure	0.137357	-0.000055424
Dialysis	0.016785	0.000007401
Menopause	0.683362	0.00094085
Hormone replacement therapy	0.379223	0.00010860
Physical/emotional trigger	1.951236	0.00097193
Anterior left side location	0.42644	0.00011250
Oppressive nature	0.90551	0.00070792
Irradiation to neck	0.41147	-0.00011320
Irradiation to left arm	0.70464	0.00025748
Vagal symptoms	0.493875	0.00003483
Severe intensity	0.624608	0.00016137
Intensity (0 – 10)	0.696121	0.00053586
Number of episodes	1.701348	0.00006361
Duration (minutes)	0.493875	0.00089453
Intensity (1 – 10 scale)	2.604802	0.00053586
Relief with nitrate	4.880035	0.00140420
Similar to previous infarction	0.696121	0.000699946
Worsening with compression	0.905519	0.000707922
Worsening with position change	0.384833	0.000041857
Worsening with arm movement	0.295489	-0.000075263
Worsening with deep breath	1.006767	0.000973174
Ischemic changes on ECG	4.880035	0.009409961
Positive troponin	7.935190	0.002336380
NT-proBNP (pg/ml)	17.39237	0.00367361
Plasma creatinine (mg/dL)	4.497093	0.00040330
Total cholesterol (mg/dL)	4.291174	0.00298651
LDL-cholesterol (mg/dL)	4.246389	0.00159658
HDL-cholesterol (mg/dL)	6.131821	0.00596194
Triglycerides (mg/dL)	5.213428	0.00397991
Plasma glucose (mg/dL)	4.115463	0.00222222
C-reactive protein (mg/L)	3.948830	0.00315613
D-dimer	3.418193	-0.00010837
White cell count	4.7122731	0.00034806
Hemoglobin (g/dL)	6.0717680	0.00230890
Platelets	5.0908595	0.00103027

CAD: coronary artery disease; LVF: left ventricular failure; NT-pro-BNP: N-terminal pro b-type natriuretic peptide; ECG: electrocardiogram; LDL: low-density lipoprotein; HDL: high density lipoprotein.

Discussion

In the present study, we tested the concept of building a machine learning tool for prediction of obstructive CAD in a small sample of patients with acute chest pain at admission, based on epidemiological data, prospectively collected, and a limited number of variables. First, we confirmed that artificial intelligence can be built from this type of data and be accurate in discrimination (yes or no) and calibration (probability prediction); second, our validation analysis suggested that artificial intelligence is not superior to traditional statistics in these circumstances.

In the fifties, the psychologist Paul Meehl demonstrated that statistical prediction is generally superior to clinical prediction by human judgement.[8] This idea was supported by the work of Nobel laureate Daniel Kahneman, who described an array of cognitive bias responsible for inaccuracies of human heuristics.[9] Such concepts supported the emphasis on using statistical models as the best evidence-based approach to diagnostic and prognostic predictions. More recently, artificial intelligence rouses as a more robust technique for building prediction tools.

Typically, artificial intelligence is derived from large databases, available from electronic records or web-based interfaces.[10] It provides precision due to the enormous sample size and no assumptions regarding the number of variables, distribution, independence of observations, multicollinearity and concerns with interactions.[1] However, since these large data sets are not collected for scientific purpose, they lack information quality.[3] On the other hand, epidemiological prospective studies with planned, standardized, and *a priori* data collection, are the best method for generating data sets of ideal quality. In this circumstances, traditional statistical modellings usually have assumptions fulfilled and good performance. Thus, the question arises: in these ideal circumstances for statistical modeling, does artificial intelligence remain a superior technique?

In the scenario of acute coronary syndromes and traditional data sets, four authors have compared machine learning versus statistics. Three of the studies evaluated prognosis in acute coronary syndrome and compared machine learning with risk scores, showing some superiority in discrimination for artificial intelligence.[11-13] However, in these studies, the variables used to build machine learning models were different from those of the TIMI and GRACE scores, which impairs any extrapolation for the concept of artificial intelligence versus statistics. The only study that built the two types of models from the same set of variables (sample size of 628; 38 variables) did not show consistent superiority of the several types of machine learning over logistic regression neither for discrimination nor calibration.[14] Also, a systematic review that assessed 71 studies comparing machine learning and logistic regression, showed no superiority of the former over the latter.[15] Therefore, based on the set of studies in patients with acute chest pain, whether machine learning is superior to traditional statistics is an unresolved issue.

Our study indicates that artificial intelligence can build an accurate model from a sample of less than a thousand patients and a few dozens of predictive variables. However, in contrast with the current hype about artificial intelligence, we did not find it superior to the logistic regression model. Our study reinforces traditional statistics applied to a data set that meet its assumptions. Similar results in favor of traditional modelling were observed for prediction of deterioration of hospitalized patients[16] or readmission of heart failure patients.[17]

Despite both models fulfilled the calibration criteria, logistic regression showed a better calibration than machine learning. This suggests that machine learning might need larger data sets to calibrate patterns and probabilities.

On the other hand, our results may be interpreted in favor of machine learning. Considering that machine learning has the ability of constantly improve its predictive value as it is exposed to new data, starting with a reasonable accuracy at baseline, it might become a better model in the long run if exposed to continuous administrative data. Hypothesis that need to be tested, but the present study gives support to invest in this possibility.

One should also contextualize artificial intelligence in terms of medical decision making: it should not be confused with a concept of certainty. Machine learning will not be a paradigm shift in decision making, because if has the same concept of providing probabilities of an outcome, instead of certainty. In this sense, medicine continues to be the "science of uncertainty and art of probability", as William Osler defined several decades ago.[18] Furthermore, decision does not only depend on prediction of outcomes, but also on their negative effects. A highly probable outcome of no serious consequences might be preferable than a low probability outcome of devastating consequences. Thus, after assessing probability through a machine learning model, physician should exercise judgment. In addition to possible damage, judgment should be based on the cost of trying to prevent the event and possible unintended consequences. Thus, clinical judgement is not to be replaced by statistical models or machine learning algorithms.

We believe our sample meets assumptions for building both statistical and artificial intelligence models. Number of events was large enough for the number of predictive variables entered into the logistic regression and for discrimination analysis. However, for calibration analysis, the number of events was low in each decile of predictive probability, making estimation of observed probabilities imprecise. These are our main limitations.

Conclusion

The present study suggests that an accurate machine learning prediction tool can be derived from a moderate size and relatively simple sample of patients. However, machine learning did not prove to be superior to the statistical model of logistic regression.

Author Contributions

Conception and design of the research: Correia L, Lopes D, Meireles AC; Acquisition of data: Correia L, Lopes D, Porto JV, Lacerda YF, Correia VCA, Bagano GO, Pontes BSB, Melo MHV, Silva TEA; Analysis and interpretation of the data: Correia L, Lopes D, Porto JV, Lacerda YF, Correia VCA; Statistical analysis: Correia L, Lopes D, Porto JV, Lacerda YF, Bagano GO, Pontes BSB, Melo MHV, Silva TEA, Meireles AC; Critical revision of the manuscript for intellectual content: Correia L, Lopes D, Porto JV, Lacerda YF, Correia VCA, Bagano GO, Pontes BSB, Melo MHV, Silva TEA, Meireles AC.

Potential Conflict of Interest

No potential conflict of interest relevant to this article was reported.

Sources of Funding

There were no external funding sources for this study.

Study Association

This study is not associated with any thesis or dissertation work.

References

1. Breiman L. Statistical Modeling: The Two Cultures. Statistical Science 2001;16(3):199-215.
2. Mortazavi BJ, Downing NS, Bucholz EM, Dharmarajan K, Manhapra A, Li SX, et al. Analysis of Machine Learning Techniques for Heart Failure Readmissions. Circ Cardiovasc Qual Outcomes. 2016;9(6):629–40.
3. Kaplan RM, Chambers DA, Glasgow RE. Big Data and Large Sample Size: A Cautionary Note on the Potential for Bias. Clin Translat Science. 2014;7(4):342-6.
4. Hermann LK, Newman DH, Pleasant W, et al. YIeld of routine provocative cardiac testing among patients in an emergency department–based chest pain unit. JAMA Intern Med. 2013;173(11):1128-33.
5. Correia LCL, Cerqueira M, Carvalhal M, Kalil F, Ferreira K,et al. A Multivariate Model for Prediction of Obstructive Coronary Disease in Patients with Acute Chest Pain: Development and Validation. Arquivos brasileiros de cardiologia 2017;108(4):304-14.
6. Tripepi G, Jager KJ, Dekker FW, Zoccali C. Linear and logistic regression analysis. Kidney Int. 2008;73(7):806–10.
7. Bewick V, Cheek L, Ball J. Statistics review 14: Logistic regression. Crit Care. 2005;9(1):112–8.
8. Meehl PE. Clinical Versus Statistical Prediction: A Theoretical Analysis and a Review of the Evidence. J Abn Psychol. 1954;10:136-8.
9. Tversky A, Kahneman D. Judgment under Uncertainty: Heuristics and Biases. Science 1974;185(4157):1124-31.
10. O'Leary DEO. Artificial Intelligence and Big Data. IEEE Intelligent Syst.2013;28:96-9.
11. Liu N, Koh ZX, Goh J, et al. Prediction of adverse cardiac events in emergency department patients with chest pain using machine learning for variable selection. BMC Med Inform Decis Mak. 201414:75.
12. Myers PD, Scirica BM, Stultz CM. Machine Learning Improves Risk Stratification After Acute Coronary Syndrome. Scient Rep. 2017;7:12692.
13. Van Houten JP, Starmer JM, Lorenzi NM, Maron DJ, Lasko TA. Machine Learning for Risk Prediction of Acute Coronary Syndrome. AMIA Ann Sympos Proc. 2014;2014:1940-9.
14. Green M, Björk J, Forberg J, Ekelund U, Edenbrandt L, Ohlsson M. Comparison between neural networks and multiple logistic regression to predict acute coronary syndrome in the emergency room. Art Intel Med. 2006;38:305-18.
15. Christodoulou E, Ma J, Collins GS, Steyerberg EW, Verbakel JY, Van Calster B. A systematic review shows no performance benefit of machine learning over logistic regression for clinical prediction models. J Clin Epidemiol. 2019;110: 12–22.
16. Churpek MM, Yuen TC, Winslow C, Meltzer DO, Kattan MW, Edelson DP. Multicenter Comparison of Machine Learning Methods and Conventional Regression for Predicting Clinical Deterioration on the Wards. Crit Care Med. 2016;44(2):368-74.
17. Frizzell JD, Liang L, Schulte PJ, Yancy CW. Prediction of 30-day all-cause readmissions in patients hospitalized for heart failure: Comparison of machine learning and other statistical approaches. JAMA Cardiol. 2017;2(2):204-9.
18. Brainyquotes. William Osler Quotes.[Cited in 2020 June 12] Available from:https://www.brainyquote.com/quotes/william_osler_.

Artificial Algorithms Outperform Traditional Models in Predicting Coronary Artery Disease

Lutfu Askin,[1] Okan Tanrıverdi,[1] Mustafa Cetin[2]

Adiyaman Universitesi Egitim ve Arastirma Hastanesi – Cardiology,[1] Adıyaman -Turkey

Sanko University – Cardiology,[2] Gaziantep – Turkey

Short Editorial related to the article: Validation of an Artificial Intelligence Algorithm for Diagnostic Prediction of Coronary Disease: Comparison with a Traditional Statistical Model

Recent clinical recommendations indicate that additional tests for assessing anatomical (extent, severity, morphology) or functional (ventricular function, presence/extent of ischemia) aspects of chronic and symptomatic coronary artery disease (CAD) may be helpful in certain cases.[1] Emergency physicians must determine whether to release the patient, do further non-invasive testing, or perform invasive angiography on patients with acute chest discomfort. Accepting anybody with chest pain may have unintended effects if discharged with unstable coronary disease.[2] The likelihood of obstructive CAD should guide medical decisions.[3] Machine learning (ML) algorithms can supplement the diagnostic and prognostic capabilities of conventional regression methods. The disparity between the applicability of such methods and the outcomes achieved with them was due to the data analysis software platforms used.[4]

ML may use thoracic phase signal features to build final mathematical models that evaluate the existence of severe CAD. Cardiac phase space analysis seems similar to the most widely used functional stress tests and needs little patient time.[5] The 2-year results showed that deep learning fractional flow reserve derived from CT (DL-FFRCT) may be used to guide revascularization, with high cancellation rate and low event rate. A positive DL-FFRCT for tandem lesions was linked with reduced major adverse cardiac events (MACEs) after 2 years.[6] The ML-ischemia risk score (ML-IRS) obtained from quantitative coronary CT angiography enhanced the prediction of future revascularization and may be used to identify individuals who are likely to need revascularization if referred for cardiac catheterization. This machine learning score is linked with invasive fractional flow reserve (FFR) measures, providing external validation across two centers and augmenting clinical risk prediction models.[7]

Even with older computed tomography (CT) scanners, the new version of fractional flow reserve derived from CT (FFRCT) demonstrated excellent diagnostic performance for flow-limiting obstructive coronary lesions, with a substantial reduction in false-positive instances, which may reduce the number of patients referred for further testing. The clinical significance of these results must be confirmed by research evaluating clinical outcomes. This program uses cutting-edge machine learning technologies to improve accessibility, speed, and save costs.[8]

Al'Aref et al.[9] found out that artificial intelligence (AI) has changed fundamental elements of human existence. ML, a type of AI in which computers autonomously learn knowledge by identifying patterns from huge datasets, is widely used in medicine, particularly in cardiovascular disease. A short introduction of ML methods for building inferential and predictive data-driven models is presented. In particular, they emphasize non-invasive imaging techniques such as coronary artery calcium scoring and coronary computed tomography angiography (CTA). In the end of their study, they discuss the current limitations of ML algorithms in the field of cardiovascular illness.

Because of its capacity to assist decision-making and improve diagnostic and prognostic performance, AI is promoting a major paradigm change in a wide range of medical fields, especially in Cardiology. A non-systematic overview of the main articles published on AI in Cardiology is presented here, focusing on its primary applications, effects, and difficulties.[10] Despite better patient outcomes, fractional flow reserve (FFR) remains underused in daily practice. Roguin et al.[11] wanted to see whether an automated AI angiography-based FFR program (AutocathFFR) may help interventional cardiologists make decisions. AutocathFFR was used to take angiographic pictures of patients who had pressure wire FFR measurements. The FFR cut-off 0.8 was computed sensitivity and specificity. Automatic lesion identification worked on all lesions with FFR 0.8 or below. A wire-based FFR >0.8 was predicted with accuracy level of 90% and an area under the curve of 0.91 by AutocathFFR. AutocathFFR is a promising technology that may help people with coronary artery disease make better decisions and choose better treatment options.

AI has grown steadily owing to technological advancements. To enhance the quality of picture collection and reconstruction while integrating information obtained from the images to build powerful prediction models, many AI algorithms have been used for CAD. In CTA, AI can help with many aspects of plaque analysis, including stenosis degree and plaque shape. An increasing body of data links some plaques, termed high-risk or susceptible plaques, to cardiovascular events, regardless of stenosis. The radiologist must understand and actively engage in the development and implementation of AI. We discuss the merits, limits, new applications, and potential advancements of using AI to characterize plaques using CT in this current literature review.[12]

Keywords

Coronary Artery Disease; Artificial Intelligence; Algorithms; Angiography Coronary CT/methods; Machine Learning; Deep Learning; Support Vector Machine.

Mailing Address: Lutfu Askin •
Adiyaman Universitesi Egitim ve Arastirma Hastanesi – Cardiology - Adıyaman Eğitim Ve Araştırma Hastanesi Kardiyoloji Bölümü Adıyaman Centry 2230 – Turkey
E-mail: lutfuaskin23@gmail.com

DOI: https://doi.org/10.36660/abc.20210823

References

1. Cesar LA, Ferreira JF, Armaganijan D, Gowdak LH, Mansur AP, Bodanese LC, et al. Sociedade Brasileira de Cardiologia. Guideline for stable coronary artery disease. Arq Bras Cardiol. 2014;103(2 Suppl 2):1-56.
2. Correia L, Lopes D, Porto JV, Lacerda YF, Correia VCA, Bagano GO, et al. Validation of an Artificial Intelligence Algorithm for Diagnostic Prediction of Coronary Disease: Comparison with a Traditional Statistical Model. Arq Bras Cardiol. 2021; 117(6):1061-1070.
3. Correia LCL, Cerqueira M, Carvalhal M, Kalil F, Ferreira K, Silva ABD, et al. A Multivariate Model for Prediction of Obstructive Coronary Disease in Patients with Acute Chest Pain: Development and Validation. Arq Bras Cardiol.2017;108(4):304-14.
4. Beunza JJ, Puertas E, García-Ovejero E, Villalba G, Condes E, Koleva G, et al. Comparison of machine learning algorithms for clinical event prediction (risk of coronary heart disease). J Biomed Inform .2019 Sep;97:103257.
5. Rabbat MG, Ramchandani S, Sanders WE Jr. Cardiac Phase Space Analysis: Assessing Coronary Artery Disease Utilizing Artificial Intelligence. Biomed Res Int. 2021 Apr 09;2021:6637039. doi:10.1155/2021/6637039
6. Liu X, Mo X, Zhang H, Yang G, Shi C, Hau WK. A 2-year investigation of the impact of the computed tomography-derived fractional flow reserve calculated using a deep learning algorithm on routine decision-making for coronary artery disease management. Eur Radiol. 2021;31(9):7039-46.
7. Kwan AC, McElhinney PA, Tamarappoo BK, Cadet S, Hurtado C, Miller RJH, et al. Prediction of revascularization by coronary CT angiography using a machine learning ischemia risk score. Eur Radiol . 2021;31(3):1227-35.
8. Morais TC, Assunção-Jr AN, Dantas Júnior RN, Silva CFGD, Paula CB, Torres RA, et al. Diagnostic Performance of a Machine Learning-Based CT-Derived FFR in Detecting Flow-Limiting Stenosis. Arq Bras Cardiol. 2021;116(6):1091-8.
9. Al'Aref SJ, Anchouche K, Singh G, Slomka PJ, Kolli KK, Kumar A, et al. Clinical applications of machine learning in cardiovascular disease and its relevance to cardiac imaging. Eur Heart J.2019;40(24):1975-86.
10. Souza Filho EM, Fernandes FA, Soares CLA, Seixas FL, Santos AASMDD, Gismondi RA, et al. Artificial Intelligence in Cardiology: Concepts, Tools and Challenges - "The Horse is the One Who Runs, You Must Be the Jockey". Arq Bras Cardiol. 2020;114(4):718-25.
11. Roguin A, Abu Dogosh A, Feld Y, Konigstein M, Lerman A, Koifman E. Early Feasibility of Automated Artificial Intelligence Angiography Based Fractional Flow Reserve Estimation. Am J Cardiol. 2021;139:8-14.
12. Cau R, Flanders A, Mannelli L, Politi C, Faa G, Suri JS, ET AL. Artificial intelligence in computed tomography plaque characterization: A review. Eur J Radiol. 2021;140:109767.

Training Non-Cardiologists Could Improve the Treatment Results of ST Elevation Myocardial Infarction

Luiz Antonio Machado Cesar,[1] Antonio Padua Mansur,[1] Rui Fernando Ramos,[2] Carlos Magalhães,[3] João Fernando Monteiro Ferreira,[1] Bruno Mahler Mioto,[1] Naide Aparecida de Oliveira,[4] Pedro Silvio Farsky,[4] Amaury Zatorre Amaral,[5] Antonio Célio Camargo Moreno[6]

InCor - Instituto do Coração do Hospital das Clínicas da FMUSP,[1] São Paulo, SP - Brazil
Instituto Dante Pazzanese de Cardiologia,[2] São Paulo, SP - Brazil
Universidade Nove de Julho,[3] São Paulo, SP - Brazil
Secretaria da Saúde do Estado de São Paulo,[4] São Paulo, SP - Brazil
Secretaria Municipal da Saúde,[5] São Paulo, SP - Brazil
Secretaria de Gestão Pública,[6] São Paulo, SP - Brazil

Abstract

Background: According to the World Health Organization, emerging countries will have an enormous growth in the number of heart attacks and related deaths. The main medical issue in Brazil is mortality caused by acute ST elevation myocardial infarction (STEMI). The Society of Cardiology in the State of São Paulo has never trained non-cardiologists as emergency personnel. Patients usually seek help from emergency departments instead of calling for an ambulance.

Objectives: We aimed at reducing in-hospital death rates from acute myocardial infarction by training emergency personnel in the city of Sao Paulo.

Methods: We used a training program for the personnel of five hospitals with >100 patients admitted with STEMI per year, and at least 15% in-hospital STEMI-associated mortality rate. We performed internet training, biannual-quarterly symposia for up to 400 participants, informative folders and handouts. Statistical analysis used the two proportion comparison test with p <0.05.

Results: Nearly 200 physicians and 350 nurses attended at least one training from May 2010 to December 2013. Initially, many emergency physicians could not recognize an acute myocardial infarction on the electrocardiogram, but tele-electrocardiography is used in some emergency departments to determine the diagnosis. The death rate in the five hospitals decreased from 25.6%, in 2009, to 18.2%, in 2010 (p=0.005). After the entire period of training, the STEMI-associated death rate in all public hospitals of São Paulo decreased from 14.31%, in 2009, to 11.25%, in 2014 (p<0.0001).

Conclusion: Even simple training programs for emergency personnel can greatly reduce acute myocardial infarction death rates in undeveloped countries.

Keywords: Acute Coronary,Syndrome; Myocardial Infarction/drug therapy; Training; Epidemiology; Mortality; Emergency Services.

Introduction

Cardiovascular disease continues to be the leading cause of death in many countries. According to the World Health Organization, emerging countries will present an enormous growth in the number of heart attacks and, consequently, in the number of deaths.[1] In 2010, Brazil, which had 200 million inhabitants, had an estimated incidence of 116 heart attacks per 100,000 people,[2] compared to 294 per 100,000 in the United States.[3] The main medical issue in Brazil is mortality caused by ST elevation myocardial infarction (STEMI), which is no longer the case for developed countries.[4] The biggest city in Brazil, the São Paulo metropolitan area, has nearly 18 million inhabitants, most of whom depend on the city's public health system. Public authorities estimate that ≥70% of the population uses public health services, from primary care to specialized treatments. The city's in-hospital mortality rate due to STEMI in 2009 was 14.1%,[5] nearly twice as much as the percentage in developed countries. At that time, the available treatment for STEMI in most of the hospitals in São Paulo was thrombolytic therapy with streptokinase. Currently, the public health system has 46 general hospitals, 139 emergency units for basic emergency care, and 400 ambulatory units. Out of the 46 general hospitals, only 6 can provide primary percutaneous coronary intervention (PCI), and there is no organized system to transfer patients to these hospitals for PCI nor to submit patients to coronary angiography immediately after thrombolysis. The Society

Mailing Address: Luiz Antonio Machado Cesar •
InCor - Instituto do Coração do Hospital das Clínicas da FMUSP - Av. Dr. Enéas Carvalho Aguiar, 44. Postal Code 05403-000, São Paulo, SP - Brazil
E-mail: dcllucesar@incor.usp.br
Manuscript received January 07, 2020, revised manuscript November 17, 2020, accepted January 27, 2021

DOI: https://doi.org/10.36660/abc.20200180

of Cardiology in the State of São Paulo, which is part of the Brazilian Society of Cardiology, thought to improve the care addressed to these patients. The Society has trained cardiologists for many years, but cardiologists are not in the emergency rooms; instead, internal medicine physicians and specialists such as gynecologists and orthopedists compose the staff of the emergency units.

Training, retraining, and revising are important tools for any medical update, but this may not be necessary for very basic training. Many similar initiatives have brought clear results in other countries.[6-12] Even considering the relative simplicity of diagnosing and treating STEMI, it is uncertain whether or not basic training can substantially reduce mortality rates. In the public hospitals of São Paulo, only those with specialized cardiology units can provide PCI, and STEMI-associated mortality is acceptable (6 to 7%) in these hospitals. Some of the 24 hospitals unable to provide interventional cardiology treatment had a >15% STEMI-associated death rate in 2009, according to data from the Health Secretariat of the State of São Paulo.[13] The Society of Cardiology in the State of São Paulo has trained cardiologists, including for the diagnosis and treatment of STEMI, since 1976, but has never trained non-cardiologist emergency personnel. The residents of São Paulo do not usually call 193 (similar to 911 in the United States) for acute chest pain, but instead go to emergency rooms, basic health units, and general hospitals in the city. Therefore, we aimed at reducing in-hospital STEMI-associated mortality rates by providing a training program to emergency personnel (physicians, nurses and other staff) in the city of São Paulo.

Methods

After three meetings with the heads of emergency units and hospital emergency departments, the Society of Cardiology, together with the Secretariat of Health in the State of São Paulo and the Secretariat of Health in the city of São Paulo, designed a training program.

We pre-determined a first target: to teach personnel in the five hospitals with more than 100 STEMI patients per year and ≥15% in-hospital STEMI-associated mortality rate. For these five hospitals, we performed on-site training on Saturdays. During the meetings, we observed that many participants feared starting thrombolytic therapy.

Besides on-site training, we used internet tools for online training, had update meetings, such as symposia for up to 400 participants 2-4 times each year, created informative online folders and handouts. On-site meetings and the symposia included a four-hour training program with three seminars discussing differential diagnosis of chest pain, thoracic pain, and diagnosis and treatment of acute myocardial infarction (AMI) in the emergency department. After each training, a Q&A session was held. Physicians, nurses and other emergency personnel were invited.

The main goal was to evaluate the effects of the training on in-hospital STEMI-associated mortality rates. During this three-year period, streptokinase was replaced with tenecteplase in some hospitals. After treatment with the thrombolytic, aspirin, clopidogrel, and enoxaparin, patients were transferred to a tertiary hospital capable of providing interventional cardiology treatment and surgery. The incidence of AMI and associated death rate was updated every semester by the Secretariat of Health in the State of São Paulo. This information came from public hospitals, which filled out forms including admission, discharge and in-hospital mortality rates.

To evaluate the influence of both the training program and the strategy of tecnecteplase followed by transfer to a reference hospital on mortality rates, we specifically monitored one hospital in which tecnecteplase was introduced and evaluated mortality rates after four months of training, and then after the onset of the tenecteplase strategy along the years, after 2013 until 2015. Besides, we took the same data from five other hospitals with ≥15% in-hospital STEMI-associated mortality rate as a control. An Institutional Review Board (IRB) approved this study, whose data was collected from the Secretariat of Health in the State of São Paulo, Brazil.

Statistical Analysis

For this study, we obtained data from the Secretariat of Health in the city of São Paulo. The database contained data from each health unit where a patient had been admitted by generating an authorization for hospitalization. We used number of deaths (N) and mortality rates (%) to perform the two proportion comparison test, using the statistic software Primer of Biostatistics®, version 4.02.9.[14] P-value was significant when < 0.05.

Results

We provided on-site training to the emergency personnel in five hospitals and extended the training to three other hospitals in 2010. The same participants were retrained in online meetings and update symposia. Twelve emergency units also trained their staff. Many other hospitals trained their emergency and intensive care unit personnel from 2011 to 2013. In total, nearly 200 physicians and 350 nurses attended at least one training session from May, 2010, to December, 2013. We observed that many emergency physicians were unable to identify an AMI on the electrocardiogram. Nearly 50 emergency departments used tele-electrocardiography, causing a five-minute delay in diagnosis. Even in those departments, the emergency staff often feared starting thrombolytic therapy. The STEMI-associated death rates in the five pre-determined hospitals (numbered from 1 to 5) with on-site training reduced their rates from 25.9%, in 2009, to 18.3%, in 2010, with significant difference ($p < 0.001$) (Table 1 and Figure 1). The five non-trained hospitals (numbered from 6 to 10) did not show differences in STEMI-associated death rates: from 17.8%, in 2009, to 21.2%, in 2010 ($p=0.138$) (Table 2 and Figure 2). After the entire training period, the in-hospital STEMI-associated death rates in all the public hospitals of São Paulo decreased from 14.31%, in 2009 (July-December), to 11.25%, in 2013 (January-July) ($p < 0.0001$, Table 3).

Table 1 – Frequency, number of deaths and mortality rate from 2008-09 to 2010 in the five trained hospitals

	Frequency (N)		Number of Deaths (N)		Mortality rate (%)		p-value
Hospital	2008-09	2010	2008-09	2010	2008-09	2010	
1	112	127	26	17	23.2	13.4	
2	121	138	26	25	21.5	18.1	
3	142	157	42	28	29.6	17.8	
4	185	189	50	28	27.0	14.8	
5	165	174	44	46	26.7	26.4	
Total	725	785	188	144	25.9	18.3	< 0.001

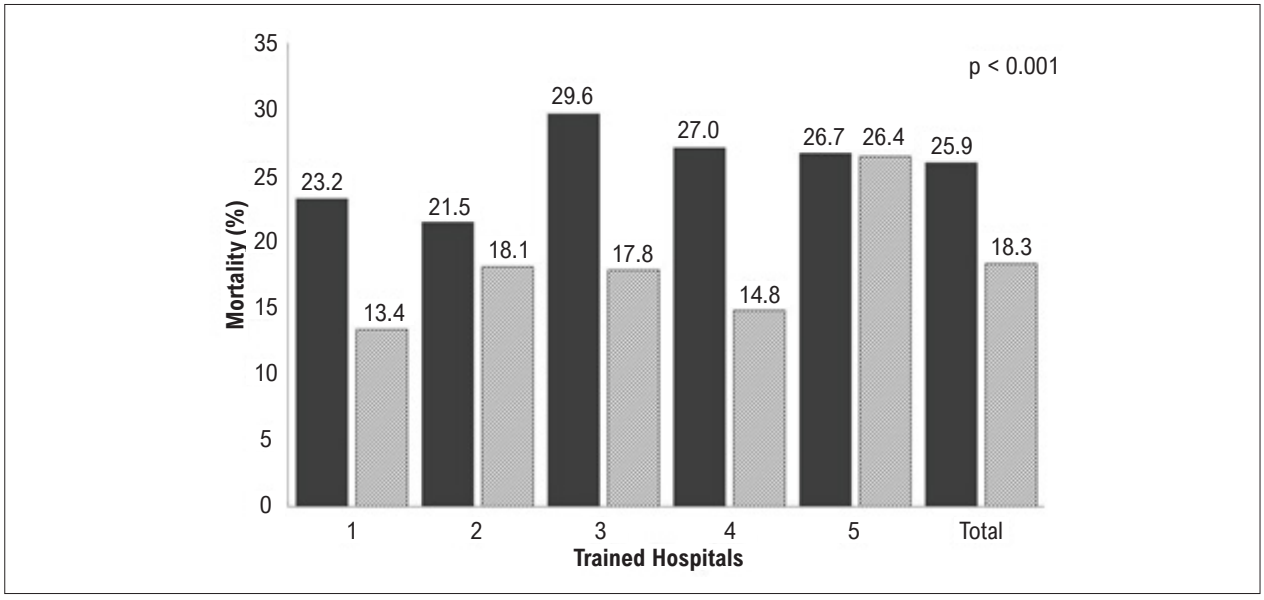

Figure 1 – *Mortality rate (%) in the first five hospitals attending the first training program. Comparison between 2008-2009 and 2010 (p-value for comparison). Columns: gray= before; and dash= after training. The numbers on the columns show the exact percentage death rate in each hospital.*

Table 2 – Frequency, number of deaths and mortality rate from 2008-09 to 2010 in the five trained hospitals

	Frequency (N)		Number of Deaths (N)		Mortality rate (%)		p-value
Hospital	2008-09	2010	2008-09	2010	2008-09	2010	
1	112	151	19	30	13.9	19.9	
2	214	172	34	28	15.9	16.3	
3	107	147	28	48	26.2	32.7	
4	73	86	16	23	21.9	26,7	
5	198	194	33	30	16.7	15.5	
Total	729	750	130	159	17.8	21.2	0.138

Over the three-year period, the number of diagnosed myocardial infarctions increased by 12.61%. However, the number of deaths decreased by 177, an absolute reduction of 3.06% and a relative risk reduction of 21.39%.

Data from the monitored hospital were as follows: this hospital (number 1 in Figure 1) had a 23.7% mortality rate before training, and even had streptokinase that was not used. Four months after the beginning of the training, mortality rates decreased to 13.9%. After the educational program, the administration of tenecteplase was started in trained hospitals and mortality rates progressively decreased, reaching 6.7% in this monitored hospital in 2015.

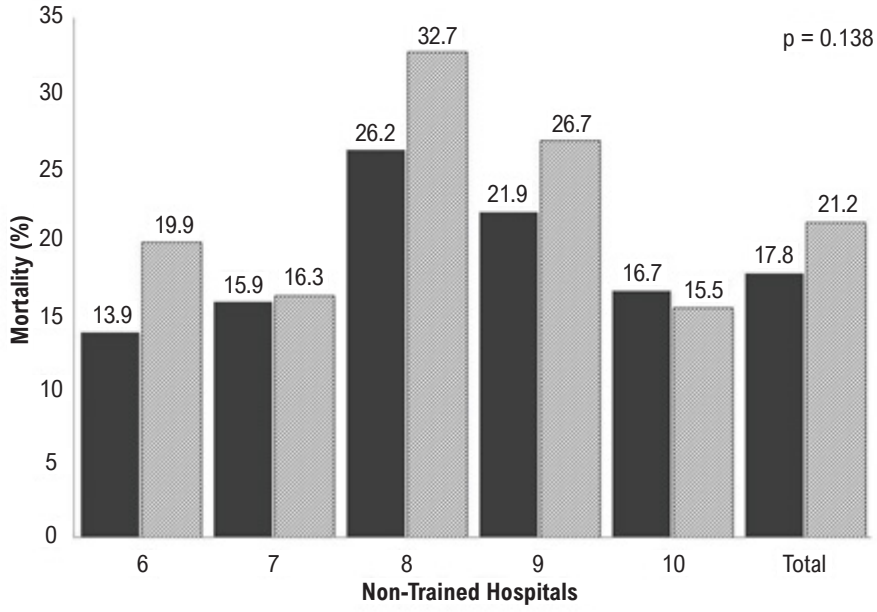

Figure 2 – *Mortality rate (%) in the five hospitals that did not receive the training program. Comparison between 2008-2009 and 2010 (p-value for comparison). Columns: gray= before; and dash= after. The number on the columns show the exact percentage death rate in each hospital.*

Table 3 – Frequency, number of deaths and mortality rate from 2010 to 2013 in all health units in the city of São Paulo

Age range (years)	Frequency (N)		Number of Deaths (N)		Mortality rate (%)		p-value
	2010	2013	2010	2013	2010	2013	
up to 39	290	275	20	21	6.9	7.64	
40-49	909	1,046	70	56	7.70	5.35	
50-59	1,955	2,252	183	141	9.36	6.26	
60-69	1,900	2,297	229	231	12.05	10.06	
70-79	1,384	1,436	280	235	20.23	16.36	
80and+	705	738	240	221	34.04	29.95	
Total	7,143	8,044	1,022	905	14.31	11.25	< 0.0001

Discussion

Although the reduced mortality rates we observed after training could have been affected by other factors, such as weather changes or *H. influenza* vaccination, we feel this is not the case. The median temperature was higher in 2013 than in 2010, especially in the winter, being 6% higher.[15] We had previously found an influence of temperature on the number of AMI-associated deaths in the city of São Paulo, showing a strong association between lower temperatures and increasing death rates. Compared to an average 24-hour day temperature of 22.6ºC, an average of 13.7ºC increased the number of deaths in 32.8%. On the other hand, we observed an increase of 11.8% in death rates when temperatures rose from 21.6-22.6ºC to 23.8-27.3ºC.[16] The temperature in São Paulo had a 6% increase in 2013, in comparison to 2010, and this could not explain the reduction in death rates observed in this study, since such an increase was more evident in the summer, which should rise – and not reduce – the number of deaths according to our data. In fact, there was a very slight growth in the number of cases of AMI in 2014,[15] but with lower death rates. In addition, the level of humidity was very similar between these two periods, so differences related to this factor could not have influenced the reduction of death rates. Another factor that could have had an impact on the results is the vaccine for the influenza virus; however, it has been available since 1998, and vaccination rates have been stable, >70%, since 2000.[16] Therefore, the expected reduction in cases of AMI due to vaccination had already occurred as of 1996-2006.[17] The other confounding factor would be an increase in the number of primary angioplasty procedures performed in São Paulo from 2010 to 2013, but this is not the case, according to the National Registry of

Interventions[18] in public hospitals. Actually, the opposite was true, because the number of primary angioplasty procedures decreased from 503, in 2010, to 185, in 2013. Based on all of these data, we believe that the extreme reduction in mortality rates observed in this study was owed to the training program, which started in May, 2010.

The percentage of deaths caused by AMI remained stable from 2002 to 2009.[5] This number was very high (14%), compared to the data in the United States (5.9%).[13] The absolute increase in the number of cases of AMI from 2010 to 2013 is in accordance with the projections from the World Health Organization,[1] and is supposed to grow even more in the next twenty years. In this study, basic training of emergency personnel caused a significant reduction in the number of deaths due to AMI (1,022 vs 905), with an absolute reduction of 3.06%. In fact, there were two main issues addressed by the training program: difficulty in interpreting an electrocardiogram; and fear of prescribing thrombolytic therapy due to the possibility of brain bleed. We know that these achieved results must be maintained, and we consider this will only be possible with a continuous training program directed to emergency personnel. We acknowledge the possibility that the strategy of treating AMI with tenecteplase, followed by transfer to a reference hospital, could have contributed with the observed reduction in mortality rates. However, as we had pre-established the monitoring of one hospital, it was possible to observe an impressive mortality reduction: from 23.7% to 13.9%, even before the beginning of the strategy with tenecteplase and just four months after the training had started. The non-trained hospitals did not show any differences in this period, and some of them even presented higher mortality rates instead. Unfortunately, mortality rates continue to rise among STEMI patients in our city, and efforts to change this scenario should strongly consider the strategy of training emergency personnel and giving support through tele- electrocardiography and telemedicine.

Study limitations

The study had some limitations. It was not possible to have all the data we wanted, such as the exact number of trained professionals, the number of retrained professionals, the onset of symptoms, the onset-to-door and door-to-balloon times, as well as door-to-thrombolysis time. The data were from a few years ago, but nowadays public hospitals that are similar to that in this study still do not have a routine to carry out thrombolysis or immediate transfer to hospitals that are capable of PCI.

Conclusion

In conclusion, the training of emergency personnel significantly reduced AMI in-hospital morbidity and mortality rates. The strategy of implementing personnel training and retraining in public hospitals is life-saving.

Author Contributions

Conception and design of the research: Cesar LAM, Ramos RF, Magalhães C, Ferreira JFM, Oliveira NA, Amaral AZ, Moreno ACC; Acquisition of data: Magalhães C, Ferreira JFM, Oliveira NA, Amaral AZ, Moreno ACC; Analysis and interpretation of the data and Statistical analysis: Cesar LAM, Mansur AP; Writing of the manuscript: Cesar LAM; Critical revision of the manuscript for intellectual content: Cesar LAM, Mansur AP, Ramos RF, Magalhães C, Ferreira JFM, Oliveira NA

Potential Conflict of Interest

No potential conflict of interest relevant to this article was reported.

Sources of Funding

There were no external funding sources for this study.

Study Association

This study is not associated with any thesis or dissertation work.

Ethics approval and consent to participate

This article does not contain any studies with human participants or animals performed by any of the authors.

Erratum

Arq Bras Cardiol. 2021; [online].ahead print, PP.0-0,

In Original Article "Training Non-Cardiologists Could Improve the Treatment Results of ST Elevation Myocardial Infarction", with DOI number: https://doi.org/10.36660/abc.20200180, published in ahead of print in the Journal Arquivos Brasileiros de Cardiologia, Arq Bras Cardiol. 2021; [online].ahead print, PP.0-0, include the authors Bruno Mahler Mioto and Pedro Silvio Farsky and their respective institutions: InCor - Instituto do Coração do Hospital das Clínicas da FMUSP, São Paulo, SP - Brazil and Secretaria da Saúde do Estado de São Paulo, São Paulo, SP - Brazil. The author Bruno Mahler Mioto insert after the author João Fernando Monteiro Ferreira and the author Pedro Silvio Farsky insert after the author Naide Aparecida de Oliveira.

References

1. Mathers CD, Loncar D. Projections of global mortality and burden of disease from 2002 to 2030. PLoS Med. 2006 [Vited 2020 July 12] Available from: url. http://www.who.int/healthinfo/global_burden_disease/projections2002/en
2. Mansur AP, Favarato. Trends in Mortality Rate from Cardiovascular Disease in Brazil, 1980-2012. Arq Bras Cardiol. 2016;107(3):20-5.
3. Kushner FG, Hand M, Smith Jr SC. 2009 Focused updates: ACC/AHA guidelines for the management of patients with STelevation myocardial infarction (updating the 2004 guideline and 2007 focused update) and ACC/AHA/SCAI guidelines on June 2013 percutaneous coronary intervention (updating the 2005 guideline and 2007 focused update): a report of the American College of Cardiology Foundation/American Heart Association Task Force on Practice Guidelines. Circulation. 2009;120(12):2271-306.
4. Mozaffarian D, Benjamin EJ, Go AS, Heart Disease and Stroke Statistics—2015 Update. A Report From the American Heart Association. *Circulation*. 2015;131 DOI: 10.1161/CIR.0000000000000152.
5. Brasil. Ministério da Saúde. Datasus. [Citado em 2015 Jun 23] Disponível em: http://tabnet.datasus.gov.br/cgi/tabcgi.exe?sim/cnv/evitb10sp.def.
6. HenryTD,SharkeySW,BurkeMN,etal. A regional system to provide timely access to percutaneous coronary intervention for ST-elevation myocardial infarction. Circulation. 2007;116(9):721-8.
7. Moyer P, Ornato JP, Brady Jr WJ. Development of systems of care for ST-elevation myocardial infarction patients: the emergency medical services and emergency department perspective. Circulation 2007;116(5):43-8.
8. Rokos IC, French WJ, Koenig WJ. Integration of pre-hospital electrocardiograms and ST-elevation myocardial infarction receiving center (SRC) networks: impact on door-to-balloon times across 10 independent regions. J Am Coll Cardiol Cardiovasc Interv 2009;2(5):339-46.
9. Jollis JG, Roettig ML, Aluko AO. Implementation of a statewide system for coronary reperfusion for ST-segment elevation myocardial infarction. JAMA 2007;298(25):2371-80.
10. Eagle KA, Nallamothu BK, Mehta RH. Trends in acute reperfusion therapy for ST-segment elevation myocardial infarction from 1999 to 2006: we are getting better but we have got a long way to go. Eur Heart J 2008;29(2):609-17.
11. Ting HH, Bradley EH, Wang Y. Factors associated with longer time from symptom onset to hospital presentation for patients with ST-elevation myocardial infarction. Arch Intern Med. 2008;168(6):959-68.
12. Studneck JR, Garvey L, Blackwell T. Association between prehospital time intervals and ST-elevation myocardial infarction system performance. Circulation 2010;122(11):1464-9.
13. OECD: "In-hospital mortality following acute myocardial infarction" In: Health at a Glance 2011: OECD Indicators, OECD Publishing; 2011. [Cited in 2019 July 12]. Available from: http://dx.doi.org/10.1787/health_glance-2011-42-en.
14. Glantz SA. Primer of biostatistics, version 4.02. New York: McGraw-Hill; 1996.
15. Boletim Climatológico Annual de Estação Metereológica do IAG/USP Seção Técnica de Serviço Metereológicos- Instituto de Astronomia, Geofísica e Ciências Atsmoféricas da Universidade de São Paulo. 2014;v.17. São Paulo: IAG/USP;2014. Disponível em: http://www.estacao.iag.usp.br/Boletins/2014.pdf.
16. Sharovsky R, Cesar LAM, Ramires, JAF. Temperature, air pollution, and mortality from myocardial infarction in São Paulo, Brazil. Temperature, air pollution, and mortality in São Paulo. Braz J Med Biol Res. 2004;37:1651-7.
17. Mansur AP, Favarato D, Avakian SD, Ramires JAF. Influenza Vaccination and Cardiovascular Mortality in Women and Men at Least 60 Years of Age in the Metropolitan Area of São Paulo, Brazil. Journal of Primary Care & Community Health. 2010;1:139–43.
18. Brasil. Ministério da Saúde. SIH/SUS Sistema de informações hospitalares SUS/ Datasus/MS-Code -0406030049 primary coronary angioplasty. Brasilia;2015. Database of Hospitals Admissions. - SIH/SUS Sistema de Informações Hospitalares SUS/ Datasus/MS. Code- 0406030049 primary coronary angioplasty. Brasilia;2015.

Optimizing Treatment for Acute Myocardial Infarction, a Continuous Effort

Ramón Corbalán[1,2]

Pontificia Universidad Catolica - Cardiovascular Division,[1] *Santiago – Chile*
División Cardiovascular, Universidad Catolica de Chile,[2] *Santiago – Chile*

Short Editorial related to the article: Training Non-Cardiologists Could Improve the Treatment Results of ST Elevation Myocardial Infarction

Early reperfusion with primary percutaneous coronary intervention (PPCI) or thrombolysis (TL) has decreased the morbimortality from acute myocardial infarction (AMI) in Latin America and worldwide. National and international guidelines recommend reperfusion, using either method, according to its availability at the medical center, for patients admitted within 12 hours of AMI symptom onset.[1,2]

PPCI has been shown to be superior to TL, especially when performed at a specialized care center with the infrastructure, staff, and experience necessary to ensure good results and minimize complications.[3-5] However, because of the high costs associated with implementing and developing cardiovascular intervention programs, the availability of centers with the capacity to perform this intervention varies by country and even by region within a given country.

International evidence also indicates that pre-hospital TL followed by timely transfer to a higher-complexity hospital for an invasive study can match or even exceed the results obtained with PPCI.[6] Given the abovementioned findings, some authors recommend a routine invasive study of thrombolyzed patients within the first 24 hours after reperfusion.[7] TL has been shown to be particularly effective if a latest-generation thrombolytic is administered in a timely fashion, that is, within the first 2-4 hours after symptom onset.[8,9] Recent studies have shown the benefits of implementing a pharmacoinvasive strategy, that is TL with Tenecteplase at weight and age-adjusted doses, followed by transfer to a PCI center to perform rescue or elective PCI, depending on the signs of positive or negative reperfusion.[9,10] Nonspecialized doctors usually prefer a transfer to a PCI center, with a long delay, and the consequent underuse of thrombolytics.[11]

The implementation of these strategies has been successfully performed in Europe and USA and whenever possible, in Latin America, but there are persistent inequities in different regions. Large cities, such as Sao Paulo, represent a challenge, particularly at public hospitals, since improving MI care needs adequate public policies. First, the people should be educated about how to recognize symptoms and the need for prompt care at the emergency services. This should be followed by an early diagnosis made by the health team (doctors and nurses), support of tele-electrocardiography to accelerate the diagnosis and the implementation of the best available reperfusion therapy at each center. This implies using TL when the chances for transfer to a tertiary center will delay the time for optimal reperfusion.

In the study performed by Machado et al.[12] and published in this issue of *Arquivos Brasileiros de Cardiologia*, the authors report their experience with the training of doctors and nurses from emergency services in five public hospitals that exhibit high MI mortality rates at baseline, and compare results with data from hospitals with non-trained staff in the long-term follow up. The obtained results are quite impressive, since they achieve a significant reduction of mortality at the trained centers.[12] Certainly, this is an initiative that should be continued over time and extended to other hospitals. Rotation of health personnel in emergency services represent an additional challenge and, for that reason, the training should be continued over time.

This experience was supported by the Society of Cardiology from the State of Sao Paulo and the Health Secretariat of Sao Paulo. Additional support should be found to add other policies such as education, tele-electrocardiography, and the building of networks with tertiary centers.[13] Last, but not least, it would be convenient that treatment of acute MI could be supported by government authorities to facilitate consultation at the nearest available hospital. These policies have been successful in other countries, where they have achieved a significant reduction in MI mortality.[14]

Keywords

Myocardial Infarction; Early Reperfusion; Education and Training.

Mailing Address: Ramón Corbalán •
Pontificia Univ Catolica - Cardiovascular Division - Marcoleta 367, Piso 8, Appt 301, Santiago, 8330024 - Chile
E-mail: corbalan@med.puc.cl

DOI: https://doi.org/10.36660/abc.20210907

References

1. O'Gara P, Kushner F, Aschem D, Casey Jr D, Chung MK, Lemos JA, et al. 2013 ACC/AHA Guidelines for the Management of ST-Elevation Myocardial Infarction. A Report of the American College of Cardiology Foundation/American Heart Association Task Force on Practice Guidelines. Circulation. 2013;127(4):e362-425.
2. Steg G, James SK, Atar D, Badano LP, Blomstrom-Lundqvist CB. ESC Guidelines for the management of acute myocardial infarction in patients presenting with ST-segment elevation. The Task Force on the management of ST-segment elevation acute myocardial infarction of the European Society of Cardiology (ESC). Eur Heart J., 2012;33(20):2569-619.
3. Keeley EC, Boura J, Grines CL Primary angioplasty versus intravenous thrombolytic therapy for acute myocardial infarction: a quantitative review of 23 randomized trials. Lancet 2003;361(9351):13-20.
4. Halvorsen S, Kuber K. The role of fibrinolysis in the era of primary percutaneous coronary intervention. Thromb Haemost. 2011;105(3):390-5.
5. Kristensen S, Lauit KG, Fajader J, Kaifoszova Z, Kala P, Di Mario C, et al. Reperfusion therapy for ST elevation acute myocardial infarction 2010/2011: current status in 37 ESC countries. Eur Heart J.2014;35(29):1957-70.
6. Bonnefoy E, Steg FG, Boutitie F, Dubien PY, Lapostolle F, Roncalli J, et al. Comparison of primary angioplasty and pre-hospital fibrinolysis in acute myocardial infarction (CAPTIM) trial: a 5-year follow-up. Eur Heart J. 2009;30(13);1598-606.
7. Armstrong PW., WEST Steering Committee. A comparison of pharmacologic therapy with/without timely coronary intervention vs. primary percutaneous intervention early after ST elevation myocardial infarction: the WEST (Which Early ST-elevation myocardial infarction Therapy) study. Eur Heart J.2006;27(13):1530-8.
8. Westerhout CM, Bonnefoy E, Welsh RC, Steg PG, Armstrong PW. The influence of time from symptom 1-year survival in ST-elevation myocardial infarction: a pooled analysis of an early fibrinolytic strategy versus primary percutaneous coronary intervention from CAPTIM and WEST. Am Heart J. 2021;161(2):283-9.
9. Armstrong PW, Gerschlick AH, Goldstein P, Danays T, Lambert Y, Sulimov V, et al. Fibrinolysis or Primary PCI in ST-Segment Elevation Myocardial Infarction. N Engl J Med. 2013; 368(15):1379-87.
10. Gershlick A,Westerhoat CM, Armstrong PW, Huber K, Halvorsen S, Steg PG, et al. Impact of pharmacoinvasive strategy when delays to primary PCI are prolonged. Hear.t 2015;101(9):692-8.
11. Oliveira GC, Ferreira JS, Oliveira JC. Lima TCR, Barreto ID. et al. Influence of geographical location on access to reperfusion therapies and mortality of patients with ST elevation MI in Sergipe: VICTIN Registry. Arq Bras Cardiol. 2021;117(1):120-9.
12. Machado Cesar LA, Mansur AP, Ramos RF, Magalhães C, Ferreira JFM, Oliveira NA, et al. Training Non-Cardiologists Could Improve the Treatment Results of ST Elevation Myocardial Infarction. Arq Bras Cardiol. 2021; 117(6):1073-1078.
13. Huber K, Goldstein P, Granger CB, Armstrong PW. The organization, function, and outcomes of ST-elevation myocardial infarction networks worldwide: current state, unmet needs and future directions. Eur Heart J.2014;35(23):1526-32.
14. Nazzal C, Campos TP, Corbalan HR, Lanas ZF, Bartolucci JJ, Sanhueza CP, et al. et al. Impacto del plan AUGE en el tratamiento de pacientes con infarto agudo al miocardio con supradesnivel del ST, en hospitales chilenos. Re Méd Chile. 2008; 136(10):1231-8.

Cardiac Fibrosis and Changes in Left Ventricle Function in Patients with Chronic Chagas Heart Disease

João Bosco de Figueiredo Santos,[1] Ilan Gottlieb,[2] Eduardo Marinho Tassi,[3] Gabriel Cordeiro Camargo,[3] Jacob Atié,[3] Sérgio Salles Xavier,[1] Roberto Coury Pedrosa,[3] Roberto Magalhães Saraiva[1]

Instituto Nacional de Infectologia Evandro Chagas/Fundação Oswaldo Cruz,[1] Rio de Janeiro, RJ - Brazil

Casa de Saúde São José,[2] Rio de Janeiro, RJ - Brazil

Hospital Universitário Clementino Fraga Filho/Faculdade de Medicina/Universidade Federal do Rio de Janeiro,[3] Rio de Janeiro, RJ - Brazil

Abstract

Background: **Chagas heart disease (CHD) is a slow progressing condition with fibrosis as the main histopathological finding.**

Objectives: To study if cardiac fibrosis increases over time and correlates with increase in left ventricular (LV) size and reduction of ejection fraction (EF) in chronic CHD.

Methods: **Retrospective study that included 20 individuals (50% men; 60±10 years) with chronic CHD who underwent two cardiac magnetic resonance imaging (MRI) with late gadolinium enhancement with a minimum interval of four years between tests. LV volume, EF, and fibrosis mass were determined by cardiac MRI. Associations of fibrosis mass at the first cardiac MRI and changes in LV volume and EF at the second cardiac MRI were tested using logistic regression analysis. P values <0.05 were considered significant.**

Results: **Patients were classified as follows: A (n=13; changes typical of CHD in the electrocardiogram and normal global and segmental LV systolic function) and B1 (n=7; LV wall motion abnormality and EF≥45%). Mean time between cardiac MRI studies was 5.4±0.5 years. LV fibrosis (in %LV mass) increased from 12.6±7.9% to 18.0±14.1% between MRI studies (p=0.02). Cardiac fibrosis mass at baseline was associated with decrease in >5 absolute units in LV EF from the first to the second MRI (OR 1.48, 95% CI 1.03-2.13, p=0.03). LV fibrosis mass was larger and increased between MRI studies in the group that presented decrease in LV EF between the tests.**

Conclusions: **Even patients at an initial stage of CHD show an increase in myocardial fibrosis over time, and the presence of LV fibrosis at baseline is associated with a decrease in LV systolic function.**

Keywords: **Chagas Cardiomyopathy; Chagas Disease; Endomyocardial Fibrosis; Ventricular Dysfunction, Left; Diagnostic, Imaging; Magnetic Resonance Imaging/methods; Electrocardiography/methods.**

Introduction

Chagas disease is caused by the protozoan *Trypanosoma cruzi* that infects around 10 million people worldwide[1] and 1 to 3 million people in Brazil.[2] Among those patients with chronic Chagas disease, 20 to 40% have the cardiac form or Chagas heart disease (CHD)[2] and around 2% of patients will progress each year from the indeterminate to the cardiac form.[3]

Histopathological studies of myocardial specimens obtained from patients with CHD revealed a low-grade chronic fibrosing cardiomyopathy with a continuous replacement of myocardial fibers by areas of fibrosis and compensatory hypertrophy of remnant myocytes, which would be correlated to CHD progression, cardiac remodeling and left ventricular (LV) systolic dysfunction.[4,5]

Cardiac magnetic resonance imaging (MRI) allows the non-invasive recognition and quantification of cardiac fibrosis, the identification of global and segmental wall motion abnormalities, and aneurysm and intracardiac thrombi, as well as evaluation of LV systolic function in patients with CHD.[6] Fibrosis mass correlates directly to functional class and inversely to the LV ejection fraction.[7] Moreover, fibrosis identified by cardiac MRI is associated to ventricular arrhythmias,[8] especially in the presence of two or more contiguous areas of transmural fibrosis.[9] Longitudinal studies found that fibrosis mass was an independent predictor of the combined end-point of cardiovascular death, sustained ventricular tachycardia,[10] and all-cause mortality.[11]

Furthermore, cardiac MRI can identify areas of fibrosis in around 20% of the patients with the indeterminate form of Chagas disease[7,8] and in 43.7% of patients at the stage A of CHD,[8] who have normal global and segmental LV systolic function on two-dimensional echocardiography.

Mailing Address: Roberto Magalhães Saraiva
Instituto Nacional de Infectologia Evandro Chagas - Fundação Oswaldo Cruz - Av. Brasil, 4365. Postal Code 21040-900, Rio de Janeiro, RJ - Brasil
E-mail: roberto.saraiva@ini.fiocruz.br
Manuscript received March 12, 2020, revised manuscript November 18, 2020, accepted January 27,

DOI: https://doi.org/10.36660/abc.20200597

On the other hand, in patients with more advanced stages of the cardiac form, cardiac fibrosis is detected in 89-100% of the patients.[7,9] Therefore, cardiac MRI can identify early cardiac involvement in Chagas disease and the prevalence of patients with cardiac fibrosis increases with the severity of the disease.

Therefore, we aimed to evaluate if cardiac fibrosis progresses over time and if it correlates with worsening of LV function and LV geometry. For that, we retrospectively evaluated a group of patients at early stages of CHD, who underwent two cardiac MRI tests with a minimum interval of four years between them.

Methods

Study subjects

This is a retrospective study that included a convenience sample composed of adult patients with chronic Chagas disease regularly followed at the institutional outpatient Chagas disease clinic.

The criteria of Chagas disease classification followed the Brazilian consensus on Chagas disease:[2] indeterminate form (no evidence of cardiac involvement), cardiac form (evidence of typical CHD changes in the electrocardiogram [ECG]), digestive form (evidence of megacolon or megaesophagus), or cardiodigestive form. Cardiac form was classified into stage A (no symptoms of heart failure [HF] with isolated changes in the ECG), stage B (no HF symptoms with segmental or global LV systolic dysfunction; B1: LV ejection fraction ≥ 45%; B2: LV ejection fraction < 45%), stage C (symptomatic HF), or stage D (end-stage HF).

All patients with CHD at stages A or B1 who underwent two cardiac MRI tests with late gadolinium enhancement (LGE) protocol within a minimum interval of four years, with cardiac fibrosis detected at the first MRI, and negative test for coronary artery disease on treadmill exercise testing at baseline were included in this study. Most patients included in this study were part of a previous study.[8]

Epidemiological and clinical data, including comorbidities, symptoms, echocardiogram, ECG, 24-hour Holter monitoring, and blood tests, were obtained by analysis of medical records.

Cardiac Magnetic Resonance Imaging (MRI)

The first cardiac MRI was performed in a GE HDxt 1.5 Tesla (T) MRI scanner (Wakeusha, Wisconsin, USA) and analyzed using the ReportCard® GE software, version 3.6, as previously described.[8] The second cardiac MRI was performed using a Siemens Avanto 1.5 T scanner (Siemens Healthcare, Germany) or a Siemens Verio 3.0 T scanner (Siemens Healthcare, Germany). LV images were obtained during a 15-s breath hold to minimize artefacts due to breathing movements. LV long-axis and short-axis images were obtained by two ECG-triggered pulse sequences at the same locations. LV and right ventricular (RV) systolic function were analyzed by cine-CMR using steady-state free precession protocol. End-diastolic LV diameter, end-diastolic and end-systolic LV volumes, LV mass, LV ejection fraction, end-diastolic RV volume and ejection fraction were determined by the Simpson's method. Papillary muscles were regarded as part of the LV cavity for calculation of LV volume and mass. Images were acquired with 8-mm slice thickness and 2-mm slice spacing up to the LV apex.

In order to evaluate myocardial fibrosis, images were acquired 10 to 20 min after intravenous bolus of 0.1mmol/kg of gadolinium-based contrast (Dotarem®, Guerbet, Aulnay Sous Bois, France) using an inversion-recovery prepared gradient-echo sequence for myocardial delayed enhancement (MDE) protocol in the long- and short-axis projections. The presence, location and pattern of fibrosis were qualitatively determined. Fibrosis mass was calculated using the ReportCard® GE software version 3.6 in the first cardiac MRI and using the CVI42 software (Circle Cardiovascular Imaging, Canada) in the second cardiac MRI). Calculation of fibrosis mass was based on semi-automatic detection of hyperintense areas compatible with fibrosis on short-axis MDE sequences. The researcher was free to edit the limits of the area of fibrosis. Signal threshold of ≥ 3 standard deviations (SDs) above the mean signal of the reference myocardium was applied to determine the scar volume for both software programs used for fibrosis mass calculation. LV fibrosis mass was defined in absolute values and as percentage of the LV mass. Segmental MDE was analyzed using LV 17-segment model.[12] Scar distribution patterns were classified as follows: 1) transmural, if there was any area of scar that occupied >50% of the wall thickness but in no more than eight segments; 2) focal, if the scar area was not transmural and identified in no more than eight segments; and 3) diffuse, if the scar areas were present in more than eight segments, regardless of the presence of transmural areas.[10] Fibrosis in individual segments was classified as subendocardial, midwall, subepicardial, or transmural.

The analyses of the first cardiac MRI were done by two observers, while the analyses of the second cardiac MRI were done by two other different observers who were unaware of the results of the first cardiac MRI.

Statistical analysis

Calculations were done using statistical software MedCalc 12.5.0.0. Continuous variables were expressed as mean ± SD, and categorical variables as absolute values and percentages. All continuous variables passed the normality test (Kolmogorov-Smirnov test) allowing the use of parametric tests. Data between first and second cardiac MRI were compared using paired Student's t-test. Associations between fibrosis mass at the first cardiac MRI and changes on LV structure and function between first and second cardiac MRI were tested using logistic regression analysis. A decrease >5 units in LV ejection fraction, an increase >10 mL/m^2 in end-diastolic LV volume, and an increase >10 mL/m^2 in end-systolic LV volume were considered events for this analysis. P values below 0.05 were considered significant.

Results

Patients' characteristics

A total of 20 patients were included in this study. All patients had CHD and 65% were at stage A and 35% at stage B1 of the disease at the time of the first cardiac MRI. Associated

digestive disease was present in 35% of the participants. There was an equal gender distribution, most patients were born in the northeast region of Brazil, were white, had elementary schooling, and had hypertension (Table 1). No participant had history of sudden cardiac arrest, HF symptoms, pacemaker, or diabetes mellitus. Most common symptom was palpitations, followed by near-syncope, and syncope (Table 1). One patient had a history of previous stroke and another of transient ischemic attack.

Regarding ECG, all patients at baseline were in sinus rhythm, and the most common ECG changes were right bundle branch block, left-anterior hemiblock, and primary T wave changes (Table 1). No participant had left bundle branch block, low QRS voltage, or periods of electrical inactivity. Except for one participant, all had 24-hour Holter monitor exams recorded on medical records. No participant had sustained ventricular tachycardia and only three had sinus pause longer than two seconds. Almost 40% had a high incidence of premature ventricular contractions and one fifth had non-sustained ventricular tachycardia on Holter exams (Table 1). Except for two patients with enlarged end-systolic LV diameter and one patient with enlarged LV diastolic diameter, all participants had normal LV diameters and ejection fraction. Half of the patients also presented normal LV diastolic function (Table 1).

At the time of the second cardiac MRI, three patients progressed from stage A to B1, one patient progressed from stage B1 to B2, and one patient progressed from stage B1 to C. No patient presented any clinical event compatible with acute coronary syndrome during the study follow-up.

Cardiac MRI

The mean time between the cardiac MRI studies was 5.4 ± 0.5 years. The proportion of the LV segments with areas of scar at the first and second cardiac MRI is depicted in Figure 1.

Fibrosis pattern was classified as focal in 13 patients (65%) and transmural in seven patients (35%) at the first cardiac MRI. Sixty-two out of 340 walls (18.2%) showed cardiac fibrosis with the following distribution: basal inferolateral (55%), apex (30%), apical lateral (30%), apical inferior (25%), apical anterior (25%), mid inferolateral (25%), basal inferior (20%), apical septal (20%), mid anterolateral (20%), basal anterolateral (15%), basal anteroseptal (10%), mid inferoseptal (10%), basal anterior (5%), basal inferoseptal (5%), mid anterior (5%), mid inferior (5%), and mid anteroseptal (5%). The fibrosis pattern was classified as midwall in 37 segments, transmural in 23 segments, subepicardial and midwall in one segment, and subendocardial and midwall in one segment.

At the second cardiac MRI, the fibrosis pattern presented by the patients was classified as focal in 13 patients (65%), transmural in three patients (15%), and diffuse in four patients (20%). The number of walls with areas of fibrosis increased to 102 (30% of 340 walls) and the frequency the walls with areas of fibrosis were: basal inferolateral (75%), basal inferior (50%), mid inferolateral (45%), apical lateral (40%), basal anterolateral (35%), mid anterolateral (35%), basal anteroseptal (30%), apex (30%), apical inferior (25%), apical anterior (25%), apical septal (25%), mid inferoseptal (20%), mid inferior (20%), basal inferoseptal (15%),mid anterior (15%), mid anteroseptal (15%), and basal anterior (10%). The fibrosis pattern was classified as midwall in 74 segments, transmural in 25 segments, subepicardial and midwall in one segment, and subendocardial and midwall in two segments.

Regarding LV size and function, mean values of end-systolic LV volume and LV mass were greater, and the LV ejection fraction was lower at the second cardiac MRI compared to the first cardiac MRI. Mean end-diastolic LV diameter and volume, and the right ventricular volume and ejection fraction did not change significantly from the first to the second cardiac MRI (Table 2).

The mean fibrosis mass in % of LV mass increased 43% from the first cardiac MRI to the second cardiac MRI (Figure 2; Table 2). Regarding the pattern of fibrosis distribution, patients with a transmural pattern showed an increase in fibrosis mass from 19.3±6.1% to 31.4±14.2%, p=0.02, and those with focal pattern presented a non-significant increase in fibrosis mass from 9.0±6.3% to 10.8±7.1%, p=0.36. The number of LV segments with scar increased in both groups: from 38 to 65 (a 71% increase) in the group classified as transmural pattern and from 24 to 37 (a 54.2% increase) in the group classified as focal pattern of fibrosis distribution. The cardiac fibrosis mass increased in 11 of the 20 patients studied (Figure 3).

From the first to the second cardiac MRI, 14 subjects showed a decrease greater than five units in LV ejection fraction, five subjects presented an increase greater than 10 mL/m^2 in end-diastolic LV volume, and seven subjects showed an increase >10 mL/m^2 in end-systolic LV volume. Cardiac fibrosis mass in % of LV mass detected at the first cardiac MRI showed a univariate significant association, with a decrease of >5 units in LV ejection fraction (OR 1.48, 95% CI 1.03 to 2.13, p=0.03) from the first to the second MRI. There was no univariate or multivariate significant association between sex, age, LV fibrosis mass at the first cardiac MRI and the changes in end-diastolic or end-systolic LV volume > 10 mL/m^2 from the first to the second cardiac MRI (Table 3).

We stratified the patients into those who had a decrease>5 units in LV ejection fraction and those who did not (Figure 3). LV fibrosis mass in % of LV mass in the first cardiac MRI was greater among those who had a decrease in LV ejection fraction than those who did not (15.8±7.3% vs. 5.1±2.2%; p=0.017). Also, the LV fibrosis mass in % of LV mass increased from the first to the second cardiac MRI only among patients who presented a decrease in LV ejection fraction (15.8±7.3% vs. 22.9±14.2%; p=0.013; Figure 3A). Among those who did not present a decrease in LV ejection fraction, the cardiac fibrosis mass in % of LV mass did not change from the first to the second cardiac MRI (5.1±2.2% vs. 6.7±2.2%; p=0.25; Figure 3B).

Discussion

CHD is a slow, relentless, silent condition characterized by a chronic fibrosing myocarditis that culminates in a myriad of cardiovascular events such as HF, stroke and life threatening arrythmias.[2,4,5] It is hypothesized that after an initial insult, cardiac damage progresses continuously until symptomatic HF supervenes.[13] In this paper, we show in a group of patients at the initial stages of CHD that the cardiac insult caused by *T. cruzi* infection, measured by cardiac fibrosis mass, increases

Table 1 – Clinical and epidemiological characteristics of study participants (n=20)

Age, years	**60.5 ± 10.4**
Male gender	**10 (50%)**
Place of origin	
Northeast	14 (70%)
Southeast	5 (25%)
Central-West	1 (5%)
Ethnicity	
Caucasian	14 (70%)
Mixed/Pardo	4 (20%)
Afro-Brazilian	2 (10%)
Schooling	
Illiterate	2 (10%)
Elementary School	12 (60%)
High school	6 (30%)
Clinical parameters	
ChD clinical form	
Cardiac – Stage A	9 (45%)
Cardiac – Stage B1	4 (20%)
Cardiodigestive A	4 (20%)
Cardiodigestive B1	3 (15%)
Symptoms	
Near-syncope	5 (25%)
Syncope	3 (15%)
Palpitations	7 (35%)
Hypertension	13 (65%)
Electrocardiogram	
RBBB	14 (70%)
LAHB	14 (70%)
Primary T wave changes	18 (90%)
Premature ventricular contraction	5 (25%)
24 h Holter **Premature ventricular contraction**	
> 30/hour	7 (36.8%)
10-30/hour	3 (15.8%)
< 10/hour	5 (26.3%)
None	4 (21%)
Nonsustained ventricular tachycardia	4 (21%)
Echocardiogram	
Left atrial diameter, cm	3.5 ± 0.5
LV end-diastolic diameter, cm	5.1 ± 0.5
LV end-systolic diameter, cm	3.3 ± 0.5
LV ejection fraction, %	64.9 ± 7.9
LV aneurysm	2 (10%)
LV diastolic function	
Normal	10 (50%)
Delayed relaxation	9 (45%)
Not determined	1 (5%)

ChD: Chagas disease; LAHB: left anterior hemiblock; LV: left ventricular; RBBB: right bundle branch block; values are mean ± SD or n (%).

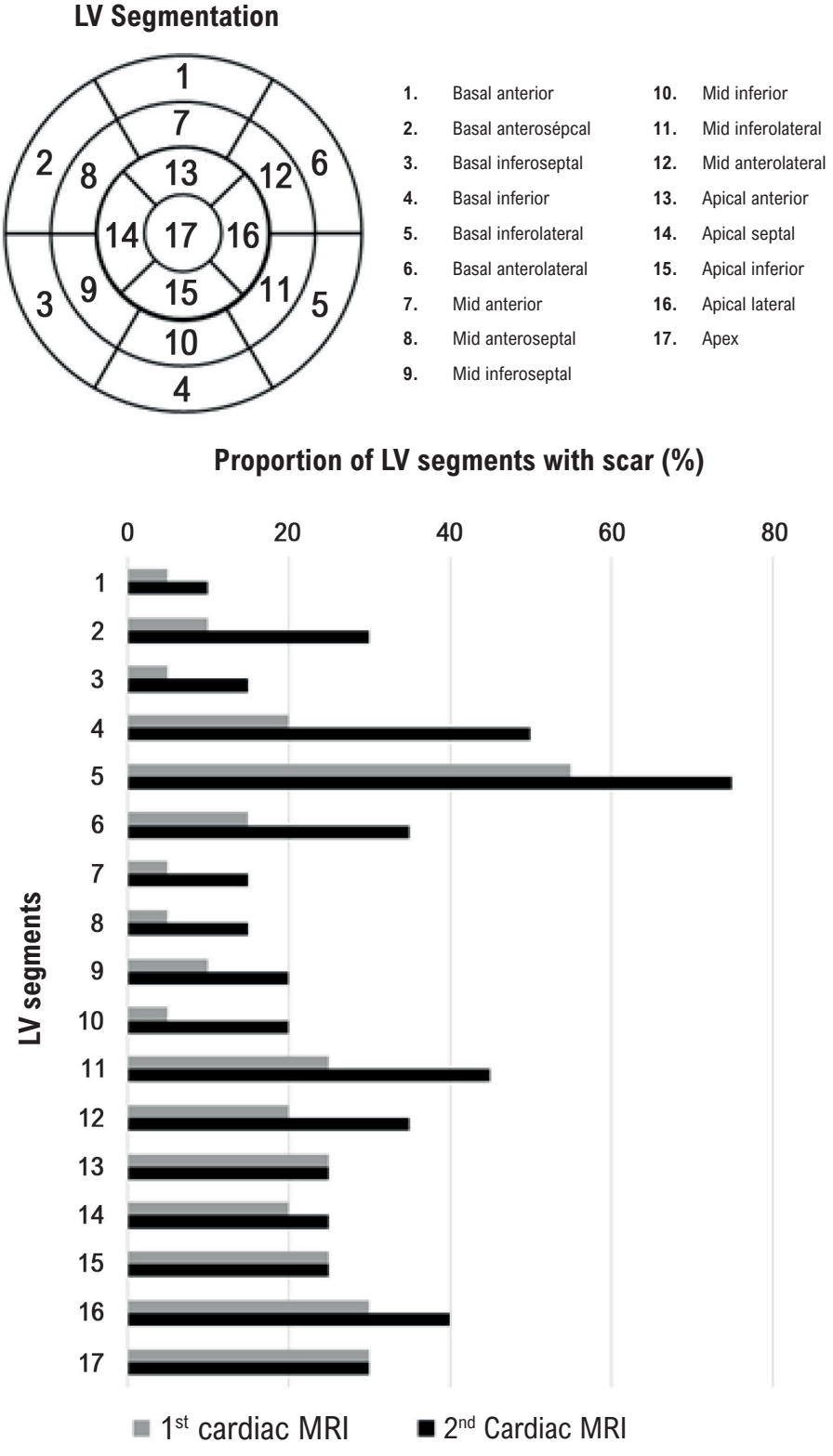

Figure 1 – *Proportion of left ventricular segments with scar at the first and second cardiac magnetic resonance imaging tests according to the 17-segment model.12 Note the increase in the frequency in almost all segments; LV: left ventricular; MRI: magnetic resonance imaging.*

Table 2 – Comparison of left ventricular fibrosis and left and right ventricular chamber size and function between the first and the second cardiac magnetic resonance imaging tests

	1st MRI	2nd MRI	p Value[a]
Fibrosis mass (grams)	12.4 ± 9.1	17.9 ± 16.7	0.03
Fibrosis mass (% of LV mass)	12.6 ± 7.9	18.0 ± 14.1	0.02
End-diastolic LV diameter, mm	53 ± 4	53 ± 7	0.90
End-diastolic LV volume, mL/m^2	76.6 ± 19.1	76.8 ± 21.7	0.94
End-systolic LV volume, mL/m^2	30.5 ± 13.1	37.9 ± 17.9	0.004
LV ejection fraction, %	61.1 ±9.5	52.5 ± 11.7	<0.0001
LV mass, g/m^2	53.9 ± 11.8	56.5 ± 12.6	0.008
End-diastolic RV volume, mL/m^2	58.9 ± 14.6	62.0 ± 15.8	0.11
RV ejection fraction, %	56.7 ± 3.2	56.1 ± 10.2	0.79

LV: left ventricular; MRI: magnet resonance imaging; RV: right ventricular. aPaired Student's t-test.

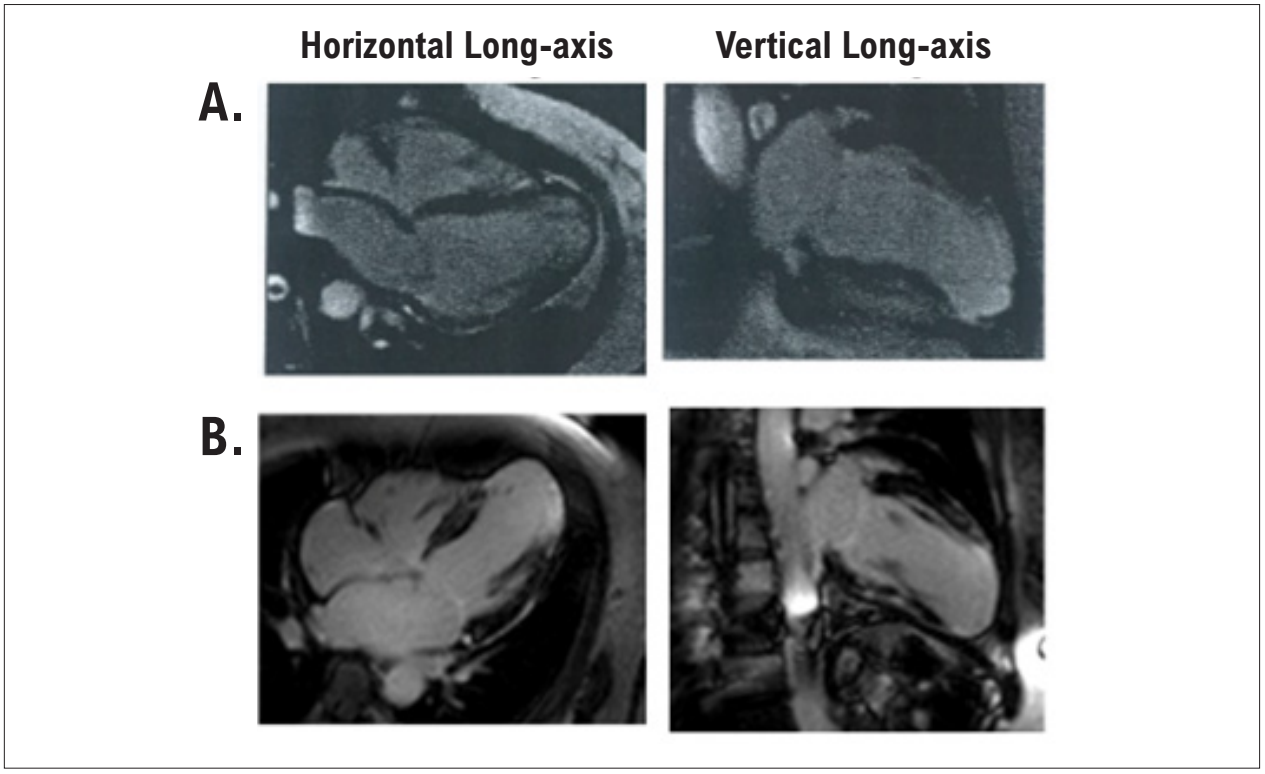

Figure 2 – *Cardiac magnetic resonance imaging of a patient with progressive changes in fibrosis mass. A) Myocardial delayed enhancement on horizontal and vertical long-axis slices depicts areas of midwall fibrosis (bright areas) in mid segments of the septum and transmural cardiac fibrosis in all apical walls and apex. Myocardial fibrosis mass was estimated in 33 grams. B) Myocardial delayed enhancement images obtained from the same patient 4.5 years later depict areas of midwall cardiac fibrosis in basal segments of inferoseptal, inferolateral, and anterolateral walls, mid segments of the septum and anterior walls, and transmural cardiac fibrosis in mid segments of inferolateral and anterolateral walls, all apical walls and apex. The estimated cardiac fibrosis mass increased to 58 grams.*

over time. Moreover, the degree of cardiac damage, *i.e.* cardiac fibrosis mass, is associated with decrease in LV ejection fraction.

Cardiac fibrosis is a hallmark of CHD and a promising prognostic index. As far as we know, this is the first study to address changes in cardiac fibrosis mass and LV structure by means of cardiac MRI in patients at an early stage of CHD. We found an increase not only in fibrosis mass, but also in the number of segments with fibrosis, together with a worsening of LV systolic function and an increase in LV end-systolic volume from the first to the second cardiac MRI after a mean follow-up time of five years. The increase in LV fibrosis occurred mainly in the group of patients with transmural fibrosis. In our study, LV fibrosis was associated with decrease in LV ejection fraction

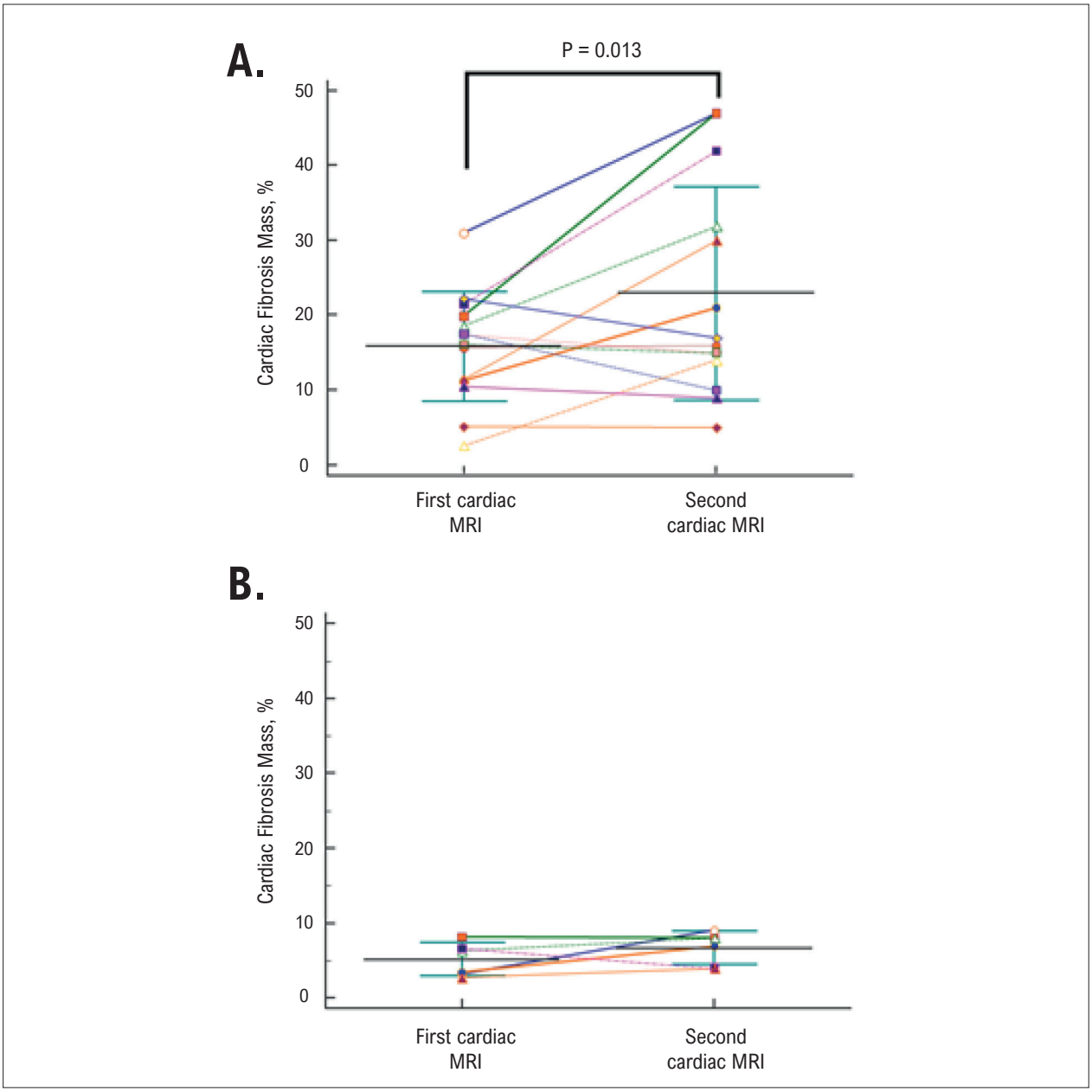

Figure 3 – *Individual changes of cardiac fibrosis mass in % of left ventricular (LV) mass from the first cardiac magnetic resonance imaging test (MRI) to the second cardiac MRI among patients who presented a decrease in LV ejection fraction over time (A) and among those who did not present a decrease in LV ejection fraction (B). Note the LV fibrosis mass is larger at baseline and increased from the first to the second cardiac MRI only in the group who showed a decrease in LV ejection fraction over time.*

over time. LV fibrosis mass was greater in the first cardiac MRI and increased from the first to the second cardiac MRI only in those patients who showed a decrease in LV ejection fraction over time.

Chagas disease patients with cardiac fibrosis have lower LV ejection fraction and higher LV volume and mass, and larger left atrial size than patients without cardiac fibrosis.[10,14] In fact, there is a negative, strong correlation between LV fibrosis mass and LV ejection fraction.[7,15] In a previous study of our group, only patents with cardiac fibrosis had worsening of Chagas disease and LV function measured by LV longitudinal and circumferential strain.[16] Myocardial fibrosis was independently associated with all-cause mortality in a retrospective study[11] and with the occurrence of the combined end-point of cardiovascular death and sustained ventricular tachycardia in a prospective study.[10]

At the first cardiac MRI, fibrosis was more commonly seen in the infero-lateral and apical segments, as previously shown in Chagas disease.[7-9] After a mean follow-up of 5.4 years, the prevalence of cardiac fibrosis increased in almost all segments,

Table 3 – Univariate and multivariate associations of the studied events with left ventricular fibrosis mass, age and sex

	Univariate Association			Multivariate Association		
	OR	95% CI	p values	OR	95% CI	p values
Decrease >5 units in LV ejection fraction						
Male sex	0.37	0.05-2.77-	0.34	0.14	0.00-15.9	0.42
Age, years	1.03	0.94-1.13	0.47	1.37	0.89-2.11	0.15
LV fibrosis mass, %	1.48	1.03-2.13	0.03	2.27	0.87-5.91	0.09
Increase >10 mL/m² in end-diastolic LV volume						
Male sex	0.58	0.07-4.56	0.61	0.56	0.04-7.65	0.66
Age, years	1.10	0.96-1.27	0.17	1.12	0.96-1.31	0.15
LV fibrosis mass, %	1.04	0.91-1.18	0.56	1.05	0.89-1.24	0.57
Increase >10 mL/m² in end-systolic LV vol						
Sex, male	0.64	0.10-4.10	0.64	1.03	0.07-14.8	0.98
Age, years	1.13	0.97-1.31	0.10	1.17	0.97-1.40	0.09
LV fibrosis mass, %	1.06	0.94-1.20	0.33	1.11	0.93-1.33	0.24

LV: left ventricular; Vol: volume logistic regression analysis (enter method).

more notably in the basal segments. There was an aggravation of cardiac fibrosis, as in four patients, fibrosis pattern changed from transmural to diffuse. This reinforces the progressive nature of the cardiac insult caused by Chagas disease.

Our data demonstrated that myocardial fibrosis mass increases over time, which may be related to a slowly progressive fibrosing myopathy with changes in extracellular matrix that leads to cardiac remodeling and HF. In fact, enzymes involved in the extracellular matrix modulation (metalloproteinases [MMP] 2 and 9), present in the pathogenesis of several cardiovascular diseases,[17] may have an important role in Chagas disease pathogenesis. Changes in the balance between MMP and their inhibitors activity may be important for cardiac remodeling.[18] In *T.cruzi* infected mice, MMP-2/MMP-9 inhibitors treatment induced a decrease in myocardial inflammation and a survival increase.[19] In patients with chronic Chagas disease, both MMP-2 and MMP-9 serum levels are higher in patients at the indeterminate and cardiac forms than controls.[20,21] However, MMP-2 serum levels were higher in patients with the cardiac form than with the indeterminate form,[21,22] while MMP-9 serum levels were higher in patients with the indeterminate form than with the cardiac form.[22] Therefore, a MMP-2/MMP-9 balance seems to be important for Chagas disease progression.[23]

Limitations

This study is limited by its retrospective design, a small convenience sample, and by the fact that the cardiac MRIs were performed in machines of different vendors and analyzed by different experts, without an assessment of interobserver variability. However, the interobserver agreement for cardiac fibrosis mass of the group that performed the first cardiac MRI was previously described as excellent.[8] In a previous study,[24] the interobserver variability for the signal threshold versus reference myocardium (STRM)-based scar quantification technique, which we used to evaluate LV fibrosis, was -1.2% (95% CI -8.8 to 9.2%).[24] In our study, six patients had a decrease in LV fibrosis mass in % of LV mass, that ranged from 1.56 to 7.48%, all within the 95% CI described for the interobserver variability. On the other hand, from the 11 patients who presented an increase in LV fibrosis mass in % of LV mass, seven showed an increase above the 95% CI described for the interobserver variability. Three other patients had a difference less than one percent between exams. Therefore, all patients with a difference between exams above the test variability showed an increase in LV fibrosis mass and corresponded to 35% of the studied population. Therefore, we believe that our results were not biased by intra or inter-observer variability.

Regarding exclusion of patients with previous coronary artery disease, a negative treadmill exercise test result does not exclude the possibility of complete occlusion of a coronary branch. However, patients denied previous clinical events compatible with acute coronary syndrome. Patients also did not undergo a second treadmill exercise test or coronary angiography before the second MRI to exclude coronary artery disease. However, no patient presented any clinical event compatible with coronary artery disease during the study follow-up.

Conclusions

In this retrospective study that included patients at an initial stage of CHD, myocardial fibrosis increased over time and LV fibrosis at baseline was associated with a decrease in LV systolic function. This important finding should be confirmed in prospective designed studies. Cardiac fibrosis must also be further studied as a prognostic index for Chagas disease progression and cardiovascular events.

Author Contributions

Conception and design of the research: Santos JBF, Xavier SS, Pedrosa RC, Saraiva RM; Acquisition of data: Santos JBF, Gottlieb I, Tassi EM, Camargo GC; Analysis and interpretation of the data: Santos JBF, Atié J, Xavier SS, Pedrosa RC, Saraiva

RM; Statistical analysis: Santos JBF, Saraiva RM; Writing of the manuscript: Santos JBF, Tassi EM, Camargo GC, Pedrosa RC, Saraiva RM; Critical revision of the manuscript for intellectual content: Santos JBF, Gottlieb I, Tassi EM, Camargo GC, Atié J, Xavier SS, Pedrosa RC, Saraiva RM.

Potential Conflict of Interest

No potential conflict of interest relevant to this article was reported.

Sources of Funding

This study was partially funded by CAPES

Study Association

This article is part of the doctoral thesis submitted by João Bosco de Figueiredo Santos, from Instituto Nacional de Infectologia Evandro Chagas/Fiocruz.

Ethics approval and consent to participate

This study was approved by the Ethics Committee of the CEP INI Fiocruz; CEP HUCFF UFRJ under the protocol numbers 3.146.237 and 11.186.956. All the procedures in this study were in accordance with the 1975 Helsinki Declaration, updated in 2013. Informed consent was obtained from all participants included in the study.

References

1. World Health Organization. (WHO). Chagas Disease (American trypanosomiasis). [Cited in 2020 Apr 12] Available at: http://www.who.int/mediacentre/factsheets/fs340/en/ . 2017.
2. Dias JC, Ramos AN Jr, Gontijo ED, Luquetti A, Shikanai-Yasuda MA, Coura JR, et al. Brazilian Consensus on Chagas Disease, 2015. Rev Soc Bras Med Trop. 2016;49(Suppl 1):3-60.
3. Sabino EC, Ribeiro AL, Salemi VM, Di Lorenzo OC, Antunes AP, Menezes MM, et al. Ten-year incidence of Chagas cardiomyopathy among asymptomatic Trypanosoma cruzi-seropositive former blood donors. Circulation 2013;127(10):1105-15.
4. Chaves AT, Menezes CAS, Costa HS, Nunes MCP, Rocha MOC. Myocardial fibrosis in chagas disease and molecules related to fibrosis. Parasite Immunol 2019;41(10):e12663.
5. Bonney KM, Luthringer DJ, Kim SA, Garg NJ, Engman DM. Pathology and Pathogenesis of Chagas Heart Disease. Annu Rev Pathol. 2019;14:421-47.
6. Nunes MCP, Badano LP, Marin-Neto JA, Edvardsen T, Fernandez-Golfin C, Bucciarelli-Ducci C, et al. Multimodality imaging evaluation of Chagas disease: an expert consensus of Brazilian Cardiovascular Imaging Department (DIC) and the European Association of Cardiovascular Imaging (EACVI). Eur Heart J Cardiovasc Imaging 2018;19(4):459-60n.
7. Rochitte CE, Oliveira PF, Andrade JM, Ianni BM, Parga JR, Avila LF, et al. Myocardial delayed enhancement by magnetic resonance imaging in patients with Chagas' disease: a marker of disease severity. J Am Coll Cardiol 2005;46(8):1553-8.
8. Tassi EM, Continentino MA, Nascimento EM, Pereira BB, Pedrosa RC. Relationship between fibrosis and ventricular arrhythmias in Chagas heart disease without ventricular dysfunction. Arq Bras Cardiol 2014;102(5):456-64.
9. Mello RP, Szarf G, Schvartzman PR, Nakano EM, Espinosa MM, Szejnfeld D, et al. Delayed enhancement cardiac magnetic resonance imaging can identify the risk for ventricular tachycardia in chronic Chagas' heart disease. Arq Bras Cardiol 2012;98(5):421-30.
10. Volpe GJ, Moreira HT, Trad HS, Wu KC, Braggion-Santos MF, Santos MK, et al. Left Ventricular Scar and Prognosis in Chronic Chagas Cardiomyopathy. J Am Coll Cardiol 2018;72(21):2567-76.
11. Senra T, Ianni BM, Costa ACP, Mady C, Martinelli-Filho M, Kalil-Filho R, et al. Rochitte CE. Long-Term Prognostic Value of Myocardial Fibrosis in Patients With Chagas Cardiomyopathy. J Am Coll Cardiol 2018;72(21):2577-87.
12. Cerqueira MD, Weissman NJ, Dilsizian V, Jacobs AK, Kaul S, Laskey WK, et al. Standardized myocardial segmentation and nomenclature for tomographic imaging of the heart. A statement for healthcare professionals from the Cardiac Imaging Committee of the Council on Clinical Cardiology of the American Heart Association. Circulation. 2002;105(4):539-42.
13. Benchimol-Barbosa PR. Nonlinear mathematical model for predicting long term cardiac remodeling in Chagas' heart disease: introducing the concepts of 'limiting cardiac function' and 'cardiac function deterioration period'. Int J Cardiol. 2010;145(2):219-21.
14. Regueiro A, Garcia-Alvarez A, Sitges M, Ortiz-Perez JT, De Caralt MT, Pinazo MJ, et al. Myocardial involvement in Chagas disease: insights from cardiac magnetic resonance. Int J Cardiol. 2013;165(1):107-12.
15. Uellendahl M, Siqueira ME, Calado EB, Kalil-Filho R, Sobral D, Ribeiro C, et al. Cardiac Magnetic Resonance-Verified Myocardial Fibrosis in Chagas Disease: Clinical Correlates and Risk Stratification. Arq Bras Cardiol. 2016;107(5):460-6.
16. Gomes VA, Alves GF, Hadlich M, Azevedo CF, Pereira IM, Santos CR, et al. Analysis of Regional Left Ventricular Strain in Patients with Chagas Disease and Normal Left Ventricular Systolic Function. J Am Soc Echocardiogr. 2016;29(7):679-88.
17. Nagase H, Visse R, Murphy G. Structure and function of matrix metalloproteinases and TIMPs. Cardiovasc Res. 2006;69(3):562-73.
18. Spinale FG. Myocardial matrix remodeling and the matrix metalloproteinases: influence on cardiac form and function. Physiol Ver. 2007;87(4):1285-342.
19. Gutierrez FR, Lalu MM, Mariano FS, Milanezi CM, Cena J, Gerlach RF, et al. Increased activities of cardiac matrix metalloproteinases matrix metalloproteinase (MMP)-2 and MMP-9 are associated with mortality during the acute phase of experimental Trypanosoma cruzi infection. J Infect Dis. 2008;197(10):1468-76.
20. Bautista-Lopez NL, Morillo CA, Lopez-Jaramillo P, Quiroz R, Luengas C, Silva SY, et al. Matrix metalloproteinases 2 and 9 as diagnostic markers in the progression to Chagas cardiomyopathy. Am Heart J. 2013;165(4):558-66.
21. Fares RC, Gomes JA, Garzoni LR, Waghabi MC, Saraiva RM, Medeiros NI, et al. Matrix metalloproteinases 2 and 9 are differentially expressed in patients with indeterminate and cardiac clinical forms of chagas disease. Infect Immun. 2013;81(10):3600-8.
22. Clark EH, Marks MA, Gilman RH, Fernandez AB, Crawford TC, Samuels AM, et al. Circulating serum markers and QRS scar score in Chagas cardiomyopathy. Am J Trop Med Hyg. 2015;92(1):39-44.
23. Medeiros NI, Gomes JAS, Correa-Oliveira R. Synergic and antagonistic relationship between MMP-2 and MMP-9 with fibrosis and inflammation in Chagas' cardiomyopathy. Parasite Immunol. 201;39(8):e12446.
24. Fine NM, Tandon S, Kim HW, Shah DJ, Thompson T, Drangova M, et al. Validation of sub-segmental visual scoring for the quantification of ischemic and nonischemic myocardial fibrosis using late gadolinium enhancement MRI. J Magn Reson Imaging. 2013;38(6):1369-76.

The Importance of Understanding the Progression of Myocardial Fibrosis in Chronic Chagas Cardiomyopathy

Carlos E. Rochitte[1,2]

Universidade de São Paulo, Faculdade de Medicina, Hospital das Clínicas - Instituto do Coração,[1] *São Paulo, SP - Brazil*
Hospital do Coração (HCOR),[2] *São Paulo, SP - Brazil*

Short Editorial related to the article: Cardiac Fibrosis and Changes in Left Ventricle Function in Patients with Chronic Chagas Heart Disease

Myocardial fibrosis is one of the most important biological markers of Chagas' cardiomyopathy and is directly related to the severity of the cardiomyopathy and the stage of the disease.[1] In addition, myocardial fibrosis has prognostic value for major cardiovascular events, with a strong and close relationship with arrhythmic events in these patients.[2-4]

Cardiac magnetic resonance (CMR) is the reference imaging method for myocardial fibrosis detection and quantification in many cardiomyopathies, including Chagas cardiomyopathy. Initial studies included patients with Chagas cardiomyopathy at different stages of the disease and clearly demonstrated that the higher the disease severity the larger the amount of myocardial fibrosis. Based on these data and on the natural history of the disease, with progression of left ventricle dysfunction, one could safely infer that myocardial fibrosis progresses with time for any given patient. However, the longitudinal data using CMR in patients with Chagas disease was not available until the publication of the original article in this issue of ABC Cardiol by Santos et al.[5] This is the first study to include data on myocardial fibrosis from two consecutive CMR of the same patient with a relatively long follow-up of 5.4 years. The authors demonstrated an impressive 43% increase of myocardial fibrosis over the follow-up period, which indicates a mean of 7.9% increase per year of myocardial fibrosis detected by CMR.

Despite the originality of this finding, which was perhaps, a hypothesis generator, this is a retrospective study with a rather small sample only 20 patients. The study also investigated the association of myocardial fibrosis with left ventricle function, which has already been demonstrated in previous studies. This, in my view, took the focus away from myocardial fibrosis progression, which was the original information of the manuscript and should have been explored more deeply and in more detail. I understand the limited sample size might not allow such a detailed analysis. For this reason, additional and larger studies are mandatory to further the knowledge on this crucial parameter that could be the "the one" to help us to understand the pathophysiology and develop new treatments for Chagas cardiomyopathy.

Mechanisms involved in the progression of myocardial fibrosis, including aspects of the myocardial microcirculation,[6] status of the epicardial coronary arteries[7] and even involvement of specific metabolic pathways[8] were not discussed in this manuscript.

A surprising result of the study was the lack of association of fibrosis with age and gender, which has been demonstrated in previous work.[9] Again, this might be the result of very small sample size.

Another interesting aspect of Chagas cardiomyopathy is the low frequency of myocardial fibrosis observed in the acute phase of Chagas disease (personal communication by João Marcos Ferreira) and the possible appearance of new cardiac abnormalities over the follow-up.[10] This may indicate that myocardial fibrosis in Chagas disease is a relentless process, depending on time and the intensity of the inflammatory process. In this regard, prior work has also shown that, differently from ischemic fibrosis, Chagas cardiomyopathy fibrosis is associated to myocardial edema detected by T2- weighted CMR images, indicating the presence of inflammation.

Myocardial fibrosis in Chagas disease is not a fixed and bystander process, but rather, a dynamic and unfolding process leading to progressive myocardial injury and inflammation. This concept is essential for developing methods to try to stop this lethal pathway.

Although the study published in this issue of ABC Cardiol[5] was not designed to investigate the mechanism of the progression of myocardial fibrosis, this knowledge is crucial if we want to advance our knowledge in the pathophysiology and treatment of Chagas cardiomyopathy in the early future.

Keywords

Chagasic Cardiomyopathy; Endomyocardial Fibrosis; Chagas Diseases; Heart Failure; Diagnostic,Imaging/méthods; Imaging Resonance Magnetic/methods.

Mailing Address: Carlos E. Rochitte•
Av. Dr. Enéas de Carvalho Aguiar 44 - Andar AB, Ressonância & Tomografia. Postal Code 05403-000, Cerqueira César, São Paulo, SP – Brazil
E-mail: rochitte@cardiol.br

DOI: https://doi.org/10.36660/abc.20210897

References

1. Rochitte CE, Oliveira PF, Andrade JM, Ianni BM, Parga JR, Avila LF, Kalil-Filho R, Mady C, Meneghetti JC, Lima JA, Ramires JA. Myocardial delayed enhancement by magnetic resonance imaging in patients with chagas' disease: A marker of disease severity. *J Am Coll Cardiol*. 2005;46(8):1553-8
2. Senra T, Ianni BM, Costa ACP, Mady C, Martinelli-Filho M, Kalil-Filho R, Rochitte CE. Long-term prognostic value of myocardial fibrosis in patients with chagas cardiomyopathy. J Am Coll Cardiol. 2018;72(21):2577-87
3. Uellendahl M, Siqueira ME, Calado EB, Kalil-Filho R, Sobral D, Ribeiro C, et al. Cardiac magnetic resonance-verified myocardial fibrosis in chagas disease: Clinical correlates and risk stratification. Arq Bras Cardiol. 2016;107(5):460-6.
4. Volpe GJ, Moreira HT, Trad HS, Wu KC, Braggion-Santos MF, Santos MK,et al. Left ventricular scar and prognosis in chronic chagas cardiomyopathy. J Am Coll Cardiol. 2018;72(21):2567-76.
5. Santos JBF,Gottlieb I, Tassi EM, Camargo GC, Atie J, Xavier S. Cardiac fibrosis and changes in left ventricle function in patients with chronic chagas heart disease. Arq Bras Cardiol. 2021; 117(6):1081-1090.
6. Campos FA, Magalhães ML, Moreira HT, Pavão RB, Lima Filho MO, Lago IM, et al. Chagas cardiomyopathy as the etiology of suspected coronary microvascular disease. A comparison study with suspected coronary microvascular disease of other etiologies. Arq Bras Cardiol. 2020;115(6):1094-101
7. Cardoso S, Azevedo Filho CF, Fernandes F, Ianni B, Torreão JA, Marques MD, et al. Lower prevalence and severity of coronary atherosclerosis in chronic chagas' disease by coronary computed tomography angiography. *Arq Bras Cardiol*.2020;115(6):1051-60
8. Miranda CP, Botoni FA, Nunes M, Rocha M. Analysis of iron metabolism in chronic chagasic cardiomyopathy. *Arq Bras Cardiol*. 2019;112(2):189-92.
9. Assunção AN Jr, Jerosch-Herold M, Melo RL, Mauricio AV, Rocha L, Torreão JA, Fernandes F, et al. Chagas' heart disease: Gender differences in myocardial damage assessed by cardiovascular magnetic resonance. *J cardiovasc Magn Reson,2016;18:88*.
10. Ortiz JV, Pereira BVM, Couceiro KDN, Silva M, Doria SS, Silva P, Lira EDF, et al. Cardiac evaluation in the acute phase of chagas' disease with post-treatment evolution in patients attended in the state of amazonas, brazil. *Arq Bras Cardiol*.2019;112(3):240-6.

Original Article

Antihypertensive Activity of Sauromatum guttatum Mediated by Vasorelaxation and Myocardial Depressant Effects

Bibi Rabia,[1] Umme Salma,[1,2] Kashif Bashir,[1] Taous Khan,[1] Abdul Jabbar Shah[1]

COMSATS University Islamabad - Abbottabad Campus - Department of Pharmacy,[1] Abbottabad, Khyber Pakhtunkhwa – Pakistan

Ibadat International University Islamabad,[2] Islamabad - Pakistan

Abstract

Background: **Sauromatum guttatum (S. guttatum) is used in the treatment of blood disorders and reportedly has a spasmolytic activity through Ca^{2+} channel inhibition.**

Objectives: **The aim of this study was to investigate the antihypertensive potential of S. guttatum in high salt-induced hypertensive Sprague-Dawley (SD) rat model (HSHRs).**

Methods: **SD rats were divided into normotensive, hypertensive, S. guttatum and verapamil treated groups. S. guttatum crude extract (Sg.Cr) (100, 150 and 300 mg/kg/day) and verapamil (5, 10 and 15 mg/kg/day) were administered orally along with NaCl. Aortic rings and right atrial strips from normotensive rats were used to investigate the underlying mechanisms. The level of statistical significance was set at 5%.**

Results: **Mean arterial pressure decreased in the Sg.Cr and verapamil-treated hypertensive groups in a dose-dependent manner ($p < 0.001$). In the vascular reactivity study, acetylcholine induced relaxations with an EC_{50} value of 0.6 μg/mL (0.3–1.0) in Sg.Cr-treated hypertensive rats (300 mg/kg), suggesting endothelial preservation. In isolated normotensive rat aorta, Sg.Cr-treated rats showed vasorelaxation with an EC_{50} value of 0.15 mg/mL (0.10-0.20), ablated by endothelial denudation or pretreatment with $_L$-NAME and atropine. Sg.Cr treatment caused relaxation against high K^+-induced contractions, like verapamil. Sg.Cr showed negative inotropic (82%) and chronotropic effects (56%) in isolated rat atrial preparations reduced with atropine. The phytochemical investigation indicated presence of alkaloids, flavonoids and tannins.**

Conclusion: **S. guttatum has a vasodilatory effect through endothelial function preservation, muscarinic receptor-mediated NO release and Ca^{2+} movement inhibition, while atrial myocardial depressant effect can be linked to the muscarinic receptor. These findings provide pharmacological base for using S. guttatum extract as an antihypertensive medication.**

Keywords: **Rats; Antihypertensive; Sauromatum guttatum; Blood Pressure; Hypertension; Vasodilatation; Calcium Channel Blockers; Cardiac Performance.**

Introduction

Hypertension is an important risk factor for cardiovascular disease and mortality due to target-organ damage.[1] There are many environmental factors that contribute to the etiology of hypertension, including high salt intake. High salt intake has remained the most important factor in the etiology of hypertension in humans.[2] In rats, high salt intake also promotes hypertension, providing a convenient model to study human hypertension.[3] Sustained consumption of a high-salt diet leads to endothelial dysfunction, which may pose a particularly significant risk factor in the development of hypertension,[4] negatively affecting the quality of life.[5]

Mailing Address: Abdul Jabbar Shah •
COMSATS University Islamabad - Abbottabad Campus - Department of Pharmacy, Abbottabad, Khyber Pakhtunkhwa - Pakistan
E-mail: jabbarshah@cuiatd.edu.pk
Manuscript received January 29, 2020, revised manuscript November 28, 2020, accepted January 27, 2021

DOI: https://doi.org/10.36660/abc.20200055

Hypertension management measures include lifestyle adjustments, diet modification, exercise, as well as conventional and alternative therapies, including herbal remedies.[6-8] *Sauromatum guttatum* (*S. guttatum*) belongs to the Araceae family, and is commonly known as "Voodoo Lilly". *Sauromatum guttatum* is known as "Sanp ki Booti" in Pakistan and India, where it is ubiquitous. *S. guttatum* is traditionally used for treating inflammation, breathing difficulties,[9] gastric troubles,[10] tuberculosis, blood disorders, snakebites and skin infections.[11] *S. guttatum* contains lectins, dimethyl sulphides, caryophyllene, indole, skatole, ammonia, trimethylamine and primary amines.[12-14] The corms contain carbon, magnesium, sulfur, oxygen, phosphorus, potassium and chlorine. *In vitro* studies revealed *S. guttatum's* mitogenic,[15] antiproliferative,[16] herbicidal,[17] lipoxygenase inhibitor,[18] antioxidant, antibacterial,[19] spasmolytic[18,20] and insecticidal activities.[17,21] It is traditionally used to manage blood disorders. It has been previously reported that its spasmolytic effect is mediated through Ca^{2+} entry blockade in the smooth muscles of the intestine.[20] Ca^{2+} entry blockers also have an important therapeutic role in the management of hypertension. All these observations provide a solid

foundation for our hypothesis that *S. guttatum* extract might have antihypertensive properties. The objective of this study was to investigate the antihypertensive potential of *S. guttatum* and to reveal the underlying mechanisms by using *in vivo* and *in vitro* methods.

Materials and methods

Preparation of crude extract and phytochemical screening

S. guttatum corms were procured in Nathia Gali, Pakistan (June-July, 2018), identified and validated by Dr. Abdul Nazir, Assistant Professor, Department of Biotechnology, COMSATS University Islamabad, Abbottabad Campus, Pakistan. CHUA-112 is voucher code for the specimen in the herbarium, Department of Pharmacy, COMSATS University Islamabad, Abbottabad Campus, Pakistan. Fresh corms were chopped and dried under the shade at room temperature. Then the dry material was powdered, soaked in a (70%) aqueous methanol solution, with occasional shaking for fifteen, seven and three days. The macerate was filtered through a muslin cloth and then through a qualitative filter paper (Whatman, Grade 1).[22] This process was repeated thrice. Then, a rotary evaporator (-760 mmHg at 37°C) was used to concentrate the liquid extract. The crude extract was analyzed phytochemically for all important constituents such as flavonoids, alkaloids, saponins, phenols and tannins.[23]

Animals

All the experiments were performed in conformity with the guidelines from the Commission on Life Sciences, Institute of Laboratory Animal Resources, National Research Council[24] and approved by the Ethical Committee. Sprague-Dawley (SD) rats were kept in the Animal House with food and water available *ad libitum*.

Pharmacological investigations

Drugs and standards

Drugs and standards were purchased from the following sources: acetylcholine chloride, phenylephrine hydrochloride, atropine sulfate, pentothal sodium from Abbott Laboratories, Pakistan; while isoprenaline hydrochloride, potassium chloride, Nω-nitro-L-arginine methyl ester hydrochloride ($_L$-NAME) and verapamil hydrochloride were obtained from Sigma chemicals company, USA.

In vivo studies

High salt-induced hypertensive rat (HSHR) model and grouping

SD rats (200-250 g) (n=60) were divided randomly into eight groups (n=5-7 in each group). The sampling was done by convenience sampling. Group 1 (normal control group) was given a normal diet. Group 2 (hypertensive group) was given NaCl (8% in diet + 1% in drinking water) for 8 weeks. Groups 3-5 (*S. guttatum*-treated group) were given NaCl (8% in diet + 1% in drinking water) and different oral doses of *S. guttatum* crude extract (100 mg/kg/day, 150 mg/kg/day and 300 mg/kg/day) once daily for 8 weeks. Groups 6-8 (standard treated group) were given oral daily doses of verapamil (5 mg/kg/day, 10 mg/kg and 15 mg/kg/day) along with a NaCl diet containing 8% NaCl + 1% NaCl in drinking water for 8 weeks.[25-27]

Invasive blood pressure recording in HSHR

The tracheal intubation of anesthetized (pentothal, 40–100 mg/kg, i.p) SD rats were performed using polyethylene tubing (PE-20). To monitor blood pressure, the right carotid artery was canulated using polyethylene tubing (PE-50) and affixed to a PowerLab Data Acquisition System (ADInstrument, Australia), through a pressure transducer (MLT 0699). An overhead lamp was used to maintain the animal's body temperature. Mean arterial pressure was monitored for 30 minutes in each group.[25,28]

Body weight profile

Body weight was determined at the beginning of the experiment in all groups and subsequently monitored weekly. After 8 weeks of treatment, the change in body weight was calculated.

In vitro studies

Vascular reactivity studies

To investigate the crude extract-induced endothelium preservation effect in HSHR, we isolated aortae from the normotensive, hypertensive and treated groups. Aortic rings were hanged in tissue baths (10 mL), containing carbogen (5% CO_2 and 95% O_2) aerated normal Kreb's solution consisting of NaCl, 118.2 mM; KCl, 4.7 mM; $MgSO_4$, 1.2 mM; KH_2PO_4, 1.3 mM; $NaHCO_3$, 25.0 mM; Glucose, 11.7 mM; $CaCl_2$, 2.5 mM, and kept at 37°C. The force was monitored by the PowerLab Data Acquisition System (ADInstrument, Australia) and a bridge amplifier (N12128) using a force displacement transducer (MLT 0201). Aortic rings were stabilized at 2 g isometric tension for 60-90 minutes by changing the Kreb's solution every 15 minutes. To determine the endothelial integrity, different concentrations of acetylcholine were used on phenylephrine (1 μM) pre-constricted aortic rings.[25,28]

Isolated SD rat aortic preparations

Aortic rings were hanged in tissue baths filled with 10 mL of carbogen (5% CO_2 and 95% O_2) aerated normal Kreb's solution maintained at 37°C, affixed to a PowerLab Data Acquisition System (ADInstrument, Australia) and a bridge amplifier (N12128) using a force displacement transducer (MLT 0201). The rings were equilibrated for 60-90 minutes at an isometric tension of 2 g, while the solution was changed after every 15 minutes. Different concentrations (0.1–10 mg/mL) of *S. guttatum* were added to PE preconstricted rings. To determine the underlying mechanism, aortic rings were pre-treated with 1 μM atropine or 10 μM $_L$-NAME for 30 minutes. In some experiments, endothelium-denuded rings from normotensive rats were used.[25,28,29]

Isolated right atrial preparations

The right atria from normotensive SD rats were dissected. The atrial preparations were hanged in tissue baths containing 10 mL of aerated Kreb's solution, maintained at 32°C, linked to PowerLab (ML 846) Data Acquisition System (ADInstrument, Australia) and bridge amplifier (N12128) via force transducer (MLT 0201). The tissues were stabilized at the resting tension of 1 g for 30 minutes. The muscarinic receptor involvement was studied in atropine (1 μM) pre-treated atrial preparations.[25,28]

Statistical analysis

Data were normally distributed, as determined by the Shapiro-Wilk's test of normality. Data were expressed as mean ± standard deviation (SD) and the median effective concentrations (EC_{50} values) with the 95% confidence interval (CI). The % of change in MAP or body weight profiles were calculated by one-way analysis of variance (ANOVA) (followed by *post-hoc* Tukey HSD test). The % of vasorelaxation in normotensive and hypertensive rats were calculated by two-way ANOVA (followed by *post-hoc* Bonferroni test) using SPSS software, v. 21 (USA). The accepted level of statistical significance was set at 5%.

Results

Phytochemical constituents

Preliminary phytochemical analysis performed on *S. guttatum* corms extract indicated presence of alkaloids, flavonoids, phenols, phytosterols, saponins and tannins.

Pharmacological investigation

In vivo studies

Invasive blood pressure monitoring

The mean arterial pressure (MAP) values measured in different experimental groups are shown in Figures 1 and 2. The MAP of the HSHR group showed a 67.7% elevation in blood pressure as compared to the normotensive control group. This elevation in MAP was reversed by Sg.Cr treatment in a dose-dependent manner ($p < 0.01$) with up to 300 mg/kg concentration, where it reached its maximal MAP lowering effect ($p < 0.001$). The MAP in verapamil-treated rats (5 mg/kg and 10 mg/kg) also decreased in a dose-dependent manner ($p < 0.01$ and $p < 0.001$ respectively) reaching the maximal effect at a 15 mg/kg concentration ($p < 0.001$).

Body weight profile

High salt intake for 8 weeks caused a significant ($p < 0.001$) decrease in body weight in the hypertensive control group (Table.1). The treatment of hypertensive rats with Sauromatum guttatum crude extract (Sg.Cr) prevented significant changes in body weight at all doses, while verapamil-treated animals at 5 mg/kg showed a significant decrease in body weight ($p < 0.05$). Animals in the verapamil-treated groups (both 10 mg/kg and 15 mg/kg) did not show any significant changes in body weight (Table.1).

In vitro studies

In vitro vascular reactivity studies

In aortas isolated from the normotensive group, acetylcholine caused complete relaxation with an EC_{50} value of 0.2 μM (0.1–0.3) (Figure 3). Aortas from hypertensive control rats, on the other hand, displayed only 5.5% acetylcholine-dependent relaxation as shown in Figure 3. *S. guttatum* crude extract treatment at doses of 100 mg/kg and 150 mg/kg partially restored the acetylcholine-induced relaxation to 38.5%, and 45.5%, respectively. However, rings from SD rats treated with 300 mg/kg *S. guttatum* crude extract showed 100% acetylcholine-dependent relaxation with an EC_{50} value of 0.6 μM (0.3–1.0) (Figure 3). Treatment with 5 mg/kg verapamil caused only a negligible relaxation, while treatment with 10 mg/kg induced relaxation up to 16%. Interestingly, the increase in verapamil concentration up to 15 mg/kg did not further increase the acetylcholine-induced relaxation (Figure 3).

In vitro rat aorta studies

Pharmacological studies were performed in normotensive rat aortae to investigate the antihypertensive effect of the *S. guttatum* crude extract. Relaxation induced by the cumulative addition of the crude extract on PE-preconstricted aortic rings showed an EC_{50} value of 0.15 mg/mL (0.10-0.20) (Figure 4). $_L$-NAME (10 μM) pre-treated rings showed relaxation with EC_{50} value of 5.1 mg/mL (3.0-7.1) (Figure 4). *S. guttatum* crude extract failed to induce relaxation in atropine (1 μM) pretreated and endothelial denuded rings. Both atropine pretreatment (1 μM) and endothelium removal decreased the crude extract-induced relaxation by 26% and 14%, respectively (Figure 4). *S. guttatum* crude extract also produced vasorelaxation in aortic rings preconstricted with high K^+ concentration, with an EC_{50} value of 9.03 mg/mL (8.06-10.00). In comparison, verapamil relaxed the high K^+ preconstricted aortas with EC_{50} value of 2.02 μM (1.02-3.02) (Figure 5).

In vitro rat right atrial study

Right atrial strips from normotensive rats were used to investigate chronotropic and inotropic effects of *S. guttatum*. The crude extract showed a dose-dependent decrease in force of contraction and heart rate with an EC_{50} value of 2.99 mg/mL (1.08-4.90) and 1.83 (1.02-2.64), respectively (Figure 6). In atropine pre-treated tissues, the decrease in force of contraction and heart rate was shown to be 29% and 44%, respectively (Figure 6).

Discussion

Traditionally, *S. guttatum* has been used in the management of blood disorders. It contains ample amounts of magnesium and potassium.[11,15] Additionally, it has been reported as an antioxidant, spasmolytic and Ca^{2+} entry blocker agent.[19, 20]

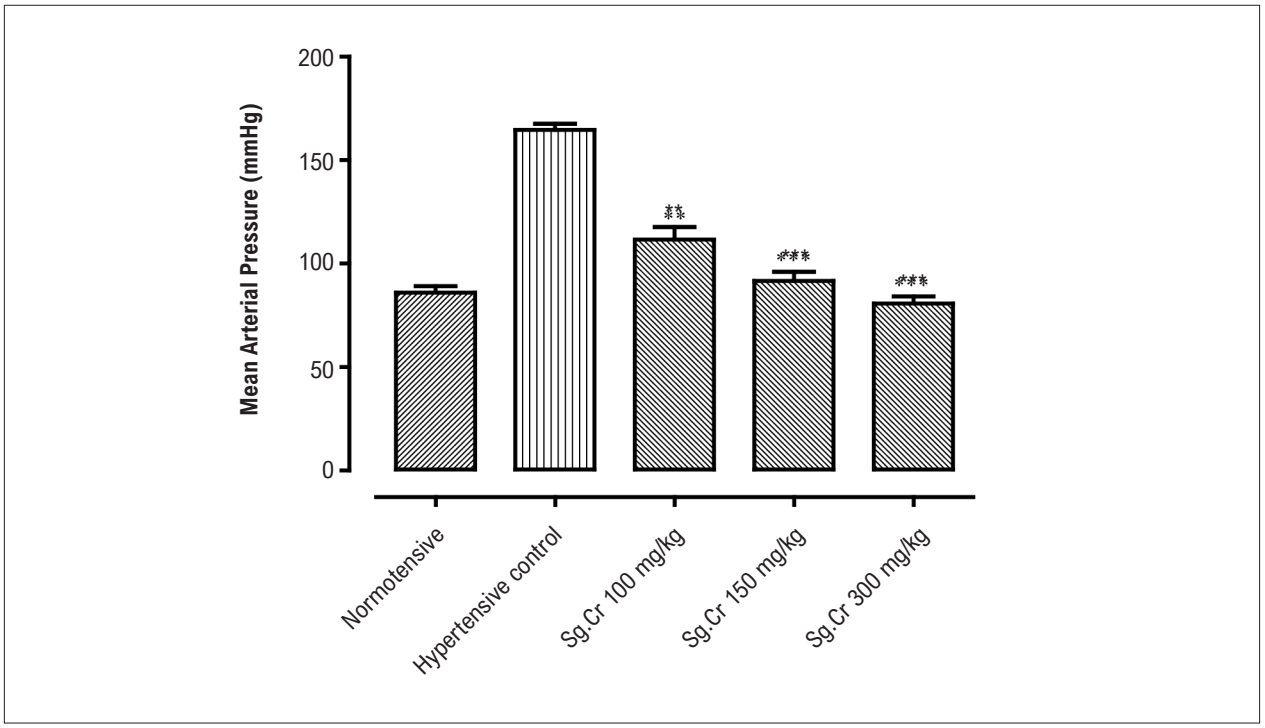

Figure 1 – *Mean arterial pressure in the normotensive, hypertensive and Sauromatum guttatum crude extract (Sg.Cr)-treated high salt-induced hypertensive rats at doses of 100 mg/kg, 150 mg/kg and 300 mg/kg (n=5-7; mean ± SEM). Compared with hypertensive control values, **p < 0.01 and ***p < 0.001*

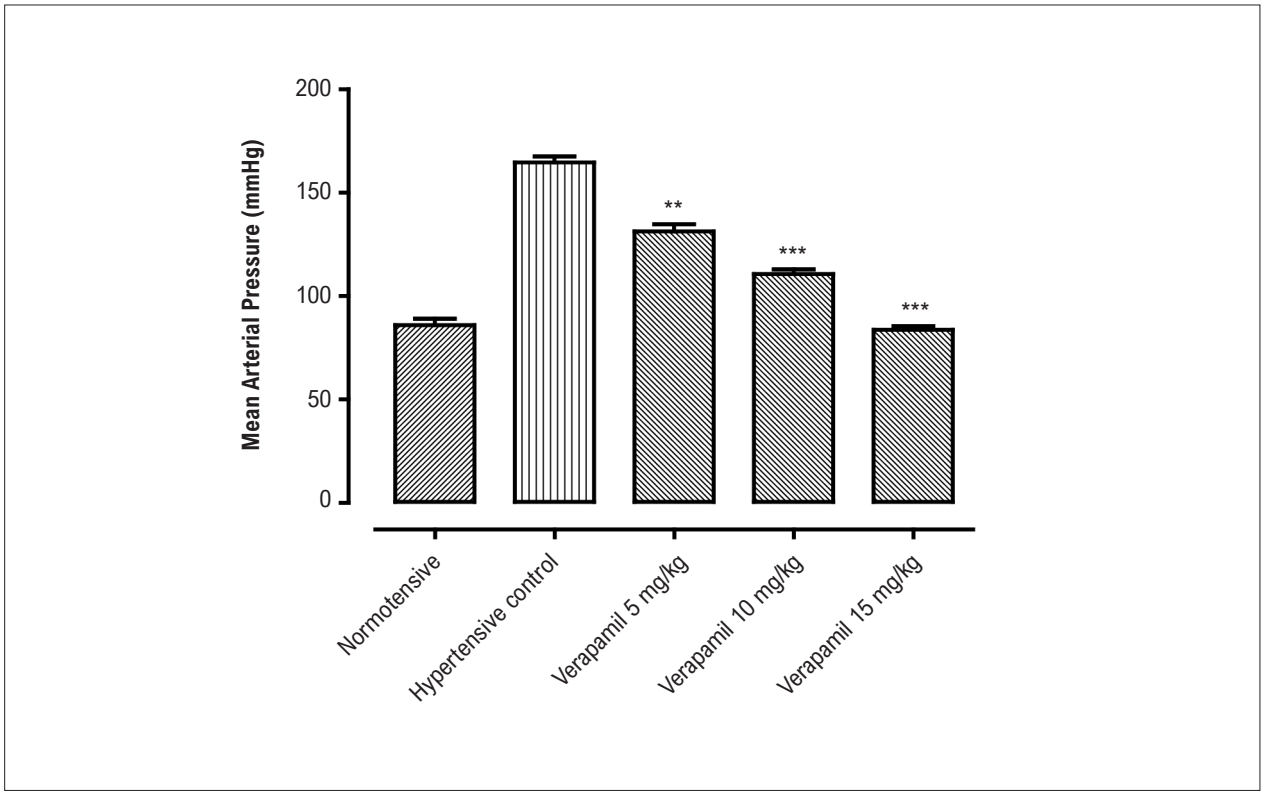

Figure 2 – *Mean arterial pressure in the normotensive, hypertensive and verapamil-treated high salt-induced hypertensive rats at doses of 5 mg/kg, 10 mg/kg and 15 mg/kg) (n=5-7; mean ± SEM). Compared with hypertensive control values, **p < 0.01 and ***p < 0.001*

Plants with antioxidant properties, DASH diet rich in potassium and magnesium and Ca^{2+} entry blockers are recommended for hypertension management.[8,30,31] The present study, using the hypertensive SD rat model, was carried out to explore the use of the crude extract from *S. guttatum* as a potential antihypertensive drug. Different doses of *S. guttatum* crude extracts were given orally to high salt diet-induced hypertensive SD rats. This treatment resulted in a significant decrease in the mean arterial pressure, with a maximum effect observed at the dose of 300 mg/kg. This effect of the crude extract was comparable to that of verapamil, which is a standard antihypertensive drug and calcium channel blocker.[31] This finding revealed that *S. guttatum* extract is effective against the development of high salt diet-induced experimental hypertension. However, further studies were needed to identify the possible underlying action mechanism.

Since blood pressure is the product of elevated peripheral vascular resistance and high cardiac output,[32] further experiments were carried out using isolated vascular and cardiac preparations. First, an attempt was made to establish how high salt intake induces endothelial dysfunction. Endothelial integrity was confirmed by applying sub maximum concentrations of acetylcholine on phenylephrine-preconstricted aortic rings from HSHR. Acetylcholine failed to induce relaxation in aortic rings in the HSHR group, indicating that the endothelium was damaged. This finding is supported by previous studies.[33-35] In aortic rings from normotensive rats, on the other hand, same concentrations of acetylcholine induced relaxation, indicating the presence of a functional endothelium. In the extract-treated groups, the response to acetylcholine was restored. These results indicate that the crude extract treatment can reverse the endothelial damage and also prevent the elevation in mean arterial pressure observed in *in-vivo*. In comparison, verapamil failed to induce vasorelaxation in aortic rings in HSHR control or treated rats, indicating that its action mechanism is different from that of the crude extract. *S. guttatum* extract exerts its antihypertensive function on experimental hypertension by partially preserving the endothelial function.

Further *in vitro* studies were carried out in the aorta to investigate the underlying action mechanism(s). In acetylcholine-preconstricted aortic rings of normotensive rats, the cumulative additions of crude extract concentrations induced vasorelaxation. Endothelial denudation completely reversed this effect, suggesting that vascular endothelial-derived factors might play a role. However, high concentrations of acetylcholine still induced relaxation, suggesting the involvement of different mechanisms. To study the involvement of nitric oxide, aortic rings were pretreated with $_{L}$-NAME, a nitric oxide synthase inhibitor.[36] Interestingly, the vasorelaxant effect of *S. guttatum* extract was reduced by about 75% at 1 mg/mL concentration, while higher concentrations shifted the response curve to the right. These findings suggest that *S. guttatum* induces vasorelaxation through both an endothelium-dependent (at a lower concentration) and endothelium-independent (at a higher concentration) pathways. The endothelium-dependent component could be attributed to nitric oxide. In vascular endothelial cells, nitric oxide release is coupled to muscarinic receptors.[37] To see if the effect of *S. guttatum* crude extract is linked to muscarinic receptors and nitric oxide, aortic rings were precontracted with atropine, a muscarinic receptor antagonist.[37] This pretreatment abolished vasorelaxation associated to the crude extract of *S. guttatum*, thus indicating an action through a muscarinic receptor-linked NO pathway. Atropine or $_{L}$-NAME failed to inhibit relaxation at higher concentrations of the crude extract, further suggesting that the extract might also act on vascular smooth muscles. To test this hypothesis, aortic rings were precontracted with high K^{+} concentration. Interestingly, the cumulative addition of the crude extract induced a vasorelaxant effect that was 10 times less potent than against PE. High K^{+} was used to induce contractions, as it activates voltage-dependent calcium channels (VDCs) and Ca^{2+} release through depolarization, resulting in vasoconstriction.[38,39] These findings indicate that the crude extract of *S. guttatum* also inhibit Ca^{2+} entry through VDCs. It also suggests that vascular NO plays a dominant role in the vasorelaxant and antihypertensive effects of *S. guttatum,* in addition to the effect on vascular smooth muscles.

To investigate the effect of *S. guttatum* extract on cardiac parameters, isolated rat atrial strips were used. *S. guttatum*

Table 1 – Effect on body weight in normal control, hypertensive control and rats treated with different doses of the crude extract of Sauromatum guttatum (Sg.Cr) and verapamil. Values are expressed as mean ± SD (n=5-7)

Groups	Weight (g)	Weight (g) after 8 weeks
Normal control	244.66 ± 6.36	267.61 ± 3.08
Hypertensive group	249.28 ± 3.25	182.10 ± 5.09***
Sg.Cr 100 mg/kg treated	241.66 ± 3.81	245.01 ± 4.66
Sg.Cr 150 mg/kg treated	245.93 ± 6.43	250.90 ± 3.53
Sg.Cr 300 mg/kg treated	239.43 ± 1.48	248.63 ± 4.52
Verapamil 5 mg/kg treated	240.50 ± 1.41	214.23 ± 3.53*
Verapamil 10 mg/kg treated	242.25 ± 5.65	247.68 ± 2.96
Verapamil 15 mg/kg treated	245.83 ± 6.36	254.48 ± 3.32

*Sg.Cr: Crude extract of Sauromatum guttatum. Values are expressed as mean ± SD (n=5-7). *p < 0.05, **p < 0.01 and ***p < 0.001 vs. pretreatment values (One-way ANOVA analysis followed by Tukey HSD post-hoc test).*

Original Article

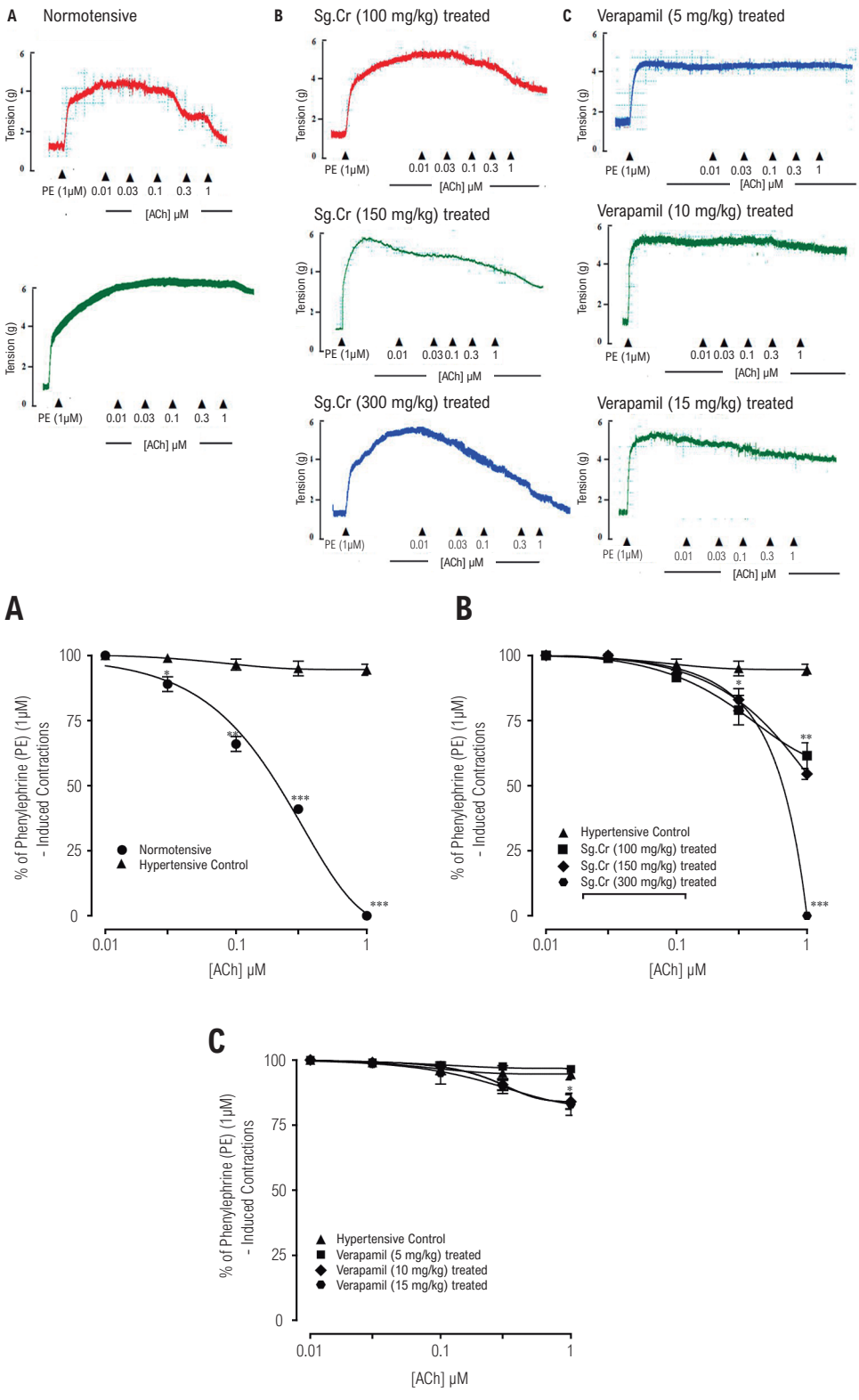

Figure 3 – *Typical tracings and graphs show the effect of acetylcholine (ACh) against phenylephrine-induced contractions in isolated rat aortic rings in normotensive, hypertensive control (A) and Sauromatum guttatum crude extract (Sg.Cr) treated high salt-induced hypertensive rats at doses of 100 mg/kg, 150 mg/kg and 300 mg/kg (B) and verapamil treated high salt-induced hypertensive rats at doses of 5 mg/kg, 10 mg/kg and 15 mg/kg (C) (n=5-7; mean ± SD). Compared with hypertensive control values, *p < 0.05, **p < 0.01 and ***p < 0.001.*

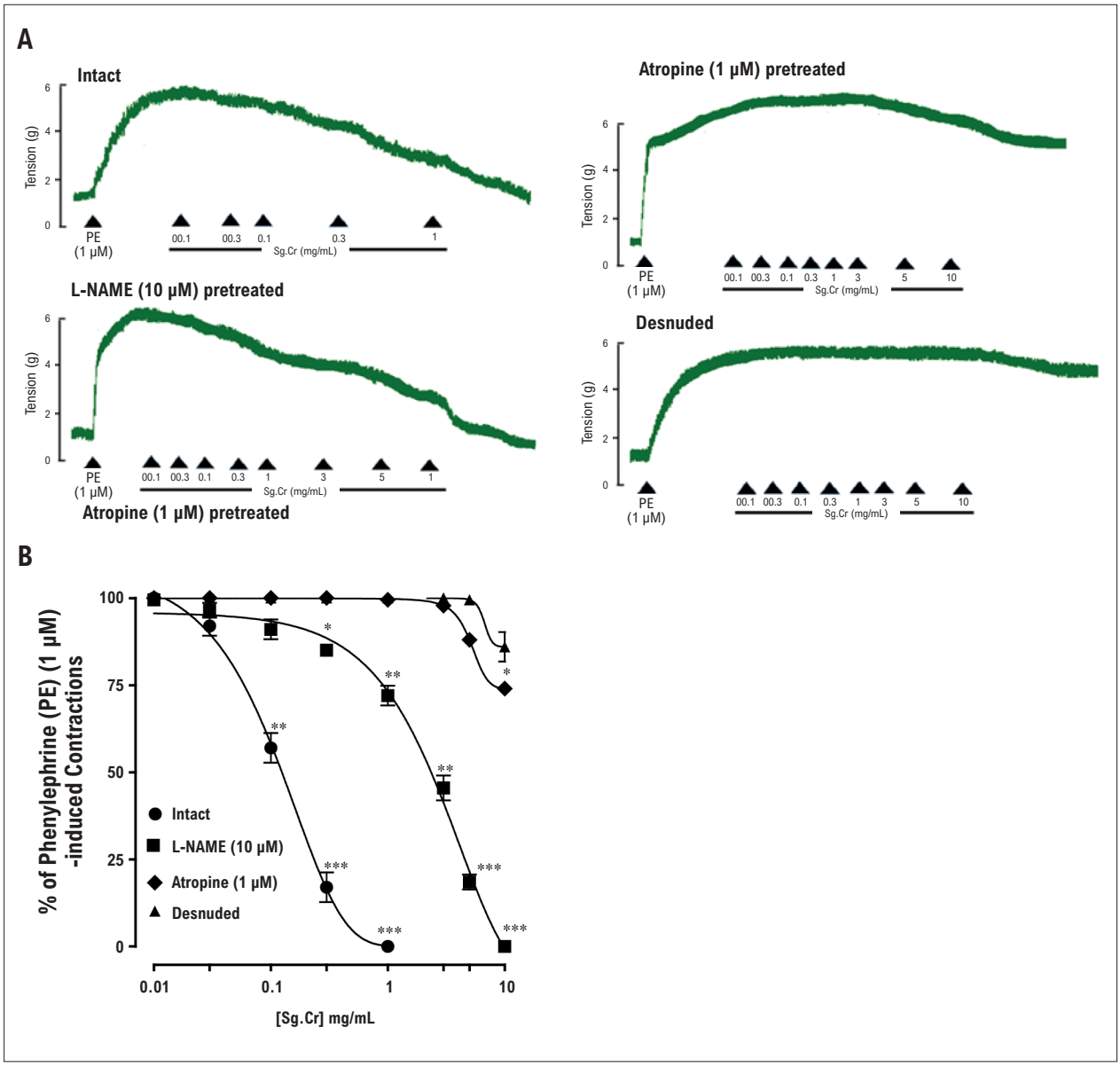

Figure 4 – *Tracing (A) and graph (B) show the effect of Sauromatum guttatum crude extract on intact, L-NAME (10 µM) and atropine (1µM) pretreated and endothelium denuded normotensive rat aorta against phenylephrine-induced contractions (n=5-7; mean ± SD). *p < 0.05, **p < 0.01 and ***p < 0.001 vs Control (pretreated values). Two-way ANOVA analysis followed by Bonferroni's post-hoc test.*

showed negative inotropic (82%) and chronotropic (56%) effects when added cumulatively to spontaneously contracting right atrial strips. To test the possible role of cardiac muscarinic receptors, atrial strips were pretreated with atropine. This pretreatment partially inhibited the effect of the crude extract of *S. guttatum*, thus indicating a possibility that the observed negative inotropic or chronotropic effect is due to cardiac muscarinic receptor activation. However, our findings revealed that the extract is more selective for the vascular than cardiac muscarinic receptors.

S. guttatum was also tested for the presence of phytochemical constituents. It was found to contain flavonoids, phenols, and tannins. Previous studies revealed the therapeutic effect of flavonoids, phenols and tannins on hypertension.[40-42] So, these constituents might be the active agents responsible for lowering blood pressure and the vascular effects in high salt-induced hypertension. Future phytochemical studies will be focused on isolating the active components and exploring the underlying mechanisms, such as calcium blocking and nitric oxide pathway at the molecular level.

Conclusion

These findings indicate that *S. guttatum* has antihypertensive activity resulting from the vasodilatory and atrial myocardium depressant effects linked to muscarinic receptors. Endothelial function preservation, muscarinic receptor dependent NO

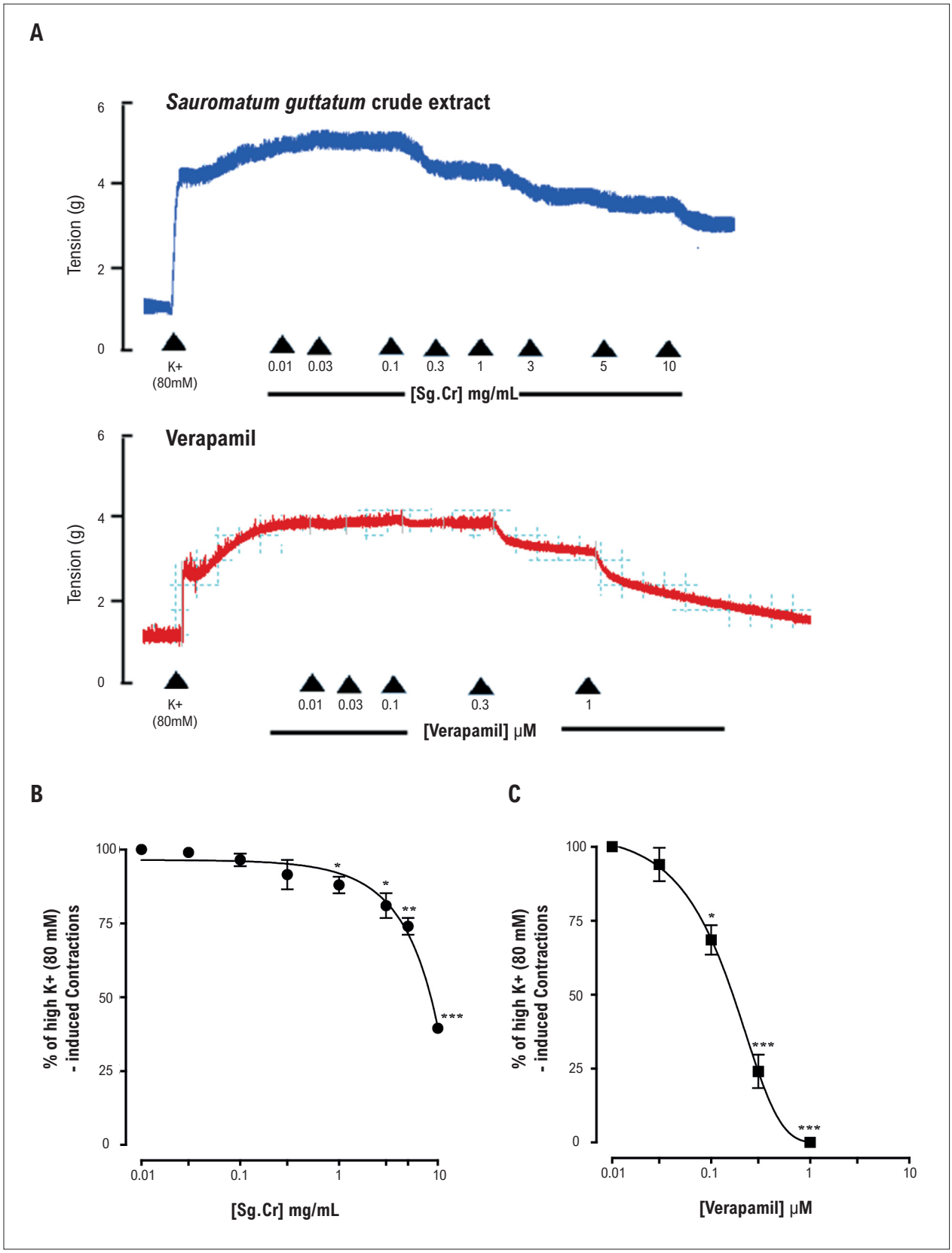

Figure 5 – *Tracing (A) and graph (B, C) show the effect of Sauromatum guttatum crude extract on high potassium (K+) (80 mM)-induced contractions in intact rat aortic preparation (n=5-7; mean ± SD). *p < 0.05, **p < 0.01 and ***p < 0.001 vs. Control (pretreated values). Two-way ANOVA analysis followed by Bonferroni's post-hoc test*

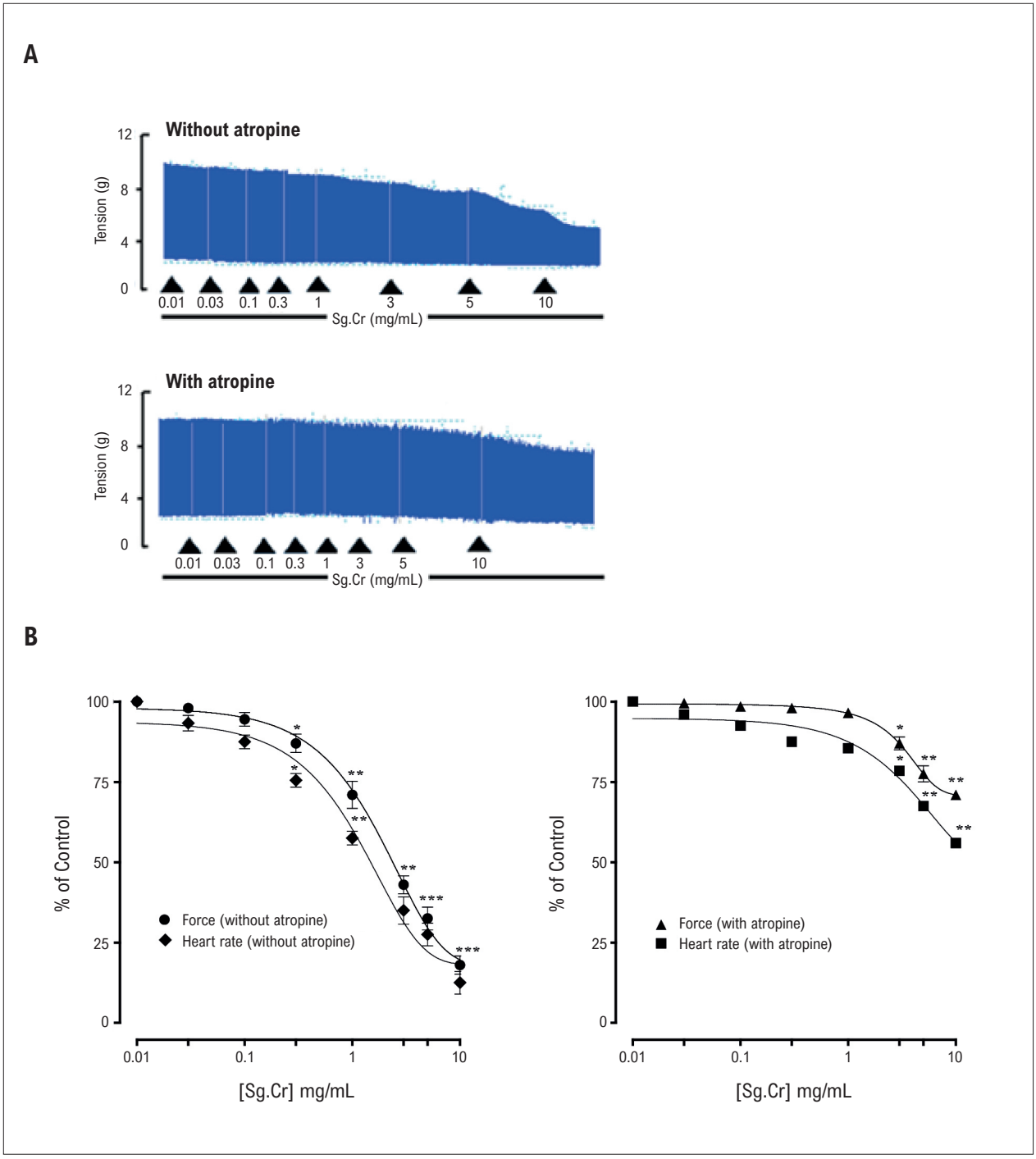

Figure 6 – *Tracing (A) and graph (B, C) show the inotropic and chronotropic effects of Sauromatum guttatum crude extract without and with atropine (1 µM) pre-treated normotensive rat right atria (n=5-7; mean ± SD). *p < 0.05, **p < 0.01 and ***p < 0.001 vs. control (pretreated values). Two-way ANOVA analysis followed by Bonferroni's post-hoc test.*

release and Ca^{+2} movement inhibition are the underlying mechanisms of vasodilation. *S. guttatum* also exerts negative inotropic and chronotropic effects, possibly due to activation of cardiac muscarinic receptors. Our results observed in the SD rat model provide pharmacological explanation for *S. guttatum* antihypertensive potential.

Acknowledgements

The manuscript was reviewed for the English language by Tamas Kriska, PhD, Department of Pharmacology and Toxicology, Medical College of Wisconsin, Watertown Plank Road 8701, WI, USA. The authors would like to thank Tamas Kriska, PhD (tkriska@mcw.edu) for his assistance.

Author Contributions

Conception and design of the research and Obtaining financing: Bibi R, Shah AJ; Acquisition of data, Analysis and interpretation of the data and Writing of the manuscript: Bibi R, Salma U, Bashir K, Khan T, Shah AJ; Statistical analysis: Bibi R, Salma U, Shah AJ; Critical revision of the manuscript for intellectual content: Bibi R, Salma U, Shah AJ.

Potential Conflict of Interest

No potential conflict of interest relevant to this article was reported.

Sources of Funding

There were no external funding sources for this study.

Study Association

This article is part of the thesis of master submitted by Bibi Rabia, from COMSATS Institute of Information Technology - Abbottabad Campus.

Ethics approval and consent to participate

This study was approved by the Ethics Committee of the COMSATS University Islamabad, Abbottabad Campus, Pakistan under the protocol number EC/PHM/07-2013/CIIT/ATD. All the procedures in this study were in accordance with the 1975 Helsinki Declaration, updated in 2013.

Erratum

December 2021 Issue, vol. 117(6), pages 1093-1103

In the Original Article "Antihypertensive Activity of Sauromatum guttatum Mediated by Vasorelaxation and Myocardial Depressant Effects", with DOI: https://doi.org/10.36660/abc.20200055, published in the journal Arquivos Brasileiros de Cardiologia, 117(6):1093-1103, in page 1093, correct the author's name Rabia Bibi to Bibi Rabia.

References

1. Chobanian AV, Bakris GL, Black HR, Cushman WC, Green LA, Izzo Jr JL, Jones DW, Materson BJ, Oparil S, Wright Jr JT, Roccella EJ. The seventh report of the joint national committee on prevention, detection, evaluation, and treatment of high blood pressure: the JNC 7 report. Jama. 2003; 289(19):2560-71.
2. Freis ED. The role of salt in hypertension. Blood pressure. 1992; 1(4):196-200.
3. Dahl LK. Possible role of salt intake in the development of essential hypertension. Int J Epidemiol. 2005; 34(5):967-72.
4. Feng W, Dell'Italia LJ, Sanders PW. Novel paradigms of salt and hypertension. Journal of the American Society of Nephrology. 2017; 28(5):1362-9.
5. Carvalho MV, Siqueira LB, Sousa AL, Jardim PC. The influence of hypertension on quality of life.Arq Bras Cardiol. 2013; 100(2):164-74.
6. Pagan LU, Gomes MJ, Okoshi MP. Endothelial function and physical exercise. Arq Bras Cardiol.. 2018; 111(4): 540-1.
7. Gilani AH, Atta-ur-Rahman. Trends in ethnopharmacology. J Ethnopharmacol. 2005; 100(1-2): 43-9.
8. Carey RM, Whelton PK. Prevention, detection, evaluation, and management of high blood pressure in adults: synopsis of the 2017 American College of Cardiology/American Heart Association hypertension guideline. Ann Intern Med. 2018; 168(5): 351-8.
9. Dass S, Mathur M. Herbal drugs: Ethnomedicine to Modern Medicine. Ramawat KG. ISBN: 9783540791164. New York, USA: Springer; 2009.
10. Patale C, Nasare P, Narkhede S. Ethnobotanical studies on the medicinal plants of Darekasa Hill range of Gondia district, Maharashtra, India. Int J Res Plant Sci. 2015; 5: 10-6.
11. Quattrocchi U. CRC World Dictionary of Medicinal and Poisonous Plants. Philadelphia: CRC Press;2016.ISBN: 9780429171482.
12. Smith BN, Meeuse BJ. Production of volatile amines and skatole at anthesis in some arum lily species. Plant Physiol. 1966; 41(2): 343-7.
13. Chen J, Meeuse B. Production of free indole by some aroids. Acta Botanica Neerlandica. 1971; 20(6): 627-35.
14. Borg-Karlson AK, Englund FO, Unelius CR. Dimethyl oligosulphides, major volatiles released from *Sauromatum guttatum* and *Phallus impudicus*. Phytochemistry. 1994; 35(2): 321-3.
15. Khan T, Ahmad M, Khan H, Ahmad W. Standardization of crude extracts derived from selected medicinal plants of Pakistan for elemental composition using SEM-EDX. Asian J Plant Sci. 2006; 5: 211-6.
16. SinghBains J, Singh J, Kamboj SS, Nijjar KK, Agrewala JN, Kumar V, et al. Mitogenic and anti-proliferative activity of a lectin from the tubers of Voodoo lily (Sauromatum venosum). Biochim Biophys Acta (BBA) 2005; 1723(1-3):163-74.
17. Khan T, Ahmad M, Khan R, Khan H, Choudhary MI. Phytotoxic and insecticidal activities of medicinal plants of Pakistan: Studies on *Trichodesma indicum, Aconitum laeve* and *Sauromatum gutatum*. J Chem Soc Pakistan. 2007; 29(3): 260-4.
18. Khan T, Ahmad M, Ahmad W, Saqib QNU, Choudhary MI. Preliminary evaluation of the antispasmodic and lipoxygenase inhibitory effects of some selected medicinal plants. Pharmaceut Biol. 2009; 47(12): 1137-41.
19. Abbasi MA, Shahwar D, Wahab M, Saddiqui MF. Antibacterial and antioxidant activities of an ethnobotanically important plant *Sauromatum venosum* (Ait.) Schott. of District Kotli, Azad Jammu & Kashmir. Pakistan J Botan. 2011; 43(1): 579-85.
20. Shah N, Shah AJ, Ahmed M, Gilani AH. Functional nature of the spasmolytic effect, phytochemical composition and acute toxicity studies on *Sauromatum guttatum*. Bangl J Pharmacol. 2014; 9(2): 203-7.
21. Kaur M, Thakur K, Kamboj SS, Kaur S, Kaur A, Singh J. Assessment of *Sauromatum guttatum* lectin toxicity against *Bactrocera cucurbitae*. J Environ Biol. 2015; 36(6); 1263.

22. Williamson EM, Okpako DT, Evans FJ. Pharmacological Methods in Phytotherapy Research. New York: John Wiley & Sons Ltd; 1996.

23. Edeoga HO, Okwu DE, Mbaebie BO. Phytochemical constituents of some Nigerian medicinal plants. African Journal of Biotechnology. 2005; 4(7): 685-688.

24. National Research Council. Guide for the Care and Use of Laboratory Animals. Washington DC, National Academy Press; 2011.

25. Salma U, Khan T, Shah AJ. Antihypertensive effect of the methanolic extract from *Eruca sativa* Mill., (Brassicaceae) in rats: Muscarinic receptor-linked vasorelaxant and cardiotonic effects. J Ethnopharmacol. 2018; 224: 409-20.

26. Lawler JE, Sanders BJ, Chen YF, Nagahama S, Oparil S. Hypertension produced by a high sodium diet in the borderline hypertensive rat (BHR). Clin Experimental Hypertens. Part A: Theory and Practice. 1987; 9(11):1713-31.

27. Vasdev S, Gill V, Longerich L, Parai S, Gadag V. Salt-induced hypertension in WKY rats: prevention by α-lipoic acid supplementation. Mol Cel Biochem. 2003; 254(1-2):319-26.

28. Qayyum R, Qamar HMUD, Khan S, Salma U, Khan T, Shah AJ. Mechanisms underlying the antihypertensive properties of *Urtica dioica*. Journal of Translational Medicine. 2016; 14(1): 254.

29. Furchgott RF, Zawadaski JV. The obligatory role of endothelial cells in the relaxation of arterial smooth muscle by acetylcholine. Nature. 1980; 299: 373–6.

30. Baradaran A, Nasri H, Rafieian-Kopaei M. Oxidative stress and hypertension: Possibility of hypertension therapy with antioxidants. J Res Med Sci. 2014; 19(4): 358.

31. Godfraind T. Discovery and development of calcium channel blockers. Front in Pharmacol. 2017; 8: 286.

32. Vincent JL. Understanding cardiac output. Crit Care. 2008; 12(4): 174.

33. Luscher TF, Vanhoutte PM, Raij L. Antihypertensive treatment normalizes decreased endothelium-dependent relaxations in rats with salt-induced hypertension. Hypertension. 1987; 9(6):III193.

34. Miyoshi A, Suzuki H, Fujiwara M, Masai M, Iwasaki T. Impairment of endothelial function in salt-sensitive hypertension in humans. Am J Hypertens. 1997; 10(10):1083-90.

35. Banday AA, Muhammad AB, Fazili FR, Lokhandwala M. Mechanisms of oxidative stress-induced increase in salt sensitivity and development of hypertension in Sprague-Dawley rats. Hypertension. 2007; 49(3):664-71.

36. Küng CF, Moreau P, Takase H, Lüscher TF. L-NAME hypertension alters endothelial and smooth muscle function in rat aorta: prevention by trandolapril and verapamil. Hypertension. 1995; 26(5): 744-51.

37. Hammer R, Giachetti A. Muscarinic receptor subtypes: M_1 and M_2 biochemical and functional characterization. Life Scienc. 1982; 31(26): 2991-8.

38. Nishimura K, Ota M, Ito K. Existence of two components in the tonic contraction of rat aorta mediated by α_1-adrenoceptor activation. Br J Pharmacol. 1991; 102(1): 215-21.

39. Godfraind T. EDRF and cyclic GMP control gating of receptor-operated calcium channels in vascular smooth muscle. Eur J Pharmacol. 1986; 126(3): 341-3.

40. Bhargava UC, Westfall BA. The mechanism of blood pressure depression by ellagic acid. Proceeding of the Society for Experimental Biology and Medicine. 1969; 132(2): 754-6.

41. Moline J, Bukharovich IF, Wolff MS, Phillips R. Dietary flavonoids and hypertension: is there a link? Med Hypotheses. 2000; 55(4): 306-9.

42. Godos J, Sinatra D, Blanco I, Mulè S, La Verde M, Marranzano M. Association between dietary phenolic acids and hypertension in a Mediterranean cohort. Nutrients. 2017; 9(10): 1069.

Searching Naturally Occurring Compounds to Treat Hypertension

Diego Santos Souza[1] *and Danilo Roman-Campos*[1]

Laboratório de CardioBiologia, Departamento de Biofísica, Escola Paulista de Medicina, Universidade Federal de São Paulo,[1] *São Paulo, SP – Brazil*

Short editorial related to the article: Antihypertensive Activity of Sauromatum guttatum Mediated by Vasorelaxation and Myocardial Depressant Effects

Cardiovascular diseases (CDs) are the major cause of death worldwide. Impressively, approximately 17.9 million people died from CDs in 2019, representing almost 32% of global deaths. Also, nearly three-quarters of deaths due to CDs occur in low- and middle-income countries, which is a risk factor for Brazilians.[1] There are several underlying mechanisms involved in CDs, and hypertension is a significant contributor. Today, it is thought that about 1.28 billion adults aged 30-79 years have hypertension in the world. Furthermore, it has been estimated that 60–70% of hypertension in adults is attributable to obesity, associated with insulin resistance, dyslipidemia and metabolic syndrome.[2] Also, almost 50% of adults with hypertension are unaware of its condition, and only 20% have hypertension under control.[3]

According to the American College of Cardiology and the American Heart Association,[4] Normal Blood pressure (BP) is considering when Systolic Blood Pressure (SBP) is <120 mm Hg and < 80 mm Hg for diastolic blood pressure (DBP). Elevated BP is considered when SBP is 120-129, and DBP is <80 mg. Stage 1 and 2 hypertension are considering when SBP is 130-139 mm Hg or > 140 mm Hg, respectively, or DBP is 80-89 mm Hg or >90 mm Hg, respectively. These values follow the most recent Brazilian guideline to diagnostic hypertension.[5]

The numbers show us that the search for new compounds to ameliorate hypertension is of great importance to treat patients worldwide. Repurposing therapies is one possibility. For example, a recent pilot study demonstrated that a single dose of infliximab could reduce mean and DBP levels immediately after its infusion, compared to placebo in patients with hypertension. However, not every patient may benefit from this type of therapy.[6]

In this scenario, natural products play an essential part. The implementation of natural products has increased over the last decades. In an in-depth review study that covered all-natural products as sources of new drugs, from 1981 to 2019 approved by the Food and Drug Administration, approximately 1946 new compounds were approved to treat human diseases. In the context of antihypertensive, 82 natural compounds were authorized.[7] However, despite the increasing number of natural compounds authorized, it is still necessary to find new compounds to treat hypertension since patients are not responsive to a given antihypertensive class or do not adhere to the treatment.

Bibi et al.[8] describe a novel crude plant extract from *Sauromatum guttatum* to treat experimental hypertension. In the manuscript, the authors evaluate the potential therapeutic application of the plant extract in the classical animal model of High salt-induced hypertension in rats (DOCA-hypertensive rats). Their study found that hypertensive animals daily treated for eight weeks with *S. guttatum* significantly attenuated Arterial Blood Pressure in a dose-dependent manner. Furthermore, 300 mg/kg of *S. guttatum* had a similar antihypertensive effect as Verapamil 15 mg/kg treated during the same time frame. The use of isolated aortic rings from hypertensive rats favored acetylcholine-dependent relaxation. Importantly, aortic Rings isolated from hypertensive rats orally treated with *S. guttatum* crude extract at 300 mg/kg for 28 days had a similar potency for acetylcholine-dependent relaxant effect against phenylephrine-induced contractions that observed for control. Interestingly, aortic rings isolated from hypertensive animals treated with Verapamil at 15 mg/kg for 28 days showed only modest improvement in the same experimental approach. Apparently, the mechanism involved in the relaxation effect of *S. guttatum* involves activating muscarinic receptors in endothelial cells and stimulating nitric oxide production. Also, the crude extract may interact with the L-type calcium channel found in aortic rings, which may also contribute to the antihypertensive effect observed. Thus, future studies should isolate the main antihypertensive active compound found in *S. guttatum* to uncover its potential further to treat hypertension in additional animal models in vivo.

Despite the growing number of natural products approved as therapeutic agents, considering hypertension, it is still necessary to find new compounds that act at low doses. Also, a natural compound could be helpful for compliance issues and patients who do not respond to a particular class of antihypertensive treatment. As hypertension is a common factor among CDs, natural products can provide a whole new treatment' spectrum for several patients. Thus, we would like to highlight the importance of natural products and perhaps stimulate the search for new (natural) therapeutic agents that act as antihypertensive, providing a scientific basis for its use.

Keywords

Cardiovascular Diseases; Hypertension; Diet;Biological Products; Mortality; Prevention and Control; Sauromatum Gluttatum/ therapeutic use; Rats

Mailing Address: Danilo Roman-Campos •
Rua Botucatu 862, ECB, 2 Andar. Postal Code 04023-062, Departamento de Biofísica, Escola Paulista de Medicina, UNIFESP. Vila Clementino, São Paulo, SP - Brazil
E-mail:drcampos@unifesp.br

DOI: https://doi.org/10.36660/abc.20210869

References

1. World Health Organization. (WHO) [Internet] {Cited in 2021 Jul 23]. Available from: https://www.who.int/news-room/fact-sheets/detail/cardiovascular-diseases-(cvds)
2. Kotchen TA. Obesity-Related Hypertension: Epidemiology, Pathophysiology, and Clinical Management. Am J Hypertens.2010;23(11):1170-8. https://doi.org/10.1038/ajh.2010.172
3. World Heath Organization. (WHO). Internet [Cited in 2021 may12] Available from:/https://www.who.int/news-room/fact-sheets/detail/hypertension
4. Whelton PK, Carey RM, Aronow WS, Casey DE, Collins KJ, Dennison C, et al. 2017 ACC/AHA/AAPA/ABC/ACPM/AGS/APhA/ASH/ASPC/NMA/PCNA Guideline for the prevention, detection, evaluation, and management of high blood pressure in adults external icon. Hypertension. 2018;71(19):e13–115.
5. Barroso WkS, Nadruz W, Bortolotto LA, Mota-Gomes MA, Brandão AA, Feitosa AD, et al. Diretrizes Brasileiras de Hipertensão Arterial – 2020. Arq Bras Cardiol. 2021; 116(3):516-658.
6. Faria AP, Ritter A, Catharina A, Souza D, Naser P, Bertolo M, et al. Resistant Hypertensive Subjects: A Randomized, Double-Blind, PlaceboControlled Pilot Study. Arq Bras Cardiol. 2021;116(3):443-51.
7. Newman DJ, Cragg GM. Natural products as sources of new drugs over the nearly for decades from 01/1981 to 09/2019. J Nat Prod. 2020;83(3):770-83.
8. Bibi R, Salma U, Bashir K, Khan T, Sha AJ. Antihypertensive Activity of Sauromatum guttatum Mediated by Vasorelaxation and Myocardial Depressant Effects. Arq Bras Cardiol. 2021; 117(6):1093-1103.

Effects of Copaiba Oil in Peripheral Markers of Oxidative Stress in a Model of Cor Pulmonale in Rats

Cristina Campos,[1] Patrick Turck,[1] Angela Maria Vicente Tavares,[1] Giana Corssac,[1] Denise Lacerda,[1] Alex Araujo,[1] Susana Llesuy,[2] Adriane Bello Klein[1]

Universidade Federal do Rio Grande do Sul,[1] Porto Alegre, RS – Brazil

Hospital Italiano de Buenos Aires,[2] Buenos Aires – Argentina

Abstract

Background: To date, copaiba oil's systemic effects have never documented in Cor pulmonale induced by monocrotaline.

Objectives: To investigate copaiba oil's effects in peripheral markers of oxidative stress in rats with Cor pulmonale.

Methods: Male Wistar rats (170±20g, n=7/group) were divided into four groups: control (CO), monocrotaline (MCT), copaiba oil (O), and monocrotaline+copaiba oil (MCT-O). MCT (60 mg/kg i.p.) was administered, and after one week, treatment with copaiba oil (400 mg/kg/day-gavage-14 days) was begun. Echocardiography was performed and, later, trunk blood collection was performed for oxidative stress evaluations. Statistical analysis: two-way ANOVA with Student-Newman-Keuls post-hoc test. P values<0.05 were considered significant.

Results: Copaiba oil reduced pulmonary vascular resistance and right ventricle (RV) hypertrophy (Fulton index (mg/mg): MCT-O=0.39±0.03; MCT=0.49±0.01), and improved RV systolic function (RV shortening fraction, %) in the MCT-O group (17.8±8.2) as compared to the MCT group (9.4±3.1; p<0.05). Moreover, in the MCT-O group, reactive oxygen species and carbonyl levels were reduced, and antioxidant parameters were increased in the peripheral blood (p<0.05). Conclusions: Our results suggest that copaiba oil has an interesting systemic antioxidant effect, which is reflected in the improvements in function and RV morphometry in this Cor pulmonale model. Cor pulmonale attenuation promoted by copaiba oil coincided with a reduction in systemic oxidative stress.

Keywords: Cor Pulmonale; Monocrotaline,Rats; Oxidative Stress; Fabaceae; Phytotherapy; Hypertrophy, Right Ventricular; Copaiba Oil

Introduction

The Amazon forest could be considered a natural laboratory, since it has a wide diversity of plants with medicinal properties. The great majority of these plants have not yet been fully studied, as it is the case of copaiba.[1] Copaiba is a large tree that grows abundantly in the northern region of Brazil. Since the 16th century, copaiba oil has been used by the native indigenous people of the country in the treatment of various diseases. These traditional uses have motivated some researchers to study this oil.[2]

According to some reports, copaiba oil presents antioxidant and anti-lipoperoxidative properties.[3,4] The antioxidant properties of copaiba oil could be very useful in the treatment of some cardiovascular diseases associated with oxidative stress. However, only two studies were found in the literature demonstrating the beneficial effects of copaiba oil on cardiovascular diseases, such as pulmonary arterial hypertension (PAH).[5,6]

PAH is a chronic and fatal disease that is associated with progressive increases in pulmonary vascular resistance and pressure. These changes impair the performance of the right ventricle (RV) and result in RV failure, and ultimately death.[7] To study the physiopathological mechanisms involved in RV dysfunction and PAH development, a monocrotaline (MCT) model was used.[8] The active metabolite of MCT causes damage in the pulmonary endothelium, leading to PAH.[9]

The MCT model mimics aspects of human PAH, including *Cor pulmonale,* which is a term used to describe pathological RV hypertrophy induced by lung dysfunction.[10] In fact, multiple studies in animal models and patients implicate oxidative stress in the development of *Cor pulmonale* and PAH.[11-13] Oxidative stress can cause damage to pulmonary endothelial cells,[14] as well as contribute to RV dysfunction and failure.[11] However, no study has explored the impact of PAH on oxidative stress markers in peripheral blood by analyzing copaiba oil's effects. It was reported that oxidative stress measured in the blood of patients with a neurodegenerative disease could represent a reflection of the oxidative brain damage in those patients.[15] In this sense, evaluating peripheral markers of oxidative stress could have clinical applicability, since obtaining a blood sample represents a minimally invasive procedure.[16] This

Mailing Address: Adriane Bello Klein •
Universidade Federal do Rio Grande do Sul - Sarmento Leite, 500. Postal Code 90040-060, Porto Alegre, RS - Brazil
E-mail: belklein@ufrgs.br
Manuscript received August 20, 2020, revised manuscript December 07, 2020, accepted January 27, 2021

DOI: https://doi.org/10.36660/abc.20200929

approach could be useful to cardiopulmonary diseases, such as PAH, in order to monitor the disease's progression, together with the need and efficacy of antioxidant therapy, such as copaiba oil.

Thus, the aim of this study was to investigate whether peripheral markers of oxidative stress reflect the structural and functional changes promoted in RV by PAH and the effects of copaiba oil under these markers.

Methods

Animals, induction of *cor pulmonale*, and groups:

All procedures were approved by the institutional Animal Ethics Committee (protocol number: 31765). In total, 28 male Wistar rats (weighing 170±20g) from the Center for Reproduction and Experimentation of Laboratory Animals (CREAL) of Universidade Federal do Rio Grande do Sul were studied. These were kept at 20-22°C and with a 12:12h dark/light photoperiod. All animals had *ad libitum* access to regular rodent chow and water, and the experiments were conducted in accordance with the Guide for the Care and Use of Laboratory Animals (U.S. Department of Health and Human Services, NIH Publication No. 86-23) and with institutional guidelines.

The number of animals per group was estimated based on previous studies from our research group,[6,7] considering the minimum difference between the groups of two standard deviations, a minimum probability of type I error of 5% (a = 0.05), and a probability of type II error of 20% (b = 0.2). This calculation was performed using the Computer Programs for Epidemiologists (PEPI - Version 4.04x) software.

Animals were divided into four experimental groups (N=7/group): control (CO), copaiba oil (O), monocrotaline (MCT), and monocrotaline+copaiba oil (MCT-O). On the first day, PAH was induced by a single *in bolus* MCT injection (60mg/kg i.p.), as described elsewhere.[10] One week after PAH induction, animals in the O and MCT-O groups received copaiba oil (400mg/kg) by gavage, once a day, for 14 days.[5] This dose corresponds to a volume of 0.63mL/kg of copaiba oil. During this period, animals from the CO and MCT groups received the same volume of water by gavage.

Echocardiographic analysis

The flow through the pulmonary artery and RV contractile function were evaluated by echocardiography after the end of treatment to estimate the effect of copaiba oil on the cardiovascular function. Animals were anesthetized (ketamine, 90mg/kg; xylazine, 20mg/kg, intraperitoneal) and placed in the left lateral decubitus position to obtain cardiac images. An EnVisor Philips system (Andover, MA) was used, with a 12–13MHz transducer, by a trained operator with experience in small animal echocardiography. The RV shortening fraction (RVSF), which estimates RV contractile function, as well as the acceleration time (AT) and the ejection time (ET) of pulmonary artery flow velocity tracings were measured, which estimates pulmonary vascular resistance.[17]

Morphometric analysis

After the end of treatment, rats were killed by decapitation. RV and left ventricle (LV) were harvested for morphometric measurement, and blood was collected from the venous trunk for oxidative stress analysis. RV and LV+septum (S) were weighed to determine cardiac hypertrophy through the Fulton index (RV weight/LV+S weight).[18]

Blood sample preparation:

Systemic antioxidant defenses and total reactive oxygen species (ROS) were evaluated in red blood cells, and carbonyls were measured in plasma. Heparinized blood samples were washed three times in a solution of sodium chloride (9g/L) and centrifuged at 3,000g for 10min. at room temperature. Washed erythrocytes were diluted 1/10 in a solution of acetic acid (1mmol/L) and magnesium sulphate (4mmol/L). The final solution was centrifuged at 4,200g for 20 min. The supernatant was stored in freezers at -80ºC for later oxidative stress measurements.[15]

Protein concentration

Protein concentration was quantified by the method established by Lowry et al.,[19] using bovine albumin as a standard solution at a concentration of 1mg/mL. All oxidative stress results were normalized by the amount of protein.[19]

Determination of total ROS levels

ROS generation was measured by DCFH-DA fluorescence emission (Sigma-Aldrich, USA). Dichlorofluorescein diacetate is a permeable membrane and is rapidly oxidized to the highly fluorescent 2,7-dichlorofluorescein (DCF) in the presence of ROS. The samples were excited at 488 nm and emission was collected with a 525nm long pass filter. ROS was expressed as nmol per milligram of protein.[20]

Carbonyl assay

This technique is based on the reaction of oxidized proteins with 2,4-dinitro-phenyl hydrazine (DNPH). Briefly, these proteins were added to a DNPH 10mmol/L in 2.5mol/L HCl solution for 1 h in the dark at room temperature, with shaking every 15 min. A 20% trichloroacetic acid (w/v) solution was then added to the plasma samples, which were centrifuged (1,000g for 5 min) to collect protein precipitates. Thereafter, the pellet was dissolved with ethanol:ethyl acetate (1:1) (v/v) and incubated for 10 min at 37ºC with 6mol/L guanidine hydrochloride solution. The absorbance was measured in a spectrophotometer at 360nm and results were expressed as nmol DNPH derivatives/mg protein.[21]

Determination of antioxidant enzyme activities:

Superoxide dismutase (SOD) activity was determined by measuring the velocity of oxidized pyrogalol formation, and expressed as units per milligram of protein, according to Marklund.[22] Catalase (CAT) activity was determined by following the decrease in 240nm absorption of hydrogen peroxide. This was expressed as ηmol of hydrogen peroxide reduced per minute per milligram of protein.[23]

Glutathione peroxidase (GPx) activity, expressed as nmol of hydroperoxide reduced per min per mg protein, was measured following NADPH oxidation at 340nm in a reaction medium containing 0.17mmol/L reduced glutathione, 0.2U/mL glutathione reductase, and 0.5mmol/L tert-butyl hydroperoxide.[24]

Total glutathione levels

Total glutathione (GSH) levels were determined as described by Akerboom and Sies,[25] with modifications. GSH was measured in erythrocytes after protein precipitation with 10% trichloroacetic acid. An aliquot of the sample was added to phosphate buffer with 500μmol/L DTNB. Color development, resulting from the reaction between DTNB and the thiols, reached a maximum in 5 min and was stable for more than 30 min. Absorbance was read at 412nm after 10 min. A standard curve of reduced glutathione was used to calculate the GSH levels in the samples.[25]

Statistical Analysis

For statistical analysis, the SigmaPlot software was used. Data are shown as mean±standard deviation. The normality test (Shapiro-Wilks) was performed to determine the data distribution. As our results presented normal distribution, statistical analysis was performed using two-way ANOVA, followed by the Student-Newman-Keuls post-hoc test. Pearson correlation was used to study the association between variables. P values less than 0.05 were considered significant.

Results

Echocardiographic evaluations

A significant decrease was observed in the AT in the MCT group, while it was increased in the O group, as compared to CO. However, copaiba oil recovered this parameter to control levels in the MCT-O group. By contrast, no difference was found among groups in the ET parameter. RVSF, which estimates RV systolic function, decreased in the MCT group, and copaiba oil prevented this change in the MCT-O animals (Table 1).

Morphometric evaluation

The right ventricular hypertrophy index (RV/LV+S weight), shown in Table 1, was significantly increased in the MCT group in comparison to the CO group. This parameter decreased significantly in the animals from the MCT-O group.

Oxidative stress analysis

There was a significant increase in the ROS and carbonyl levels (Figure 1A and 1B, respectively) in the MCT group in comparison with CO. No significant difference was found between the MCT group and the MCT-O, or between the MCT-O and the O group in ROS levels. However, carbonyl levels, which increased in the MCT group, were reduced in MCT-O.

Antioxidant analysis

Antioxidant enzyme activities (SOD, CAT, and GPx), and GSH concentration were significantly lower in the MCT group, when compared to the CO group. Treatment with copaiba oil significantly recovered these parameters in the animals from the MCT-O group (Figure 2A, 2B, 2C, 2D, respectively).

Correlations

A positive correlation ($R=0.688$; $p<0.05$) was observed between total ROS and the RV weight/LV+S weight ratio (Figure 3A), as compared to a negative correlation ($R=0.614$; $p<0.05$) between GSH concentration and the RV weight/LV+S weight ratio (Figure 3B).

Discussion

The main findings of the present study where that copaiba oil modulated MCT-induced *Cor pulmonale*, since it promoted reduction in the pulmonary artery resistance, as well as in RV hypertrophy and dysfunction. In parallel with these changes, it was found that: copaiba oil treatment reversed the systemic oxidative stress increased by MCT, which was observed by enhanced ROS and carbonyl levels, and a reduction in antioxidant defenses.

According to the literature, the elevation in the pulmonary artery resistance is accompanied by RV hypertrophy, which characterizes *Cor pulmonale*.[10] In fact, in this study, a decrease in the acceleration time through pulmonary artery (AT) was observed, which indicates an increase in pulmonary artery resistance and an increase in RV hypertrophy in animals from the MCT group. On the other hand, copaiba oil treatment was able to mitigate these effects. The reduction of resistance in the pulmonary artery, which contributed to an improvement in RV

Table 1 – Echocardiographic and morphometric results

	CO	MCT	O	MCT-O
AT (s)	0.029±0.005	0.018±0.001[a]	0.034±0.001[a]	0.025±0.003[b]
ET (s)	0.099±0.01	0.106±0.007	0.098±0.01	0.11±0.001
RVSF (%)	21.2±2.4	9.4±3.1[a]	18.8±2.4	17.8±8.2[b]
Fulton index (mg/mg)	0.29±0.02	0.49±0.01[a]	0.29±0.01	0.39±0.03[b]

Data are expressed as mean±SD. a P<0.05 vs CO; b P<0.05 vs MCT. CO:control; O: Copaiba oil; MCT: Monocrotaline; MCT-O: Monocrotaline+Oil; AT: acceleration time; ET: ejection time; RV: right ventricle; RVSF: right ventricle shortening fraction. Fulton index: RV weight/LV+Septum weight; N: 7 animals per group.

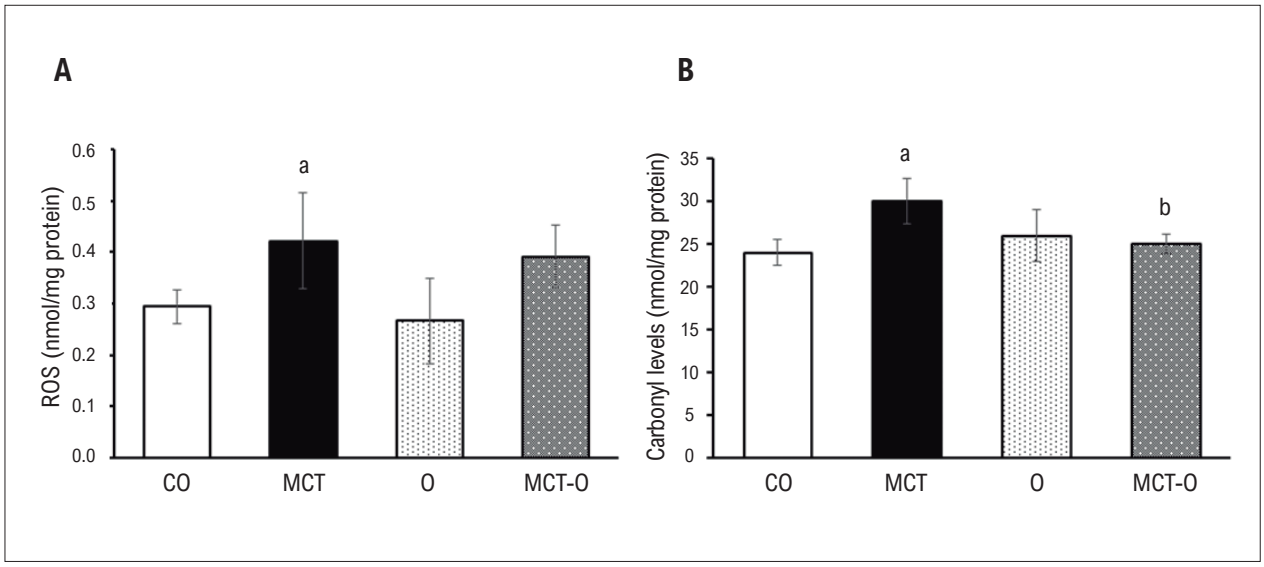

Figure 1 – *Oxidative stress A) Total reactive oxygen species concentration; B) Carbonyl levels. Data are expressed as mean±SD. a P<0.05 vs CO; b P<0.05 vs MCT. Control group: CO; Monocrotaline group: MCT, Copaiba oil group: O, Monocrotaline+Copaiba oil group: MCT-O.*

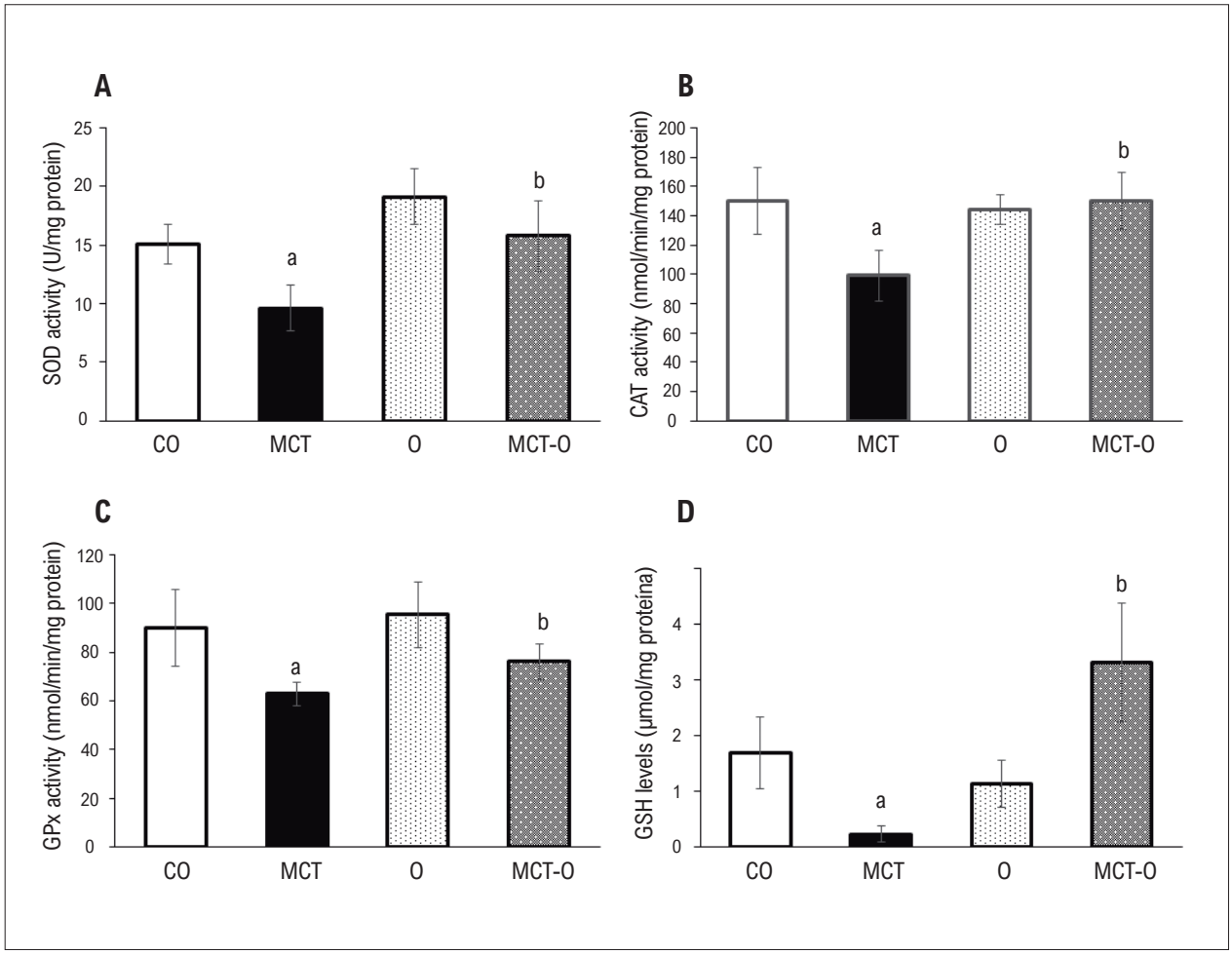

Figure 2 – *Antioxidant measurements. A) Superoxide dismutase activity; B) Catalase activity; C) Glutathione peroxidase activity; D) Total glutathione levels. Data are expressed as mean±SD. a P<0.05 vs CO; b P<0.05 vs MCT. Control group: CO; Monocrotaline group: MCT; Copaiba oil group: O; Monocrotaline+Copaiba oil group: MCT-O.*

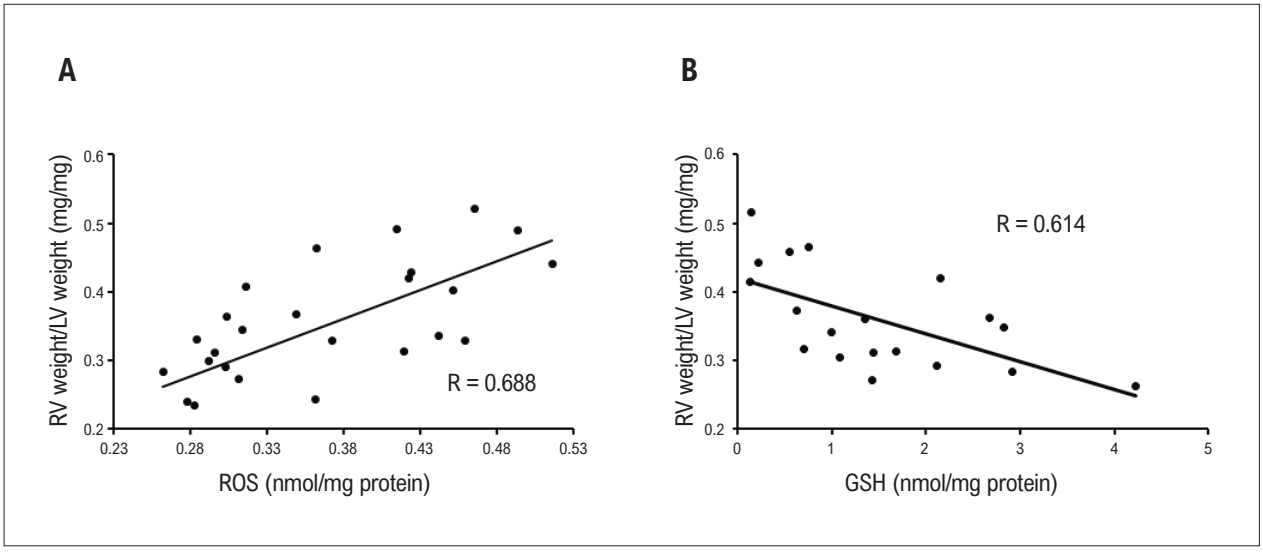

Figure 3 – *Correlations between RV weight/LV+S weight and (A) ROS (p < 0.05); and (B) GSH (p<0.05). RV: right ventricle; LV: left ventricle; ROS: reactive oxygen species; GSH:Total glutathione levels.*

remodeling, could contribute to improving the RV function. Previous investigations in patients with PAH indicate that a RV function impairment is related to adverse clinical outcomes and reduced survival,[26] which highlights the importance of a treatment, such as copaiba oil, which softens this harmful damage in the RV. Moreover, a decrease was found in the RV shortening fraction (RVSF) in the MCT group, which indicates impairment of the RV contractile function. This result is in accordance with others[27,28] that have studied this disease. Conversely, as described in a previous work, copaiba oil was able to increase this parameter, which indicates that this oil could improve the RV function.[6]

According to Jim et al.,[29] there is an increase in systemic ROS production in a rat model of pulmonary hypertension. Moreover, Mohammadi [30] also observed a decrease in the CAT, SOD, GPx activities, and GSH concentration measured in the blood in an MCT-induced PAH. Those data encouraged us to investigate the antioxidant effects of copaiba oil on PAH. Our data have shown that copaiba oil reversed oxidative damage by elevating the systemic antioxidant defenses and reducing carbonyl to levels close to that observed in control rats, suggesting that this oil has enlarged the antioxidant reserve.

In a previous study from our group, copaiba oil composition was evaluated.[5] Chemical analysis of this oil was carried out using gas chromatography – mass spectroscopy. It was found that copaiba oil is composed of terpenes with the predominance of β-caryophyllene. This compound has antioxidant activity, leading to a reduction in ROS due to its free radical-scavenging effect against superoxide anions, hydroxyl anions, and lipid peroxides.[31]

Thus, it is reasonable to believe that the antioxidant effects observed after treatment with copaiba oil are due to the β-caryophyllene present in this oil. On the other hand, the antioxidant effects of copaiba oil may also be due to an interaction between its various components. As reported in a previous study, copaiba oil is composed of a large variety of other sesquiterpenes and diterpenes, which also have antioxidant properties.[5]

Oxidative stress is involved in the development of pathologic cardiac hypertrophy and in a bad prognosis.[32] The reduction in RV hypertrophy found in the present study could be associated with the copaiba oil antioxidant effect. In fact, a positive correlation was found between ROS levels and cardiac hypertrophy in this study. On the other hand, increased levels of GSH, an endogenous non-enzymatic antioxidant, were correlated with lower rates of cardiac hypertrophy. Thus, it is suggested that copaiba oil can protect RV against cardiac hypertrophy through its antioxidant proprieties. This finding is of tremendous importance because, according to Rosca et al., RV hypertrophy is correlated with an increased risk of sudden cardiac death.[33] Since there was an association between systemic oxidative stress and a cardiac morphometric alteration, these markers may be a reflection of the changes in the RV promoted by PAH.

The present study was the first to test the systemic effect of copaiba oil in a *Cor pulmonale* model. Some oxidative stress peripheral markers to detect changes in the systemic redox state were evaluated. Evaluations in the peripheral blood are important and useful because they reflect the organism's general state of health. Blood samples are easily accessible, available in large quantity, and its collection is less invasive than a tissue biopsy, for example. Thus, the evaluation of oxidative stress markers in the blood of patients with PAH could be useful to monitor the development of *Cor pulmonale* and the applied treatment, as performed in the animals used in the present study.

Conclusions

The results obtained suggest that copaiba oil has an interesting systemic antioxidant effect, which is reflected in

the RV morphometric and function improvement in this *Cor pulmonale* model. These results highlight the importance of copaiba oil as a potential adjuvant treatment for PAH.

Author Contributions

Conception and design of the research: Campos C, Llesuy S, Klein AB; Acquisition of data and Analysis and interpretation of the data: Campos C, Turck P, Tavares AMV, Corssac G, Lacerda D; Statistical analysis: Campos C, Araujo A; Obtaining financing: Klein AB; Writing of the manuscript: Campos C, Klein AB; Critical revision of the manuscript for intellectual content: Araujo A, Llesuy S, Klein AB.

Potential Conflict of Interest

No potential conflict of interest relevant to this article was reported.

Sources of Funding

This study was funded by Coordenação de Aperfeiçoamento de Pessoal de Nível Superior (CAPES) and Conselho Nacional de Desenvolvimento Científico e Tecnológico (CNPq).

Study Association

This article is part of the thesis of post doctoral submitted by Cristina Campos, from Universidade Federal do Rio Grande do Sul.

Ethics approval and consent to participate

This study was approved by the Ethics Committee of the Universidade Federal do Rio Grande do Sul under the protocol number 31765. All the procedures in this study were in accordance with the 1975 Helsinki Declaration, updated in 2013.

References

1. Kanis LA, Prophiro JS, Vieira Eda S, Nascimento MP, Zepon KM, Kulkamp-Guerreiro IC, et al. Larvicidal activity of copaifera sp. (leguminosae) oleoresin microcapsules against aedes aegypti (diptera: Culicidae) larvae. Parasitol Res. 2012;110(3):1173-8.
2. Veiga Junior VF, Rosas EC, Carvalho MV, Henriques MG, Pinto AC. Chemical composition and anti-inflammatory activity of copaiba oils from copaifera cearensis huber ex ducke, copaifera reticulata ducke and copaifera multijuga hayne--a comparative study. J Ethnopharmacol. 2007;112(2):248-54.
3. Paiva LA, Gurgel LA, Campos AR, Silveira ER, Rao VS. Attenuation of ischemia/reperfusion-induced intestinal injury by oleo-resin from copaifera langsdorffii in rats. Life Sci. 2004;75(16):1979-87.
4. Silva JJ, Pompeu DG, Ximenes NC, Duarte AS, Gramosa NV, Carvalho KM, et al. Effects of kaurenoic acid and arginine on random skin flap oxidative stress, inflammation, and cytokines in rats. Aesthetic Plast Surg. 2015;39(6):971-7.
5. Campos C, de Castro AL, Tavares AM, Fernandes RO, Ortiz VD, Barboza TE, et al. Effect of free and nanoencapsulated copaiba oil on monocrotaline-induced pulmonary arterial hypertension. J Cardiovasc Pharmacol. 2017;69(2):79-85.
6. Carraro CC, Turck P, Seolin BG, Tavares AM, Lacerda D, Corssac GB, et al. Copaiba oil attenuates right ventricular remodeling by decreasing myocardial apoptotic signaling in monocrotaline-induced rats. J Cardiovasc Pharmacol. 2018;72(5):214-21.
7. Chin KM, Rubin LJ. Pulmonary arterial hypertension. J Am Coll Cardiol. 2008;51(16):1527-38.
8. Hessel MH, Steendijk P, Adel B, Schutte CI, van der Laarse A. Characterization of right ventricular function after monocrotaline-induced pulmonary hypertension in the intact rat. Am J Physiol Heart Circ Physiol. 2006;291(5):H2424-30.
9. Maruyama H, Watanabe S, Kimura T, Liang J, Nagasawa T, Onodera M, et al. Granulocyte colony-stimulating factor prevents progression of monocrotaline-induced pulmonary arterial hypertension in rats. Circ J. 2007;71(1):138-43.
10. Farahmand F, Hill MF, Singal PK. Antioxidant and oxidative stress changes in experimental cor pulmonale. Mol Cell Biochem. 2004;260(1-2):21-9.
11. Lacerda DS, Turck P, Lima-Seolin B, Colombo R, Ortiz V, Bonetto JH, et al. Pterostilbene reduces oxidative stress, prevents hypertrophy and preserves systolic function of right ventricle in cor pulmonale model. Br J Pharmacol. 2017;174(19):3302-14.
12. Fessel JP, West JD. Redox biology in pulmonary arterial hypertension (2013 grover conference series). Pulm Circ. 2015;5(4):599-609.
13. Tabima DM, Frizzell S, Gladwin MT. Reactive oxygen and nitrogen species in pulmonary hypertension. Free Radic Biol Med. 2012;52(9):1970-86.
14. Grobe AC, Wells SM, Benavidez E, Oishi P, Azakie A, Fineman JR, et al. Increased oxidative stress in lambs with increased pulmonary blood flow and pulmonary hypertension: Role of nadph oxidase and endothelial no synthase. Am J Physiol Lung Cell Mol Physiol. 2006;290(6):L1069-77.
15. Repetto MG, Reides CG, Evelson P, Kohan S, de Lustig ES, Llesuy SF. Peripheral markers of oxidative stress in probable alzheimer patients. Eur J Clin Invest. 1999;29(7):643-9.
16. Fois AG, Paliogiannis P, Sotgia S, Mangoni AA, Zinellu E, Pirina P, et al. Evaluation of oxidative stress biomarkers in idiopathic pulmonary fibrosis and therapeutic applications: A systematic review. Respir Res. 2018;19(1):51.
17. Urboniene D, Haber I, Fang YH, Thenappan T, Archer SL. Validation of high-resolution echocardiography and magnetic resonance imaging vs. High-fidelity catheterization in experimental pulmonary hypertension. Am J Physiol Lung Cell Mol Physiol. 2010;299(3):L401-12.
18. Winter RL, Ray Dillon A, Cattley RC, Blagburn BL, Michael Tillson D, Johnson CM, et al. Effect of heartworm disease and heartworm-associated respiratory disease (hard) on the right ventricle of cats. Parasit Vectors. 2017;10(Suppl 2):492.
19. Lowry OH, Rosebrough NJ, Farr AL, Randall RJ. Protein measurement with the folin phenol reagent. J Biol Chem. 1951;193(1):265-75.
20. LeBel CP, Ischiropoulos H, Bondy SC. Evaluation of the probe 2',7'-dichlorofluorescin as an indicator of reactive oxygen species formation and oxidative stress. Chem Res Toxicol. 1992;5(2):227-31.
21. Reznick AZ, Packer L. Oxidative damage to proteins: Spectrophotometric method for carbonyl assay. Methods Enzymol. 1994;233:357-363.
22. Marklund SL. Superoxide dismutase isoenzymes in tissues and plasma from new zealand black mice, nude mice and normal balb/c mice. Mutat Res. 1985;148(1-2):129-34.
23. Boveris A, Chance B. The mitochondrial generation of hydrogen peroxide. General properties and effect of hyperbaric oxygen. Biochem J. 1973;134(3):707-16.
24. Flohe L, Gunzler WA. Assays of glutathione peroxidase. Methods Enzymol. 1984;105:114-21.

25. Akerboom TP, Sies H. Assay of glutathione, glutathione disulfide, and glutathione mixed disulfides in biological samples. Methods Enzymol. 1981;77:373-82.

26. Vanderpool RR, Pinsky MR, Naeije R, Deible C, Kosaraju V, Bunner C, et al. Rv-pulmonary arterial coupling predicts outcome in patients referred for pulmonary hypertension. Heart. 2015;101(1):37-43.

27. Turck P, Lacerda DS, Carraro CC, de Lima-Seolin BG, Teixeira RB, Bonetto JH, et al. Trapidil improves hemodynamic, echocardiographic and redox state parameters of right ventricle in monocrotaline-induced pulmonary arterial hypertension model. Biomed Pharmacother. 2018;103:182-90.

28. Ruiter G, de Man FS, Schalij I, Sairras S, Grunberg K, Westerhof N, et al. Reversibility of the monocrotaline pulmonary hypertension rat model. Eur Respir J. 2013;42(2):553-6.

29. Jin H, Liu M, Zhang X, Pan J, Han J, Wang Y, et al. Grape seed procyanidin extract attenuates hypoxic pulmonary hypertension by inhibiting oxidative stress and pulmonary arterial smooth muscle cells proliferation. J Nutr Biochem. 2016;36:81-8.

30. Mohammadi S, Najafi M, Hamzeiy H, Maleki-Dizaji N, Pezeshkian M, Sadeghi-Bazargani H, et al. Protective effects of methylsulfonylmethane on hemodynamics and oxidative stress in monocrotaline-induced pulmonary hypertensive rats. Adv Pharmacol Sci. 2012;2012:507278.

31. Calleja MA, Vieites JM, Montero-Melendez T, Torres MI, Faus MJ, Gil A, et al. The antioxidant effect of beta-caryophyllene protects rat liver from carbon tetrachloride-induced fibrosis by inhibiting hepatic stellate cell activation. Br J Nutr. 2013;109(3):394-401.

32. Madamanchi NR, Runge MS. Redox signaling in cardiovascular health and disease. Free Radic Biol Med. 2013;61:473-501.

33. Rosca M, Calin A, Beladan CC, Enache R, Mateescu AD, Gurzun MM, et al. Right ventricular remodeling, its correlates, and its clinical impact in hypertrophic cardiomyopathy. J Am Soc Echocardiogr. 2015;28(11):1329-38.

A New Therapeutic Alternative for the Treatment of Pulmonary Hypertension?

Ricardo J Gelpi[1]

Institute of Cardiovascular Physiopathology, Department of Pathology, Faculty of Medicine, University of Buenos Aires,[1] *Buenos Aires - Argentina*

Short Editorial related to the article: Effects of Copaiba Oil in Peripheral Markers of Oxidative Stress in a Model of Cor Pulmonale in Rats

In this issue of the journal *Arquivos Brasileiros de Cardiologia,* important and original research work on rats is published.[1] The work is important because pulmonary hypertension represents a serious pathology that is very difficult to treat. The only way to relieve patients is lung transplantation, but are very well known the difficulties and limitations of this treatment. The work is also original because a lot has been published about the beneficial effects of copaiba oil, such as its anti-inflammatory action, analgesic effect, and ability to prevent infections and improve the healing process. However, the beneficial effect of copaiba oil on pulmonary hypertension had not been described. In this sense, the group led by Adriane Belló Klein has been working for several years on this important issue of pulmonary hypertension in general,[2-4] and the effects of copaiba oil on this particular pathology,[5,6] which has made this research group an international benchmark on this theme.

It is important to mention that pulmonary hypertension induced in rats by monocrotaline produces vascular lesions very similar to those found in patients with this pathology.[7,8] In essence, what the work published in this issue of the journal *Arquivos Brasileiros de Cardiologia*[1] shows is that the administration of copaiba oil to a group of rats with pulmonary hypertension induced by monocrotaline produces a clear beneficial effect, through the decrease in peripheral blood indicators of oxidative stress, a reduction in pulmonary vascular resistance, and a favorable remodeling of the right ventricle, with a reduction in hypertrophy, which translates into a better systolic function of that ventricle. This finding is very important because it is well known that myocardial hypertrophy is one of the most important causes of heart failure and sudden death. The positive relationship between the degree of hypertrophy and the decrease in oxidative stress shown by the authors is clearly proven in this work by the high r-value obtained when these two variables were correlated. However, and beyond this important correlation, future studies should determine if the beneficial effect on the right ventricle is due to the reduction of oxidative stress or if there is also a direct effect of copaiba oil on myocardial fibers. Perhaps experiments that could be carried out on isolated hearts would make it possible to detect or not a direct impact of this natural agent. In this sense, it is important to mention that the authors of this study also published an interesting work previously[5] where they showed that the administration of copaiba oil decreased apoptosis signals in the hypertrophic right ventricle and attributed the better remodeling to a possible decrease in the apoptosis mentioned above; obviously this same mechanism could be acting in the work that we are commenting now. Nevertheless, here it is important to make some clarifications that may allow a better understanding of what is happening in these hearts with hypertrophy secondary to pulmonary hypertension.

In previous work, we have shown[9] that apoptosis that develops during hypertrophy does not correlate with ventricular function. That is, apoptosis is not necessarily responsible for the decrease in ventricular function as has been previously suggested, and in addition, and even more important, cardiac apoptosis is not only of myocytes, but the vast majority is due to nonmyocyte cells, which includes endothelial cells, fibroblasts, or macrophages. Therefore, it could be that the decrease in apoptosis due to copaiba oil in these hearts with hypertrophy secondary to pulmonary hypertension is not mainly in myocardial cells and therefore, this decrease in apoptosis does not affect ventricular function, not being involved in the beneficial effect of copaiba oil. Although variables related to apoptosis were not measured in the present work, the fact that the same authors have suggested in a previous work that this mechanism could have been included in the beneficial effect of copaiba oil, I think, justifies this comment on apoptosis. In other words, we are commenting in this editorial an excellent experimental work, well designed, with clear, important and original results, showing strong experimental evidence of a beneficial effect of copaiba oil in inhibiting oxidative stress. Perhaps in future works, other mechanisms involved could be described, which could include, in addition to the effect of oxidative stress, direct action on the myocardial fiber or a more detailed study of apoptosis.

Keywords

Cor Pulmonale; Hypertension,Pulmonary, Lung Transplantation; Rats; Monocrotaline; Heart Failure; Oxidative Stress; Cardiomegaly, Copaiba Oil; Phytotherapy; Fabaceae

Mailing Address: Ricardo J. Gelpi •
J. E. Uriburu 950, 2nd floor. 1114 Buenos Aires - Argentina
E-mail: rgelpi@fmed.uba.ar

DOI: https://doi.org/10.36660/abc.20210935

References

1. Campos C, Turck P, Tavares AMV, Corssac G, Lacerda D, Araujo A, Llesuy S, Klein AB. Effects of Copaiba Oil in Peripheral Markers of Oxidative Stress in a Model of Cor Pulmonale in Rats. Arq Bras Cardiol. 2021; 117(6):1106-1112.
2. Zimmer A, Teixeira RB, Constantin RL, Fernandes-Piedras TRG, Campos-Carraro C, et al. Thioredoxin system activation is associated with the progression of experimental pulmonary arterial hypertension. Life Sci. 2021 Nov 1; 284:119917.
3. Zancan LR, Bruinsmann FA, Paese K, Türck P, Bahr A, Zimmer A, et al. Oral delivery of ambrisentan-loaded lipid-core nanocapsules as a novel approach for the treatment of pulmonary arterial hypertension. Int J Pharm. 2021 Oct 12; 610:121181.
4. Zimmer A, Teixeira RB, Constantin RL, Campos-Carraro C, Aparicio Cordero EA, Ortiz VD, et al. The progression of pulmonary arterial hypertension induced by monocrotaline is characterized by lung nitrosative and oxidative stress, and impaired pulmonary artery reactivity. Eur J Pharmacol. 2021 Jan 15; 891:173699.
5. Campos-Carraro C, Turck P, de Lima-Seolin BG, Tavares AMV, Dos Santos Lacerda D, Corssac GB, et al. Copaiba Oil Attenuates Right Ventricular Remodeling by Decreasing Myocardial Apoptotic Signaling in Monocrotaline-Induced Rats. J Cardiovasc Pharmacol. 2018 Nov;72(5):214-21.
6. Campos C, de Castro AL, Tavares AM, Fernandes RO, Ortiz VD, Barboza TE, et al. Effect of Free and Nanoencapsulated Copaiba Oil on Monocrotaline-induced Pulmonary Arterial Hypertension. J Cardiovasc Pharmacol. 2017 Feb;69(2):79-85.
7. Gewehr DM, Salgueiro GR, Noronha L, Kubrusly FB, Kubrusly LF, Coltro GA,et al. Plexiform Lesions in an Experimental Model of Monocrotalin-Induced Pulmonary Arterial Hypertension. Arq Bras Cardiol. 2020;115(3):480-90.
8. Calderaro D, Alves Junior JL, Fernandes CJCDS, Souza R. Pulmonary Hypertension in General Cardiology Practice. Arq Bras Cardiol. 2019;113(3):419-28.
9. Gelpi RJ, Park M, Gao S, Dhar S, Vatner DE, Vatner SF. Apoptosis in severe, compensated pressure overload predominates in nonmyocytes and is related to the hypertrophy but not function. Am J Physiol Heart Circ Physiol. 2011;300(3):H1062-8.

Physiology or Angiography-Guided Coronary Artery Bypass Grafting: A Meta-Analysis

José Martins,[1] Vera Afreixo,[2] Luís Santos,[1] Luís Fernandes,[3] Ana Briosa[1]

Baixo Vouga Hospital Centre,[1] Aveiro - Portugal

CIDMA/IBIMED/Department of Mathematics, University of Aveiro,[2] Aveiro - Portugal

Centre for Health Economics, University of York,[3] York - United Kingdom

Abstract

Background: While invasive coronary angiography is considered the gold standard for the diagnosis of coronary artery disease (CAD) involving the epicardial coronary vessels, coronary physiology-guided revascularization represents a contemporary gold-standard practice for the invasive management of patients with intermediate CAD. Nevertheless, the long-term results of assessing the severity of stenosis through physiology compared to the angiogram as the guide to bypass surgery – coronary artery bypass grafting (CABG) are still uncertain. This meta-analysis aims to assess the clinical outcomes of a physiology guided CABG compared to the angiography-guided CABG.

Objectives: We sought to determine if outcomes differ between a physiology guided CABG compared to an angiography-guided CABG.

Methods: We searched Medline, EMBASE, and the Cochrane Library. The last date for this search was June 2020, and all of the previous studies were included. We conducted a pooled risk-ratio meta-analysis for four main outcomes: all-cause death, myocardial infarction (MI), target vessel revascularization (TVR) and major adverse cardiovascular events (MACE). P-value <0.05 was considered as statistically significant. Heterogeneity was assessed with Cochran's Q test and quantified by the I^2 index.

Results: We identified five studies that included a total of 1,114 patients. A pooled meta-analysis showed no significant difference between a physiology guided strategy and an angiography-guided strategy in MI (risk ratio [RR] = 0.72; 95%CI, 0.39–1.33; I2 = 0%; p = 0.65), TVR (RR = 1.25; 95%CI = 0.73–2.13; I2 = 0%; p = 0.52), or MACE (RR = 0.81; 95%CI = 0.62–1.07; I2 = 0%; p = 1). The physiology guided strategy has 0.63 times the risk of all-cause death compared to the angiography-guided strategy (RR = 0.63; 95%CI = 0.42–0.96; I2 = 0%; p = 0.55).

Conclusion: This meta-analysis demonstrated a reduction in all-cause death when a physiology guided CABG strategy was used. Nevertheless, the short follow-up period, small sample size of the included studies and the non-discrimination of the causes of death can largely justify these conclusions. Studies with an extended follow-up period of observation are required to draw more robust and definitive conclusions.

Keywords: Coronary Artery Disease; Angiography; Metanalysis; Coronary Artery/physiology; Coronary Angiography; Coronary Artery Bypass.

Introduction

Invasive coronary angiography is considered as the *gold standard* for the diagnosis of coronary artery disease (CAD) involving the epicardial coronary vessels.[1] Nevertheless, visual assessment by traditional coronary angiography is unable to distinguish if a coronary stenosis is hemodynamically significant, particularly in intermediate CAD, so there are often discordances between the angiographic severity and the physiological significance of CAD.[2,3] Discrepancies occur because, unlike angiography, physiology incorporates the combined and inter-related effects of coronary flow and microvascular resistance.[3]

There is growing evidence supporting the clinical benefit and cost-effectiveness of coronary physiology guided percutaneous revascularization, either by indices based on hyperemia or indices based on pressure difference during a specific period in diastole, compared to percutaneous revascularization based on coronary angiography.[4-7] However, the long-term results of assessing the severity of stenosis through physiology compared to the angiogram as the guide to bypass surgery are still uncertain.

Cardiac surgeons are, in the light of the results, progressively guiding multivessel disease (MVD) revascularization based on coronary physiology. However, whether this decision entails better long-term clinical

Mailing Address: José Martins •
Baixo Vouga Hospital Centre - Avenida Ravara, 3814-501, Aveiro - Portugal
E-mail: zeluismartins@gmail.com
Manuscript received July 11, 2020, revised manuscript October 11, 2020, accepted December 04, 2020

DOI: https://doi.org/10.36660/abc.20200763

outcomes or not is still unclear. Recommendations on the use of CABG compared with medical therapy or percutaneous coronary intervention (PCI) are entirely based on studies that used anatomical and non-functional criteria to guide revascularization.[8-12]

Given this data, several authors have already evaluated the potential clinical benefit of physiology guided coronary bypass surgery in addition to anatomic detail for surgical decisions.[13-20] In this article, we extend the work of Spadaccio et al.[20] by pooling all results from randomized and non-randomized studies to assess the effect on clinical outcomes between a physiology guided CABG compared to angiography-guided CABG. [20]

Methods

Data sources and searches

We systematically searched Medline, Embase, and the Cochrane Library for relevant published articles. The last date for this search was June 2020, and all of the previous studies were included in the search. Previous qualitative and systematic reviews, if available, were checked for additional studies. The following query term was used: "Coronary physiology" or "Fractional Flow Reserve" or "FFR" or "Instant Wave-Free Ratio" or "iFR" or "Coronary Artery Bypass Graft" or "CABG". Further studies were sought by means of a manual search of secondary sources, including references from primary articles. No language restrictions were enforced.

Study selection

Citations were first screened at the title/abstract level by two independent reviewers (JM and LS), and complete manuscripts were retrieved if potentially pertinent. Disagreements were resolved after consensus. The identified articles were independently appraised by the same reviewers according to the following inclusion criteria: articles with clinical outcomes comparing the two strategies for CABG revascularization (physiology vs angiography). Disputes regarding the inclusion criteria were resolved by consensus. Studies comparing the two strategies that did not report clinical outcomes were excluded. Studies that, despite the evaluation of clinical outcomes, did not report the strategy used in detail, were also excluded (Figure 1).

Endpoints

The studied endpoints were: all-cause death, myocardial infarction (MI), target vessel revascularization (TVR) and major adverse cardiovascular events (MACE) during the follow-up period.

MACE was defined as a composite of death, myocardial infarction, or any revascularization by Moscona et al.,[16] Fournier et al.[18] and as composite of death, myocardial infarction, stroke, or any revascularization in the FARGO, FUTURE and GRAFFITI studies during the follow-up period.[13-19]

Statistical analysis

To calculate the pooled effect estimates, we used the inverse variance assuming a fixed-effect model and the DerSimonian and Laird method assuming a random-effect model.[21] Homogeneity among the studies was evaluated using the Cochran's Q test and the I2 statistic (the values of 0.25, 0.50, and 0.75 indicated low, moderate, and high levels of heterogeneity, respectively). *P*-value <0.05 was considered

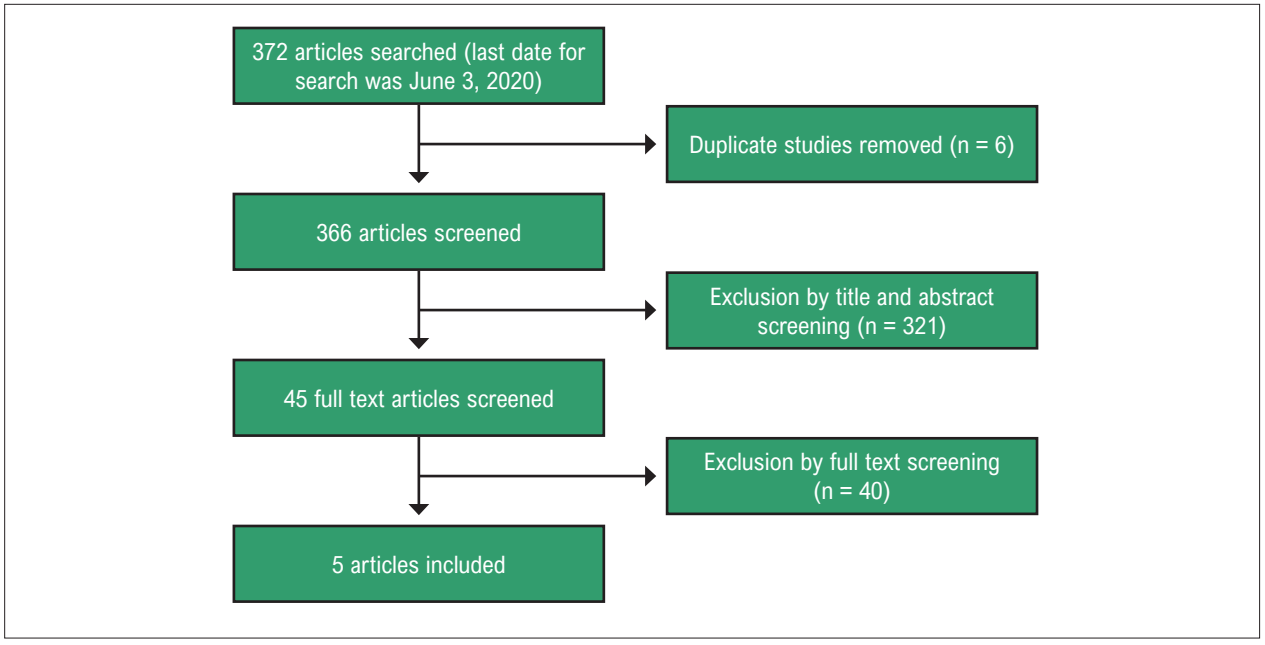

Figure 1 – *Flow chart of studies included in the meta-analysis.*

statistically significant. Publication bias was evaluated using the funnel plot. We performed a sensitivity analysis to show the impact of each study on the results. MetaXL 2.0 (EpiGear International Pty Ltd, Wilston, Queensland, Australia) was used to calculate the pooled risk difference effect size (difference between the risk between revascularization and conservative management groups).

Results

Study identification

Database searches initially retrieved 372 citations. Of these, 6 duplicate studies and 321 articles were excluded after the review of the title or abstract. After a thorough assessment according to the selection criteria, we further excluded 40 studies. A final total of five studies were included in the analysis. These five studies included 1,114 patients: 403 in the physiology guided group and 711 the angiography-guided group.

Characteristics of the included studies

Of the five included studies, three were randomized and two were non-randomized, observational, and retrospective in design (Tables 1 and 2).

Quantitative synthesis of outcomes

All-cause death. All-cause death was reported in five studies, which we considered for pooled analysis, for a total of 1,114 patients. The physiology guided strategy has 0.63 times the risk of all-cause death compared to the angiography-guided strategy (RR = 0.63; 95%CI = 0.42–0.96). Figure 2 describes the weighted meta-analysis for all-cause death. The pooled analysis showed negligible heterogeneity among the studies (I2 = 0%; p = 0.55). Under a sensitivity analysis, by recalculating the pooled results of the primary analysis by excluding each single study in turn, in the study by Fournier et al. this risk difference disappears. This effect also disappeared when we limited the analysis to Randomized Controlled Trials (RCTs) (RR = 1.09; 95%CI = 0.28–4.3). Figure 3 describes the weighted meta-analysis for all-cause death when only RCTs were included.

Myocardial infarction. To analyze the occurrence of MI, four studies that included a total of 1,093 patients were pooled. No significant difference was noted between the two strategies (RR = 0.72; 95%CI = 0.39–1.33) and there was no significant heterogeneity among the studies (I2 = 0%; p = 0.65). The exclusion of any single study and the non-RCTs did not alter the overall combined result.

Target vessel revascularization. To analyze TVR, four studies that included a total of 1,093 patients were pooled. No significant difference was noted between the two strategies (RR = 1.25; 95%CI = 0.73–2.13) and there was no significant heterogeneity among the studies (I2 = 0%; p = 0.55). The exclusion of any single study and the non-RCTs did not alter the overall combined result.

MACE. To analyze MACE, five studies that included a total of 1,114 patients were pooled. No significant difference was noted between the two strategies (RR = 0.81; 95%CI = 0.62–1.07) and there was no significant heterogeneity among the studies (I2 = 0%; p = 1). The exclusion of any single study and the non-RCTs did not alter the overall combined result.

Study Bias

The visual inspection of the funnel plot for the outcomes did not reveal any asymmetry among the studies (Figure 4). Further, the Begg's rank correlation test was not statistically significant.

Discussion

Survival has a significant negative correlation with the burden of angiographic obstructive CAD. The SYNTAX score stratifies the angiographic complexity of coronary artery disease and establishes the prognosis of patients with MVD, being an important tool to decide on the best revascularization strategy.[22,23]

There are often discordances between the severity of angiography and the physiological significance of CAD, so the functional SYNTAX score, which is obtained by counting only ischemia-provoking lesions, can overcome this limitation. Compared with the classic SYNTAX score, the functional SYNTAX score has better reproducibility and prognostic value, reclassifying up to 32% of CABG candidates, with implications in terms of the therapeutic guidance that this entails.[22-24]

Whether or not the favorable impact of coronary physiology on PCI outcomes could be translated to surgical practice became the subject of our investigation.

Our meta-analysis showed a 37% reduction in all-cause death in the group guided by physiology, with a non-statistically significant reduction in MI and MACE; these outcomes were not associated with an increase in TVR. These results must be interpreted within the limitations intrinsic to each of the studies, including selection bias, since this reduction disappears when only RCTs have been pooled for analysis.

When clinical outcomes in revascularization are evaluated, important considerations must be addressed. The first consideration to take into account is related to the (peri) procedural outcomes. The type of MI must be clearly established when comparing strategies, as it is now universally accepted that the prognosis of spontaneous MI is not similar to peri-procedural MI or type 2 MI.[25,26]

The natural history of the disease is another important point to consider as a new paradigm focusing on the disease itself (atherosclerosis), rand not on the symptom (ischemia). [25,27] The composition of the plaque, evaluated by certain imaging features, seems to be the main determinant of prognosis, more than the level of coronary stenosis or its location.[28-30] This may explain the better prognosis associated with complete revascularization in the context of acute coronary syndrome, in which plaques in non-culprit lesions appear to have unstable characteristics, in contrast to what is found in stable coronary disease.[31]

The third important consideration is the type of revascularization. The well-defined benefits of CABG compared with angiography-guided PCI as reported in the ASCERT, SYNTAX, FREEDOM and BEST trials used anatomical and non-functional criteria to guide revascularization and are prior to the newer generation drug-eluting stent technology.[8-12]

Table 1 – Characteristics of the included studies

Author	Year	N total	N Strategy	FU	Study design	Conduits	Graft patency FU	Major clinical conclusions
Moscona et al.[16]	2018	109	FFR/iFR-guided: 14 Angiography-guided: 95	18 months	Retrospective	Arterial conduits: 92.9% (FFR-group; 90.5% Angiography-group) SVG: 85.7% (FFR-group;76.8% Angiography-group)	NR	A trend toward reduction in MACE (7.1% *vs.* 11.6%, P=0.369) and angina (0.0% *vs.* 6.3%, P=0.429) in the FFR/iFR group compared to the angiography group
Thuesen et al.[14]	2018	97	FFR-guided: 49 Angiography-guided: 48	Six months	RCT	Arterial conduits: 37%	Graft failures of all grafts were similar in both groups (16% vs. 12%; p = 0.97).	Rates of death, MI, and stroke were similar in the study groups. All-cause mortality at six months was 0% in the FFR-guided group and 4.1% in the angiography-guided group; one patient died because of pulmonary embolism, and one died because of mediastinitis
Rioufol et al.[17]	2018	109	FFR-guided: 55 Angiography-guided: 54	One year	RCT	NR	NR	FFR in all-comer multivessel-disease patients did not demonstrate any improvement in the primary composite endpoint composite of all-cause mortality, MI, repeat revascularization, or stroke through one year (14.6% vs 14.4%; HR 0.97; 95%CI 0.69-1.36) Risk of death was significantly higher in the FFR-guided arm (3.7% vs 1.5%; *P* = 0.036)
Fournier et al.[15]	2019	627	FFR-guided: 198 Angiography-guided: 429	Six years	Retrospective	Arterial conduits: 64% SVG: 36%	The occlusion rate was significantly lower with FFR-guided as compared with angiography-guided grafts	FFR-guided CABG is associated with a significant reduction in the rate of overall death or myocardial infarction (HR 0.59 [95% CI, 0.38–0.93]; *P*=0.020)
Toth et al.[19]	2019	172	FFR-guided: 88 Angiography-guided: 84	One year	RCT	NR Arterial conduits-to-SVG ratio: 1:1	No difference in overall graft patency (80% vs 81%) p=0.885)	No difference in the composite of death, myocardial infarction, target vessel revascularization and stroke (HR 1.275; 95% CI: 0.391 to 4.160, *p*=0.674)

FU: follow-up; FFR: Fractional flow reserve; iFR: instant wave-free ratio; N: patients included in the study; MI: myocardial infarction; TVR: target vessel revascularization; NR: not reported; RCT: randomized controlled trial; SVG: saphenous vein graft; CABG: coronary artery bypass grafting. A value of p < 0.05 was considered significant in all included studies.

Table 2 – Characteristics of the included studies

Author	Year	N total	N Strategy	Death	MI	TVR	MACE
Moscona et al.[16]	2018	109	FFR/iFR-guided: 14 Angiography-guided: 95	FFR/iFR: 1 Angiography: 5	FFR/iFR: 0 Angiography: 2	FFR/iFR: 0 Angiography: 4	FFR/iFR: 1 Angiography: 11
Thuesen et al.[14]	2018	97	FFR-guided: 49 Angiography-guided: 48	FFR: 0 Angiography: 2	FFR: 1 Angiography: 0	FFR: 2 Angiography: 0	FFR: 6 Angiography: 6
Rioufol et al.[17]	2018	109	FFR-guided: 55 Angiography-guided: 54	FFR: 1 Angiography: 0	NR	NR	HR 0.845 (0.108-6.612)
Fournier et al.[15]	2019	627	FFR-guided: 198 Angiography-guided: 429	FFR: 21 Angiography: 79	FFR: 11 Angiography: 34	FFR: 17 Angiography: 27	FFR: 42 Angiography: 113
Toth et al.[19]	2019	172	FFR-guided: 88 Angiography-guided: 84	FFR: 3 Angiography: 2	FFR: 0 Angiography: 2	FFR: 2 Angiography: 4	FFR: 5 Angiography: 6

MI: myocardial infarction; TVR: target vessel revascularization.

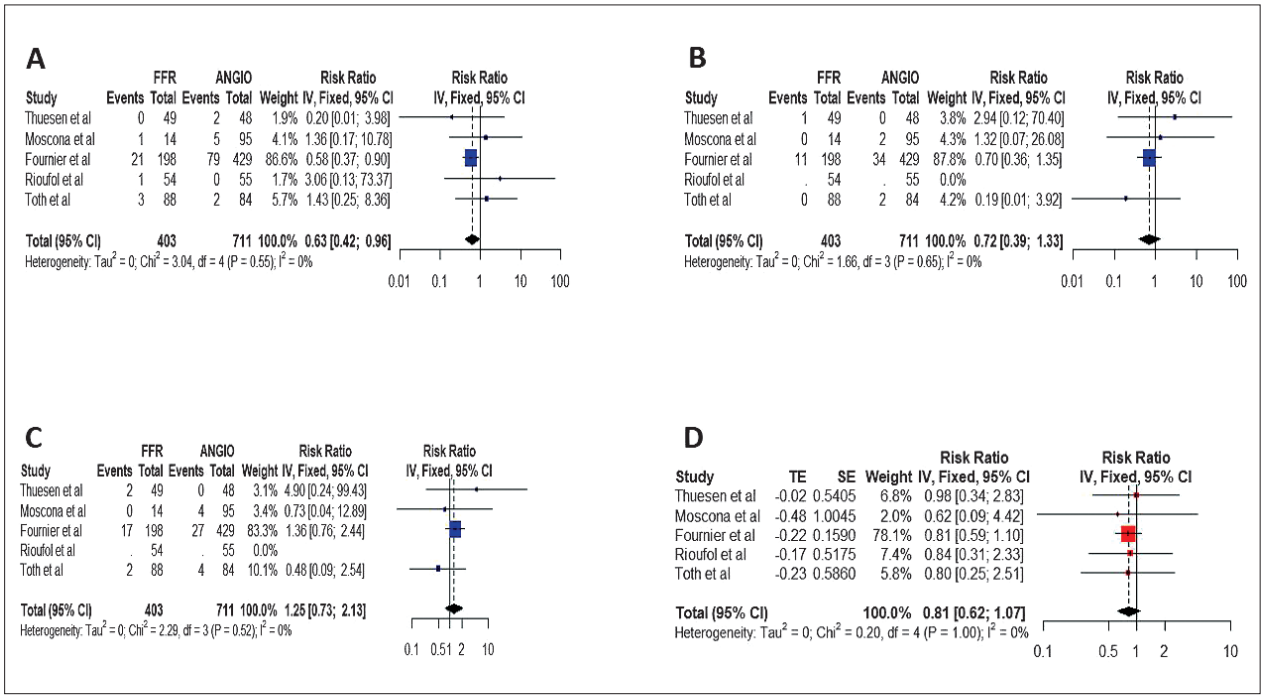

Figure 2 – *Forest plot of the pooled risk ratio for the outcomes: (A) all cause death; (B) MI; (C) TVR; (D) MACE. The sizes of data markers indicate the weight of the study. CI: confidence interval; MI: myocardial infarction; TVR: target vessel revascularization.*

An important difference between CABG and PCI depends on the protective effects of atherosclerotic disease progression. It is known that most stenoses related to MI are located in the proximal third of the coronary tree. We also know that most MIs arise from non-significant plaques. Surgical bypass grafts are usually implanted distally in the coronary circulation, providing "a collateralization effect" on revascularization, and it seems conceivable that the prognostic benefit of CABG can be explained by protection against coronary events, regardless of the severity of the stenosis of the grafted vessel. The concept of revascularization based on physiology, and not on the type of plaque, eliminates the protective effect of the surgical bypass.[28-30,32]

The concept of complete revascularization arose from the early studies on CABG, whereas some publications demonstrated that patients who were completely revascularized experienced a mortality benefit over those who were incompletely revascularized, thus setting the standard for the field of CABG.[33-35]

The revascularization based on physiology also raises the concept of complete anatomical vs. functional revascularization. If, on the one hand, the use of coronary physiology reduces the

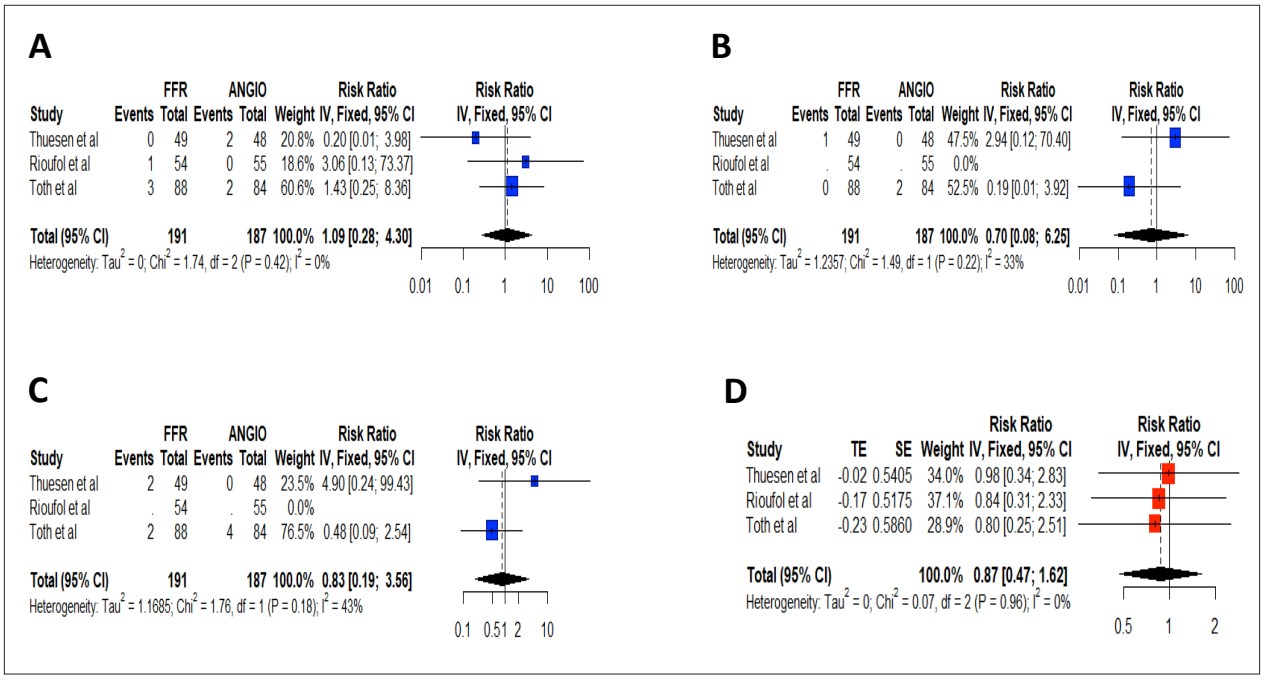

Figure 3 – *Forest plot of the pooled risk ratio for the outcomes when only RCTs were included: (A) all-cause death; (B) MI; (C) TVR; (D) MACE. The sizes of data markers indicate the weight of the study. CI: confidence interval; MI: myocardial infarction; TVR: target vessel revascularization.*

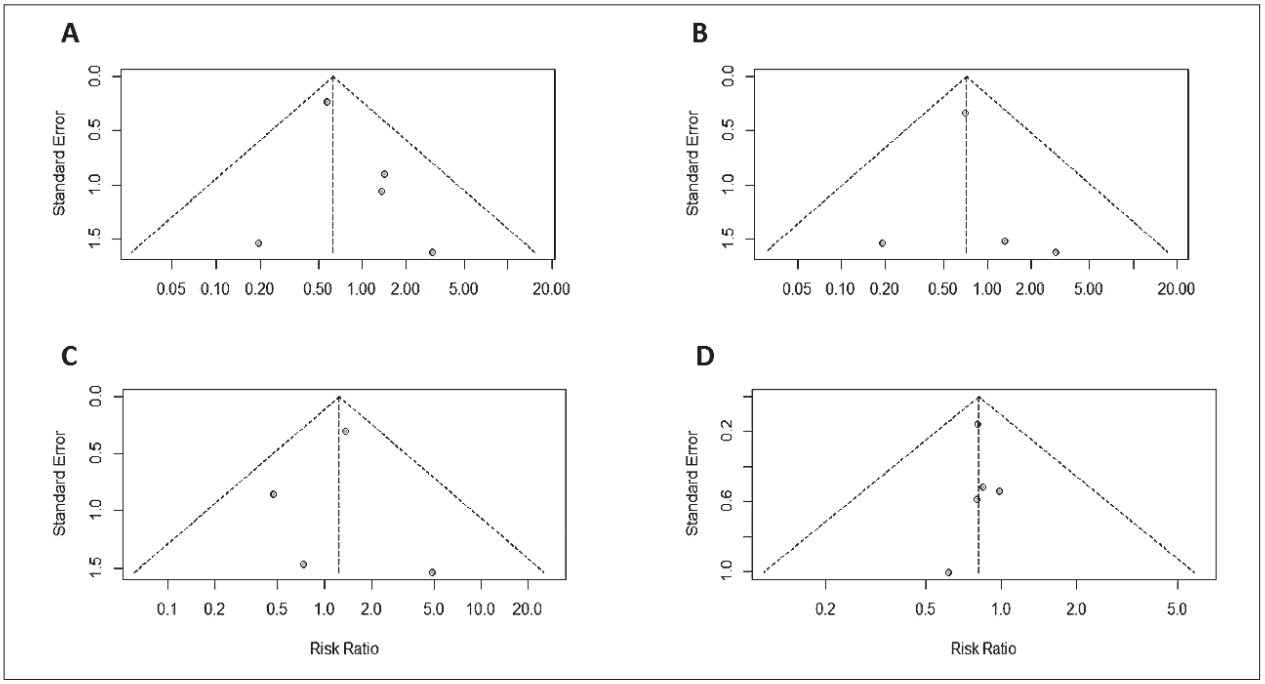

Figure 4 – *Publication bias for: (A) all-cause death; (B) MI; (C) TVR; (D) MACE. Circles represent individual studies of the meta-analysis and the vertical line represents the pooled estimate of the Risk Ratio for all cause death, MI, TVR and MACE. MI: myocardial infarction; TVR: target vessel revascularization.*

number of grafted vessels, or even surgery, without extracorporeal circulation, on the other hand, it increases the rate of anatomically defined incomplete revascularization.[19]

The use of physiology guided revascularization has been shown to reduce the MACE rate in patients with MVD, with the FFR 0.78 cut-off point showing a significant association between the preoperative FFR measurement of the target vessel and the anastomotic functionality at six months. These conclusions are also supported by Botman et al.,[36] for whom lesions with FFR> 0.75 are associated with a significant increase in the risk of graft occlusion ($p < 0.0001$).[18,19,36,37]

In light of the differences described in susceptibility to competitive flow, it seems likely that the type of conduit used in the FARGO and GRAFFITI trials (in which a large proportion of grafts were SVGs) versus IMPAG (in which only arterial grafts were used) may explain the contradictory results.[14,19,38]

The FAME 3 study will compare in a multicenter, randomized fashion FFR-guided PCI with contemporary drug-eluting stents to CABG in patients with 3-vessel coronary artery disease. It will not answer, however, the question of physiology guided CABG compared to angiography-guided CABG.[39]

Finally, the role of follow-up in this context would also be interesting to consider. The more severe the coronary stenosis, the higher the risk of MI, but it is the non-significant plaques that are responsible for most MIs. We also know that the main cause of death in these patients with CAD is cardiac-related, and that MI is a cause of cardiac death, so therapies that reduce the MI or cardiovascular death will subsequently decrease mortality.[32]

We should take the STICH trial as an example, comparing treatment with medical therapy plus CABG and medical therapy alone in patients with CAD and heart failure, with reduced ejection fraction. At five years of follow-up, the intention-to-treat analysis demonstrated no significant difference between the two strategies with respect to the primary outcome of all-cause death. However, after the follow-up period was extended to ten years, a significant reduction in mortality was found for CABG plus medical therapy compared to medical therapy alone (HR, 0.84; 95%CI: 0.73-0.97; p=0.02). Another example is the FAME 2 trial, in which the data published at five years show a strong tendency of lower rates of myocardial infarction in the PCI group (HR 0.66; 95%CI 0.43-1.00; p = 0.049), a difference that was only significant for spontaneous MI (HR 0.62; 95%CI; p = 0.04), not periprocedural MI. Recently, the ISCHEMIA trial showed that, in early follow-up, the primary composite outcome (cardiovascular death, MI, or hospitalization for unstable angina or heart failure) was more frequent in the invasive strategy group than in the conservative strategy group (5.3% vs. 3.4% at six months), due to procedure-related MI's. However, in a posterior follow-up, after about two years, the event curves crossed, and at five years, the incidence of the primary outcome was slightly higher in the conservative strategy group (18.2% and 16.4%). So, it seems that in order to have an impact on hard outcomes, like all-cause death, we have to extend the duration of the observation period.[25,40,41]

In our study, the reduction of all-cause death in a context of non-significant reduction of MI and MACE should be interpreted with caution, since this situation could be owed to deaths from non-cardiac causes. It would be interesting not only to assess if these deaths were cardiac-related, but also to extend the follow-up of the studies to observe if the curves of the hard outcomes diverge on longer follow-up periods, allowing to reach definitive conclusions. It should be noted that only the study by Fournier et al.[18] has a follow-up period longer than five years, which can explain the results, since the reduction in the composite endpoint all-cause death or MI supporting a physiology guided strategy was only found when the follow-up was extended.[15]

Limitations

The conclusions drawn from this meta-analysis are subjected to the limitations and differences of the original studies included in the analysis. A limitation of this meta-analysis is the presence of trials with small samples and wide-ranging, long-term survival results. Another limitation is represented by an intrinsic selection bias. Several revascularization decisions in the physiology guided strategy were deviated from the functional indication in the included trials, justified by some authors to be related to technical causes and, in some cases ,the reluctance to defer revascularization. As aforementioned, as the cause of death was not known, this includes non-cardiac deaths unrelated to the choice of revascularization strategy. Another limitation was that with the inclusion of two retrospective and observational studies, some patients included in this registry might have been treated with physiology guided PCI instead of CABG.

Conclusion

This meta-analysis demonstrates a reduction in all-cause death when a physiology guided CABG strategy was used. Nevertheless, the short follow-up period, small sample size of the included studies and the non-discrimination of the causes of death can largely justify these conclusions. Studies with an extended follow-up observation period are required to reach more robust and definitive conclusions.

Author Contributions

Conception and design of the research: Martins J, Santos L; Acquisition of data and Writing of the manuscript: Martins J; Analysis and interpretation of the data and Statistical analysis: Martins J, Afreixo V; Critical revision of the manuscript for intellectual content: Martins J, Santos L, Fernandes L, Briosa A.

Potential Conflict of Interest

No potential conflict of interest relevant to this article was reported.

Sources of Funding

There were no external funding sources for this study.

Study Association

This study is not associated with any thesis or dissertation work.

Ethics approval and consent to participate

This article does not contain any studies with human participants or animals performed by any of the authors.

References

1 Knuuti J, Wijns W, Saraste A, Capodanno D, Barbato E, Funck-Brentano C, et al. 2019 ESC Guidelines for the diagnosis and management of chronic coronary syndromes: The Task Force for the diagnosis and management of chronic coronary syndromes of the European Society of Cardiology (ESC). Eur Heart J. 2020;41(3):407-77.

2. Masdjedi K, Daemen J. Angiography-Based FFR: Reevaluating the Role of the Pressure Wire. Card Interv Today. 2019;13(3):28-33.

3. Morris PD, Curzen N, Gunn JP. Angiography-derived fractional flow reserve: more or less physiology?. J Am Heart Assoc. 2020;9(6):e015586.

4. Neumann FJ, Sousa-Uva M, Ahlsson A, Alfonso F, Banning AP, Benedetto U, et al. 2018 ESC/EACTS guidelines on myocardial revascularization. Eur Heart J. 2019;40(2):87-165.

5. De Bruyne B, Pijls NH, Kalesan B, Barbato E, Tonino PAL, Piroth Z, et al. Fractional flow reserve-guided PCI versus medical therapy in stable coronary disease. N Engl J Med. 2012;367:991-1001.

6. Pijls NH, Schaardenburgh P, Manoharan G, Boersma E, Bech JW, van't Veer M, et al. Percutaneous coronary intervention of functionally nonsignificant stenosis: 5-year follow-up of the DEFER study. J Am Coll Cardiol. 2007;49(21):2105-11.

7. Tonino PA, De Bruyne B, Pijls NH, Siebert U, Ikeno F, van't Veer M, et al. Fractional flow reserve versus angiography for guiding percutaneous coronary intervention. N Engl J Med. 2009;360(3):213-24.

8. Weintraub WS, Grau-Sepulveda MV, Weiss JM, O'Brien SM, Peterson ED, Kolm P, et al. Comparative effectiveness of revascularization strategies. N Engl J Med. 2012;366(16):1467-76.

9. Serruys PW, Morice MC, Kappetein AP, Colombo A, Holmes DR, Mack MJ, et al. Percutaneous coronary intervention versus coronary-artery bypass grafting for severe coronary artery disease. N Engl J Med. 2009;360(10):961-72.

10. Mohr FW, Morice MC, Kappetein AP, Feldman TE, Ståhle E, Colombo A, et al. Coronary artery bypass graft surgery versus percutaneous coronary intervention in patients with three-vessel disease and left main coronary disease: 5-year follow-up of the randomised, clinical SYNTAX trial. Lancet. 2013;381(9867):629-38.

11. Farkouh ME, Domanski M, Sleeper LA, Siami FS, Dangas G, Mack M, et al. Strategies for multivessel revascularization in patients with diabetes. N Engl J Med. 2012;367(25):2375-84.

12. Park SJ, Ahn JM, Kim YH, Park DW, Yun SC, Lee JY, et al. Trial of everolimus-eluting stents or bypass surgery for coronary disease. N Engl J Med. 2015;372(13):1204-12.

13. Toth G, De Bruyne B, Casselman F, De Vroey F, Pyxaras S, Serafino L, et al. Fractional flow reserve-guided versus angiography- guided coronary artery bypass graft surgery. Circulation. 2013;128(13):1405-11.

14. Thuesen AL, Riber LP, Veien KT, Christiansen EH, Jensen SE, Modrau I, et al. Fractional flow reserve versus angiographically-guided coronary artery bypass grafting. J Am Coll Cardiol. 2018;72(22):2732-43.

15. Fournier S, Toth GG, De Bruyne B, Johnson NP, Ciccarelli G, Xaplanteris P, et al. Six-year follow-up of fractional flow reserve-guided versus angiography-guided coronary artery bypass graft surgery. Circ Cardiovasc Interv. 2018;11(6):e006368.

16. Moscona JC, Stencel JD, Milligan G, Salmon C, Maini R, Katigbak P, et al. Physiologic assessment of moderate coronary lesions: a step towards complete revascularization in coronary artery bypass grafting. Ann Transl Med. 2018;6(15):300.

17. Rioufol G. FUTURE trial: Treatment strategy in multivessel coronary disease patients based on fractional flow reserve. Presented at: European Society of Cardiology (ESC) 2018. August 25, 2018. Munich, Germany.

18. Fournier S, Toth GG, Colaiori I, De Bruyne B, Barbato E. Long-term patency of coronary artery bypass grafts after fractional flow reserve-guided implantation. Circ Cardiovasc Interv. 2019;12(5):e007712.

19. Toth GG, De Bruyne B, Kala P, Ribichini FL, Casselman F, Ramos R, et al. Graft patency after FFR-guided versus angiography- guided coronary artery bypass grafting. The GRAFFITI trial. EuroIntervention. 2019;15(11):e999-1005.

20. Spadaccio C, Glineur D, Barbato E, Di Franco A, Oldroyd KG, Biondi-Zoccai G, et al. Fractional Flow Reserve-Based Coronary Artery Bypass Surgery: Current Evidence and Future Directions. JACC Cardiovasc Interv. 2020;13(9):1086-96.

21. DerSimonian R, Laird N. Meta-analysis in clinical trials. Control Clin Trials. 1986;7(3):177-88.

22. Serruys PW, Morice MC, Kappetein AP, Colombo A, Holmes DR, Mack MJ, et al. Percutaneous coronary intervention versus coronary-artery bypass grafting for severe coronary artery disease. N Engl J Med. 2009;360(10):961-72.

23. Thuijs DJFM, Kappetein AP, Serruys PW, Mohr FW, Morice MC, Mack MJ, et al. Percutaneous coronary intervention versus coronary artery bypass grafting in patients with three-vessel or left main coronary artery disease: 10-year follow-up of the multicentre randomised controlled SYNTAX trial. Lancet. 2019;394(10206):1325-34.

24. Serruys PW, Kogame N, Katagiri Y, Modolo R, Buszman PE, Íñiguez-Romo A, et al. Clinical outcomes of state-of-the-art percutaneous coronary revascularisation in patients with three-vessel disease: two-year follow-up of the SYNTAX II study. EuroIntervention. 2019;15(3):e244-52.

25. Maron DJ, Hochman JS, Reynolds HR, Bangalore S, O'Brien SM, Boden WE, et al. Initial Invasive or Conservative Strategy for Stable Coronary Disease. *N Engl J Med*. 2020;382:1395-407.

26. Ben-Yehuda O, Chen S, Redfors B, McAndrew T, Crowley A, Kosmidou J, et al. I Impact of large periprocedural myocardial infarction on mortality after percutaneous coronary intervention and coronary artery bypass grafting for left main disease: an analysis from the EXCEL trial. Eur Heart J. 2019;40(24):1930-41.

27. Lardinois CK. Atherosclerosis - Know your risk -is time for a paradigm shift? US Endocrinol. 2014;10(2):105-10.

28. Jeon C, Candia SC, Wang JC, Holper EM, Ammerer M, Kuntz RE, et al. Relative spatial distributions of coronary artery bypass graft insertion and acute thrombosis: a model for protection from acute myocardial infarction. Am Heart J. 2010;160(1):195-201.

29. Wang JC, Normand SL, Mauri L, Kuntz RE. Coronary artery spatial distribution of acute myocardial infarction occlusions. Circulation. 2004;110(3):278-84.

30. Mushtaq S, Goncalves P, Garcia-Garcia HM, Pontone G, Bartorelli A, Bertella E, et al. Long-term prognostic effect of coronary atherosclerotic burden: validation of the computed tomography-Leaman score. Circ Cardiovasc Imaging. 2015;8(2):e002332.

31. Al-Abdouh A, Barbarawi M, Bizanti A, Abudaya I, Upadhrasta S, Elias H, et al. Complete revascularization in patients with STEMI and multi-vessel disease: A meta-analysis of randomized controlled trials. Cardiovasc Revasc Med. 2020;21(5):684-91.

32. Doenst T, Haverich A, Serruys P, Bonow RO, Kappetein P, Falk V, et al. PCI and CABG for treating stable coronary artery disease: JACC Review Topic of the Week. J Am Coll Cardiol. 2019;73(8):964-76.

33. Buda AJ, Macdonald IL, Anderson MJ, Strauss HD, David TE, Berman ND. Long-term results following coronary bypass operation. Importance of preoperative actors and complete revascularization. J Thorac Cardiovasc Surg. 1981;82(3):383-90.

34. Bell MR, Gersh BJ, Schaff HV, Holmes Jr DR, Fisher LD, Alderman EL, et al. Effect of completeness of revascularization on long-term outcome of patients with three-vessel disease undergoing coronary artery bypass surgery. A report from the Coronary Artery Surgery Study (CASS) Registry. Circulation. 1992;86(2):446-57.

35. Ong AT, Serruys PW. Complete revascularization: coronary artery bypass graft surgery versus percutaneous coronary intervention. Circulation. 2006;114(3):249-55.

36. Botman K, Pijls NH, Bech JW, Aarnoudse W, Peels K, Straten BV, et al. Percutaneous coronary intervention or bypass surgery in multivessel disease? A tailored approach based on coronary pressure measurement. Catheter Cardiovasc Interv. 2004;63(2):184-91.

37. Kern MJ, Seto AH. High FFR strongly predicts arterial graft dysfunction: pure benefit in a pure population? Eur Heart J. 2019;40(29):2429-31.

38. Glineur D, Grau JB, Etienne PY, Benedetto U, Fortier JH, Papadatos S, et al. Impact of preoperative fractional flow reserve on arterial bypass graft anastomotic function: the IMPAG trial. Eur Heart J. 2019;40(29):2421-28.

39. Zimmermann FM, De Bruyne B, Pijls NH, Desai M, Oldroyd KG, Park SJ, et al. Rationale and design of the Fractional Flow Reserve versus Angiography for Multivessel Evaluation (FAME) 3 Trial: a comparison of fractional flow reserve-guided percut aneous coronary intervention and coronary artery bypass graft surgery in patients with multivessel coronary artery disease. Am Heart J. 2015;170(4):619-26.e2.

40. Petrie MC, Jhund PS, She L, Adlbrecht C, Doenst T, Panza JA, et al. Ten-Year Outcomes After Coronary Artery Bypass Grafting According to Age in Patients With Heart Failure and Left Ventricular Systolic Dysfunction: An Analysis of the Extended Follow-Up of the STICH Trial (Surgical Treatment for Ischemic Heart Failure). Circulation. 2016;134(18):1314-24.

41. Xaplanteris P, Fournier S, Pijls NHJ, Fearon WF, Barbato E, Tonino PAL, et al. Five- year outcomes with PCI guided by fractional flow reserve. N Engl J Med. 2018;379(3):250-9.

Physiology-guided CABG: Is it Time for Cardiac Surgeons to Incorporate FFR Into Their Practice?

Tannas Jatene,[1,2] Fabrício Ribeiro Las Casas,[1,2] Rogerio Lobo de Andrade Las Casas,[1,2] Vinicius Daher Vaz,[1,2] Alberto de Almeida Las Casas[1,2]

Hospital do Coração Anis Rassi,[1] Goiânia, GO – Brazil

Hospital Israelita Albert Einstein,[2] Goiânia, GO – Brazil

Short Editorial related to the article: Physiology or Angiography-Guided Coronary Artery Bypass Grafting: A Meta-Analysis

According to most recent international guidelines on myocardial revascularization, fractional flow reserve (FFR)-guided percutaneous coronary intervention should be considered in patients with multivessel disease. That would include evaluation of all lesions between 40 to 90% diameter stenosis before implanting a stent.[1,2] The same guidelines suggest prioritizing completeness of revascularization when the decision is made for coronary artery bypass graft surgery (CABG), which means bypassing all lesions >50% diameter stenosis.[2]

In this issue of *Arquivos Brasileiros de Cardiologia*, Martins et al.,[3] approached this paradox with a meta-analysis of five studies and 1,114 patients, comparing physiology-guided CABG and conventional angiography-guided CABG. Although the pooled meta-analysis showed no difference in myocardial infarction and target vessel revascularization rates, a 37% relative risk reduction in all-cause death was associated with physiology-guided CABG.

Multiple studies over the last two decades revealed improved outcomes and lower cost with the use of FFR-guided angioplasty, with revascularization of only functionally significant lesions.[4-6] In addition, reclassifying patients by adding FFR information to the SYNTAX score improve its correlation with events after revascularization, the so-called functional SYNTAX score.[7] All these robust data have been translated into incorporation of invasive physiology to the toolbox of most cath-labs.

In the operating rooms, however, bypassing angiographic stenosis above 50% diameter is still the standard. The FAME (FFR versus Angiography for Multivessel Evaluation) trial showed that only 35% of the 50-70% diameter stenosis lesions were hemodynamically significant,[8] but surgeons still bypass those lesions with the rationale of preventing possible progression of atherosclerosis. However, it has been demonstrated that bypassing lesions not hemodynamically relevant not only results in early graft failure but also accelerate progression of coronary artery disease in the native vessel.[9-11] Moreover, previous studies revealed the reduction in the number of graft anastomoses and lower rate of on-pump surgery with FFR-guided versus angiography-guided CABG.[12] All these arguments have not been enough to convince surgeons.

The present meta-analysis adds to this controversy. Three randomized controlled trials and two retrospective studies were evaluated together. The reduction in mortality could possibly persuade cardiac surgeons to use FFR in their decision-making process. However, major weakness of the study prevents this turnaround: 1) the small sample sizes and the consequent low number of events in the randomized controlled trials; 2) the study with the highest number of patients had a retrospective design, hence subject to inherent biases; 3) absence of long-term follow-up, when possible benefits of complete revascularization would be more evident; 4) the reduced mortality reported by Martins et al.,[3] is difficult to explain without reduction in myocardial infarction and target vessel revascularization, and would be more convincing if a cardiovascular mortality reduction was revealed.

Although the DEFER trial[4] showed a myocardial infarction incidence of only 2.2% in a group of patients with non-significant lesions on the basis of FFR after a 15-year follow-up and the recent ISCHEMIA trial raised questions about the benefits of any revascularization procedure, "surgical collateralization" and "completeness of revascularization" will be the arguments of cardiac surgeons until we have a large randomized trial with long-term follow-up comparing FFR- versus angiography-guided CABG.

For the time being, the heart team should follow the guidelines and use intracoronary physiology as much as possible before deciding about the necessity of any myocardial revascularization. If the decision is for percutaneous coronary intervention, then FFR or non-hyperemic indices should be used to guide the procedure. If the decision is for CABG, FFR benefit is still to be proved.

Keywords

Coronary Angiography/physiology; Coronary Artery Disease/physiopathology;Coronary Arteryry Bypass;Factional Flow Reserve Myocardial

Mailing Address: Tannas Jatene •
Hospital do Coração Anis Rassi, Av. A, 453 . Postal Code 74110-020, Goiânia, GO - Brazil
E-mail: tjatene@hotmail.com

DOI: https://doi.org/10.36660/abc.20210921

References

1. Feres F, Costa RA, Siqueira D, Costa Jr JR, Chamié D SR et. a. Diretriz Sobre Intervenção Coronária Percutânea. Arq Bras Cardiol. 2017;109(1 Suppl 1):1-81.
2. Neumann FJ, Sousa-Uva M, Ahlsson A, Alfonso F, Banning AP, Benedetto U, et al. 2018 ESC/EACTS Guidelines on myocardial revascularization. Eur Heart J. 2019;40(2):87–165.
3. Martins J, Afreixo V, Santos L, Fernandes L, Briosa A. Physiology or Angiography-Guided Coronary Artery Bypass Grafting: A Meta-Analysis. Arq Bras Cardiol. 2021; 117(6):1115-1123.
4. Zimmermann FM, Ferrara A, Johnson NP, Van Nunen LX, Escaned J, Albertsson P, et al. Deferral vs. performance of percutaneous coronary intervention of functionally non-significant coronary stenosis: 15-year follow-up of the DEFER trial. Eur Heart J. 2015;36(45):3182–8.
5. Xaplanteris P, Fournier S, Pijls NHJ, Fearon WF, Barbato E, Tonino PAL, et al. Five-Year Outcomes with PCI Guided by Fractional Flow Reserve. N Engl J Med. 2018;379(3):250–9.
6. Quintella EF, Ferreira E, Azevedo VMP, Araujo D V., Sant anna FM, Amorim B, et al. Clinical outcomes and cost-effectiveness analysis of FFR compared with angiography in multivessel disease patient. Arq Bras Cardiol. 2019;112(1):40–7.
7. Nam CW, Mangiacapra F, Entjes R, Chung IS, Sels JW, Tonino PAL, et al. Functional SYNTAX score for risk assessment in multivessel coronary artery disease. J Am Coll Cardiol 2011;58(12):1211–8.
8. Tonino PAL, Fearon WF, De Bruyne B, Oldroyd KG, Leesar MA, Ver Lee PN, et al. Angiographic Versus Functional Severity of Coronary Artery Stenoses in the FAME Study. Fractional Flow Reserve Versus Angiography in Multivessel Evaluation. J Am Coll Cardiol 2010;55(25):2816–21.
9. Harskamp RE, Alexander JH, Ferguson TB, Hager R, MacK MJ, Englum B, et al. Frequency and Predictors of Internal Mammary Artery Graft Failure and Subsequent Clinical Outcomes. Circulation. 2016;133(2):131–8.
10. Manninen HI, Jaakkola P, Suhonen M, Rehnberg S, Vuorenniemi R, Matsi PJ. Angiographic predictors of graft patency and disease progression after coronary artery bypass grafting with arterial and venous grafts. Ann Thorac Surg. 1998;66(4):1289–94.
11. Botman CJ, Schonberger J, Koolen S, Penn O, Botman H, Dib N, et al. Does Stenosis Severity of Native Vessels Influence Bypass Graft Patency? A Prospective Fractional Flow Reserve-Guided Study. Ann Thorac Surg. 2007;83(6):2093–7.
12. Toth G, De Bruyne B, Casselman F, De Vroey F, Pyxaras S, Di Serafino L, et al. Fractional flow reserve-guided versus angiography-guided coronary artery bypass graft surgery. Circulation. 2013;128(13):1405–11.

Original Article

Arterial Stiffness and Left Ventricular Myocardial Function in Children with a Well-Functioning Bicuspid Aortic Valve

Pelin Kosger,[1] Tugcem Akin,[2] Hikmet Kiztanir,[1] Birsen Ucar[1]

Eskisehir Osmangazi University, Faculty of Medicine, Department of Pediatric Cardiology,[1] Eskisehir - Turkey
Eskisehir State Hospital, Pediatric Cardiology Clinic,[2] Eskisehir - Turkey

Abstract

Background: **Arterial stiffness is an important predictor factor of aortopathy and myocardial remodeling in patients with a bicuspid aortic valve and it might be increased in childhood.**

Objective: **To assess the arterial stiffness and left ventricular myocardial function in children with a well-functioning bicuspid aortic valve.**

Methods: **Forty-four children with a bicuspid aortic valve and 41 healthy peers with a tricuspid aortic valve were included in this case-control study. Diameters and the related z-scores of the aortic root and ascending aorta were obtained. As for the left ventricular myocardial function, along with the mitral inflow velocities and M-Mode parameters, myocardial velocities and time intervals were assessed with tissue Doppler imaging. A pulse wave analysis was performed by oscillometric device (Mobil-o-Graph). A p value <0.05 was considered significant.**

Results: **The left ventricular mass index, mitral inflow A velocity, diameter and z-score of the ascending aorta, and myocardial performance index were significantly higher in patients (p=0.04, p=0.02,p=0.04, p<0.001,and p<0.001 respectively). The myocardial performance index was positively correlated with the diameter of the ascending aorta and A velocity (r=0.272;p=0.01, r=356;p=0.001, respectively). The multivariate analysis revealed that the myocardial performance index was related to the ascending aorta diameter (p=0.01). The augmentation index and pulse wave velocity were similar between the groups (p>0.05).**

Conclusion: **According to the oscillometric pulse wave analysis, the children with a well-functioning bicuspid aortic valve had similar arterial stiffness to that of the healthy peers. The ascending aorta diameter was established as an independent predictor of left ventricular myocardial function. Arterial stiffness may not be a severe risk factor in pediatric patients without marked ascending aorta dilation.**

Keywords: **Aortic Stiffness; Dilatation Pathologic; Ventricular Function, Left; Pulse Wave Analysis; Myocardial; Child.**

Introduction

A bicuspid aortic valve is the most common congenital cardiac malformation and occurs in 1-2% of the general population.[1] In addition to impaired valvular function, individuals are also at risk of aortopathy, which may result in aortic dissection and aneurysm formation.[2,3] There is no direct association between valvular dysfunction and aortopathy.[4] The presence of aorta dilation, even in patients with normal valvular function, may be related to a different pathophysiology of aortopathy.[5] In comparison with healthy controls, patients with bicuspid aortic valve without apparent valvular dysfunction have shown decreased aortic elasticity and increased central aortic stiffness.[6] Furthermore, in these individuals, central aortic stiffness measured using the ambulatory pulse wave velocity monitoring method is positively correlated with the degree of aortic dilation.[7] Therefore, vascular remodeling has been identified as the primary cause of arterial stiffness that impacts the monitoring process in these patients.[8] The level of arterial stiffness, a predictor of the course of cardiovascular diseases, tends to increase with age. However, examination of intraoperative biopsy and necropsy samples have shown that in many cases of congenital heart diseases, arterial stiffness increases as from childhood.[9,10] Patients with a bicuspid aortic valve show progressive aortic dilation during their childhood, and data regarding aortic elasticity and arterial stiffness are based on ultrasonographic methods, which are highly limited in number.[11,12] The gold standard method of arterial stiffness measurement is pulse wave analysis and the most commonly pulse wave analysis technique is tonometry; however, this technique can be time-consuming and challenging, especially when used in young children.[13] Oscillometric devices are user-friendly, practical for use in the clinical setting, and a reliable method for evaluating central blood pressure and arterial stiffness parameters, even in children.[14,15]

Mailing Address: Pelin Kosger •
Eskisehir Osmangazi University, Faculty of Medicine, Department of Pediatric Cardiology, Eskisehir - Turkey
E-mail: pelinkosger@gmail.com
Manuscript received June 14, 2020, revised manuscript October 02, 2020, accepted January 20, 2021

DOI: https://doi.org/10.36660/abc.20200657

The patients with a bicuspid aortic valve also suffer from myocardial remodeling, regardless of valvular functions and aortopathy. However, to confirm that myocardial remodeling is not only associated with valvular functions, studies including cases with intact valve function without additional risk factors are required. Pediatric cases comprise an ideal group of patients for this purpose, and currently there are only a few studies in the literature reporting that the left ventricular diastolic functions are affected in pediatric patients.[12,16] We aimed to evaluate arterial stiffness using the oscillometric method and to determine whether it is compatible with the level of ultrasonographic arterial elasticity in children with a well-functioning bicuspid aortic valve. Furthermore, it is aimed to assess the global myocardial function via tissue Doppler imaging-derived myocardial performance index in our study.

Materials and Methods

Study population

A total of 44 patients (7-18 years of age) followed in a pediatric cardiology clinic with a diagnosis of bicuspid aortic valve were enrolled in the study. These patients had no apparent aortic valvular dysfunction, neither had they received preventive medication for aortopathy. Forty-one children who had healthy tricuspid aortic valves and with similar demographic and anthropometric characteristics were included as the control group. Patients with moderate to severe valve insufficiency, with a valve velocity >2m/s, who had undergone prior surgery or percutaneous intervention, and had an additional repaired or unrepaired heart disease (e.g., coarctation of the aorta), as well as those with a body mass index and systolic blood pressure of >95th percentile were excluded from the study. Moreover, patients who had received preventive medication were not included, aiming to avoid the confounding effects of medications on myocardial mechanics and arterial stiffness. As demonstrated by laboratory tests, none of the children in the study population had hypercholesterolemia. Patients gave a written informed consent to participate in the study and the study was approved by the local Ethics Committee of Eskisehir Osmangazi University on April 04, 2018.

Echocardiography

Transthoracic echocardiography was performed by a single experienced pediatric cardiologist using the commercially available equipment Affinity 70 (Philips Medical Systems, Bothell, WA, USA) with 2–4 and 4–8 MHz broadband probes. The vascular examination was performed using VIVID I color Doppler ultrasonography (General Electric Ultrasound Systems, Mountain View, CA, USA) equipment with a 12-MHz linear probe.

Assessment of aortic valve morphology and functions

Aortic valve morphology was evaluated on the parasternal long and short axis sections. Probe frequency was selected according to patient size. A definitive bicuspid aortic valve was diagnosed when only two valve leaflets were unequivocally identified at systole and diastole, with a clear fish-mouth appearance in systole. Leaflet phenotype was defined as anteroposterior (left and right cusp fusion) or right–left (right and noncoronary cusp fusion). For aortic valve stenosis evaluation, peak aortic velocity was measured using continuous wave Doppler while the cursor was maintained at the level of the Valsalva sinus in the five-chamber view, and a value of >2.5 m/s was considered indicative of aortic stenosis.[17] To determine the degree of aortic valve insufficiency, we used the proportion of the aorta insufficiency diameter measured on the color Doppler images, which were obtained from the long-axis section, in relation to the left ventricular outflow tract diameter. Ratios <25%, 25-64%, and ≥65% generally indicate mild, moderate, and severe aortic regurgitation, respectively.[18]

Measurement of aortic root and ascending aorta diameter

Measurements of the four aortic segments, including the aortic annulus, Valsalva sinus, sinotubular junction, and proximal ascending aorta 2 cm above the sinotubular junction, were obtained in the parasternal long-axis view at the end diastole, leading-edge-to-leading-edge, and perpendicular to the long axis of the aorta.[19] Aortic dimensions were normalized to the body surface area. A z-score of >2 was considered abnormal.

Left ventricular M-mode and tissue Doppler echocardiography

Left ventricular internal dimensions, interventricular septum thickness, and posterior wall thickness were measured at the end diastole using two-dimensional M-mode echocardiography according to the pediatric guidelines of the American Society of Echocardiography.[20] Left ventricular mass was calculated according to the Devereux Formula[21] and indexed to the height. Left ventricular ejection fraction was calculated using the Teichholz formula.[22] The Doppler sample volume was placed at the tips of mitral leaflets to obtain the left ventricular inflow waveforms from the apical four-chamber view. The mitral inflow early diastolic velocity (E) and the late diastolic velocity (A) were also measured. To measure the longitudinal myocardial velocities, the sample volume was placed on the septal corner of the mitral annulus to obtain waveforms from the apical four-chamber view. Early diastolic mitral annular velocity (Ea) and late diastolic mitral annular velocity (Aa) were measured, and their ratio (Ea/Aa) was calculated to estimate left ventricular filling pressure. Cardiac time intervals, including the isovolumic relaxation time, isovolumic contraction time, and ejection time, were obtained by tissue Doppler imaging, and the myocardial performance index calculated according to Tei's formula: myocardial performance index = (isovolumic contraction time + isovolumic relaxation time)/ejection time.[23] For each quantitative parameter, three consecutive beats were averaged.

Assessment of aortic elasticity

Aortic elasticity was assessed using the two-dimensional guided M-mode evaluation of systolic and diastolic aortic diameters, 2 cm above the aortic valve; diastolic diameter was obtained at the R wave peak at the simultaneously recorded

electrocardiogram, whereas systolic diameter was measured at the maximal anterior motion of the aortic wall.

Aortic strain, aortic distensibility, and aortic stiffness index were calculated using the formulas below:

Aortic strain = 100 (Systolic diameter-Diastolic diameter) / Diastolic diameter

Aortic stiffness index = natural logarithm (Systolic blood pressure/Diastolic blood pressure) / [(Systolic diameter-Diastolic diameter/Diastolic diameter]

Aortic distensibility ($cm^2/dyn/10^{-6}$) = 2x (Systolic diameter-Diastolic diameter) / [(Systolic blood pressure – Diastolic blood pressure) X Diastolic diameter][24]

Arterial stiffness measurement

For pulse wave analysis and blood pressure monitoring, the Mobil-O-Graph (IEM, Industrielle Entwicklung Medizintechnik und Vertriebsgesellschaft mbH, Stolberg, Germany) device and the ARCSolver pulse wave analysis software (AIT Austrian Institute of Technology GmbH, Vienna, Austria) were used. 24-hour blood pressure monitoring was performed by connecting a cuff of an appropriate size for upper arm circumference. During the test, the peripheral and central systolic blood pressure, peripheral and central diastolic blood pressure, pulse, pulse wave velocity and augmentation index were measured.

The Mobil-O-Graph is an oscillometric ambulatory blood pressure measurement device that is appropriate for use in children.[25,26] After blood pressure measurement, the cuff is inflated to the brachial diastolic pressure level and the oscillations (pulse waves) are recorded for 10 seconds. After the 24-hour measurement circle, all measurements are transferred to the HMS client software and analyzed using the ARCSolver software, which has been applied to children.[27]

Aortic pulse wave velocity and augmentation index at a heart rate (HR) of 75 beats/minute (AIx@75) are markers of arterial stiffness.[28] Aortic pulse wave velocity is the speed at which pulse waves travel in the aortic wall and is a central arterial stiffness measure. AIx@75 is derived from the augmentation pressure and pulse pressure of a pulse wave. Pulse wave is a summation of forward (producing first systolic peak) and reflected (producing second peak) waves. Increase in the pulse wave amplitude due to pulse wave reflection is known as pulse augmentation, and its contribution to pulse wave amplitude is known as augmentation pressure. Moreover, the percentage of pulse wave amplitude due to augmentation pressure is known as augmentation index, which is dependent on heart rate. Mobil-o-Graph provides it at heart rate 75, a measure of peripheral arterial stiffness.[29]

Statistical Analysis

Statistical analysis was performed using the Statistical Package for Social Sciences, version 18 (SPSS, Chicago, USA). The sample size was determined by the G-power analysis software with a statistical power of 85%. The Kolmogorov-Smirnov test was used for the assessment of normal distribution. The results of continuous variables were expressed as mean ± standard deviation (SD) or median (percentile 25 and 75, interquartile range, IQR). The groups were compared using independent samples' T test for continuous variables, and the Mann–Whitney U test was used for non-normally distributed variables. The Chi-square test was used for the gender comparison between the groups. Spearman's correlation test was used for correlations. Multiple linear regression analysis using the Backward method was performed to assess the independent predictor of the myocardial performance index in patients with bicuspid aortic valve. The statistical significance level was set at $p < 0.05$.

Results

The median age of the entire study population (n = 85) was 12 (IQR=8.5–14) and ranged from 7 to 18 years. Twelve patients in the bicuspid aortic valve group (12/44) and 18 cases in the control group (18/41) were females (p=0.084). There was no significant difference in terms of age, weight, height, body surface area, body mass index, serum lipid profile, and glucose levels between the groups (Table 1).

Echocardiographic and aortic elasticity parameters are summarized in Tables 2 and 3. Mitral inflow A velocity, isovolumetric relaxation time, isovolumetric contraction time, and myocardial performance index were significantly higher in patients than in controls (p = 0.03, <0.001, <0.001, <0.001, respectively). Fusion of the left and right coronary cusps defined as the anteroposterior phenotype was the predominant phenotype (63.6%). Along with the aortic velocity, the ascending aorta diameter and z-score was higher in patients ($p < 0.001$, $p = 0.04$, $p < 0.001$, respectively). All aortic elasticity parameters were similar between the groups. The central and peripheral hemodynamic variables, AIx@75 and pulse wave velocity values, which showed no significant difference between the groups, are shown in Table 4.

The correlation analysis showed that the myocardial performance index was positively correlated with the ascending aorta diameter ($r= 0.275$; $p= 0.01$), aortic velocity ($r= 0.501$; $p <0.001$) and A velocity ($r= 0.351$, $p = 0.001$). Also, the ascending aorta diameter was positively correlated with the left ventricular mass index ($r= 0.273$, $p= 0.02$). The multiple linear regression analysis disclosed an independent association between the myocardial performance index and the ascending aorta diameter ($p= 0.01$) and aortic velocity ($p <0.001$). A multicollinearity analysis was also performed, and the variance influence factor (VIF) values of independent variables were found to be less than 5 (VIF = 1.349, 1.467, respectively).

Discussion

Arterial stiffness in children with a bicuspid aortic valve with preserved valvular function was not found to be increased when using the oscillometric method in our study. However, greater ascending aorta diameters and impaired global myocardial functions were detected in these children, when compared to their healthy peers.

Table 1 – Baseline demographic, anthropometric and clinical characteristics of the groups

Variable	Patients (n = 44)	Controls (n = 41)	p-value
Age (years)	12 (9 - 15)	12 (8 -14)	0.609
Gender (female,%)	12 (27.27)	18 (43.90)	0.084
Height (cm)	147.8 ± 20.1	146.8 ± 15.5	0.798
Weight (kg)	42.3 ± 16.4	38.6 ± 14	0.268
BMI (kg/m^2)	18 ± 0.3	17 ± 0.3	0.088
TC (mg/dl)	141.1 ± 23.1	148.3 ± 28.4	0.308
TG (mg/dl)	91.6 ± 38.9	86.6 ± 31.9	0.113

BMI: Body mass index; TC: total cholesterol; TG: total triglycerides. Continuous variables with normal distribution are expressed as mean ± standard deviation, and those with non-normally distribution as median (interquartile range).

Table 2 – Echocardiographic measurements in patients and controls

Variable	Patients (n = 44)	Controls (n = 41)	p-value
IVSDd (mm)	6.9 ± 1.0	6.7 ± 0.9	0.429
LVEDd (mm)	45 (41 – 48)	42 (39.5 – 45)	0.114
LVPWDd (mm)	6.4 ± 1.0	6.3 ± 1.6	0.674
LVMI (gr/m$^{2.7}$)	68.9 ± 13.7	62.9 ± 12	0.039
EF (%)	68.9 ± 13.7	62.9 ± 12	0.171
E (cm/s)	98.95 (88.8 – 114)	95 (80.75 – 100)	0.166
A (cm/s)	54.35 (43.92 – 72.6)	48 (40.85 – 57.3)	0.027
Ea (cm/s)	12.1 ± 2.2	11.8 ± 1.9	0.627
Aa (cm/s)	5.8 ± 1.2	6.1 ± 1.4	0.383
Sa (cm/s)	7.5 ± 1.0	7.2 ± 1.0	0.210
E/Ea	8.32 (6.49 – 10.56)	7.91 (6.93 – 8.89)	0.261
IVCT	54.1 ± 7.6	47.6 ± 7.1	<0.001
IVRT	55.9 ± 9.1	46.9 ± 8.3	<0.001
ET	282.5 ± 23.6	283.2 ± 22.5	0.889
MPI	0.38 ± 0.05	0.33 ± 0.04	<0.001

IVSDd: Interventricular septum diameter; LVEDd: end-diastolic left ventricular internal diameters; LVPWDd: end-diastolic left ventricular posterior wall thickness; LVMI: left ventricular mass index; IVCT: isovolumetric contraction time; IVRT: isovolumetric relaxation time; ET: ejection time; MPI: myocardial performance index. Continuous variables with normal distribution are expressed as mean ± standard deviation, those with non-normally distribution as median (interquartile range).

As observed in patients with a bicuspid aortic valve, the aortopathy characterized by ascending aorta dilation and increased arterial stiffness, constitutes a risk for aortic dissection, frequently occurring during adulthood.[30] Using applanation tonometry-based pulse-wave analysis, Shim et al.[7] revealed that the central aorta is stiffer in adult patients with a bicuspid aortic valve.[7] Similarly, Wang et al.[5] reported lower flow-mediated vasodilation related to the enlarged size and impaired elastic properties of the ascending aorta in adults with a bicuspid aortic valve without significant valvular dysfunction.[5] In studies investigating the properties of aortic elasticity in pediatric patients, ultrasonographic measurements are prevalently used to identify the elasticity characteristics of the ascending aorta.[11,12,16] Erroz et al. reported higher aortic stiffness index and lower aortic strain and distensibility in children with an isolated bicuspid aortic valve in a manner consistent with increased arterial stiffness and decreased elasticity.[11] Similarly, Ekici et al.[12] and Weisman et al.[16] reported impaired elastic properties of the ascending aorta in children with a well-functioning bicuspid aortic valve. In contrast to these studies, which focused only on the ascending aorta, the study by Eroğlu et al.[31] assessed the descending thoracic aorta as well and reported that the ascending aorta in children with a bicuspid aortic valve is more distensible and less stiff compared with that in their healthy peers. They also reported that there was no difference between the groups in terms of

Table 3 – Aortic valve characteristics, aortic size and elasticity parameters

Variable	Patients (n = 44)	Controls (n = 41)	p-value
Anulus (mm/m^2)	14.03 (12.75 – 16.87)	14.28 (12.51 – 17.02)	0.363
Anulus z-score	0.06 ± 1.1	-0.24 ± 0.96	0.185
Sinus of Valsalva (mm/m^2)	20.4 ± 4.8	20.5 ± 3.7	0.939
Sinus of Valsalva z-score	-0.19 ± 1.3	0.23 ± 0.83	0.08
Sinotubular junction (mm/m^2)	15.87 (14.19 – 20.07)	15.80 (14.33 – 18.42)	0.239
Sinotubular junction z-score	0.03 ± 1.2	-0.03 ± 0.8	0.76
Ascending aorta (mm/m^2)	20.1 ± 5.1	18.2 ± 3	0.04
Ascending aorta z- score	1.37 ± 1.24	0.4 ± 0.9	<0.001
Aortic velocity (m/s)	1.6 (1.4 – 1.9)	1.1 (0.95 – 1.25)	<0.001
SI	2.69 (1.81 – 3.35)	2.5 (2.09 – 3.92)	0.529
DI	0.01± 0.004	0.009 ± 0.004	0.736
Strain	21.7 ± 8.6	21.4 ± 10.2	0.883

SI: Stiffness index; DI: distensibility index. Continuous variables with normal distribution are expressed as mean ± standard deviation, those with non-normally distribution as median (interquartile range).

Table 4 – Peripheral and central hemodynamics

Variable	Patients (n = 44)	Controls (n = 41)	p-value
Peripheral SBP (mmHg)	109.2 ± 7.2	109.2 ± 6	0.996
Peripheral DBP (mmHg)	64.7 ± 5.5	64.2 ± 5.4	0.675
Heart rate (beats/dk)	79.5 ± 11.5	80.9 ± 12.4	0.578
Peripheral PP	44.4 ± 6	44.8 ± 5.8	0.759
Central SBD	98 (94.25-102)	98 (91 – 101)	0.437
Central DBP	66.5 ± 5.8	65.8 ± 5.4	0.588
AIx@75 (%)	18.5 ± 8.3	20.6 ± 8.8	0.256
PWV (m/sec)	4.5 (4.4 – 4.6)	4.5 (4.4 – 4.6)	0.528

SBP: systolic blood pressure; DBP: diastolic blood pressure; PP: pulse pressure; AIx@75, augmentation index normalized for a heart rate of 75 beats/min; PWV: pulse wave velocity. Continuous variables with normal distribution are expressed as mean ± standard deviation, those with non-normally distribution as median (interquartile range).

elasticity at older ages. In the same study, the level of arterial stiffness measured by flow-mediated vasodilation was reported to be similar between patients and healthy peers in all age groups. In the present study, in agreement with the literature, the children with a bicuspid aortic valve had wider ascending aortas than the healthy peers. This finding supports the fact that aortopathy begins in childhood, regardless of valve function. However, similar to the findings by Eroğlu et al.,[31] the pediatric patients had similar characteristics as their healthy peers in terms of elasticity of the ascending aorta, and there was no difference between the groups regarding arterial stiffness level based on the oscillometric pulse-wave analysis results, which is described as a more objective and reliable method in our study. The reason for the lack of a significant difference in terms of arterial elasticity and stiffness may be related with the absence of patients with significant aortic dilation. However, aortic dilation was observed to be at a moderate level, as there was no patient with an ascending aorta z-score >4. On the other hand, most pediatric cardiologists start medication to slow down aortic dilation and decrease the risk of dissection.[32] These medications that have positive effects on vascular and myocardial remodeling decrease arterial stiffness.[33] The present study did not include patients receiving preventive medication, therefore our results are more reliable.

In the present study, as the global indicator of left ventricular myocardial function, a high myocardial performance index was caused by the significantly prolonged isovolumetric contraction time and isovolumetric relaxation time. This suggested that both the systolic and diastolic functions were sub-clinically affected in children with a well-functioning bicuspid aortic valve. In addition, the significantly high levels of A velocity

indicated the alteration in the left ventricular diastolic function. The potential causes of myocardial remodeling identified in patients with a bicuspid aortic valve has been explained as an increased load caused by concomitant aortic valve stenosis and/or dysfunction, and myocardial systolic load caused by arterial stiffness, which was found to be increased compared with that in healthy controls.[6] The present study does not include cases with hemodynamically significant functional valvular abnormality at a level that might affect the myocardial structure, aortic diameter, or arterial functions, as well as the fact that the arterial stiffness levels in the patients were determined to be similar to those in their healthy peers. Hence, independent from aortic valvular functions and arterial stiffness, the common features in the aortopathy etiology may also play a role in left ventricular remodeling. The association between the ascending aorta sizes and myocardial performance index, support the presence of common histopathological changes. Thus, aortic dilation in patients with a bicuspid aortic valve has been associated with lower endothelial nitric oxide levels, elastic fiber degeneration, smooth muscle cell apoptosis, abnormal extracellular remodeling, and aortic cystic medial necrosis rather than hemodynamic factors.[5,8,31] In previous studies, in agreement with the present study findings, the histopathological changes that have an effect on the occurrence of aortic dilation might have also played a role in the myocardial remodeling identified in patients with a bicuspid aortic valve in which valvular functions were preserved.[6]

Limitations and strengths

Applanation tonometry is the most commonly used method to measure arterial stiffness. We did not perform applanation tonometry because of its use limitations in children, such as maintaining a sufficiently strong signal, cooperation, and heart rate variability. The studies about the validation of the oscillometric method for children are limited in the literature; however, it was reported that it is a user-friendly and reliable method for evaluating arterial stiffness parameters.[14] In addition, aortic elasticity parameters, which were widely used for the assessment of arterial stiffness in other studies in children with a bicuspid aortic valve were also performed in our study. Another limitation of our study is the fact that patients with marked aortic dilation were not included, as patients receiving preventive medication were excluded. Thus, the confounding effect of medication was excluded.

Conclusion

A bicuspid aortic valve is a disease that is not limited to the aortic valve only and where remodeling starts in the ascending aorta and left ventricular myocardium during childhood. The ascending aorta size may be more predictive than valvular functions in myocardial remodeling. Arterial stiffness, which plays an important role in the emergence of aortic complications in patients with a bicuspid aortic valve, may not be a serious risk factor in pediatric patients without marked ascending aorta dilation. Although the oscillometric method seems reliable for the assessment of arterial stiffness in children with an isolated bicuspid aortic valve, further comprehensive studies are needed on this issue.

Author Contributions

Conception and design of the research, Acquisition of data and Analysis and interpretation of the data: Kosger P, Akin T, Kiztanir H, Ucar B; Statistical analysis and Writing of the manuscript: Kosger P; Critical revision of the manuscript for intellectual content: Kosger P, Ucar B.

Potential Conflict of Interest

No potential conflict of interest relevant to this article was reported.

Sources of Funding

There were no external funding sources for this study.

Study Association

This study is not associated with any thesis or dissertation work.

Ethics approval and consent to participate

This study was approved by the Ethics Committee of the Eskisehir Osmangazi University under the protocol number 80558721-050.99-E43242. All the procedures in this study were in accordance with the 1975 Helsinki Declaration, updated in 2013. Informed consent was obtained from all participants included in the study.

References

1. Ward C. Clinical significance of the bicuspid aortic valve. Heart. 2000;83(1):81-5.
2. Michelena HI, Prakash SK, Della Corte A, Bissell MM, Anavekar N, Mathieu P, et al. Bicuspid aortic valve: identifying knowledge gaps and rising to the challenge from the International Bicuspid Aortic Valve Consortium (BAVCon). *Circulation.* 2014;129(25):2691-704.
3. Mordi I, Tzemos N. Bicuspid aortic valve disease: a comprehensive review. *Cardiol Res Pract*. 2012;2012:196037. https://doi: 10.1155/2012/196037.
4. Tadros TM, Klein MD, Shapira OM. Ascending aorta dilatation associated with bicuspid aortic valve. Pathophsiology, molecular biology, and clinical implications. *Circulation.* 2009;119(6):880-90.
5. Wang YB, Li Y, Deng YB, Zhang J, Sun J, Zhu Y, Li L, et al. Enlarged size and impaired elastic properties of the ascending aorta are associated with endothelial dysfunction and elevated plasma Matrix Metalloproteinase-2 level in patients with bicuspid aortic valve. *Ultrasound Med Bio.l* 2018;44(5):955-62.
6. Li Y, Deng YB, Bi XJ, Liu YN, Zhang J, Li L, et al. Evaluation of myocardial strain and aortic elasticity in patients with bicuspid aortic valve. *J Huazhong Univ Sci Technolog* Med Sci .2016;36(5):747-51.
7. Shim CY, Cho IJ, Yang WI, Kang MK, Park S, Ha JW, et al. Central aortic stiffness and its association with ascending aorta dilation in subjects with a bicuspid aortic valve. *J Am Soc Echocardiogr.* 2011;24(8):847-52.

8. Aicher D, Urbich C, Zeiher A, Dimmeler S, Schäfers HJ. Endothelial nitric oxide synthase in bicuspid aortic valve disease. *Ann Thorac Surg.* 2007;83(4):1290-4.

9. Ahmadizar F, Voortman T. Arterial stiffness in childhood: A predictor for later cardiovascular disease; Structural abnormalities of great arterial walls in congenital heart disease: Light and electron microscopic analyses. *Eur J Prev Cardiol.* 2018;25(1):100-2.

10. Niwa K, Perloff JK, Bhuta SM, Laks H, Drinkwater DC, Child JS, et al. Structural abnormalities of great arterial walls in congenital heart disease: Light and electron microscopic analyses. *Circulation.* 2001;103(3): 393–400.

11. Oulego-Erroz I, Alonso-Quintela P, Mora-Matilla M, Gautreaux Minaya S, Lapeña-López de Armentia S. Ascending aorta elasticity in children with isolated bicuspid aortic valve. *Int J Cardiol.* 2013168(2):1143-6.

12. Ekici F, Uslu D, Bozkurt S. Elasticity of ascending aorta and left ventricular myocardial functions in children with bicuspid aortic valve. *Echocardiography.* 2017;34(11):1660-6.

13. Laurent S, Cockcroft J, Van Bortel L, Boutouyrie P, Giannattasio C, Hayoz D, et al. Expert consensus document on arterial stiffness: methodological issues and clinical applications. *Eur Heart J.* 2006;27(21):2588–605.

14. Vanderschuren MM, Uiterwaal CS, van der Ent CK, Eising JB. Feasibility and characteristics of arterial stiffness measurement in preschool children. *Eur J Prev Cardiol*.2017;24-17)1895-902.

15. Tokgöz S, Yılmaz D, Tokgöz Y, Çelik B, Bulut Y. The evaluation of arterial stiffness of essential hypertension and white coat hypertension in children: A case-control study. *Cardiol Young.* 2018;28(3):403-8

16. Weismann CG, Lombardi KC, Grell BS, Northrup V, Sugeng L. Aortic stiffness and left ventricular diastolic function in children with well-functioning bicuspid aortic valves. *Eur Heart J Cardiovasc Imaging.* 2016;17(2):225–30.

17. Baumgartner H, Hung J, Bermejo J, Chambers JB, Evangelista A, Griffin BP, et al. American Society of Echocardiography; European Association of Echocardiography. Echocardiographic assessment of valve stenosis: EAE/ASE recommendations for clinical practice. *J Am Soc Echocardiogr*.2009;22(1):1-23.

18. Zoghbi WA, Adams D, Bonow RO, Enriquez-Sarano M, Foster E, Grayburn PA, et al. Recommendations for noninvasive evaluation of native valvular regurgitation: A Report from the American Society of Echocardiography developed in collaboration with the Society for Cardiovascular Magnetic Resonance. *J Am Soc Echocardiogr.* 2017;30(4):303-.71.

19. S.A. Goldstein, A. Evangelista, S. Abbara, Arai A, Asch FM, Badano LP, et al. Multimodality imaging of diseases of the thoracic aorta in adults: from the American Society of Echocardiography and the European Association of Cardiovascular Imaging: endorsed by the Society of Cardiovascular Computed Tomography and Society for Cardiovascular Magnetic Resonance. *J Am Soc Echocardiogr* 2015;28(2):119-82.

20. Lopez L, Colan SD, Frommelt PC, Ensing GJ, Kendall K, Younoszai AK, et al. Recommendations for quantification methods during the performance of a pediatric echocardiogram: a report from the Pediatric Measurements Writing Group of the American Society of Echocardiography Pediatric and Congenital Heart Disease Council. *J Am Soc Echocardiogr.* 2010;23(5):465–95.

21. Devereux RB, Alonso DR, Lutas EM, Gottlieb GJ, Campo E, Sachs I, et al. Echocardiographic assessment of left ventricular hypertrophy: comparison to necropsy findings. *Am J Cardiol* 1986;57(6):450-8.

22. Chengode S. Left ventricular global systolic function assessment by echocardiography. *Ann Card Anaesth.* 2016;19(Supplement):S26–S34.

23. Tei C., Ling L.H., Hodge D.O. New index of combined systolic and diastolic myocardial performance: a simple and reproducible measure of cardiac function—a study in normals and dilated cardiomyopathy. *J Cardiol.* 1995;26(6):357–66.

24. Fahey M, Ko HH, Srivastava S, Lai WW, Chatterjee S, Parness IA, et al. A comparison of echocardiographic techniques in determination of arterial elasticity in the pediatric population. *Echocardiography* 2009;26(5):567–73.

25. Stoner L, Lambrick DM, Westrupp N, Young J, Faulkner J. Validation of oscillometric pulse wave analysis measurements in children. *Am J Hypertens.* 2014;27(6):865-72.

26. Weber T, Wassertheurer S, Rammer M, Maurer E, Hametner B, Mayer CC, et al. Validation of a brachial cuff-based method for estimating central systolic blood pressure. *Hypertension* 2011;58(5):825–32.

27. Elmenhorst J, Weberruss H, Mayr M, Pfister K, Oberhoffer R. Comparison of two measurement devices for pulse wave velocity in children: which tool is useful to detect vascular alterations caused by overweight? *Front Pediatr.* 2019;7:334.

28. Solanki JD, Munshi HB, Mehta HB, Shah CJ. Central hemodynamics and arterial stiffness in Gujarati diabetics not receiving any antihypertensive: A case-control study based on oscillometric pulse wave analysis. *J Family Med Prim Care.* 2019 Aug 20;8:1352–8.

29. Warner PJ, Al-Quthami A, Brooks EL, Kelley-Hedgepeth A, Patvardhan E, Kuvin JT, et al. Augmentation index and aortic stiffness in bicuspid aortic valve patients with non-dilated proximal aortas. *BMC Cardiovasc Disord.* 2013 Mar 15;13:19. https://doi:10.1186/1471-2261-13-19.

30. Pepe G, Nistri S, Giusti B, Sticchi E, Attanasio M, Porciani C, et al. Identification of Fibrillin 1 gene mutations in patients with bicuspid aortic valve (BAV) without Marfan syndrome. *BMC Med Genet.* 2014;15:23. https://doi.org/10.1186/1471-2350-15-23

31. Eroğlu E, Akalın F, Çetiner N, Şaylan BÇ. Aortic elasticity and the influence of valve morphology in children with bicuspid aortic valve. *Cardiol Young.* 2018;28(11):1338-44.

32. Hussain A, Warren A.E, Chen RPC, Dhillon SS. Practice variation among Canadian pediatric cardiologists in medical management of dilated ascending aorta in patients with bicuspid aortic valve. *CJC Open.* 2019;1(3)119-22.

33. Shahin Y, Khan J.A, Chetter I. Angiotensin converting enzyme inhibitors effect on arterial stiffness and wave reflections: a meta-analysis and meta-regression of randomised controlled trials. *Atherosclerosis.* 2012;221(1):18-33.

Original Article

Dexmedetomidine Preconditioning Reduces Myocardial Ischemia-Reperfusion Injury in Rats by Inhibiting the PERK Pathway

YuJiao Chen,[1,2] Song Cao,[1] Hui Chen,[1] CunZhi Yin,[1] XinPeng Xu,[1] ZaiQun Yang[1]

Zunyi Medical University,[1] Zunyi, Guizhou – China

Affiliated Hospital of North Sichuan Medical College,[2] NanChong, SiChuan - China

Abstract

Background: **Ischemic heart disease has attracted much attention due to its high mortality rates, treatment costs and the increasing morbidity in the young population. Strategies for reperfusion have reduced mortality. However, reperfusion can lead to cardiomyocyte death and subsequent irreversible myocardial damage. At present, the timely and targeted treatment of ischemia-reperfusion (I/R) injury is often lacking.**

Objectives: **To evaluate if dexmedetomidine (DEX) has a protective effect in myocardiual I/R and explore the possible mechanism behind it.**

Methods: **Rat hearts were perfused with a Langendorff perfusion system, and randomly assigned to five groups: control group, perfused with Krebs-Henseleit (K-H) solution for 205 minutes without ischemia; and four test groups that underwent 40 minutes of global ischemia and 120 min of reperfusion. The DEX group, the yohimbine (YOH) group and the DEX + YOH group were perfused with DEX (10 nM), YOH (1 μM) or the combination of DEX and YOH prior to reperfusion, respectively. Cardiac hemodynamics, myocardial infarct size, and myocardial histology were evaluated. The expression of glucose-related protein 78 (GRP78), protein kinase R-like ER kinase (PERK), phosphorylated PERK, eukaryotic initiation factor 2α (eIF2α), phosphorylated eIF2α, activating transcription factor 4 (ATF4), and CCAAT/enhancer-binding protein homologous protein (CHOP) were assessed. P<0.05 was considered to indicate a statistically significant difference.**

Results: **DEX preconditioning improved the cardiac function of I/R hearts, reduced myocardial infarction, myocardial apoptosis, and the expression of GRP78, p-PERK, eIF2α, p-eIF2α, ATF4 and CHOP.**

Conclusions: **DEX pretreatment reduced myocardial I/R injury by suppressing apoptosis, which was induced by the PERK pathway.**

Keywords: **Dexmedetomidine; Ischemic Cardiomyopathy/mortality; Myocardial Reperfusion; Hipnotics and Sedatives; Protein Kinases; Rats.**

Introduction

Ischemic heart disease has attracted much attention due to its high mortality rates, treatment costs and the increasing morbidity in the young population. In the past three decades, reperfusion strategies to alleviate ischemic injury have been widely included in clinical practice. However, reperfusion can lead to cardiomyocyte death, and subsequent irreversible myocardial damage.[1]

Myocardial ischemia-reperfusion injury (MIRI) is a long-term and complex pathophysiological process. The process of restoring blood flow to the ischemic myocardium can induce a wide range of basic biological changes, including impaired ion homeostasis, oxygen radical bursts, autophagy, ATP metabolic disorders, inflammation, oxidative stress, mitochondrial dysfunction, and apoptosis.[2] Recent studies have demonstrated that the damage inflicted on the myocardium involves two processes: ischemia and reperfusion injury (I/R injury). I/R injury is a major determinant of long-term mortality; thus, the possibility of ameliorating the extent of the injury is of great individual and socioeconomic value.[3-7]

It has been demonstrated that cardiomyocyte apoptosis is a major mechanism of myocardial I/R-injury.[8] Cardiomyocyte apoptosis is triggered by the mitochondrial and death receptor pathways under the conditions of myocardial reperfusion.[9] However, these mechanisms have yet to be fully determined.[2] Recent studies have explored the association between the endoplasmic reticulum (ER) and myocardial I/R-injury.[9-11] Stress conditions such as I/R, hypoxia, and oxidative stress have been identified in the dysregulation of ER functions, thus triggering ER stress.[12] The pathological consequences of ER lumen disruption and miscommunication have been implicated in myocardial I/R-injury.[13,14] However, it is still unclear whether or not ER stress induces apoptosis by activating PERK during myocardial reperfusion injury.[15]

At present, due to the shortage of specific drugs and standard therapies, the timely and targeted treatment of I/R injury is often lacking. Dexmedetomidine (DEX) is a highly selective α_2 adrenergic receptor (AR) agonist, which has limited

Mailing Address: Hui Chen •
Zunyi Medical College Affiliated Hospital - 149 Dalian road, Zunyi, Guizhou Zunyi 563003 – China
E-mail: 2267390140@qq.com
Manuscript received July 12, 2020, revised manuscript October 27, 2020, accepted January 27, 2021

DOI: https://doi.org/10.36660/abc.20200672

impact on hemodynamics and breathing, thus providing the ideal sedation and analgesia for patients undergoing cardiovascular surgery.[16] Previous studies have demonstrated that DEX preconditioning showed cardioprotective effects in ischemic hearts.[17-20] However, the molecular mechanism of DEX protection, to date, remains unknown. The present study hypothesized that pre-treatment with DEX protects the heart from I/R injury by PERK pathway activation, which is dependent on the activation of the α_2 receptor. Therefore, the present study used an isolated heart I/R model to evaluate the effects of DEX on I/R injury and its potential mechanism.

Methods

Experimental animals

Male adult Sprague-Dawley rats (8-10 weeks old; 260-280g) were obtained from the animal experiment center of Changsha (Changsha, China). All experimental procedures were in accordance with the "Guide for the Care and Use of Laboratory Animals", published in China (No.1492, 2001), and were approved by the Experimental Animal Care and Use committee of the Zunyi Medical University. All rats were housed under standard conditions (room temperature, 22°C; 12 h light/dark cycle) with free access to food and water in the Guizhou Key Laboratory of Anesthesiology and Organ Protection of Zunyi Medical University.

Isolation of adult rat hearts

Rats were anesthetized with sodium pentobarbital (45 mg/kg, intraperitoneally). After the successful anesthesia, the heart was immediately excised from the chest by sternotomy and immersed in ice-cold Krebs-Henseleit (K-H) solution (NaCl, 119 mM; KCl, 6.0 mM; $CaCl_2$, 1.24 mM; $NaHCO_3$, 20.1 mM; KH_2PO_4, 1.24 mM; $MgSO_4$, 1.24 mM; glucose, 11.2 mM). The excised heart was retrogradely placed in a Langendorff perfusion setup via the aorta (PanLab). The K-H solution was perfused at a constant perfusion pressure of 75-80 mmHg and balanced with a mixture of 95% O_2 and 5% CO_2 to a pH of 7.35-7.45 at 37°C. A latex balloon connected to a pressure transducer was inserted in the left ventricle through the mitral valve, and filled with normal saline to produce a left ventricular end-diastolic pressure (LVEDP) of 2-10 mmHg. The balloon volume was maintained constant throughout the experiment. Heart rate (HR), LVEDP, left ventricular developed pressure (LVDP = LVSP - LVEDP), left ventricular pressure peak rates of positive and negative changes ($\pm dp/dt_{max}$) and rate pressure product (RPP = HR x LVDP) were recorded by the Lab Chart system.

I/R and DEX preconditioning in isolated rat heart

For each test, following a 15-minute equilibration of perfusion, the hearts in which the baseline LVDP and HR were >50mmHg and >200 beats/min were randomly assigned to five groups in a sealed envelope randomization assignment. The specimens in all groups were perfused for 30 minutes prior to 40 minutes of normothermic global ischemia, followed by 120 minutes of reperfusion with the exception of the control group (n= 6): (i) control group, no preconditioning protocol, perfused with normal K-H solution; (ii) I/R group, no preconditioning protocol, perfused with normal K-H solution prior to ischemia; (iii) DEX group, preconditioned with 10 nM DEX prior to ischemia; (iv) yohimbine (YOH) group, preconditioned with1 μM YOH prior to ischemia; and(v) DEX + YOH group, preconditioned with 10 nM DEX + 1μM YOH prior to ischemia. The concentrations of DEX (Hengrui pharmaceutical) and antagonist were selected based on previous studies. Yohimbine (YOH) was used as an α_2-AR antagonist. DEX and YOH were dissolved in the modified Krebs-Ringer solution (Figure 1).

Infarct size determination

Infarct size was assessed by the triphenyl tetrazolium chloride (TTC) staining method. After reperfusion, the tissues that were adherent to the arterial root were removed, and the whole heart was frozen. The frozen heart was cut into 1-2 mm thick slices. The slices were immersed in a vial with 1% TTC and incubated in a water bath for 30 minutes at 37°C. The vial was continuously agitated to obtain an even staining. The slices were subsequently placed in 10% formaldehyde for 24 hours, placed on a glass plate, and a cover glass was placed over the slices. Shims of 2 mm were placed in the corners between the glasses to obtain the desired slice thickness, and digital photographs were taken. Areas of infarction and normal areas were determined in a blinded manner by planimetry with the Image-Pro Plus 6.0 software (Media Cybernetics, Inc.), and infarct size was expressed as a percentage of the total area.

Histopathological examination

Myocardial tissues harvested from the rats were cut into 1 cm sections, fixed in 4% paraformaldehyde and embedded in paraffin. To quantify the extent of myocardial damage, the biopsies were cut into 5 μm sections, which were stained with hematoxylin and eosin (H&E) for 90 minutes, at room temperature, and six fields of view (magnification, x200) were randomly selected for evaluation in each group.

TUNEL assay

Terminal deoxynucleotidyl transferase dUTP nick end labeling (TUNEL) assays were performed to determine the extent of apoptosis in the myocardium using a commercially available kit (Baiao Cisco Biological Technology) according to the manufacturer's instructions. Green nuclear labeling was defined as TUNEL-positive cells. To determine the extent of myocardial apoptosis, five fields (magnification, x 200) were randomly selected from two sections in each group, and the apoptosis index (AI) was calculated using Image-Pro Plus 6.0 (AI) as follows: AI = number of apoptotic cells / total number of cells counted.

Western blotting

The heart was homogenized and lysed with a RIPA buffer (Thermo Fisher scientific, Inc.). The tissues were centrifuged at 125 x g for six minutes and the supernatant was collected. The concentration of the protein was determined by a BCA protein assay (Thermo Fisher scientific, Inc.). The samples were separated by 10% sodium dodecyl sulphate polyacrylamide gel electrophoresis and transferred onto

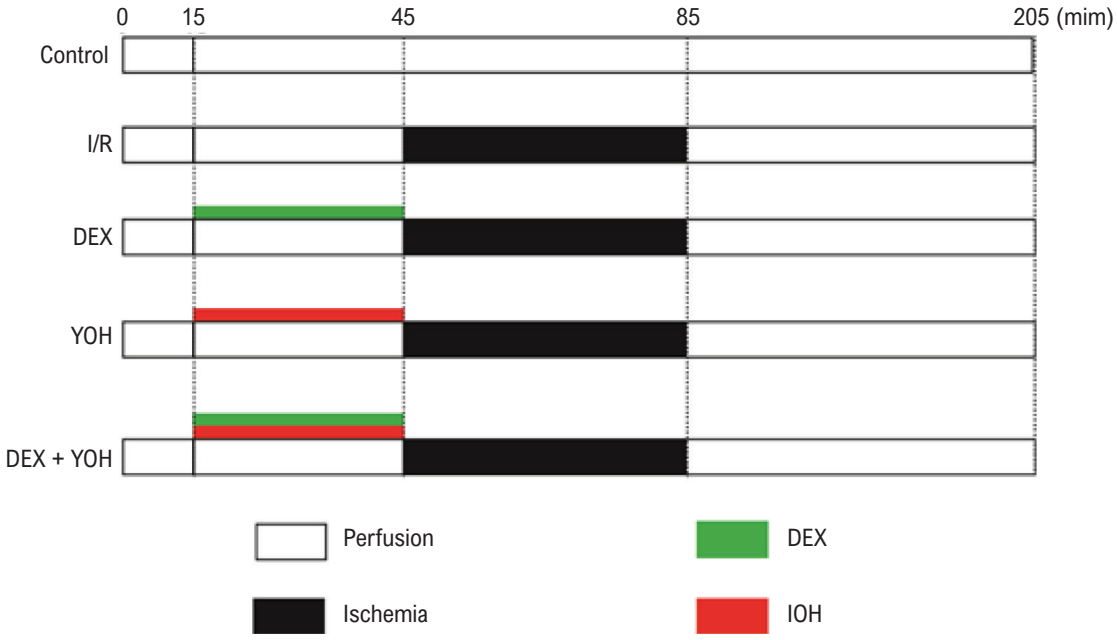

Figure 1 – *Langendorff myocardial ischemia-reperfusion injury model. For each test, after a 15-minute equilibration of perfusion, the prepped hearts were randomly assigned to five groups for baseline LVDP and HR, which were less than 50 mmHg and 200 beats/min. The specimens in control group were continuously perfused with K-H solution for 205 minutes. The specimens in four other groups were perfused for 30 minutes prior to 40 minutes of normothermic global ischemia, followed by 120 minutes of reperfusion. The specimens in the I/R group had no preconditioning protocol perfused with normal K-H solution before ischemia; the specimens in DEX group were perfused with DEX (10 nM) before ischemia; the specimens in YOH group were perfused with YOH (1 μM) before ischemia; the specimens in DEX + YOH group were perfused with DEX (10 nM)+YOH (1 μM) before ischemia. LVDP: left ventricular developed pressure, HR: heart rate, K-H: Krebs-Henseleit, I/R: ischemia-reperfusion, DEX: dexmedetomidine, YOH: yohimbine*

nitrocellulose membranes. The membranes were blocked with 5% skimmed milk for two hours, membranes were probed with anti-GRP78 (1:1000; cat no. PA1-014A; Thermo Fisher scientific), anti-PERK (1:1000; cat no. PA5-79193; Thermo Fisher scientific), anti-p-PERK (1:1000; cat no. MA5-15033; Thermo Fisher scientific), anti-eIF2α (1:1000; cat no. MA1-079; Thermo Fisher scientific), anti-p-eIF2α (1:1000; cat no. 44-728G; Thermo Fisher scientific), anti-ATF4 (1:1000; cat no. PA5-68802; Thermo Fisher scientific), anti-CHOP (1:1000; cat no. PA5-86145; Thermo Fisher scientific), anti-GAPDH (1:1000; cat no. MA5-32539; Thermo Fisher scientific) primary antibodies at 4°C overnight. After washing the membranes three times, the blots were incubated with horseradish peroxidase-conjugated secondary antibodies (1:1000; cat no. G-21234; Thermo Fisher scientific) for two hours. The content of the protein was determined by a gel imaging system (Tanon Science & Technology).

Statistical analysis

The sample size of this study was based on the preliminary experiment. Means of LVEDP in the control group, the DEX group and the I/R group following reperfusion for 120 minutes were 12.52, 16.23, 22.39, respectively, and Standard deviations were 1.45, 2.44 and 145, respectively. The α-level test was considered as 0.05, $Z0.05/2 = 1.96$. The power level, $1 - \beta$, was considered as 0.8. For the control and the EDX groups, a sample size of six was required for each group. For the I/R and the DEX groups, a sample size of four was required for each group. So, a sample size of six was determined per group.

Data are presented as mean ± standard deviation (SD). SPSS 20.0 (IBM, Corp) was used for statistical analyses. Differences between groups were analyzed with the one-way analysis of variance (ANOVA). The Shapiro-Wilk test was employed to verify normality. The LSD test was used for the comparison of homogeneous variance, and the Dunnett's T3 test was used for the comparison of uneven variance. $P<0.05$ was considered to indicate a statistically significant difference.

Results

DEX improves cardiac recovery from the I/R injury

To determine the effects of DEX on myocardial I/R-injury, an isolated perfused heart preparation was performed by perfusing rat hearts for 30 minutes with modified K-H solution prior to 40 minutes of global ischemia, followed

by 120 minutes of reperfusion. The analysis of variance demonstrated there were no significant differences in hemodynamics between the groups at the end of the balance point. After 45 minutes of perfusion, no significant differences were observed in HR, $\pm dp/dt_{max}$, LVDP, LVEDP and RPP, with the exception of the YOH group and the DEX + YOH group. In the control group, HR, $\pm dp/dt_{max}$, LVDP, and RPP were higher and LVEDP was lower compared with the other groups after reperfusion for 120 minutes, which suggested that 40-minute ischemia at room temperature was challenging for rat hearts. During the second half of the 120-minute reperfusion, a number of hearts exhibited failure and arrhythmia (~10%). However, in the DEX group, HR, $\pm dp/dt_{max}$, LVDP, and RPP were higher and LVEDP was lower compared with the other groups after reperfusion for 120 minutes, with the exception of the control group. Therefore, DEX preconditioning significantly improved the hemodynamics following myocardial I/R injury, and the effects were reversed by the AR antagonist YOH (Figure 2).

Pre-treatment with DEX reduces myocardial infarct size

TTC staining, which is the gold standard for testing myocardial infarct, was used to evaluate the cardio-protective function of DEX. In the control group, the percentage of infarct was low; however, it was significantly increased in the I/R, YOH and DEX + YOH groups (Figure 3A). In rats that were pre-treated with DEX, the infarct area was significantly smaller when compared with that in the I/R group. Additionally, no differences were observed between the YOH and the DEX + YOH groups compared with the I/R group. Therefore, the addition of YOH reversed the DEX-mediated protective effects on myocardial injury (Figure 3).

Pretreatment with DEX attenuates myocardial tissue damage

Myocardial injury was further measured in the H&E-stained sections. H&E staining revealed that myocardial structure was complete and exhibited regular arrangement, normal cardiac muscle fibers and no necrosis, with mild cardiomyocyte edema in the control group, whereas the structure of the myocardium was severely damaged after the I/R injury. The I/R group exhibited disordered myofibril arrangement and ruptured cardiac muscle fibers. As shown in Figure 3C, DEX preconditioning significantly improved these pathological changes; however, YOH partially reversed the protective effect.

Pretreatment with DEX suppresses myocardial apoptosis

The TUNEL assay was used to determine the effects of DEX on cardiomyocytic apoptosis in isolated rat hearts after I/R. Compared with the control group (apoptotic rate, 0.00±0.00%), the number of TUNEL-positive cells increased significantly in the I/R (apoptotic rate, 58.17±0.60%), YOH (apoptotic rate, 57.11±1.39%) and DEX + YOH (apoptotic rate, 57.62±1.50%) groups, whereas no significant differences were observed in apoptotic rate among the I/R, YOH and the DEX + YOH groups (Figure 4C). Compared with the I/R, YOH and DEX + YOH groups, apoptotic rate was significantly decreased in the DEX group. Therefore, DEX may decrease myocardial apoptosis. However, YOH completely reversed this effect (Figure 4).

DEX pret-reatment alleviates apoptosis by inhibiting the ER stress-mediated PERK pathway

To elucidate the successful establishment of an ER stress model induced by myocardial I/R injury, the activation of GRP78 and PERK was evaluated. In the present study, GRP78, which is an important marker for the occurrence of ER stress, was extensively upregulated at the protein level in all experimental groups compared with the control group (Figure 5). As GRP78 is a direct target of PERK, which is a highly conserved ER stress-mediated apoptosis transducer, the expression levels of PERK and p-PERK protein were examined. Under physiological conditions, the overexpression of GRP78 did not change the activation of PERK as indirectly determined by PERK phosphorylation (Figure 6). The expression of p-PERK protein in the I/R, YOH and DEX + YOH groups was higher compared with that in the control and the DEX groups (Figure 6). By contrast, this was successfully blocked by the DEX treatment. These results suggested that DEX may participate in ER stress-mediated protection against reperfusion injury, whereas the protective effect of DEX was reversed by YOH compared with the DEX + YOH group. To further determine the effects of DEX on the PERK pathway and its potential molecular mechanism, downstream components of the PERK pathway in ER stress response were investigated, including the eukaryotic initiation factor 2α (eIF2α), activating transcription factor 4 (ATF4) and CCAAT/enhancer-binding protein homologous protein (CHOP). The results demonstrated that the levels of p-eIF2α, ATF4 and CHOP were notably upregulated in the I/R, YOH and DEX + YOH groups in comparison with the control group, whereas pre-treatment with DEX inhibited the expression of the three proteins (Figure 5, Figure 6). The examination by TUNEL assay confirmed these results. Therefore, the results indicated that DEX may relieve myocardial I/R injury-mediated apoptosis by suppressing the activation of the PERK pathway.

Discussion

The present study indicated that DEX may protect against myocardial I/R injury, which was in accordance with a previous study.[21] The protective effects of DEX on myocardial I/R injury through the inhibition of apoptotic pathways have been previously confirmed.[22] Similarly, the results of the present study indicated that DEX improved cardiac hemodynamics and decreased apoptosis, which was revealed by the changes in apoptotic morphology and apoptotic rates in the TUNEL assay. Excessive ER stress has been demonstrated to serve an important role in myocardial I/R injury and lead to apoptosis.[23] GRP78, which is an ER chaperone protein, belongs to one of the heat-shock protein 70 (Hsp70) family, which indicates the occurrence of ER stress and regulates ER homeostasis at a certain point.[24] Previous studies have demonstrated that I/R induces the expression of GRP78 protein.[25,26] The results of the present study

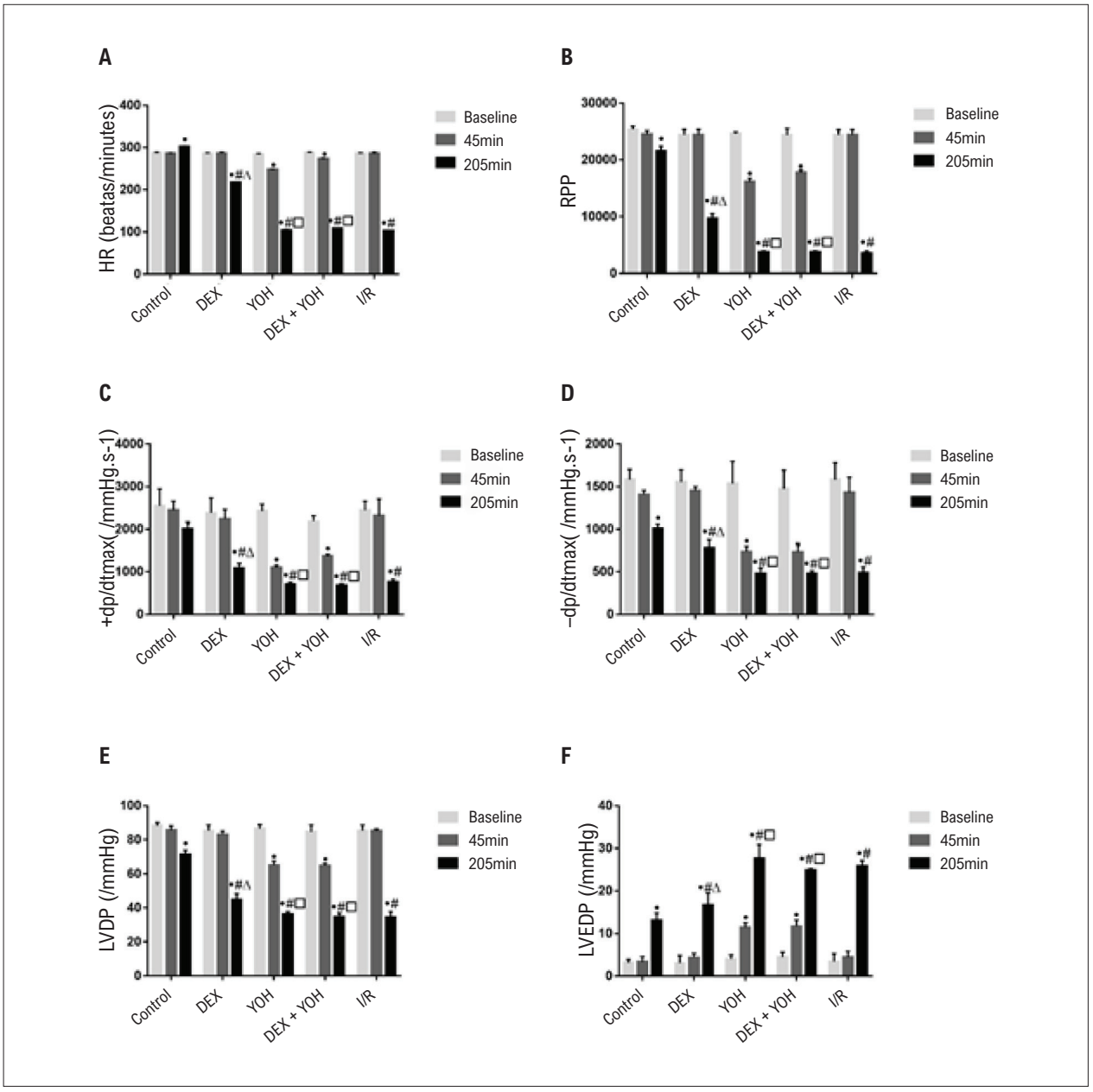

Figure 2 – *Dexmedetomidine improves cardiac function of ischemia-reperfusion rat hearts. A-F: effect of dexmedetomidine on the HR, rate pressure product (RPP = HR×LVDP), left ventricular pressure peak rates of positive and negative changes (±dp/dt$_{max}$) of I/R injury in rats, LVDP, LVEDP. Data are presented as the mean ± standard deviation. n=12. *P<0.05, vs. ischemia beginning point, #P<0.05, vs. control group at reperfusion for 120 minutes. ΔP<0.05, vs. I/R group at reperfusion for 120 minutes. P<0.05, vs. DEX group at reperfusion for 120 minutes. Baseline: at the end of the balance point, 45 minutes: ischemia beginning point, 205 minutes: 120 minutes of reperfusion. HR, heart rate, I/R: ischemia-reperfusion, LVDP: left ventricular developed pressure, RPP: rate pressure product, ±dp/dt$_{max}$: left ventricular pressure peak rates of positive and negative changes, LVDP: left ventricular developed pressure, LVEDP: left ventricular end diastolic pressure, DEX: dexmedetomidine.*

demonstrated that the GRP78 protein was induced by I/R, whereas the DEX treatment decreased GRP78 expression, which indicated that DEX may exert its protective effects by suppressing ER stress.

PERK is a stress receptor on the ER with serine-threonine kinase activity, which is activated by trans-autophosphorylation and oligomerization. Under prolonged ER stress conditions, the PERK/eIF2α/ATF4/CHOP pathway contributes with apoptosis during myocardial I/R injury.[27,28] A previous study has reported that membrane-localized GRP78 is crucial for PERK phosphorylation,[26] which was also observed in the present study. It is reported that the highest expression of GRP78 protein was detected in the myocardium from the isolated and perfused rat heart with 40-minute ischemia and 120-minute reperfusion.[29]

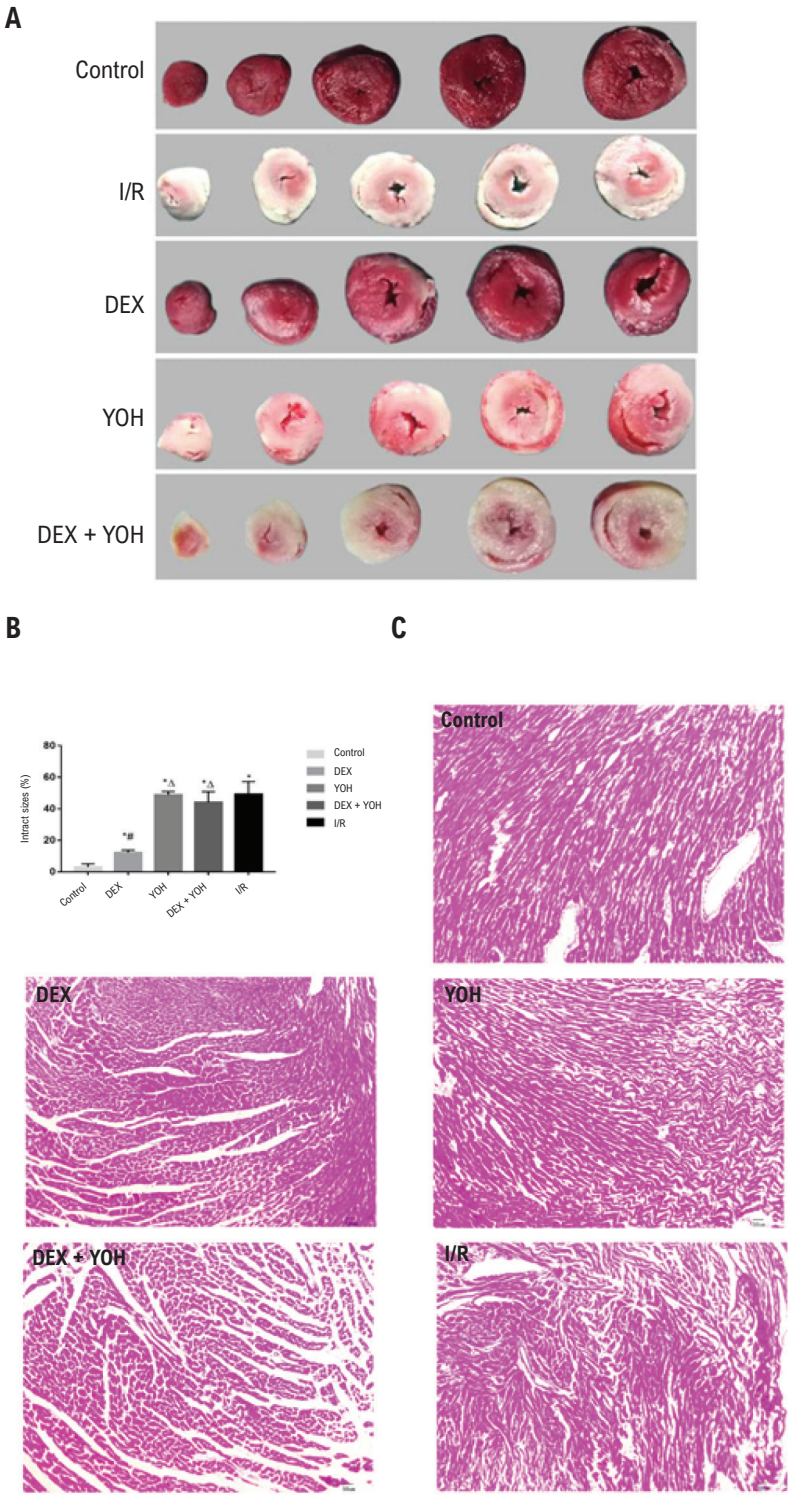

Figure 3 – *TTC staining and HE staining of Langendorff hearts after ischemia-reperfusion injury. (A) Representative images of TTC stained samples showing the infarct area (white) and the non-infarct area (red). (B) Analysis of the myocardial infarct size in control and in I/R-induced isolated heart. Data are presented as the mean ± standard deviation. n=6. *P<0.05, vs. control group; #P<0.05, vs. I/R group; ΔP<0.05, vs. DEX group. (C) Representative images of HE stained samples (magnification, ×200) demonstrating histopathological changes in the myocardium. TTC: triphenyl tetrazolium chloride staining technique. HE: hematoxylin and eosin, I/R: ischemia-reperfusion.*

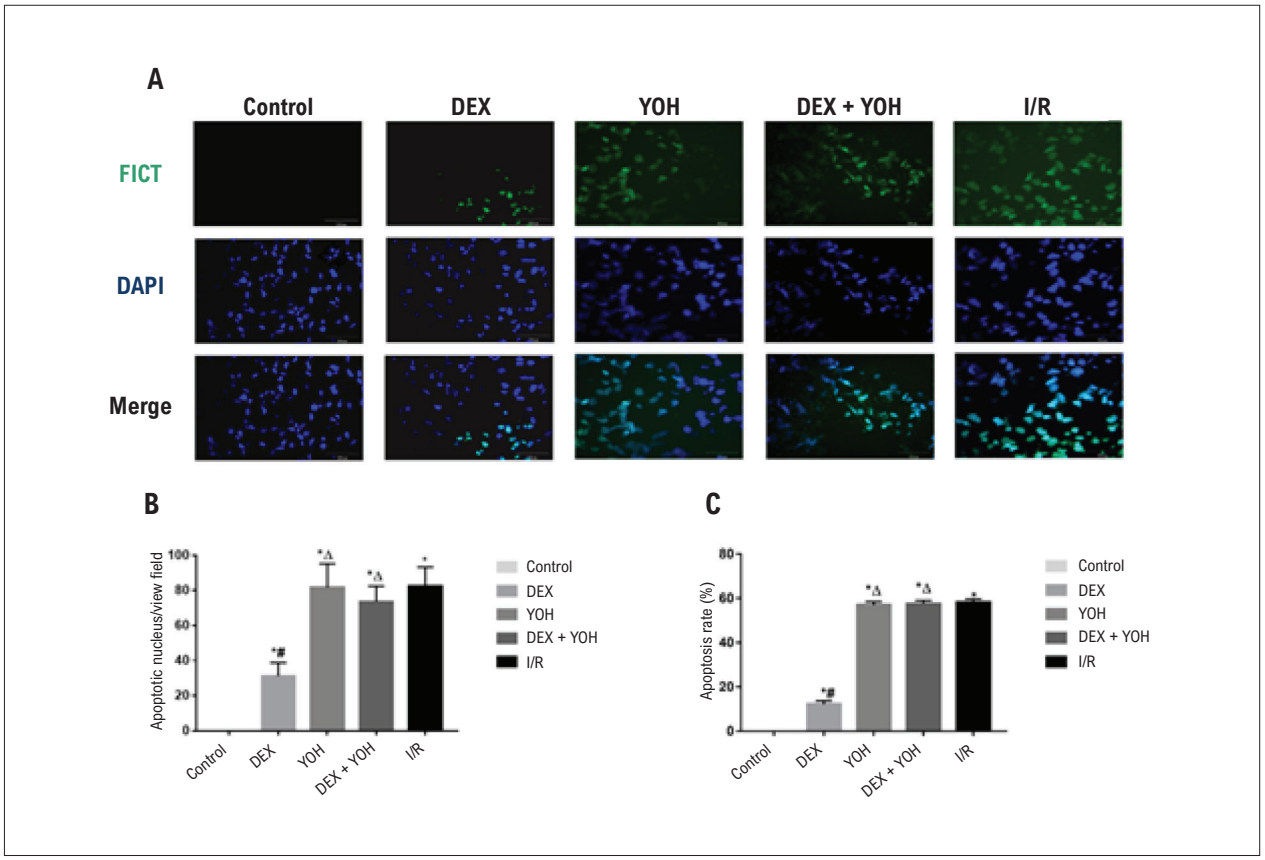

Figure 4 – *TUNEL assays to detect apoptosis in ischemia-reperfusion hearts. (A) Representative images of TUNEL assays (magnification, ×400) showing the total nucleus (blue) and apoptotic nucleus (green). (B) Analysis of the cardiomyocytic apoptotic nucleus in the control group and in I/R-induced isolated heart. (C) Analysis of the cardiomyocytic apoptosis rates in control group and in I/R-induced isolated heart. Data are presented as the mean ± standard deviation. n=6. *P<0.05, vs. control group; #P<0.05, vs. I/R group; ΔP<0.05, vs. DEX group. TUNEL: Terminal deoxynucleotidyl transferase dUTP nick end labeling.*

In addition, we previously found that 40-minute ischemia was optimal for the Langendorff ischemia-reperfusion rat hearts,[30] therefore, we selected 40-minute ischemia and 120-minute reperfusion in the present *ex vivo* ERS ischemia reperfusion injury model. It is also reported that the activation of the PERK kinase domain in the early stages of ER stress leads to the phosphorylation of eIF2α, which reduces transcriptional initiation and protein folding, and maintains homeostasis in the endoplasmic reticulum. Advanced phosphorylation of eIF2α through the activation of ATF4 induces the overexpression of the apoptosis protein CHOP, which leads to apoptosis.[31,32] Related studies have shown that the mechanisms of DEX against myocardial I/R injury are mediated by the activation of α_2-ARs and anti-inflammatory processes,[22] whereas the effect of DEX on ER stress in myocardial I/R injury has rarely been investigated. The results of the present study have demonstrated that DEX inhibited the ER stress-mediated PERK/eIF2α/ATF4/CHOP pathway during myocardial I/R injury. A previous study has described that myocardial I/R causes abnormal accumulation of unfolded proteins in the lumen of the endoplasmic reticulum, and contributes with the autophosphorylation of PERK.[33] In the present study, p-PERK protein expression level was increased in the I/R group, but decreased with the DEX pretreatment. With the activation of PERK, the phosphorylation of downstream protein eIF2α inhibited 80S ribosome assembly and massive protein synthesis.[34,35] Another study has indicated that the dephosphorylation of eIF2α suppressed downstream ATF4/CHOP signaling.[36] Therefore, eIF2α may be a key component in PERK-mediated signaling. The results of the present study demonstrated that after the DEX treatment, the level of p-eIF2α was reduced compared with the I/R group. ATF4 plays a role in promoting apoptosis, which is induced by the phosphorylation of eIF2α.[37-39] The results of the present study suggested that ATF4 may be responsible for cardiomyocyte apoptosis during I/R induced ER stress, whereas DEX treatment may downregulate ATF4. CHOP, which is a member of the CCAAT/enhancer binding protein family of transcription factors,[40] is a classic marker of apoptosis initiation, which plays an important role in ER stress-mediated myocardial apoptosis.[41,42] Our results suggested that the expression of CHOP protein increased in the I/R group, which corresponded to the results of the apoptosis assay. The present study demonstrated that DEX had an anti-apoptotic effect, and the mechanism may be dependent on the ER stress-mediated PERK pathway.

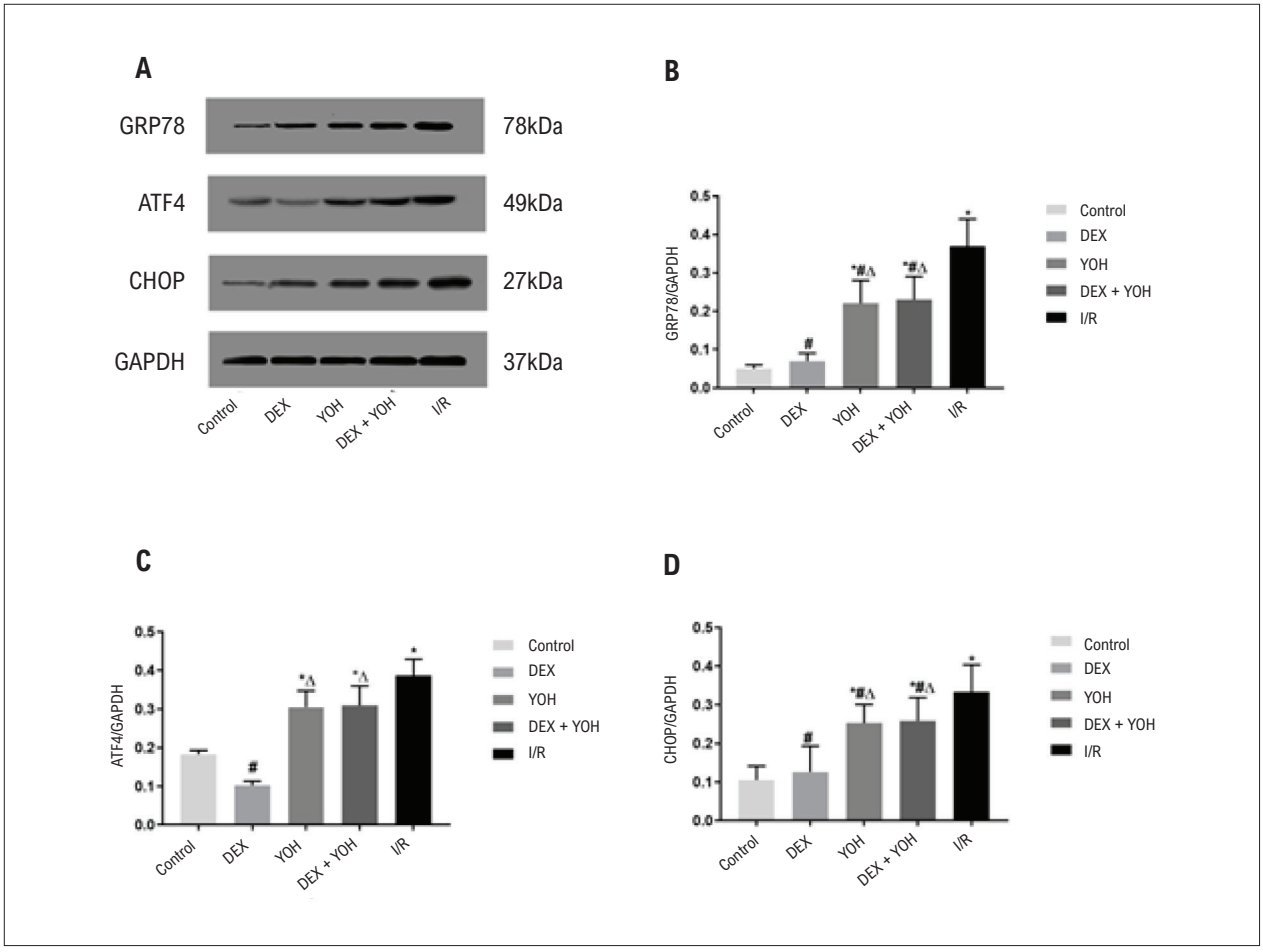

Figure 5 – *Dexmedetomidine protected the myocardium from I/R injury and reduced apoptosis. (A) Western-blotting detecting of GRP78, ATF4, CHOP protein expression. (B-D) Analysis of the expression of ATF4, GRP78 CHOP in control and I/R-induced isolated heart. Data are presented as the mean ± standard deviation. n=6. *P<0.05, vs. control group. #P<0.05, vs. I/R group, ΔP<0.05, vs. DEX group. I/R: ischemia-reperfusion. GRP78: glucose-related protein 78, ATF4: activating transcription factor 4, CHOP: CCAAT/enhancer-binding protein homologous protein.*

YOH is a selective blocker of presynaptic α_2-AR, which dilates vascular smooth muscle, decreases sympathetic tone, and increases peripheral parasympathetic tone. In the present study, YOH reversed the protective effects of DEX pretreatment in the myocardium of rats, which resulted in increased myocardial infarct size and cardiomyocyte apoptosis; in addition, the expression levels of the PERK pathway proteins were increased. Together, these results indicated that the protective effect of DEX preconditioning in rat myocardium may be antagonized by an AR blocker, which is consistent with a previous study.[43]

Although the results of the present study identified an important role for the PERK pathway in the survival of cardiomyocytes, there were certain limitations to the study. Future work is necessary to analyze other potential mechanisms besides apoptosis and the PERK pathway. In addition, apoptosis is considered to occur in the context of excessive stress in the ER; by contrast, ER promotes normal cell survival by providing nutrients from digesting damaged organelles and proteins when ER stress levels are mild, which is termed ER stress-induced autophagy. Further analysis is required to determine the threshold between PERK exerting protective self-adaptation and injurious apoptosis in myocardial I/R injury.

Conclusion

This study confirmed that DEX preconditioning reduced myocardial I/R injury and improved cardiac function by inhibiting PERK-mediated apoptosis pathway.

Acknowledgements

This study was supported by The Science and Technology Development Plan of Guizhou Province (grant no.2016[1175]), and The Postgraduate Research Fund of Guizhou Province (grant no. KYJJ2017034).

Author Contributions

Conception and design of the research: Chen Y, Chen H; Acquisition of data: Chen Y, Cao S, Chen H, Yin C, Xu

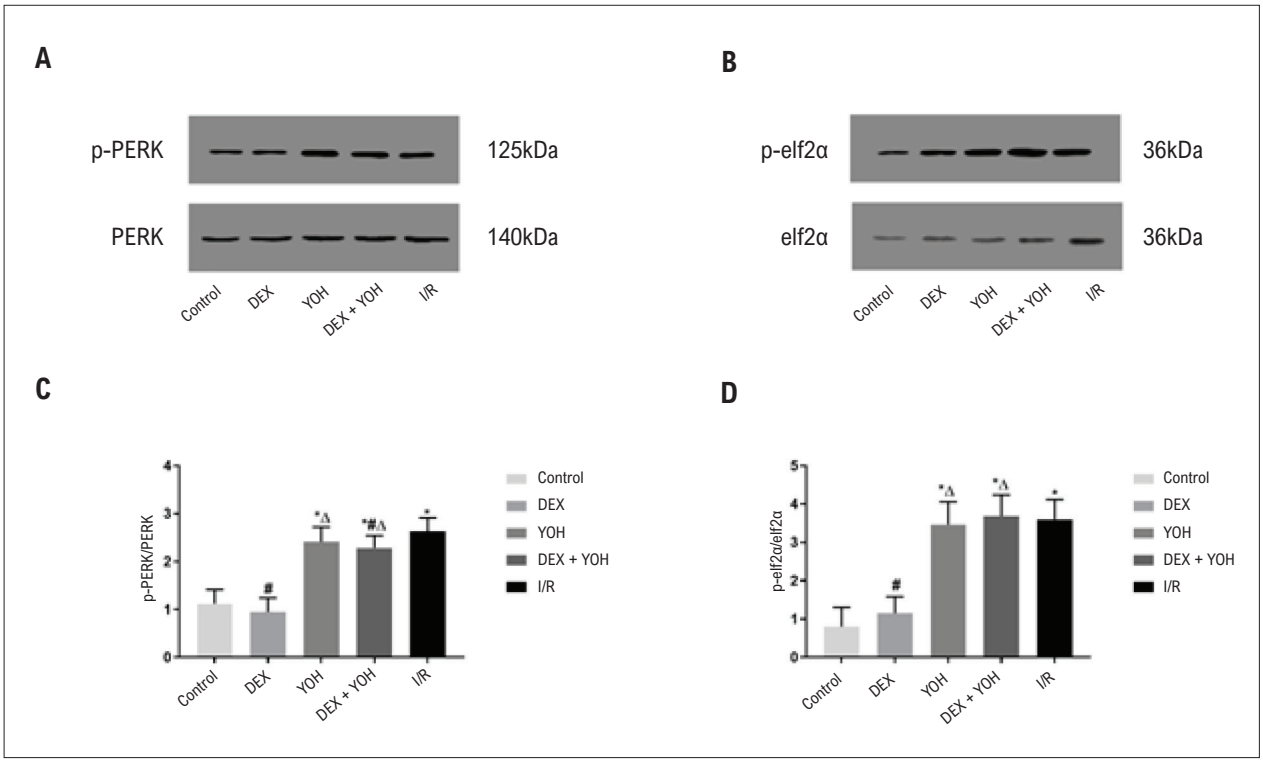

Figure 6 – *Effect of DEX on the expression of p-PERK and p-eIF2α. (A, B) Western-blotting detecting of PERK, p-PERK, eIF2α, p-eIF2α protein expression. (C, D) Analysis of the expression of PERK, p-PERK, eIF2α, p-eIF2α in control and I/R-induced isolated heart. Data are presented as the mean ± standard deviation. n=6. *P<0.05, vs. control group. #P<0.05, vs. I/R group, ΔP<0.05, vs. DEX group. I/R: ischemia-reperfusion. PERK: protein kinase R-like ER kinase, p-PERK: phosphorylation-protein kinase R-like ER kinase, eIF2a: eukaryotic initiation factor 2a, p-eIF2α: phosphorylation-eukaryotic initiation factor 2a.*

X, Yang Z; Analysis and interpretation of the data: Chen Y, Yang Z; Statistical analysis: Chen Y, Cao S, Yin C; Obtaining financing and Writing of the manuscript: Chen Y; Critical revision of the manuscript for intellectual content: Chen Y, Xu X.

Potential Conflict of Interest

No potential conflict of interest relevant to this article was reported.

Sources of Funding

This study was partially funded by The Science and Technology Development Plan of Guizhou Province (grant no.2016[1175]), and The Postgraduate Research Fund of Guizhou Province (grant no. KYJJ2017034).

Study Association

This study is not associated with any thesis or dissertation work.

Ethics approval and consent to participate

This study was approved by the Ethics Committee of the Experimental Animal Care and Use committee of Zunyi Medical University under the protocol number 1492, 2001. All the procedures in this study were in accordance with the 1975 Helsinki Declaration, updated in 2013.

References

1. Yellon DM, Hausenloy DJ. Myocardial reperfusion injury. *N Engl J Med*. 2007; *357* (11):1121-35.
2. Xu J, Hu H, Chen B, Yue R, Zhou Z, Liu Y, et al. Lycopene Protects against Hypoxia/Reoxygenation Injury by Alleviating ER Stress Induced Apoptosis in Neonatal Mouse Cardiomyocytes. *PloS one*. 2015; *10* (8):e0136443.
3. Ibanez B, Heusch G, Ovize M, Van de Werf F. Evolving therapies for myocardial ischemia/reperfusion injury. *J Am Coll Cardiol*. 2015; *65* (14):1454-71.
4. Hausenloy DJ, Yellon DM. Myocardial ischemia-reperfusion injury: a neglected therapeutic target. *J Clin Invest*. 2013; *123* (1):92-100.
5. Vinten-Johansen J. Involvement of neutrophils in the pathogenesis of lethal myocardial reperfusion injury. *Cardiovascular research*. 2004; *61*(3):481-97.
6. Park JL, Lucchesi BR. Mechanisms of myocardial reperfusion injury. *Ann Thorac Surg. 1999 Nov;68(5):1905-12*
7. Xiao Y, Ding L, Gu YH. [Progress of Acupuncture and Moxibustion Research on the Signal Transduction Pathways Involved in Cell Apoptosis in Myocardial Ischemia Reperfusion Injury]. *Zhen Ci Yan Jiu. 2017 Oct 25;42(5):463-6.*
8. Szegezdi E, Duffy A, O'Mahoney ME, Logue SE, Mylotte LA, O'Brien T, et al. ER stress contributes to ischemia-induced cardiomyocyte apoptosis. *Biochem Biophys Res Commun. 2006 Nov 3;349(4):1406-11.*

9. Qiu B, Hu S, Liu L, Chen M, Wang L, Zeng X, et al. CART attenuates endoplasmic reticulum stress response induced by cerebral ischemia and reperfusion through upregulating BDNF synthesis and secretion. *Biochem Biophys Res Commun. 2013 Jul 12;436(4):655-9.*

10. Wu CX, Liu R, Gao M, Zhao G, Wu S, Wu CF, et al. Pinocembrin protects brain against ischemia/reperfusion injury by attenuating endoplasmic reticulum stress induced apoptosis. *Neurosci Lett. 2013 Jun 24;546:57-62.*

11. Glembotski CC. Endoplasmic reticulum stress in the heart. *Circ Res. 2007 Nov 9;101(10):975-84.*

12. Wu H, Ye M, Yang J, Ding J. Endoplasmic reticulum stress-induced apoptosis: A possible role in myocardial ischemia-reperfusion injury. *Int J Cardiol. 2016 Apr 1;208:65-6.*

13. Wu H, Ye M, Yang J, Ding J. Modulating endoplasmic reticulum stress to alleviate myocardial ischemia and reperfusion injury from basic research to clinical practice: A long way to go. *Int J Cardiol. 2016 Nov 15;223:630-1.*

14. Liu Z, Lv Y, Zhao N, Guan G, Wang J. Protein kinase R-like ER kinase and its role in endoplasmic reticulum stress-decided cell fate. *Cell Death Dis. 2015 Jul 30;6(7):e1822.*

15. Venn M, Newman J, Grounds M. A phase II study to evaluate the efficacy of dexmedetomidine for sedation in the medical intensive care unit. *Intensive Care Med. 2003 Feb;29(2):201-7.*

16. Mason KP, Robinson F, Fontaine P, Prescilla R. Dexmedetomidine offers an option for safe and effective sedation for nuclear medicine imaging in children. *Radiology. 2013 Jun;267(3):911-7.*

17. Biccard B, Goga S, De Beurs J. Dexmedetomidine and cardiac protection for non-cardiac surgery: A meta-analysis of randomised controlled trials. *Anaesthesia. 2008 Jan;63(1):4-14.*

18. Wijeysundera DN, Bender JS, Beattie WS. Alpha-2 adrenergic agonists for the prevention of cardiac complications among patients undergoing surgery. *Cochrane Database Syst Rev. 2009 Oct 7;(4):CD004126.*

19. Okada H, Kurita T, Mochizuki T, Morita K, Sato S. The cardioprotective effect of dexmedetomidine on global ischaemia in isolated rat hearts. *Resuscitation. 2007 Sep;74(3):538-45.*

20. Dong J, Guo X, Yang S, Li L. The effects of dexmedetomidine preconditioning on aged rat heart of ischaemia reperfusion injury. *Res Vet Sci. 2017 Oct;114:489-92.*

21. Cai Y, Xu H, Yan J, Zhang L, Lu Y. Molecular targets and mechanism of action of dexmedetomidine in treatment of ischemia/reperfusion injury. *Mol Med Rep. 2014 May;9(5):1542-50.*

22. Liu XH, Zhang ZY, Sun S, Wu XD, Ischemic postconditioning protects myocardium from ischemia/reperfusion injury through attenuating endoplasmic reticulum stress. *Shock. 2008 Oct;30(4):422-7.*

23. Rao RV, Peel A, Logvinova A, del Rio G, Hermel E, Yokota T, et al. Coupling endoplasmic reticulum stress to the cell death program: role of the ER chaperone GRP78. *FEBS Lett. 2002 Mar 13;514(2-3):122-8.*

24. Wang ZV, Deng Y, Gao N, Pedrozo Z, Li DL, Morales CR, et al. Spliced X-box binding protein 1 couples the unfolded protein response to hexosamine biosynthetic pathway. *Cell. 2014 Mar 13;156(6):1179-92.*

25. Bi X, Zhang G, Wang X, Nguyen C, May HI, Li X, et al. Endoplasmic Reticulum Chaperone GRP78 Protects Heart From Ischemia/Reperfusion Injury Through Akt Activation. *Circ Res. 2018 May 25;122(11):1545-1554.*

26. Harding HP, Zhang Y, Bertolotti A, Zeng H, Ron D. Perk is essential for translational regulation and cell survival during the unfolded protein response. *Mol Cell. 2000 May;5(5):897-904.*

27. Yu L, Li B, Zhang M, Jin Z, Duan W, Zhao G, et al. Melatonin reduces PERK-eIF2alpha-ATF4-mediated endoplasmic reticulum stress during myocardial ischemia-reperfusion injury: role of RISK and SAFE pathways interaction. *Apoptosis. 2016 Jul;21(7):809-24.*

28. Degabriele NM, Griesenbach U, Sato K, Post MJ, Zhu J, Williams J, et al. Critical appraisal of the mouse model of myocardial infarction. *Exp Physiol. 2004 Jul;89(4):497-505.*

29. Cao S, Liu Y, Wang H, Mao X, Chen J, Liu J, et al. Ischemic postconditioning influences electron transport chain protein turnover in Langendorff-perfused rat hearts. *PeerJ. 2016 Feb 16;4:e1706.*

30. Lai E, Teodoro T, Volchuk A. Endoplasmic reticulum stress: signaling the unfolded protein response. *Physiology (Bethesda). 2007 Jun;22:193-201.*

31. Tabas I, Ron D. Integrating the mechanisms of apoptosis induced by endoplasmic reticulum stress. *Nat Cell Biol. 2011 Mar;13(3):184-90.*

32. Vaughn LS, Snee B, Patel RC. Inhibition of PKR protects against tunicamycin-induced apoptosis in neuroblastoma cells. *Gene. 2014 Feb 15;536(1):90-6.*

33. Locker N, Easton LE, Lukavsky PJ. HCV and CSFV IRES domain II mediate eIF2 release during 80S ribosome assembly. *EMBO J. 2007 Feb 7;26(3):795-805.*

34. Thompson SR, Gulyas KD, Sarnow P. Internal initiation in Saccharomyces cerevisiae mediated by an initiator tRNA/eIF2-independent internal ribosome entry site element. *Proc Natl Acad Sci U S A. 2001 Nov 6;98(23):12972-7.*

35. Chambers JE, Dalton LE, Clarke HJ, Malzer E, Dominicus CS, Patel V, et al. Actin dynamics tune the integrated stress response by regulating eukaryotic initiation factor 2alpha dephosphorylation. Elife. 2015 Mar 16;4:e04872.

36. Chen Y, Gao H, Yin Q, Chen L, Dong P, Zhang X, et al. ER stress activating ATF4/CHOP-TNF-alpha signaling pathway contributes to alcohol-induced disruption of osteogenic lineage of multipotential mesenchymal stem cell. *Cell Physiol Biochem. 2013;32(3):743-54.*

37. Su N, Kilberg MS. C/EBP homology protein (CHOP) interacts with activating transcription factor 4 (ATF4) and negatively regulates the stress-dependent induction of the asparagine synthetase gene. *J Biol Chem. 2008 Dec 12;283(50):35106-17.*

38. Cao J, Dai DL, Yao L, Yu HH, Ning B, Zhang Q, et al. Saturated fatty acid induction of endoplasmic reticulum stress and apoptosis in human liver cells via the PERK/ATF4/CHOP signaling pathway. *Mol Cell Biochem. 2012 May;364(1-2):115-29.*

39. Xu Q, Chen C, Lin A, Xie Y. Endoplasmic reticulum stress-mediated membrane expression of CRT/ERp57 induces immunogenic apoptosis in drug-resistant endometrial cancer cells. *Oncotarget. 2017 May 8;8(35):58754-64*

40. Qing G, Li B, Vu A, Skuli N, Walton ZE, Liu X, et al. ATF4 regulates MYC-mediated neuroblastoma cell death upon glutamine deprivation. *Cancer Cell. 2012 Nov 13;22(5):631-44.*

41. Minamino T, Kitakaze M. ER stress in cardiovascular disease. *J Mol Cell Cardiol. 2010 Jun;48(6):1105-10.*

42. Yang YF, Peng K, Liu H, Meng XW, Zhang JJ, Ji FH. Dexmedetomidine preconditioning for myocardial protection in ischaemia-reperfusion injury in rats by downregulation of the high mobility group box 1-toll-like receptor 4-nuclear factor kappaB signalling pathway. *Clin Exp Pharmacol Physiol. 2017 Mar;44(3):353-61.*

Original Article

Preconditioning in Ischemia-Reperfusion Lesion

Mariana Gatto,[1] Gustavo Augusto Ferreira Mota,[1] Luana Urbano Pagan,[1] Mariana Janini Gomes,[2] Marina Politi Okoshi[1]

Departamento de Clínica Médica - Faculdade de Medicina de Botucatu - Universidade Estadual Paulista (UNESP),[1] Botucatu, SP – Brazil
Brigham and Women's Hospital, Harvard Medical School,[2] Boston, MA – USA

Short Editorial related to the article: Dexmedetomidine Preconditioning Reduces Myocardial Ischemia-Reperfusion Injury in Rats by Inhibiting the PERK Pathway

Ischemic heart disease is characterized by a decrease in myocardial blood flow, which reduces the relationship between oxygen supply and demand. The condition has attracted the attention of the scientific community due to its high incidence, elevated morbidity and mortality, and high therapeutic cost.[1] The treatment primarily relies on myocardial revascularization. Paradoxically, reperfusion and restoration of blood flow can cause additional damage, called myocardial ischemia-reperfusion (IR) injury.[2] Several mechanisms are involved in the IR injury, such as ionic homeostasis change, intracellular calcium transient alteration, metabolic and mitochondrial dysfunction, inflammation, and reactive oxygen species increase.[3,4] These factors may contribute to an increase in the myocardial necrosis size, post-ischemia heart failure, and death.[3]

First identified in the mid-1980s, ischemic preconditioning is a process whereby repeated application of short periods of ischemia alternating with reperfusion protect the myocardium from longer ischemic insults, therefore reducing the infarction size.[5,6] The beneficial effect of ischemic preconditioning was shown in angina patients; when evolving to myocardial infarction, they had a smaller infarcted area and a better clinical prognosis than previously asymptomatic patients.[7,8] Additionally, preconditioning of rats with acute physical stress prior to the IR insult reduced infarct size and improved hemodynamic parameters.[9]

Currently, methods to induce ischemia-reperfusion have been used experimentally to assess whether different pharmacological and non-pharmacological therapies are effective in protecting the heart from ischemia and reperfusion injury. However, investigations to evaluate potential drugs, such as atorvastatin, anti-inflammatory medicines, or antioxidants did not result in cardioprotection after myocardial ischemia.[10] The CIRCUS multicenter clinical trial evaluated the effects of cyclosporine A administration before revascularization with percutaneous coronary intervention in acute myocardial infarction patients. Despite a reduction in the infarcted area, there was no long-term clinical improvement.[11] Currently, there are no specific drugs to prevent or attenuate IR injury.

Dexmedetomidine (DEX) is an α2-adrenergic receptor agonist used in clinical practice mainly to induce analgesia and sedation. Preconditioning with DEX improved left ventricular function in rats.[12] However, molecular mechanisms related to DEX-induced cardioprotection are still not fully understood. In this edition of ABC, we read with great interest the study by Chen et al.[13] evaluating the protective effects of DEX administration prior to myocardial ischemia-reperfusion in rats. DEX treatment improved hemodynamic and cardiac function variables and attenuated the infarcted area compared to the untreated animals. Cardiac improvement was combined with reduced myocardial apoptosis, assessed by morphological analysis, and inhibited expression of proteins of the apoptotic pathway PERK/eIF2α/TCF-4/CHOP. The authors also observed a decrease in the expression of the GRP78 protein, an important marker of endoplasmic reticulum stress.

The results are exciting and show the need for additional studies to better clarify the molecular effects of dexmedetomidine on cardioprotection after myocardial injury induced by ischemia followed by reperfusion.

Keywords

Physical Conditioning, Drug Therapy; Animal; Myocardial Reperfusion; Myocardial Ischemia; Apoptosis, Rats.

Mailing Address: Mariana Gatto •
Universidade Estadual Paulista Júlio de Mesquita Filho Campus de Botucatu Faculdade de Medicina - Rua Prof. Armando Alves, s/n. Postal Code 18618-687, Rubião Junior, Botucatu, SP - Brazil
E-mail: mariana.gatto@unesp.br

DOI: https://doi.org/10.36660/abc.20210908

References

1. Jensen RV, Hjortbak MV, Bøtker HE. Ischemic Heart Disease: An Update. Semin Nucl Med. 2020 May;50(3):195–207.
2. Hausenloy DJ, Yellon DM. Ischaemic conditioning and reperfusion injury. Nat Rev Cardiol. 2016 Apr;13(4):193–209.
3. Sprick JD, Mallet RT, Przyklenk K, Rickards CA. Ischaemic and hypoxic conditioning: potential for protection of vital organs. Exp Physiol. 2019;104(3):278–94.
4. Xu J, Hu H, Chen B, Yue R, Zhou Z, Liu Y, et al. Lycopene Protects against Hypoxia/Reoxygenation Injury by Alleviating ER Stress Induced Apoptosis in Neonatal Mouse Cardiomyocytes. PLoS One. 2015;10(8):e0136443.
5. Murry CE, Jennings RB, Reimer KA. Preconditioning with ischemia: a delay of lethal cell injury in ischemic myocardium. Circulation. 1986 Nov;74(5):1124–36.
6. Przyklenk K, Bauer B, Ovize M, Kloner RA, Whittaker P. Regional ischemic "preconditioning" protects remote virgin myocardium from subsequent sustained coronary occlusion. Circulation. 1993 Mar;87(3):893–9.
7. Muller DW, Topol EJ, Califf RM, Sigmon KN, Gorman L, George BS, et al. Relationship between antecedent angina pectoris and short-term prognosis after thrombolytic therapy for acute myocardial infarction. Thrombolysis and Angioplasty in Myocardial Infarction (TAMI) Study Group. Am Heart J. 1990 Feb;119(2 Pt 1):224–31.
8. Eitel I, Thiele H. Cardioprotection by pre-infarct angina: training the heart to enhance myocardial salvage. Eur Hear journal Cardiovasc Imaging. 2013 Nov;14(11):1115–6.
9. Imani A, Parsa H, Chookalaei LG, Rakhshan K, Golnazari M, Faghihi M. Acute Physical Stress Preconditions the Heart Against Ischemia/Reperfusion Injury Through Activation of Sympathetic Nervous System. Arq Bras Cardiol. 2019;113(3):401–8.
10. Hausenloy DJ, Erik Bøtker H, Condorelli G, Ferdinandy P, Garcia-Dorado D, Heusch G, et al. Translating cardioprotection for patient benefit: position paper from the Working Group of Cellular Biology of the Heart of the European Society of Cardiology. Cardiovasc Res. 2013 Apr 1;98(1):7–27.
11. Cung T-T, Morel O, Cayla G, Rioufol G, Garcia-Dorado D, Angoulvant D, et al. Cyclosporine before PCI in Patients with Acute Myocardial Infarction. N Engl J Med 2015 Sep 10;373(11):1021–31.
12. Dong J, Guo X, Yang S, Li L. The effects of dexmedetomidine preconditioning on aged rat heart of ischaemia reperfusion injury. Res Vet Sci. 2017 Oct;114:489–92.
13. Chen Y, Cao S, Chen H, Yin C, Xu X, Yang Z. Dexmedetomidine Preconditioning Reduces Myocardial Ischemia-Reperfusion Injury in Rats by Inhibiting the PERK Pathway. Arq Bras Cardiol. 2021; 117(6):1134-1144.

Cardioprotective Effect of Maternal Supplementation with Resveratrol on Toxicity Induced by Doxorubicin in Offspring Cardiomyocytes

Verônica Bidinotto Brito,[1,2] Leopoldo Vinicius Martins Nascimento,[1] Dinara Jaqueline Moura,[1] Jenifer Saffi[1]
Universidade Federal de Ciências da Saúde de Porto Alegre,[1] Porto Alegre, RS – Brazil
Faculdades Integradas de Taquara,[2] Taquara, RS – Brazil

Abstract

Background: **Doxorubicin (DOX) is frequently used to treat many types of cancers, despite its dose-dependent cardiotoxicity. Alternatively, resveratrol is a polyphenol that has shown useful cardioprotective effects in many heart dysfunction models.**

Objective: **This study investigated whether resveratrol treatment in pregnant rats protects against doxorubicin-induced toxicity in offspring cardiomyocytes.**

Methods: **Wistar rats (n=8) were supplemented with dietary resveratrol during pregnancy. Upon the offspring's birth, hearts (9-11) were used to obtain the primary culture of cardiomyocytes. DOX-induced cardiotoxicity and the effects of resveratrol supplementation were evaluated by oxidative stress markers, such as dichlorofluorescein diacetate oxidation, decrease in the activity of antioxidant enzymes, and oxidation of total sulfhydryl content, in addition to cell viability evaluation, DNA damage generation, and DNA damage repair response. A value of $p<0.05$ was considered statistically significant.**

Results: **Neonatal cardiomyocytes from resveratrol supplemented rats exhibiting an increase ($p<0.01$) in cell viability and lower ($p<0.0001$) apoptotic/necrotic cells after DOX treatment, which correlates with the activities of antioxidant enzymes and dichlorofluorescein production. Moreover, resveratrol protected cardiomyocytes from DOX-induced DNA damage, showing a decrease ($p<0.05$) in DNA breaks induced by oxidative stress, evaluated by the activity of DNA-repair enzymes endonuclease III and formamidopyrimidine glycosylase. Supplementation with resveratrol increased ($p<0.05$) the expression of the repair protein Sirt6 in the cardiomyocytes of the pups.**

Conclusion: **This research indicates that supplementation with resveratrol during the gestational period has a notable cardioprotective effect on the offspring's heart against DOX-induced toxicity, which may well be due to its antioxidant function, and the increase in the DNA damage repair response.**

Keywords: **Rats; Resveratrol; Doxorubicin; Cardiomyocytes; DNA Repair Enzymes.**

Introduction

Anthracycline doxorubicin (DOX) is a chemotherapeutic agent generally used to treat leukemia and a wide range of solid tumors.[1] Its cytotoxic action in tumor cells is related to topoisomerase II inhibition; DNA intercalation and damage, producing double-strand breaks; and an increase in the generation of free radicals, which compromises the replication and transcription process.[2] Recently, DOX has been proven to evict histones from specific regions in the genome, causing chromatin damage with consequent epigenomic and transcriptional alterations.[3]

The treatment with DOX can cause severe side effects, showing a limited therapeutic action due its strong cardiotoxicity, which can lead to dose-dependent cardiomyopathy.[4] At the intracellular level, many pathways may be involved in DOX-induced toxicity. In many of these, reactive oxygen species (ROS) generated by DOX metabolism play an important role in the outcome of myocardial dysfunction due to oxidative stress.[5]

It is currently unclear whether the adverse effects of treatment with DOX are necessary for its anti-tumor efficacy. With a look at its cardiotoxicity, some strategies to reduce toxicity have been investigated, but to date the iron chelating agent dexrazoxane is clinically an alternative method for preventing DOX-induced cardiotoxicity.[6]

Therefore, the present challenge is to design a cardioprotective protocol for short or long treatments with DOX, without hampering its antitumor activity. Many therapeutic strategies, such as supplementation with antioxidants or an increase in antioxidant capacity by exercise, have already been proposed to restrain DOX toxicity.[7,8] Remarkably, recently published data by our research group have demonstrated that maternal

Mailing Address: Verônica Bidinotto Brito •
Universidade Federal de Ciências da Saúde de Porto Alegre - Rua Sarmento Leite, 245. Postal Code 90050-170, Porto Alegre, RS – Brazil
E-mail: veronicab@ufcspa.edu.br
Manuscript received July 23, 2020, revised manuscript December 01, 2020, accepted January 27, 2021

DOI: https://doi.org/10.36660/abc.20200752

exercise during pregnancy is able to reduce the DOX-induced cardiotoxic effects on cardiomyocytes of rat pups.[9]

In line with this, resveratrol is a polyphenolic compound that has received attention due to its potential protection against cardiovascular diseases.[10] Its cardiovascular benefits are related to the effects on biological systems - preventing platelet aggregation,[11] decreasing the expression of nitric oxide synthase,[12] exerting antioxidant effects, and scavenging free radicals.[13] The global demand for more reasonable therapeutics has identified important features for human health in resveratrol associated with cost-effectiveness: low toxicity and high availability.[14] Moreover, the interest in this bioactive compound recently increased after the identification of its protective action against skin cancer.[15]

Bioactive molecules present in the rats' maternal diet have received recent importance due their participation in the offspring's metabolism reprograming.[16,17] As resveratrol crosses the placental membrane, supplementation by the mother during pregnancy has already been associated with beneficial effects in experimental models, such as preventing embryo death in the course of gestational diabetes[18] and controlling hypertension in the progeny of spontaneously hypertensive animals.[19] However, the cardioprotective effect on the offspring of resveratrol present in the maternal diet has not yet been investigated.

Therefore, considering the bioactive effects of resveratrol on cardiovascular diseases, this study tested the hypothesis that resveratrol, present in the maternal diet during the gestational period, has a cardioprotective effect on DOX-induced toxicity in an offspring cardiomyocyte culture through its possible effects on the antioxidant defense system and the response to DNA damage.

Methods

Animals

Adult female and male Wistar rats (Center of Animals Reproduction of the UFCSPA), weighing 70-100 g were housed under controlled light, temperature, and humidity conditions (12h light/dark period, at 22ºC ± 2, and 55% ± 5 relative humidity), with water and standard diet *ad libitum*. This research was conducted according to national and institutional guidelines on the use of animals for science, approved by the UFCSPA Ethics Committee, and logged under protocol number 183/13.

Experimental protocol

The mating procedure was conducted after the first estrous period. On the subsequent morning after the mating procedure, vaginal smears were analyzed to detect spermatozoon, which was the confirmation of the gestational day zero. Subsequently, the females were assigned to the following groups:

Control group (C-G, n=8): without supplementation with resveratrol. These received saline solution with 0.05% of Tween 80 by gavage, and were manipulated once a day, 5 days/week, during 21 gestational days, totaling 15 days of gavage.

Resveratrol group (RV-G, n=8): supplemented with resveratrol 2.5 mg/Kg body weight[20] (dispersed in saline with 0.05% of Tween 80)[21] by gavage (once a day, 5 days/week, during 21 gestational days, totaling 15 days of supplementation).

For the estimation of sample size, the research of Singh et al.[18] was used as the reference. For this, a two tailed-test was applied, with a significance level at 5% and a power of 95%. A minimal difference between groups of 12 ŋmol/mg protein was estimated, with a 0.096 standard deviation, to result in a significant evaluation of a sulfhydryl test, used for sample estimation. The sample size estimation resulted in eight animals per group.

At the end of the gestational period, pups up to 3 days old were euthanized and their hearts[9-11] were used to obtain a pool of cardiomyocytes used for the primary culture, as demonstrated in a simplified time line in Figure 1.

Cardiomyocyte culture

The primary culture from hearts of neonatal rats was obtained as previously described by our research group.[9]

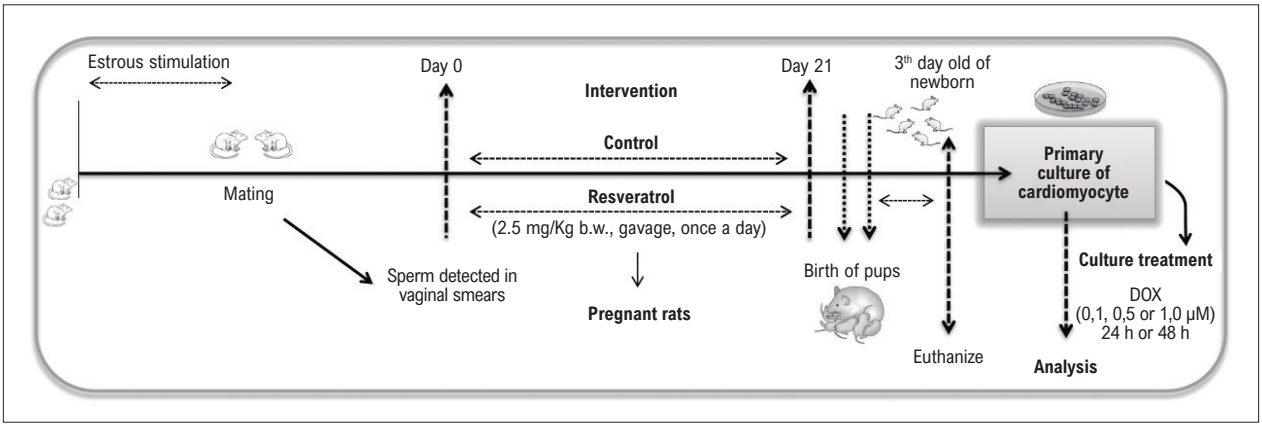

Figure 1 – *Simplified time line of the experimental protocol.*

Briefly, the hearts were submitted to repeated cycles of an enzymatic digestion in a buffer containing pancreatin and BSA, at 37°C. At the end of the cycles, the pool of cells was plated in a 75 cm^2 bottle culture for fibroblast adhesion. The cell suspension was aspirated, centrifuged, and plated in culture plates treated with gelatin (0.1% in PBS) for cardiomyocyte adhesion. When the cells had acquired confluence, the culture was treated with DOX (0.1, 0.5 or 1.0 μM) for 24 or 48 h for the analysis described below. All experiments were conducted in triplicates to ensure the accuracy of the results.

Assay of cell viability and mechanisms of death

The trypan blue (TB) test was used to evaluate the viability of cells.[22] The number of viable and dead cells was counted in an Automated Cell Counter (Countess®), which enables the estimation of the percentage of viable cells (ratio of viable cells/total cells). Thereafter, the mechanism of death was evaluated by the flow cytometric analysis. After DOX treatment, the cardiomyocyte culture was washed, centrifuged, and resuspended in binding buffer (100 μL) with Annexin V-PE (3 μL) and 7-AAD (3 μL), and then incubated in the dark for 15 min. Analyses by flow cytometry, considering 5,000 events/sample, were used to access the viable, apoptotic, or necrotic cells (FACS Calibur with CellQuest software).

DNA damage detection

The DOX-induced genotoxicity was assessed by the DNA damage index, through the previously described alkaline comet assay.[23,24] After treatment, the cardiomyocyte culture was washed, trypsinized, centrifuged, and resuspended in PBS. Thirty μL of cell suspension was dissolved in 0.75% agarose (low melting) which was distributed on a slide pre-covered with 1% agarose (normal melting point). Microscope slides were then incubated in a lysis solution during 24 hours at 4°C. To evaluate the presence of oxidative damage in DNA, slides were withdrawn from the lysis solution, washed, and incubated with repair enzymes - endonuclease III (EndoIII) or formamidopyrimidine glycosylase (FPG) - (300 mU/gel; 45 min 37°C). After lysis and/or incubation with EndoIII or FPG, DNA was unwound for 20 min in a horizontal electrophoresis system containing fresh alkaline buffer (300 mM NaOH/1 mM EDTA at pH 13.0). The DNA expression alkali-labile sites occurred by migration of DNA damage under an electric current (25 V; 300 mA; 0.9 V/cm). Slides were neutralized and stained beforehand as previously described;[25] 100 cells/slide were visualized by optical microscopy and scored according to the method previously described above.[26]

Cardiomyocyte protein extracts

After 24 or 48 hours of treatment with DOX, the cell medium was removed and protein extracts of cardiomyocytes were prepared as previously described,[9] which were used for all additional analyses described below.

Quantification of oxidative stress

Dichlorofluorescein diacetate (H_2DCF-DA) is a probe that is hydrolyzed by esterases of intracellular medium to form a non-fluorescent H_2DCF that is oxidized by intracellular oxidants into a fluorescent dichlorofluorescein (DCF).[27] Briefly, H_2DCF-DA was incubated with cardiomyocyte protein extract as previously described,[9] and the intensity of fluorescence was measured in a microplate reader (SpectraMax M2e, Molecular Devices, California) at 480 ηm (EX) and 535 ηm (EM).

Antioxidant defense system

The activity of the antioxidant defense system of neonatal cardiomyocytes was evaluated by means of catalase (CAT) and superoxide dismutase (SOD) enzymatic activity, as previously described.[28,29] Total sulfhydryl content, which inversely correlated with the oxidative damage in proteins, was estimated by the method previously described.[30]

DNA damage response

The response of cardiomyocytes to DNA damage DOX-induced was assessed by immunoblotting analysis of Sirt6 (sirtuin6), a histone deacetylase that acts as a scaffold protein in DNA damage repair. For this assay, 25 μg of a cardiomyocyte protein were separated by a 12% SDS-PAGE in a previously described method.[31] Membranes were incubated with anti-sirt6 and actin (C-2), at 1:500. Blot was revealed using a chemiluminescence kit (ECL, Thermo Scientific). Optical densities of immunoblots were determined with the ImageJ 1.48v software (Wayne Rasband, National Institutes of Health, USA).

Protein quantification

Protein concentration of the protein extracts was determined as previously described.[32]

Statistical analysis

Data were analyzed using the Statistical Package for the Social Sciences (SPSS) version 16.0 (IBM Company, Armonk, NY, USA). Normal distribution and homogeneity of variances were evaluated by the Kolmogorov-Smirnov and Levene's tests, respectively. One-way Analysis of Variance (ANOVA) and Tukey post-hoc test were used by comparison between groups. Correlations were performed by Pearson's correlation coefficient. Data were expressed as mean ± standard error of mean (S.E.M) and a $p<0.05$ was considered significant.

Results

Resveratrol attenuated DOX-induced apoptosis and necrosis in neonatal cardiomyocytes

The effects of maternal supplementation with resveratrol during pregnancy were initially evaluated by the trypan blue (TB) exclusion test (Figure 2), which demonstrated a concentration-dependent DOX-induced cell death. However, supplementation with resveratrol during pregnancy protected neonatal cells from death induced after 48 h of DOX treatment with 1.0 or 0.5 μM DOX (Figure 2B), in relation to neonatal cardiomyocytes from non-supplemented rats.

Subsequently, the main mechanism of cardiomyocyte death was explored by flow cytometry (Figure 3). The results confirmed those obtained by TB assay, showing an increase in cardiomyocyte death related to DOX treatment, exhibiting the highest fraction

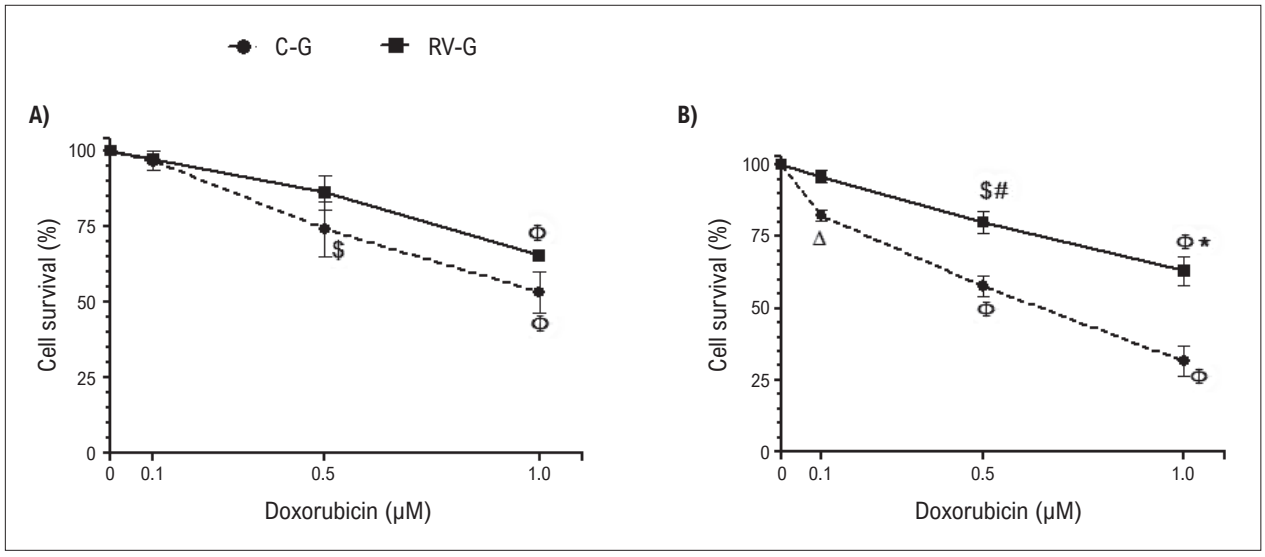

Figure 2 – Viability of neonatal cardiomyocytes exposed to DOX (0.1, 0.5 or 1.0 μM) for 24 h (A) or 48 h (B), by trypan blue (TB) exclusion test. Cardiomyocyte culture of the offspring from rats supplemented (2.5 mg/Kg) with resveratrol (RV-G) or the control group (C-G). Values are mean±S.E.M (n=8). Symbol * indicates p<0.001, # p<0.01, and & p<0.05 between RV-G and C-G. Symbol Φ indicates p<0.001, $ p<0.01, and Δ p<0.05 from control cells (not exposed to DOX), by One-Way ANOVA, Tukey post-hoc test.

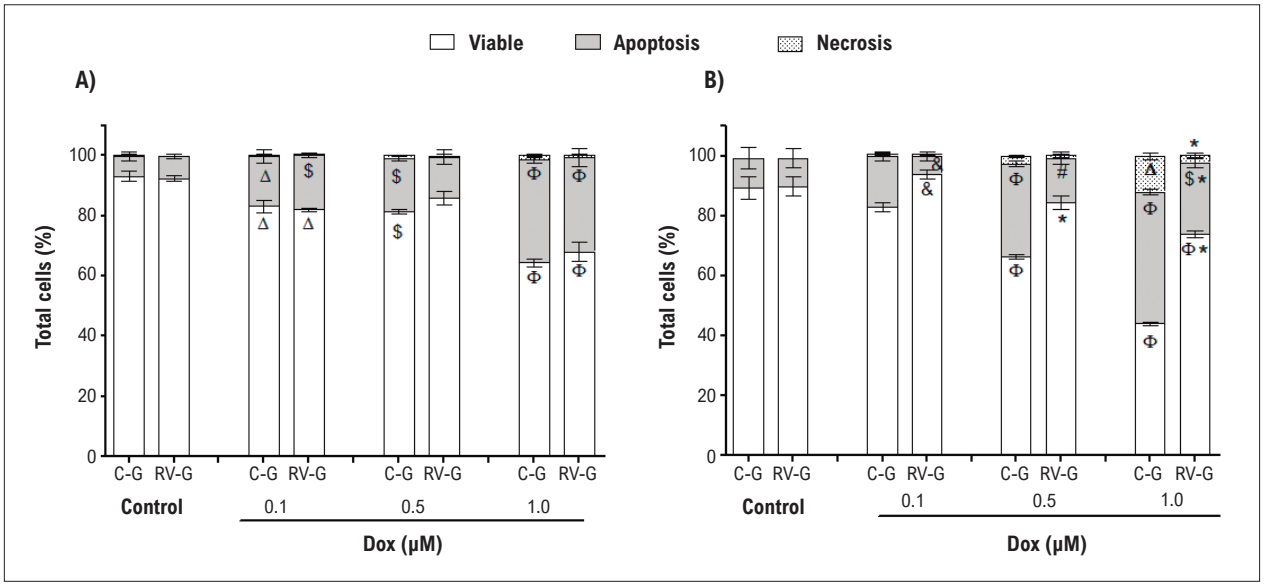

Figure 3 – *Cardiomyocyte culture of the offspring from rats supplemented (2.5 mg/Kg) with resveratrol (RV-G) or the control group (C-G) were analyzed by flow cytometry analysis. After 24 h (A) or 48 h (B) of DOX treatment (DOX (0.1, 0.5 or 1.0 μM), viability, apoptosis, or necrosis of neonatal cardiomyocytes were analyzed. Control indicates cells without DOX. Values are mean±S.E.M, n=8. Symbol * indicates p<0.001, # p<0.01, and & p<0.05 between RV-G and C-G. Symbol Φ indicates p<0.001, $ p<0.01, and Δ p<0.05 from control cells (not exposed to DOX), by One-Way ANOVA, Tukey post-hoc test.*

of cell death by apoptosis at a concentration of 1 μM DOX (p<0.001). These results also demonstrate that apoptosis is the main mechanism of death induced by DOX in neonatal cardiomyocytes (Figure 3A), corroborating previous results from our research group.[9] Moreover, the resveratrol protected neonatal cardiomyocytes against DOX-induced death 48 h after treatment, with an increase in viable cells (p<0.001) and decrease in apoptotic and necrotic cells (p<0.001) (Figure 3B).

Oxidative stress is attenuated in neonatal cells by gestational resveratrol supplementation

The most accepted mechanism for DOX-induced toxicity is the formation of ROS, which in turns leads to the formation of oxidative stress.[5] Figure 4A and B show that neonatal cardiomyocytes exposed to DOX showed an increase (p<0.001) in intracellular oxidant production, in relation to the Control (cells not exposed to DOX). Importantly,

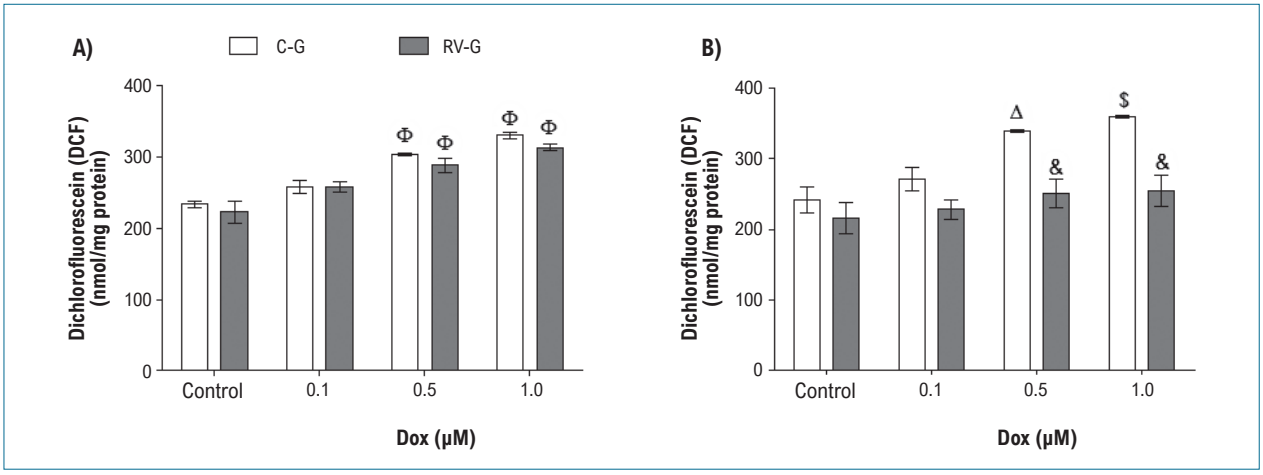

Figure 4 – *Oxidative stress in neonatal cardiomyocytes treated with DOX (0.1, 0.5 or 1.0 μM) for 24 h (A) or 48 h (B). Values are mean±S.E.M, n=8. Symbol & indicates p<0.05 between RV-G and C-G. Symbol Φ indicates p<0.001, $ p<0.01, and Δ p<0.05 from control cells (not exposed to DOX), by One-Way ANOVA, Tukey post-hoc test.*

supplementation of mothers with resveratrol during pregnancy attenuated ($p<0.05$) oxidative stress in neonatal cells after treatment with 0.5 or 1.0 μM DOX (Figure 4B) in relation to the control group (C-G). Moreover, cell viability and oxidative stress production, also measured by DCF oxidation, are inversely correlated, both at 24 and 48 h ($r=-0.8$, $p<0.0001$ and $r=-0.789$, $p<0.001$), respectively. Notably, a direct correlation between intracellular oxidative stress production and apoptosis ($r=0.836$, $p<0.0001$, $r=0.817$, $p<0.0001$) was observed after DOX treatment, 24 h and 48 h respectively.

Resveratrol reduces oxidative DNA damage DOX-induced in neonatal cardiomyocytes

The DOX-induced genotoxic stress was evaluated by the alkaline Comet assay, which detects alkali-labile sites and strand breaks in the DNA.[33] The results show an increase in DNA damage induced by DOX in neonatal cells from all groups of mothers (Figure 5A-B), which was concentration-dependent. However, gestational supplementation with resveratrol protected cardiomyocytes from DNA damage induced by DOX.

Considering that DOX-induced oxidative stress production was reduced ($p<0.05$) by resveratrol (Figure 4), the evaluation of the DNA damage related to the DOX-generated oxidative stress becomes an important question. Thus, the activity of DNA-repair enzymes of endonuclease III (EndoIII) and formamidopyrimidine glycosylase (FPG) were examined, which improve the Comet test specificity, recognizing damaged bases by oxidative stress and converting them into single-strand breaks.[26,34] Figure 5 (C-F) shows the magnitude of oxidative damage in the DNA caused by DOX treatment, which was recognized by the repair enzymes. Notably, neonatal cardiomyocytes from supplemented mothers exhibited a decrease ($p<0.001$) in oxidative damage observed in DNA. Additionally, resveratrol supplementation was able to decrease oxidative DNA damage of neonatal cardiomyocytes not exposed to DOX, both 24 and 48 h after DOX treatment.

Neonatal cardiomyocytes from resveratrol supplemented mothers showed a more efficient antioxidant defense system

With the purpose of evaluating whether resveratrol effects on oxidative stress generation and DNA damage are associated with an increase in the antioxidant defense system, the activities of CAT and SOD enzymes (Table 1) were examined, as was the total sulfhydryl content (Figure 6). DOX reduced SOD and CAT activities in neonatal cardiomyocytes from control mothers when compared to resveratrol supplemented neonatal cells (Table 1).

Correlation analysis demonstrated that CAT activity showed an inverse correlation with oxidative stress production ($r=-0.763$, $p<0.0001$ and $r=-0.808$, $p<0.0001$) both at 24 and 48 h after DOX treatment, respectively. The same effect was verified for SOD, with an inverse correlation with oxidative stress ($r=-0.527$, $p<0.004$ and $r=-0.671$, $p<0.0001$) at 24 and 48h of DOX treatment, respectively. Particularly, resveratrol blocked the decrease in total sulfhydryl content in neonatal cells, in both times of DOX treatment (Figure 6), without a protective effect at 1.0 μM DOX (Figure 6B).

Sirt6 expression and response to DNA damage are increased in cardiomyocytes from supplemented mothers

Immunoblotting analysis showed that resveratrol supplementation of rats during pregnancy induced an increase ($p<0.01$) in the expression of the Sirt6 protein of neonatal cardiomyocytes in relation to neonatal cells from the controls. Importantly, this increase in Sirt6 expression was dependent on the DOX concentration (Figure 7).

Discussion

The present study confirmed the hypothesis that resveratrol, present in the maternal diet during the gestational period, has a cardioprotective effect on DOX-induced toxicity in an offspring cardiomyocyte culture, through an increase in the antioxidant defense system and the response to DNA damage.

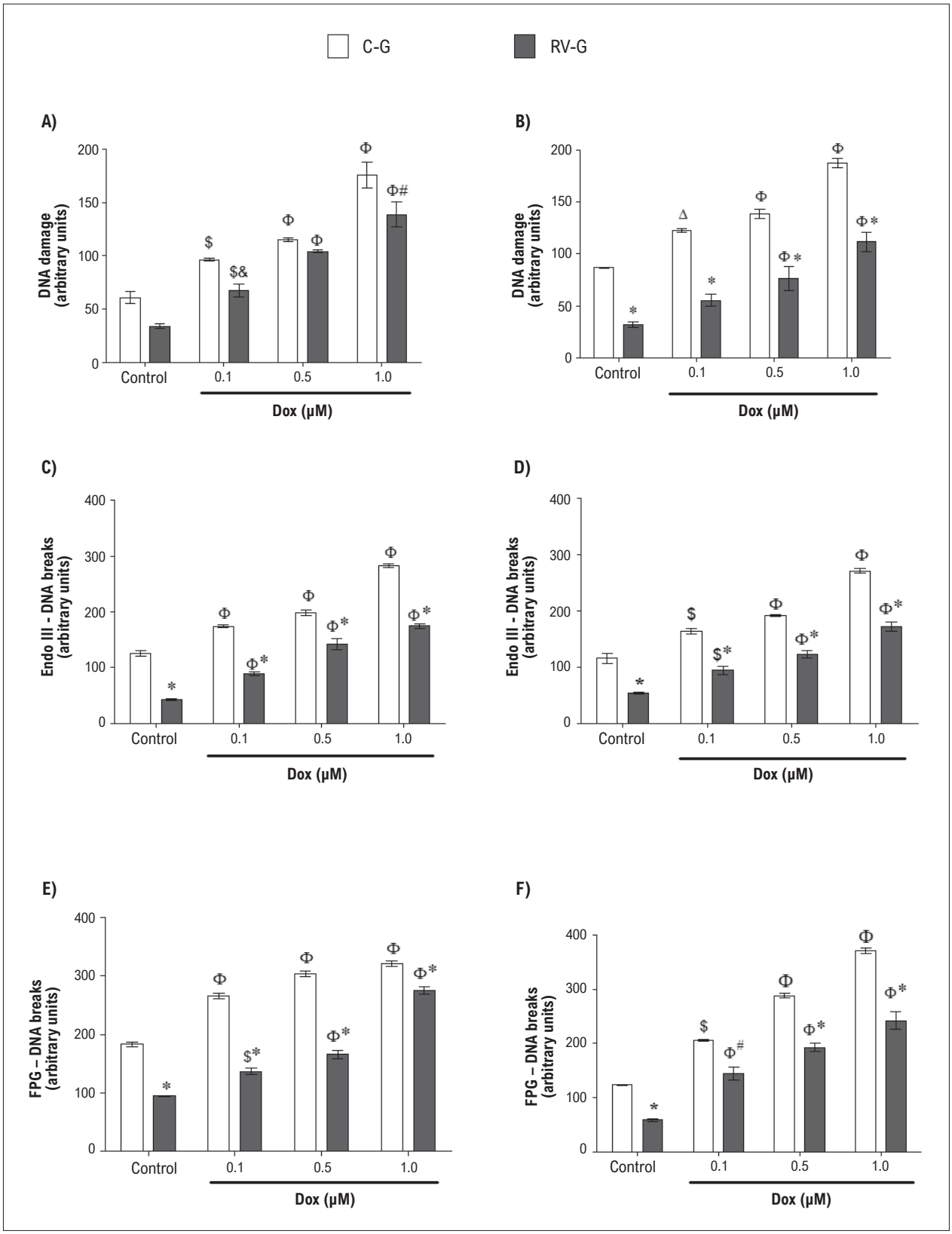

Figure 5 – *DNA damage in cardiomyocytes treated with DOX (0.1, 0.5 or 1.0 μM) for 24 h (A) or 48 h (B). Oxidative DNA damage was analyzed by endonuclease III (EndoIII) and formamidopyrimidine glycosylase (FPG) enzymes in cells treated with DOX for 24 h (C and E) or 48 h (D and F). Values are mean±S.E.M, n=8. Symbol * indicates p<0.001, # p<0.01, and & p<0.05 between RV-G and C-G. Symbol Φ indicates p<0.001, $ p<0.01, and Δ p<0.05 from control cells (not exposed to DOX), by One-Way ANOVA, Tukey post-hoc test.*

Table 1 – Effects of gestational supplementation with resveratrol on SOD and CAT activities of neonatal cardiomyocytes exposed to DOX

	Control	Resveratrol	Control	Resveratrol
	SOD (U/mg protein)			
	24 hours		48 hours	
Control	4.61 ± 0.31	6.26 ± 0.61*	4.46 ± 0.15	6.00 ± 0.73
0.1 µM DOX	3.90 ± 0.39	5.31 ± 0.19*	3.98 ± 0.05#	6.06 ± 0.50*
0.5 µM DOX	3.22 ± 0.42#	5.22 ± 0.37*	3.03 ± 0.37#	5.12 ± 0.42*
1.0 µM DOX	2.83 ± 0.20#	5.56 ± 0.32*	2.53 ± 0.54#	5.19 ± 0.69*
	CAT (U/mg protein)			
	24 hours		48 hours	
Control	12.15 ± 1.25	24.08 ± 1.31*	12.30 ± 0.54	27.11 ± 1.28*
0.1 µM DOX	6.16 ± 0.41#	13.00 ± 2.15*#	7.85 ± 0.59#	13.56 ± 1.31*#
0.5 µM DOX	4.04 ± 0.28#	9.47 ± 1.26*#	5.35 ± 0.36#	12.24 ± 1.94*#
1.0 µM DOX	2.62 ± 0.11#	8.78 ± 1.86*#	2.68 ± 0.75#	8.36 ± 0.80*#

*Cells were treated with DOX (0.1, 0.5 or 1.0 µM) during 24 or 48 h. Values are mean ± S.E.M (n=8). * indicates p < 0.05 between resveratrol and control group, and # indicates p < 0.05 from Control (cells without DOX), by One-Way ANOVA, Tukey post-hoc test.*

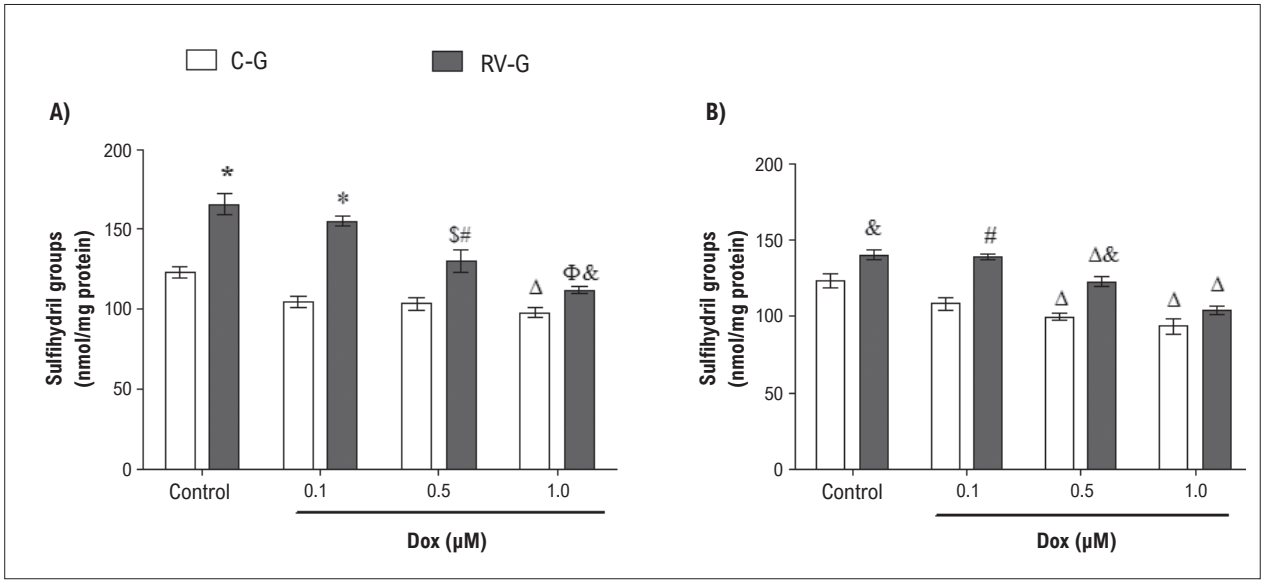

Figure 6 – *Total sulfhydryl groups of neonatal cardiomyocytes treated with DOX (0.1, 0.5 or 1.0 µM) for 24 h (A) or 48 h (B). Values are mean±S.E.M (n=8). Symbol * indicates p<0.001, # p<0.01, and & p<0.05 between RV-G and C-G. Symbol Φ indicates p<0.001, $ p<0.01, and Δ p<0.05 from control cells (not exposed to DOX), by One -Way ANOVA, Tukey post-hoc test.*

A concentration-related cardiotoxicity induced by DOX was observed in neonatal cardiomyocytes from non-supplemented mothers, with an increase in cell death. In accordance with previously elucidated mechanisms of cell toxicity induced by DOX, in this study, apoptosis was also the main mechanism of cardiomyocyte death. Maternal supplementation with 2.5 mg/Kg resveratrol per day, during the gestational period, protected neonatal heart against DOX-induced cardiotoxicity, with an increase in cell viability, also decreasing the apoptotic cells, which was correlated with the decrease in oxidative stress production both at 24 and 48 hours. Moreover, resveratrol prevented the decrease in DOX-induced SOD activity and led to an increment in CAT activity, in neonatal cells from supplemented mothers. Besides antioxidant enzymes, neonatal cardiomyocytes from resveratrol supplemented mothers exhibited an increase in total sulfhydryl content, thus protecting against the oxidative effects induced by DOX. These results are favorable to the hypothesis that maternal supplementation with resveratrol during pregnancy can modulate the responses to stressful agents of progeny.

DOX is a chemotherapeutic drug frequently used in clinics, despite its dose-related cumulative cardiotoxic

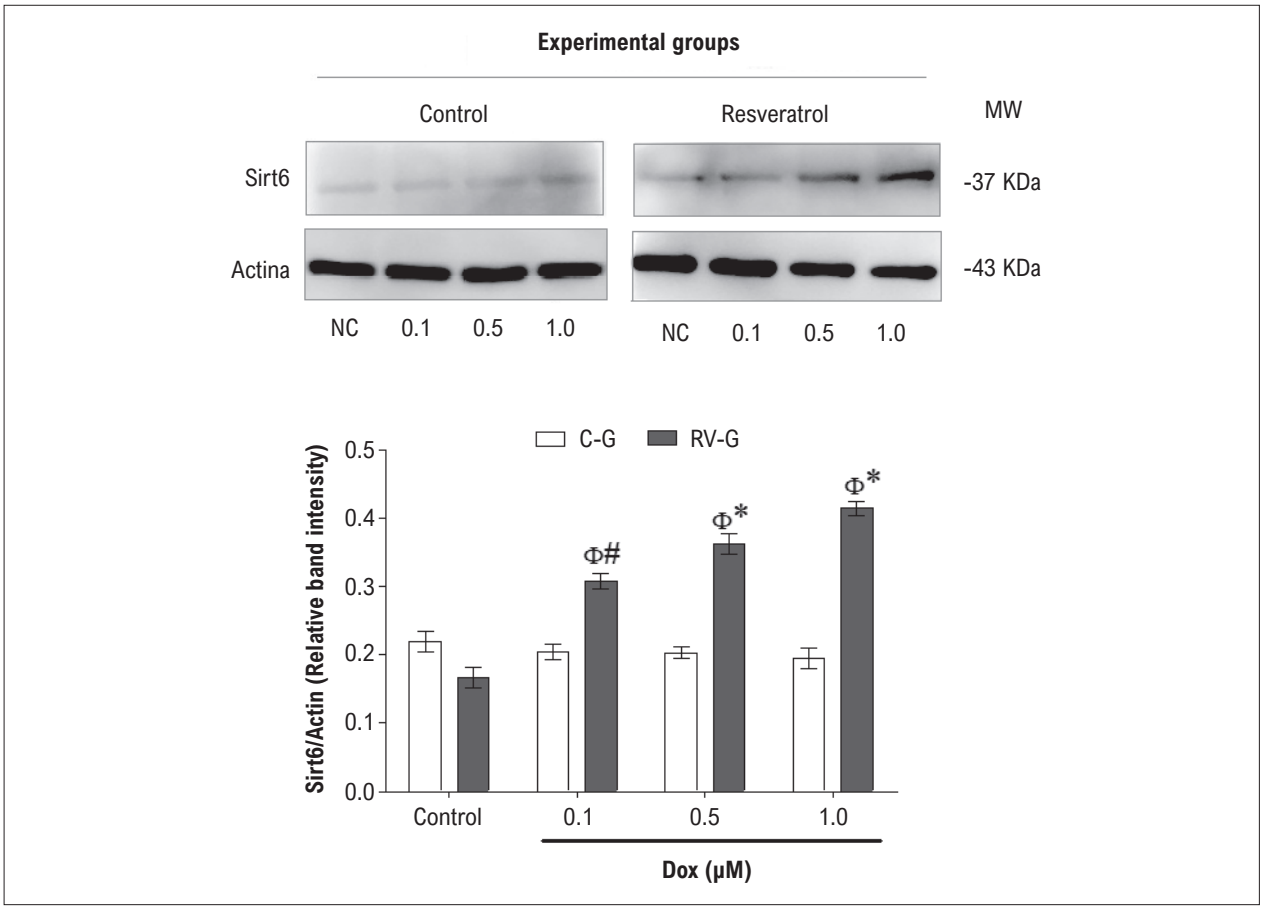

Figure 7 – *Sirt6 protein expression of neonatal cardiomyocytes treated with DOX (0.1, 0.5 or 1.0 μM) for 48 h. Bar graph corresponds to mean±SE.M of the quantification values of Sirt1/Actin ratio from all samples. Symbol * indicates p<0.001 and # p<0.01 between RV-G and C-G. Symbol Φ indicates p<0.001 from control cells (not exposed to DOX), by One-Way ANOVA, Tukey post-hoc test.*

effects.[1] Development of additional therapeutic strategies to reduce the treatment outcomes is essential, considering the increase in life expectancy for decades after anti-cancer therapy. Experimental and clinical studies, as well as preventive medicine, have highlighted the benefits of resveratrol on cardiovascular and metabolic diseases,[10] and more recently on the offspring of animals that received resveratrol during pregnancy.[18,19]

Structurally, resveratrol can be present in *cis* or *trans* isoforms, with a biological activity mainly related to *trans* isomer.[35] Due to the aromatic rings present in its structure, resveratrol acts as an antioxidant, scavenging hydroxyl radicals and the generation of oxidative stress.[36] Additionally, other protective effects on the cardiovascular system can be related to its scavenging action on H_2O_2, delaying the oxidative stress and preventing endothelial ROS-induced cell death.[37] Since resveratrol is able to cross the placental membrane, directly affecting the fetus,[18] it is possible that the cardioprotective effects observed in this study might be a direct action of resveratrol in the scavenging of DOX-induced ROS. Moreover, the decrease in oxidative stress production can also be due to an upregulation of the enzymatic and non-enzymatic antioxidant defense system, which in turn defuses the futile cycle of ROS production during DOX mitochondrial metabolization. In line with this, recent data published by our group demonstrated that an up-regulation of the antioxidant defense system in neonatal cardiomyocytes is induced by exercise during pregnancy and protects neonatal cells against toxicity induced by DOX.[9]

DOX forms adducts with DNA, which can activate DNA damage responses and induce cell death regardless of topoisomerase II.[38] DOX also acts as a topoisomerase II poisoning, generating double-strand DNA breaks and cell death.[39] Cell action of DOX also involves the chromatin damage, mediated through histone eviction at specific genomic sites.[3] By contrast, DOX can mediate cell death through the generation of oxidative stress that results in DNA damage and cell death.[2,40] It was recently proposed by Qiao et al.[41] that DOX-induced cardiotoxicity requires the combination of both cell activities, particularly the combination of DNA and chromatin damage induced by cardiotoxicity. Moreover, chromatin damage caused by the eviction of histones in the genome is highlighted as the essential action for the drug's chemotherapeutic efficacy, which must be uncoupled of double-strand breaks and DNA damage in cells, which together are responsible for the cardiotoxicity of DOX.[3,41]

In our research, neonatal cells treated with DOX exhibited an increase in oxidative DNA damage, evaluated by the activities of FPG and EndoIII enzymes, which was correlated with the increase in oxidative stress production generated by DOX. However, neonatal cells from supplemented mothers showed a reduction in DNA strand-breaks through EndoIII or FPG evaluation. This cardioprotection provided by resveratrol may well be due to its antioxidant profile, as mentioned above, since it is able to cross the placental barrier. However additional mechanisms can be involved, such as a regulation of DNA damage repair enzymes.

In line with this, Sirt6 is a histone deacetylase (HDAC) with a key role in DNA repair.[42,43] Our results demonstrated that neonatal cardiomyocytes, from supplemented rats exposed to DOX, showed an increase in Sirt6 expression, which can justify the protective action of resveratrol on the DNA damage induced in our model. Sirt6 is a scaffold protein that, following DNA damage, is attracted to strand break sites, activating DNA damage repair agents toward an efficient repair.[42,44] Moreover, Sirt6 binds to PARP-1, an enzyme with an important function in the regulation of cellular and subcellular processes, including DNA repair, cell cycle, gene expression, and cell death.[45,46]

Similarly to other class III HDACs, the activity of Sirt6 is dependent of NAD^+ - a coenzyme with a core role in the metabolic redox reactions.[47] This relationship between NAD^+ and Sirt6 in the heart is confirmed during a cardiac hypertrophy situation, where NAD^+ levels decrease and Sirt6 is inactivated.[44] The cardioprotection given by resveratrol in this model may well be due to the increase in NAD^+ levels, since the resveratrol inhibits mitochondrial ATP synthase activity by binding to its G-subunit, hindering mitochondrial ATP phosphorylation.[48] Consequently, resveratrol raises the ratio AMP/ATP, activating the energy-sensing AMPK (AMP-activated protein kinase),[49] and increases NAD^+, which act as a metabolic sensor to Sirt6 activation. It was also shown that resveratrol protects mouse embryonic fibroblasts against DOX-induced cardiotoxicity through the activation of AMPK and through a decrease in ROS production.[50]

However, Sirt6 expression was not changed in neonatal cardiomyocytes from the control group, which exhibited an increase in DOX-induced oxidative DNA-damage and oxidative stress production, suggesting that the lack of cardioprotection is dependent on Sirt6 expression. Notably, Sirt6 expression was not changed in the cardiomyocytes that were not exposed to DOX, regardless of maternal supplementation with resveratrol. As Sirt6 is viewed as a defense protein, which activates its defense pathways to survive under stressful situations, such as hypoxic damage to heart or cardiac hypertrophy,[44,51] it is possible that the DOX-induced toxicity on cardiomyocytes was the missing trigger.

Therefore, in this study, the beneficial effects of resveratrol on toxicity induced by DOX on the hearts of rat pups was demonstrated, for the first time through the supplementation of mothers during pregnancy. Regarding the antioxidant properties of resveratrol observed in this research, most of its cardioprotective effects were mediated by the overexpression of Sirt6 and the increase in DNA damage response, preserving the DNA integrity. These effects together with the modulation of antioxidant enzymes and the reduction in cellular oxidative stress, contribute to cardiomyocyte survival under DOX toxicity. However, additional studies are necessary to define the role of Sirt6 deacetylation targets, and epigenetics in the cardioprotective phenotype generated by resveratrol in offspring in this model of DOX cardiotoxicity.

Limitations

The main limitations of this study were the impossibility of using methods to quantify the dosage of resveratrol in the blood of the offspring, which could evidence or rule out the direct effect of resveratrol. In addition, the evaluation of Sirt6 deacetylation targets could clarify the role of epigenetic modulation in this model.

Conclusion

Our study demonstrates, for the first time, that supplementation of rats with low doses of resveratrol during pregnancy is able to protect the cardiomyocytes of pups against DOX-induced toxicity. This protection occurred through the regulation of oxidative stress by the antioxidant defense system and the increase in the DNA damage repair response, mediated by Sirt6 overexpression. Taken together, these results denote an important involvement of the maternal environment in the responses to stressful agents of progeny throughout life.

Acknowledgements

We wish thank to FAPERGS (Fundação de Amparo à Pesquisa do Estado do Rio Grande do Sul) and CAPES (Coordenação de Aperfeiçoamento de Pessoal de Nível Superior) for the fellowships granted to VBB and LVMN.

Author Contributions

Conception and design of the research: Brito VB, Moura DJ, Saffi J; Acquisition of data: Brito VB, Nascimento LVM; Analysis and interpretation of the data and Critical revision of the manuscript for intellectual content: Brito VB, Nascimento LVM, Moura DJ, Saffi J; Statistical analysis and Writing of the manuscript: Brito VB; Obtaining financing: Saffi J.

Potential Conflict of Interest

No potential conflict of interest relevant to this article was reported.

Sources of Funding

This study was partially funded by FAPERGS and CAPES.

Study Association

This article is part of the thesis of Doctoral submitted by Verônica Bidinotto Brito, from Universidade Federal de Ciências da Saúde de Porto Alegre.

References

1. Deng Y, Li F, He P, Yang Y, Yang J, Zhang Y, et al. Triptolide sensitizes breast cancer cells to Doxorubicin through the DNA damage response inhibition. Mol Carcinog. 2018 Jun 1;57(6):807–14.
2. Minotti G, Menna P, Salvatorelli E, Cairo G, Gianni L. Anthracyclines: molecular advances and pharmacologic developments in antitumor activity and cardiotoxicity. Pharmacol Rev. 2004 Jun;56(2):185–229.
3. Pang B, Qiao X, Janssen L, Velds A, Groothuis T, Kerkhoven R, et al. Drug-induced histone eviction from open chromatin contributes to the chemotherapeutic effects of doxorubicin. Nat Commun. 2013 Jan;4:1908. doi:https//doi.org/10.1038/ncomms2921
4. McGowan J V, Chung R, Maulik A, Piotrowska I, Walker JM, Yellon DM. Anthracycline Chemotherapy and Cardiotoxicity. Cardiovasc Drugs Ther. 2017 Feb 9;31(1):63–75.
5. Štěrba M, Popelová O, Vávrová A, Jirkovský E, Kovaříková P, Geršl V, et al. Oxidative Stress, Redox Signaling, and Metal Chelation in Anthracycline Cardiotoxicity and Pharmacological Cardioprotection. Antioxid Redox Signal. 2013 Mar 10;18(8):899–929.
6. Schlitt A, Jordan K, Vordermark D, Schwamborn J, Langer T, Thomssen C. Cardiotoxicity and oncological treatments. Dtsch Ärzteblatt Int. 2014 Mar 7;111(10):161–8.
7. Andreadou I, Mikros E, Ioannidis K, Sigala F, Naka K, Kostidis S, et al. Oleuropein prevents doxorubicin-induced cardiomyopathy interfering with signaling molecules and cardiomyocyte metabolism. J Mol Cell Cardiol. 2014;69:4–16.
8. Marques-Aleixo I, Santos-Alves E, Mariani D, Rizo-Roca D, Padrão AI, Rocha-Rodrigues S, et al. Physical exercise prior and during treatment reduces sub-chronic doxorubicin-induced mitochondrial toxicity and oxidative stress. Mitochondrion. 2015;20:22–33.
9. Brito VB, Nascimento LVM, Nunes RB, Moura DJ, Lago PD, Saffi J. Exercise during pregnancy decreases doxorubicin-induced cardiotoxic effects on neonatal hearts. Toxicology. 2016 Aug 10;368–369:46–57.
10. Catalgol B, Batirel S, Taga Y, Ozer NK. Resveratrol: French paradox revisited. Front Pharmacol. 2012 Jan;3:141.
11. Bonechi C, Lamponi S, Donati A, Tamasi G, Consumi M, Leone G, et al. Effect of resveratrol on platelet aggregation by fibrinogen protection. Biophys Chem. 2017 Mar;222:41–8.
12. Bariani MV, Correa F, Leishman E, Domínguez Rubio AP, Arias A, Stern A, et al. Resveratrol protects from lipopolysaccharide-induced inflammation in the uterus and prevents experimental preterm birth. MHR Basic Sci Reprod Med. 2017 Aug 1;23(8):571–81.
13. Zhang H-X, Duan G-L, Wang C-N, Zhang Y-Q, Zhu X-Y, Liu Y-J. Protective effect of resveratrol against endotoxemia-induced lung injury involves the reduction of oxidative/nitrative stress. Pulm Pharmacol Ther. 2014;27(2):150–5.
14. Aggarwal BB, Prasad S, Reuter S, Kannappan R, Yadev VR, Park B, et al. Identification of novel anti-inflammatory agents from Ayurvedic medicine for prevention of chronic diseases: "reverse pharmacology" and "bedside to bench" approach. Curr Drug Targets. 2011 Oct;12(11):1595–653.
15. Jin H, Wu G, Wu G, Bao Y. Combining the mammalian target of rapamycin inhibitor, rapamycin, with resveratrol has a synergistic effect in multiple myeloma. Oncol Lett. 2018 Mar 5;15(5):6257–64.
16. Mathias PCF, Elmhiri G, De Oliveira JC, Delayre-Orthez C, Barella LF, Tofolo LP, et al. Maternal diet, bioactive molecules, and exercising as reprogramming tools of metabolic programming. Eur J Nutr. 2014;53(3):711–22.
17. de Velasco PC, Chicaybam G, Ramos-Filho DM, dos Santos RMAR, Mairink C, Sardinha FLC, et al. Maternal intake of trans-unsaturated or interesterified fatty acids during pregnancy and lactation modifies mitochondrial bioenergetics in the liver of adult offspring in mice. Br J Nutr. 2017 Aug 11;118(1):1–12.
18. Singh CK, Kumar A, Hitchcock DB, Fan D, Goodwin R, LaVoie HA, et al. Resveratrol prevents embryonic oxidative stress and apoptosis associated with diabetic embryopathy and improves glucose and lipid profile of diabetic dam. Mol Nutr Food Res. 2011 Aug;55(8):1186–96.
19. Care AS, Sung MM, Panahi S, Gragasin FS, Dyck JRB, Davidge ST, et al. Perinatal Resveratrol Supplementation to Spontaneously Hypertensive Rat Dams Mitigates the Development of Hypertension in Adult OffspringNovelty and Significance. Hypertension. 2016 May;67(5):1038–44.
20. Movahed A, Yu L, Thandapilly SJ, Louis XL, Netticadan T. Resveratrol protects adult cardiomyocytes against oxidative stress mediated cell injury. Arch Biochem Biophys. 2012 Nov 15;527(2):74–80.
21. Venturini CD, Merlo S, Souto AA, Fernandes MDC, Gomez R, Rhoden CR. Resveratrol and red wine function as antioxidants in the nervous system without cellular proliferative effects during experimental diabetes. Oxid Med Cell Longev. 2010;3(6):434–41.
22. Robichová S, Slameňová D. Effects of vitamins C and E on cytotoxicity induced by N-nitroso compounds, N-nitrosomorpholine and N-methyl-N′-nitro-N-nitrosoguanidine in Caco-2 and V79 cell lines. Cancer Lett. 2002 Aug 8;182(1):11–8.
23. Singh NP, McCoy MT, Tice RR, Schneider EL. A simple technique for quantitation of low levels of DNA damage in individual cells. Exp Cell Res. 1988 Mar;175(1):184–91.
24. Hartmann A, Speit G. The contribution of cytotoxicity to DNA-effects in the single cell gel test (comet assay). Toxicol Lett. 1997 Feb 7;90(2–3):183–8.
25. Nadin SB, Vargas-Roig LM, Ciocca DR. A silver staining method for single-cell gel assay. J Histochem Cytochem. 2001 Sep;49(9):1183–6.
26. Hartmann A, Agurell E, Beevers C, Brendler-Schwaab S, Burlinson B, Clay P, et al. Recommendations for conducting the in vivo alkaline Comet assay. 4th International Comet Assay Workshop. Mutagenesis. 2003 Jan;18(1):45–51.
27. LeBel CP, Ischiropoulos H, Bondy SC. Evaluation of the probe 2′,7′-dichlorofluorescin as an indicator of reactive oxygen species formation and oxidative stress. Chem Res Toxicol. 1992 Mar;5(2):227–31.
28. Misra HP, Fridovich I. The role of superoxide anion in the autoxidation of epinephrine and a simple assay for superoxide dismutase therRole of superoxide anion in the epinephrine and a simple assay for superoxide dismutase. J Biol Chem. 1972;247(10):3170–5.
29. Aebi H. Catalase in vitro. Methods Enzymol. 1984 Jan;105:121–6.doi:10.1016/s0076-6879(84)0516-3
30. Ellman GL. Tissue sulfhydryl groups. Arch Biochem Biophys. 1959 May;82(1):70–7.
31. Towbin H, Staehelin T, Gordon J. Electrophoretic transfer of proteins from polyacrylamide gels to nitrocellulose sheets: procedure and some applications. Proc Natl Acad Sci. 1979 Sep 1;76(9):4350–4.
32. Lowry OH, Rosebrough NJ, Farr AL, Randall RJ. Protein measurement with the Folin phenol reagent. J Biol Chem. 1951 Nov;193(1):265–75.
33. Dušinská M, Collins A. Detection of oxidised purines and UV-induced photoproducts in DNA of single cells, by inclusion of Lesion-specific enzymes in the comet assay. ATLA Altern to Lab Anim. 1996;24(3):405–11.
34. Collins AR, Duthie SJ, Dobson VL. Direct enzymic detection of endogenous oxidative base damage in human lymphocyte DNA. Carcinogenesis. 1993 Sep;14(9):1733–5.
35. Zhu H-L. Resveratrol and Its Analogues: Promising Antitumor Agents. Anticancer Agents Med Chem. 2011 Jun 1;11(5):479–90.
36. Kotora P, Šeršěn F, Filo J, Loos D, Gregáň J, Gregáň F. The scavenging of DPPH, galvinoxyl and ABTS radicals by imine analogs of resveratrol. Molecules. 2016 Jan 21;21(1):127.
37. Andriantsitohaina R, Auger C, Chataigneau T, Étienne-Selloum N, Li H, Martínez MC, et al. Molecular mechanisms of the cardiovascular protective effects of polyphenols. Br J Nutr. 2012 Nov;108(09):1532–49.

38. Cutts SM, Rephaeli A, Nudelman A, Ugarenko M, Phillips DR. Potential Therapeutic Advantages of Doxorubicin when Activated by Formaldehyde to Function as a DNA Adduct-Forming Agent. Curr Top Med Chem. 2015;15(14):1409–22.

39. Pommier Y, Leo E, Zhang H, Marchand C. DNA topoisomerases and their poisoning by anticancer and antibacterial drugs. Chem Biol. 2010 May 28;17(5):421–33.

40. Stěrba M, Popelová O, Vávrová A, Jirkovský E, Kovaříková P, Geršl V, et al. Oxidative stress, redox signaling, and metal chelation in anthracycline cardiotoxicity and pharmacological cardioprotection. Antioxid Redox Signal. 2013 Mar 10;18(8):899–929.

41. Qiao X, van der Zanden SY, Wander DPA, Borràs DM, Song J-Y, Li X, et al. Uncoupling DNA damage from chromatin damage to detoxify doxorubicin. Proc Natl Acad Sci U S A. 2020 Jun 30;117(26):15182–92.

42. Toiber D, Erdel F, Bouazoune K, Silberman DM, Zhong L, Mulligan P, et al. SIRT6 Recruits SNF2H to DNA Break Sites, Preventing Genomic Instability through Chromatin Remodeling. Mol Cell. 2013 Aug 22;51(4):454–68.

43. Kugel S, Mostoslavsky R. Chromatin and beyond: the multitasking roles for SIRT6. Trends Biochem Sci. 2014 Feb;39(2):72–81.

44. Cai Y, Yu S-S, Chen S-R, Pi R-B, Gao S, Li H, et al. Nmnat2 protects cardiomyocytes from hypertrophy via activation of SIRT6. FEBS Lett. 2012;586(6):866–74.

45. Van Meter M, Simon M, Tombline G, May A, Morello TD, Hubbard BP, et al. JNK Phosphorylates SIRT6 to Stimulate DNA Double-Strand Break Repair in Response to Oxidative Stress by Recruiting PARP1 to DNA Breaks. Cell Rep. 2016 Sep 6;16(10):2641–50.

46. Chang AR, Ferrer CM, Mostoslavsky R. SIRT6, a Mammalian Deacylase with Multitasking Abilities. Physiol Rev. 2020 Jan 1;100(1):145–69.

47. Radak Z, Koltai E, Taylor AW, Higuchi M, Kumagai S, Ohno H, et al. Redox-regulating sirtuins in aging, caloric restriction, and exercise. Free Radic Biol Med. 2013 May;58:87–97. doi:10.1016/j.freeradbiomed.2013.01.004

48. Ahmad Z, Hassan SS, Azim S. A Therapeutic Connection between Dietary Phytochemicals and ATP Synthase. Curr Med Chem. 2017 Nov 20;24(35):3894–906.

49. Koltai E, Szabo Z, Atalay M, Boldogh I, Naito H, Goto S, et al. Exercise alters SIRT1, SIRT6, NAD and NAMPT levels in skeletal muscle of aged rats. Mech Ageing Dev. 2010;131(1):21–8.

50. Balteau M, Van Steenbergen A, Timmermans AD, Dessy C, Behets-Wydemans G, Tajeddine N, et al. AMPK activation by glucagon-like peptide-1 prevents NADPH oxidase activation induced by hyperglycemia in adult cardiomyocytes. Am J Physiol Heart Circ Physiol. 2014 Oct 15;307(8):H1120-33.

51. Maksin-Matveev A, Kanfi Y, Hochhauser E, Isak A, Cohen HY, Shainberg A. Sirtuin 6 protects the heart from hypoxic damage. Exp Cell Res. 2015 Jan 1;330(1):81–90.

Cardioprotection during Chemotherapy: Prospects of Antioxidant Strategies

Thiago Gomes Heck[1]

Grupo de Pesquisa em Fisiologia, Programa de Pós-Graduação em Atenção Integral à Saúde (PPGAIS), Programa de Pós-Graduação em Modelagem Matemática e Computacional (PPGMMC), Universidade Regional do Noroeste do Estado do Rio Grande do Sul (UNIJUÍ), Ijuí, RS – Brazil

Short Editorial related to the article: Cardioprotective Effect of Maternal Supplementation with Resveratrol on Toxicity Induced by Doxorubicin in Offspring Cardiomyocytes

The concept of oxidative stress, well defined as a situation in which cells, tissues, or the whole body present an imbalance between reactive oxygen species (ROS) and antioxidant defenses in favor of ROS levels, is found in several acute and chronic diseases, including cancer. The equilibrium between ROS production and the ability of cells to avoid oxidative damage is a natural challenge for mammalian species since the energy production by oxidative pathways in mitochondria allows the continuous production of free radical and oxidative molecules.[1] Pharmacological agents may generally use the modulation of oxidative balance to treat some diseases, or oxidative imbalance may represent a side effect of the drugs. Also, we need to keep in mind that oxidative stress caused by environmental (e.g., air pollution) and metabolic (e.g., obesity and diabetes) conditions is also associated with an increased risk of a variety of cancers.[2]

Hyperproliferation of tumor cells is accompanied by high ROS production, but it is well known that cell stress response, antioxidant defenses, and resistance against the cytotoxic effects of chemotherapy is quite different in tumor compared to immune cells and other tissues. Thus, the tumor is able to adapt to conditions of oxidative burden while other cells may not present sufficient self-defense against oxidative damage. The mechanism of tumor self-protection involves increasing the levels of the major non-enzymatic antioxidant defense, glutathione (GSH).[2] As a "hungry" cell, considering the common high-energy demand mainly by glucose uptake, tumors activate glucose-6-phosphate dehydrogenase (G6PD) and reroute glucose metabolism from glycolysis through the oxidative arm of the pentose phosphate pathway (PPP) toward nucleotide synthesis. In turn, the increase in nicotinamide adenine dinucleotide phosphate (NADPH) allows the increase in GSH and other antioxidant systems. Also, at a molecular level, the tumor evocates many transcription factors, including activator protein 1 (AP-1), heat shock factor 1 (HSF1), nuclear factor κB (NF-κB), nuclear factor-erythroid 2 p45-related factor 2 (NRF2), and tumor protein p53, representing a proliferative strategy accompanied by a robust cell stress defense.[2,3]

In the middle of this storm, it is necessary to attack the tumor with aggressive agents. Anthracyclines, such as doxorubicin (DOX), are highly effective against acute lymphoblastic and myeloblastic leukemias and also against solid tumors (e.g., breast cancer). However, anthracycline-induced cardiotoxicity may occur acutely (during treatment or immediately after), inducing pericarditis-myocarditis or arrhythmias, chronically promoting complications, and increasing the risk of death. In the heart, as an organ with an intense oxidative metabolism by nature, DOX can increase ROS production by metabolizing the drug. Mitochondria enzymes such as NADPH oxidase, cytochrome P-450 reductase, and xanthine oxidase can transform DOX and other anthracyclines in the form of quinone into semiquinone, which in turn generates ROS as superoxide anion and others. Also, DOX-derived ROS may activate p53 and pro-inflammatory signaling such as NF-κB-centered pathways, resulting in an imbalance between pro-and anti-apoptotic and anti-inflammatory proteins. Finally, DOX could affect the transcription and expression of cardiac-specific proteins impairing the function of cardiomyocytes leading to myofibrillar deterioration, disruption of sarcomere organization, and reduction of contractile function.[4]

Avoiding the oxidative scenario, the basic search is for antioxidant strategies. In this issue, a study[5] showed that supplementation with resveratrol during the gestational period has a cardioprotective effect on the offspring's heart against DOX-induced toxicity. This antioxidant treatment induced an increase in neonatal cardiomyocyte cell viability and decreased apoptotic/necrotic markers. These effects were associated with improved antioxidant defense and decreased DNA oxidative damages, and promoted the expression of proteins related to cell stress response pathways (Sirt6) in the cardiomyocytes of the pups. Furthermore, these exciting results showed the relevance of antioxidant supplementation during cancer treatment and highlighted the relevance of including antioxidant-related interventions (e.g. exercise)[6,7] in maternal environments in response to stress agents for the offspring health to avoid cardiotoxicity.

Keywords

Cardioprotection; Drug Therapy; Antioxidants; Oxidative Stress; Resveratrol.

Mailing Address: Thiago Gomes Heck •
Universidade Regional do Noroeste do Estado do Rio Grande do Sul - Programa de Pós-Graduação em Atenção Integral à Saúde - Rua do Comércio, 3000. Postal Code 98700-000, Ijuí, RS - Brazil
E-mail: thiago.heck@unijui.edu.br

DOI: https://doi.org/10.36660/abc.20210914

References

1. Sies H. Oxidative stress: a concept in redox biology and medicine. Redox Biology. 2015;4:180-3. https://doi.org/10.1016/j.redox.2015.01.002
2. HayesJD, Dinkova-Kostova AT,Tew KD. Oxidative Stress in Cancer. Cancer Cell.2020;38(2):67-97. https://doi.org/10.1016/j.ccell.2020.06.001
3. Kolberg A, Rosa TG,Puhl MT,Scola G, da Rocha Janner D, Maslinkiewicz et al. Low expression of MRP1/GS-X pump ATPase in lymphocytes of Walker 256 tumour-bearing rats is associated with cyclopentenone prostaglandin accumulation and cancer immunodeficiency. Cell Biochem Func. 2006;24(1): 23–39. https://doi.org/10.1002/cbf.1290
4. Angsutararux P, Luanpitpong S, Issaragrisil S. Chemotherapy-Induced Cardiotoxicity: Overview of the Roles of Oxidative Stress. Oxid Med Cell Longev.2015;795602.2015: 795602. https://doi.org/10.1155/2015/795602
5. Brito VB, Nascimento LVM, Moura DJ, Saffi J. Cardioprotective Effect of Maternal Supplementation with Resveratrol on Toxicity Induced by Doxorubicin in Offspring Cardiomyocytes. Arq Bras Cardiol. 2021; 117(6):1147-1158.
6. Cezar MD, Oliveira Junior AS, Damatto RL. Moderate-Intensity Resistance Training Improves Oxidative Stress in Heart. Arq Bras Cardiol. 2021;116(1):12-3. https://doi.org/10.36660/abc.20200561
7. Hajjar L A, Costa I, Lopes M, Hoff P, Diz M, Fonseca S., Bittar CS, et al. Brazilian Cardio-oncology Guideline - 2020. Diretriz Brasileira de Cardio-oncologia . Arq Bras Cardiol.2020;115(5):1006-43.

Influence of an Early Mobilization Protocol on the Autonomic Behavior of Patients Undergoing Percutaneous Transluminal Coronary Angioplasty

Bárbara Oliveira Silveira,[1] Jade Lara de Melo,[1] Graziella Paula de Oliveira Neri,[1] Michele Lima Gregório,[2] Moacir Fernandes de Godoy,[3] Marilita Falangola Accioly[1]

Universidade Federal do Triângulo Mineiro,[1] Uberaba, MG – Brazil

Faculdade de Medicina de São José do Rio Preto (FAMERP) - Pós Graduação Enfermagem,[2] São Jose do Rio Preto, SP – Brazil

Faculdade de Medicina de São José do Rio Preto (FAMERP) - Cardiologia e Cirurgia Cardiovascular,[3] São Jose do Rio Preto, SP – Brazil

Abstract

Background: **Recurrence Plots (RP) enable a nonlinear analysis of Heart Rate Variability (HRV) and provide information on the Autonomic Nervous System (ANS).**

Objectives: **To evaluate whether early ambulation in patients undergoing Percutaneous Transluminal Coronary Angioplasty (PTCA) influences the quantitative and qualitative components of RP.**

Methods: **A total of 32 participants who underwent PTCA were divided into a Control Group (CG - no physical exercises) and an Early Ambulation Group (EAG – with physical exercises). Beat-to-beat heart rate was recorded using a heart rate monitor in both groups upon admission and discharge. The linear indices in the time and frequency domains were analyzed, and nonlinear indices were obtained through RP. The Early Ambulation Physical Therapy Protocol began 12-18 hours after PTCA. A two-tailed unpaired t-test was used for comparisons, and p-values < 0.05 were accepted as significant.**

Results: **When comparing both groups, upon discharge, EAG showed an increase in SDNN (23.55 ± 12.05 to 37.29 ± 16.25; p=0.042), Triangular Index (8.99 ± 3.03 to 9.66 ± 3.07; p=0.014), and VLF (694.20 ± 468.20 to 848.37 ± 526.51; p=0.004), but without significant changes in the nonlinear evaluation. In addition, in the qualitative analysis of RP, a more diffuse and less geometric pattern was observed in EAG, indicating greater variability, while in CG, an altered and more geometric pattern was noted.**

Conclusion: **The Early Ambulation Protocol promotes an improvement in autonomic behavior as evaluated by HRV and by RP, which can thus be considered a useful procedure for better recovery of patients undergoing PTCA.**

Keywords: **Cardiovascular Diseases/mortality; Myocardial Infarction; Early Ambulation/methods; Exercise; Autonomic Nervous System; Angioplasty.**

Introduction

Cardiovascular diseases account for the highest number of deaths worldwide.[1] Among them, Acute Myocardial Infarction (AMI) is the leading cause of death in Brazil.[2] However, survival of these patients has increased as a result of technological advances, such as Percutaneous Transluminal Coronary Angioplasty (PTCA).[3,4]

Associated with PTCA, multidisciplinary interaction plays an important role in reducing mortality,[5] since early ambulation avoids bed confinement and its many deleterious effects, such as functional decline and reduced quality of life after discharge.[6] However, it is still very common for patients to remain confined to a bed for fear of hemodynamic instability.[7]

In contrast, the analysis of cardiac autonomic modulation through Heart Rate Variability (HRV) has been used as a predictor of cardiovascular risks in various conditions.[8,9] However, most studies used the linear analysis of HRV.[10-12]

The human body is a good illustration of a natural "Complex System" characterized by the continuous interaction of its multiple organs to maintain life. Its complexity results in a mode of behavior that is typically nonlinear in normal situations.[13] Thus, the methods related to nonlinear dynamics are usually more clinically relevant for a better interpretation of the pathophysiological behavior of HRV under various conditions and, consequently, its prognostic value, complementing the information obtained with traditional evaluations.[14]

Recurrence Plots (RP) are a nonlinear analysis method idealized by Eckmann et al.,[15] which proposes the analysis

Mailing Address: Marilita Falangola Accioly •
Universidade Federal do Triangulo Mineiro - Departamento de Fisioterapia Aplicada - Av. Frei Paulino, 30. Postal Code 38025-180, Uberaba, MG Brazil
E-mail: marilitafisio@gmail.com
Manuscript received April 08, 2020, revised manuscript December 06, 2020, accepted January 27, 2021

DOI: https://doi.org/10.36660/abc.20200296

of the behavior of a system, represented by a time series, in an abstract space called phase space, enabling the quantification and qualification of HRV.[15,16]

In addition, little is known about acute responses to early exercise in autonomic modulation and cardiovascular function in the immediate postoperative period of patients undergoing myocardial revascularization and PTCA.[17]

Therefore, the present study aimed to evaluate whether early ambulation in patients undergoing PTCA influences the quantitative and qualitative components of RP.

Methods

Sample

This is a prospective, controlled and quasi-experimental clinical trial. The sample included individuals who underwent PTCA at the University Hospital of the University of Triângulo Mineiro.

The sample size was calculated considering the prevalence of individuals requiring angioplasty and hospitalized in a coronary care unit. For the calculation, the following formula was used: $n = Z^2 \times p (p-100) / e^2$, where Z is the constant critical value that corresponds to the 95% confidence interval (95% CI); p is the prevalence of the disease/main variable; and e is sampling error, which may vary up to 10% of the true value of the population selected for the sample, suggesting a sample of 15 individuals for each group.

The flowchart for sample recruitment and selection is displayed in Figure 1.

The sample consisted of 32 participants who met the following inclusion criteria: be at least 18 years old; show a medical diagnosis of uncomplicated AMI (Killip I and II), with or without ST segment elevation and/or indication of elective PTCA (successful PTCA with residual stenosis of less than 50%); and be able to understand the instructions to perform the physical exercises. Next, the participants were divided into two groups: Early Ambulation (EAG) with 16 participants submitted to the Early Ambulation Protocol; and Control (GC) with 16 participants not submitted to the Early Ambulation Protocol. The sample was matched for age, sex, and medical diagnosis.

Individuals with at least one of the following characteristics were excluded from the study: history of previous AMI, complicated AMI (Killip III and IV), pacemaker implantation, 2nd or 3rd degree atrioventricular block, sequelae of stroke, inferior limb amputation, severe aortic stenosis, previous myocardial revascularization surgery, heart failure, hemodynamic instability at rest, worsening of the general clinical condition, feverish condition, and respiratory failure (need for mechanical ventilation).

The study procedures followed all the norms of CNS Resolution No. 466 and was approved by the Ethics and Research Committee of the Federal University of Triângulo Mineiro under Resolution 2.319.890 and the Brazilian Registry of Clinical Trials RBR-9w378x.

Figure 1 - Flowchart showing recruitment and selection of study participants. AMI: Acute Myocardial Infarction. CPA: Cardiopulmonary Arrest. PTCA: Percutaneous Transluminal Coronary Angioplasty. MV: Mechanical Ventilation.

Experimental Protocol

The experimental protocol consisted of four phases. Phase I was conducted with interviews and assessments of medical records. Phase II was performed 12 to 18 hours after PTCA and consisted of recording beat-to-beat heart rate, using a Polar® heart rate monitor model RS800CX (Polar Kempele, Finland), and the tachogram was collected continuously for 20 minutes. During the entire collection process, the participant remained at rest, in the supine position, in silence and awake. Phase III was characterized by the implementation of an Early Ambulation Protocol, performed only by EAG.

In Phase IV, a new electrocardiogram was performed to analyze HRV, following the same procedures as in Phase II.

Early Ambulation Protocol

The Early Ambulation Protocol was adapted from the protocol used at the Grady Memorial Hospital and Emory University School of Medicine,[18] consisting of progressive steps in different positions, as described in Table 1. The protocol was started and applied in the positions according to the participants' functional status, which was verified by evaluations and communication with the multidisciplinary team. The EAG performed the protocol throughout the hospitalization period, which consisted of two sessions per day (4 interventions during ICU stay).

The following criteria were used to discontinue the Early Ambulation Protocol: signs and/or symptoms of fatigue, chest pain, dyspnea, cyanosis, pallor, tachycardia (>120 beats per minute), bradycardia, complex arrhythmias, and hypotension (Mean Blood Pressure <65mmHg).

Evaluation of autonomic modulation

For the analysis of HRV indices, RR interval records were transmitted to a computer using the Polar Precision Performance software (version 4.01.029)[19] and converted to text files. Only those series with more than 95% of sinus beats were analyzed, following the selection of the 1,000 most stable points (Kubios HRV Software, version 2.0, University of Kuopio, Finland). The data were filtered using the Polar Precision Performance standard software filter (version 4.01.029), with a moderate filter. Next, a graphical computational filtering tool called T-RR Filter[20] was used.

Among the linear methods, the time domain measures normal RR intervals (iR-R), and various measurements are calculated from these intervals, including: standard deviation of the mean normal iR-R (SDNN), which corresponds to sympathetic and parasympathetic effects and represents global variability; the percentage of adjacent iR-Rs with a difference of duration greater than

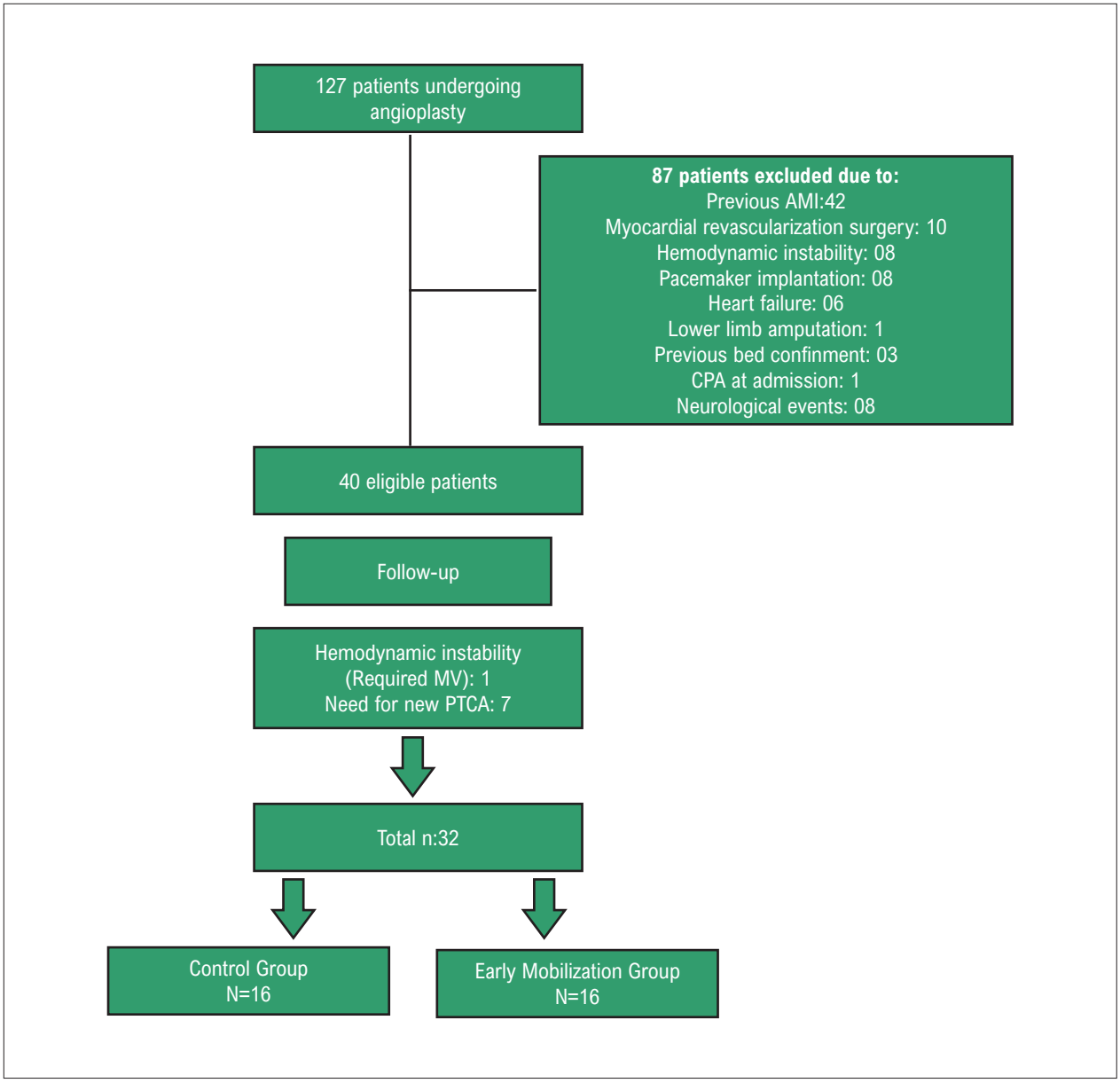

Figure 1 – *Flowchart showing recruitment and selection of study participants. AMI: Acute Myocardial Infarction. CPA: Cardiopulmonary Arrest. PTCA: Percutaneous Transluminal Coronary Angioplasty. MV: Mechanical Ventilation.*

50 milliseconds (pNN50); and the root mean square of the successive differences between the usual adjacent iR-Rs (RMSSD). The RMSSD and pNN50 variables are related only to parasympathetic behavior, while SDNN reflects all components responsible for variability. The Triangular Index refers to the number of all iR-Rs divided by the frequency of these iR-Rs in the modal compartment of the histogram, thus reflecting the global variability.[21]

For the analysis of the frequency domain, the cubic splines interpolation method at 4Hz was applied and the power spectral density of the most stable segment was calculated using the Fast Fourier Transform (FFT), calculating, in milliseconds squared (ms^2), the spectral components for Very Low Frequency (VLF) (<0.04Hz), Low Frequency (LF) (0.04-0.15 Hz), and High Frequency (HF) (0.15 to 0.40 Hz), in addition to the ratio of these components (LF/HF).

LF represents the sympathetic and parasympathetic modulation; HF represents the vagal modulation activity.[22] VLF reflects humoral, vascular, thermal regulations, as well as the activity of the renin-angiotensin-aldosterone system.[22] Moreover, the LF and HF ratio can be considered a measure of sympathovagal balance.[22,23]

RP were used for nonlinear analysis of HRV, which was made in a qualitative and quantitative manner. The qualitative analysis was performed by visualizing the graphic

Table 1 – Early Ambulation Protocol

Position	Exercises
Supine	A) One-set diaphragmatic exercises associated with active-assisted or active-free diagonal movement of the upper limb (10 times for each limb);
	B) Repeat the exercise over 1 set with both members simultaneously (10 times);
	C) Repeat the exercise over 1 set with both members simultaneously (10 times);
	D) Active assisted or active free lower limbs - triple flexion (10 times) + abduction / hip adduction (10 times for each limb);
	E) Ankle flexion-extension (10 times) for each foot;
	F) Ankle circumference (10 times) for each foot.
Sitting	Active exercises from A to F
Orthostatism	Active exercises from A to F and active for lower limbs (supported if necessary)
	G) Standing on tiptoe (10 times) with both limbs simultaneously;
	H) Half squats (10 times);
	I) Stationary gait (for 30 seconds);
	J) Ambulation in the room (1 round).

pattern and the quantitative analysis used the following indices: Recurrence (REC), Determinism (DET), Shannon entropy (ES), Laminarity (LAM), Trapping time (TT), and Maximum line (MaxLine).[15] The following parameters were used in RP: embedding dimension = 10; time delay = 1, radius = 70, line = 2,[24] and color scheme = Volcano.

A time series is used for the construction of RP. According to the ranges of values between measurements (dimension) and distances or time intervals (radius), it can be verified whether or not recurrence values exist. The use of different colors represents different radii complementing the typical visual appearance of RP.[24]

RP can be analyzed by small and large scale patterns. The small scale patterns fit the points, diagonal and vertical lines, which enable a qualitative analysis. For example, in healthy individuals, RP show a diagonal line and fewer apparent squares, indicating higher HRV. In individuals with some autonomic modulation impairment, RP show more squares defined in the graph, more geometric shapes, indicating the inherent periodicity, linear behavior and a low HRV.[24,25]

In the quantitative analysis, some indices are generated: recurrence rate (REC%), which quantifies the percentage of recurrent points within a specific radius; Percentage of Determinism (DET%), representing the diagonals formed by recurrence points; average Length of Diagonal Lines (Lmean) and Maximum Length of Diagonal Lines (Lmax), representing the largest diagonal except the main one; Laminarity (LAM), which are the recurrence points that form vertical lines; Trapping Time (TT), which is the average length of vertical lines; Entropy, representing Shannon's entropy, which measures the distribution complexity of diagonal lines. In this case, unlike other interpretations, it is understood that the higher the Shannon entropy is, the more linear the time series will be.[25]

For the qualitative analysis, chaotic, randomized, periodic, and linear systems constructed by mathematical formulation reported by Takakura et al.[24] were used as RP models, as shown in Figure 2.

Statistical Analysis

A descriptive analysis of continuous and categorical variables was performed. The presence or absence of normal distribution of variables was assessed by Shapiro-Wilk tests. Continuous data with Gaussian distribution were expressed as mean ± standard deviation. Categorical variables were expressed as absolute and percentage values.

A two-tailed unpaired t-test was set for all intergroup analyses being admitted an alpha error of 5%. All analyses were performed with Stats Direct Statistical Software version 3.3.3.

Results

The analyzed sample was homogeneous regarding clinical diagnosis, systemic blood pressure, heart rate at rest, length of hospital stay, number of implanted stents, and HRV indices. Table 2 describes the sample characterization of both groups.

The drugs used by CG were beta-blockers (81.3%), hypolipidemics (62.5%), Ieca (50%), Aspirin (62.5%), and Ticlopidine/clopidogrel (18.8), while EAG used beta-blockers (87.5%), hypolipidemics (53.6%), Ieca (50%), Aspirin (62.5%), and Ticlopidine/clopidogrel (37.5%).

Table 3 summarizes the analysis of linear indices for the time and frequency domains, in which we can observe a statistically significant difference in SDNN, Triangular Index, and VLF when comparing CG with EAG. Table 4 shows the quantitative analysis of nonlinear indices by the Visual Recurrence Analysis Software. There was no statistical difference between both moments when comparing CG and EAG.

However, an overall worsening of the Control Group pattern can be observed in Figure 3, which shows the visual (qualitative) analysis of RP. Upon discharge, there are a greater number of dark squares and more geometric shapes, indicating higher linearity, and therefore less system homeostasis when compared with admission. Moreover, when comparing EAG with GC, a more chaotic pattern can

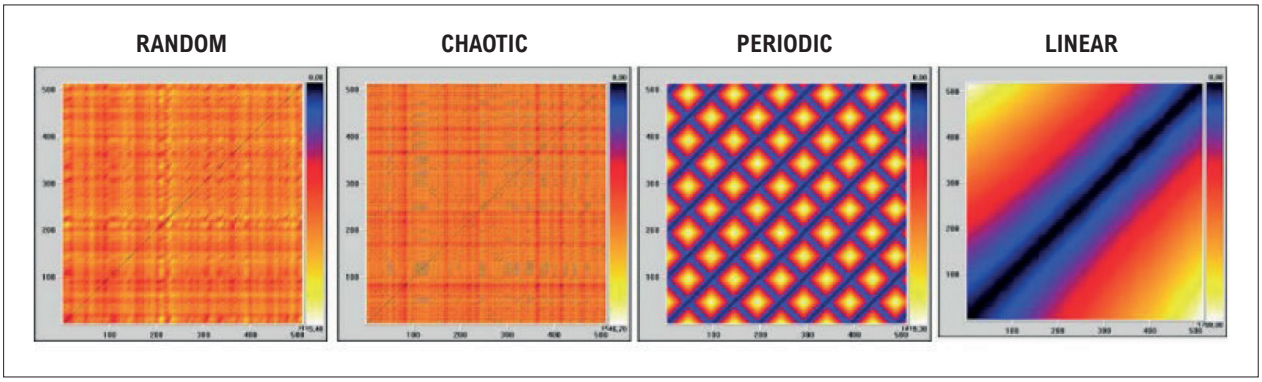

Figure 2 – *RP of randomized, chaotic, periodic, and linear systems, obtained with mathematical formulation. Source: Takakura et al.[21]*

Table 2 – Sample Characterization

	Control Group (N=16)	Early Ambulation Group (N=16)	p-value*
Sociodemographic profile			
Age: years	61.00 ±8.34	63.50 ±9.64	0.439
Sex: male (n)	08 (50%)	08 (50%)	
BMI (kg/m^2)	27 ±3	29 ±3	0.467
Diagnostic			
Coronary Artery Disease (n)	08 (50%)	08 (50%)	
Acute Myocardial Infarction (n)	08 (50%)	08 (50%)	
BP / HR (at rest)			
Heart Rate (bpm)	71.38 ±11.09	71.19 ±10.08	0.960
Systolic blood pressure (mmHg)	130.25 ±22.62	134.38±19.26	0.583
Diastolic Blood Pressure (mmHg)	76.50 ±17.29	72.06 ±9.95	0.383
Mean blood pressure (mmHg)	94.06 ±21.22	92.69 ±13.05	0.827
Coronary obstruction			
Right Coronary Artery (n)	12 (75%)	10 (62.5%)	
Anterior Descending (n)	8 (50%)	8 (50%)	
Circumflex (n)	2 (12.5%)	3 (18.8%)	
Length of stay in hospital (days)	3.94 ±1.48	3.75 ±1.18	0.113
Number of stents	1.63 ±0.71	1.94 ±0.85	0.215

N: number of participants; mean ± standard deviation; BM: body mass index; kg/m2; kilogram per square meter; BP: blood pressure; HR: heart rate; bpm: beats per minute; mmHg: millimeters of mercury. unpaired Student's t-test.*

be observed, with fewer apparent and more homogeneous squares in EAG, indicating greater complexity and improvement of homeostasis.

Discussion

The major findings of the intragroup analysis of EAG were the significant increase in the linear indices (SDNN and PNN50) upon discharge, when compared with those upon admission. In the EAG intergroup analysis, a chaotic and more complex pattern was observed.

This increase in linear indices is indicative of high HRV, represented by the increase in parasympathetic activity in PNN50 and global autonomic activity in SDNN, following the application of the Early Ambulation Protocol. This result infers improvement of overall health of the cardiovascular system, given that increased parasympathetic activity is related to higher HRV, and lower cardiovascular mortality,[26,27] demonstrating the beneficial influence of exercises performed in the ICU.

In the intergroup analysis, the indices for SDNN, Triangular Index, and VLF show a statistically significant difference upon

Table 3 – Heart Rate Variability analyzed by Linear Methods: Control vs. Early Ambulation

HRV indices	Control		Early Ambulation		Control x Early Ambulation	
	Admission	Discharge	Admission	Discharge	Admission	Discharge
	Mean (SD)	Mean (SD)	Mean (SD)	Mean (DP)	p-value	p-value
Time Domain						
Mean RR	894.58 ±112.65	825.29 ±85.04	890.60 ±147.14	908.12 ±140.25	0.9321	0.0544
SDNN	27.73 ±18.91	27.4 ±8.71	23.55 ±12.05	37.29 ±16.25	0.4610	0.0428*
RMSSD	21.98 ±11.10	15.69 ±9.09	19.68 ±11.03	20.48 ±13.47	0.5601	0.2482
PNN50	4.19 ±7.65	3.83 ±6.85	2.30 ±5.26	5.12 ±6.53	0.7046	0.4864
Triangular Index	9.34 ±4.99	7.23 ±2.09	8.99 ±3.03	9.66 ±3.07	0.8126	0.0148*
TINN	142.81 ±54.25	131.25 ±39.39	120.62 ±63.03	130.0 ±70.75	0.2944	0.9513
Frequency Domain						
VLF power (ms^2)	927.23 ±1395.20	407.56 ±237.61	694.20 ±468.20	848.37 ±526.51	0.5308	0.0043*
LF power (ms^2)	300.06 ±367.49	177.81 ±154.94	233.93 ±165.23	380.50 ±513.86	0.5165	0.1414
HF power (ms^2)	148.43 ±174.09	159.87 ±223.07	94.12 ±117.58	177.68 ±159.76	0.4677	0.3282
LF/HF power (ms^2)	2.86 ±2.12	3.39 ±2.49	2.80 ±1.61	3.94 ±3.65	0.9295	0.6205

*Mean RR: mean of RR intervals; RMSSD: root mean square of the successive differences between the usual adjacent iR-Rs; pNN50: percentage of adjacent RR intervals that differ by duration greater than 50 milliseconds; SDNN: standard deviation of the average of normal RR intervals; RR tri index: triangular index RR; TINN: Triangular interpolation of the NN interval histogram. Data expressed as mean (standard deviation); VLF: Very Low Frequency; HF: High Frequency; LF: Low Frequency; LF/HF: Ratio between Low and High Frequency *: statistically significant difference (p <0.05). unpaired Student's t-test (Control x Early Ambulation).*

Table 4 – Heart Rate Variability analyzed by Nonlinear Methods: Control x Early Ambulation

HRV indices	Control		Early Ambulation		Control x Early Ambulation	
	Admission	Discharge	Admission	Discharge	Admission	Discharge
	Mean (SD)	Mean (SD)	Mean (SD)	Mean (SD)	p-value	p-value
Visual Recurrence Analysis (VRA)						
Mean	890.64±147.15	908.22±140.36	893.71±101.13	843.18±90.72	0.9457	0.1318
Percentage of Recurrence	40.71 ±7.56	40.18 ±2.41	38.54 ±3.15	43.60±13.66	0.3021	0.3389
Percentage of Determinism	86.35 ±10.99	86.65 ±11.37	83.71 ±13.78	86.63±11.39	0.553	0.8099
Percentage of Laminarity	92.38 ±6.29	91.05 ±9.61	89.62 ±9.66	91.51 ±9.77	0.3477	0.8941
Trapping Time	11.65 ±12.15	8.73 ±3.11	7.68 ±3.67	7.82 ±2.40	0.2271	0.3668
Ratio	2.14 ±0.23	2.12 ±0.22	2.16 ±0.25	2.14 ±0.28	0.8472	0.8257
Entropy	3.79 ±0.75	3.83 ±0.52	3.66 ±0.60	3.71 ±0.48	0.5886	0.5117
MaxLine	219.93±191.23	241.68±223.29	238.12±166.34	171.12±95.56	0.7761	0.2587

Data expressed as mean (standard deviation) *: statistically significant difference (p <0.05). Paired t-test (parametric samples) and Wilcoxon test (nonparametric sample). unpaired Student's t-test (Control x Early Ambulation).

discharge. The SDNN indices infer the global information on both parasympathetic and sympathetic modulation; the Triangular Index expresses RR interval variability, closely related to SDNN; and VLF is related to the angiotensin-aldosterone renin system, thermoregulation, and peripheral vasomotor tone.[25]

Some studies[27,28] have presented evidence that early ambulation improves autonomic modulation in individuals after AMI. However, these studies used linear methods for their analyses, and recent studies point out that our body has a nonlinear behavior. Therefore, the analysis of the autonomic modulation by nonlinear methods is paramount.[14]

Nonlinear analysis, unlike linear analysis, measures quality, scale, and correlation of signal properties, thus providing an interpretation of the unpredictability, complexity, and fractability of the system.[14] Meyerfeldt et al.[26] found higher "sensitivity" of nonlinear analysis when

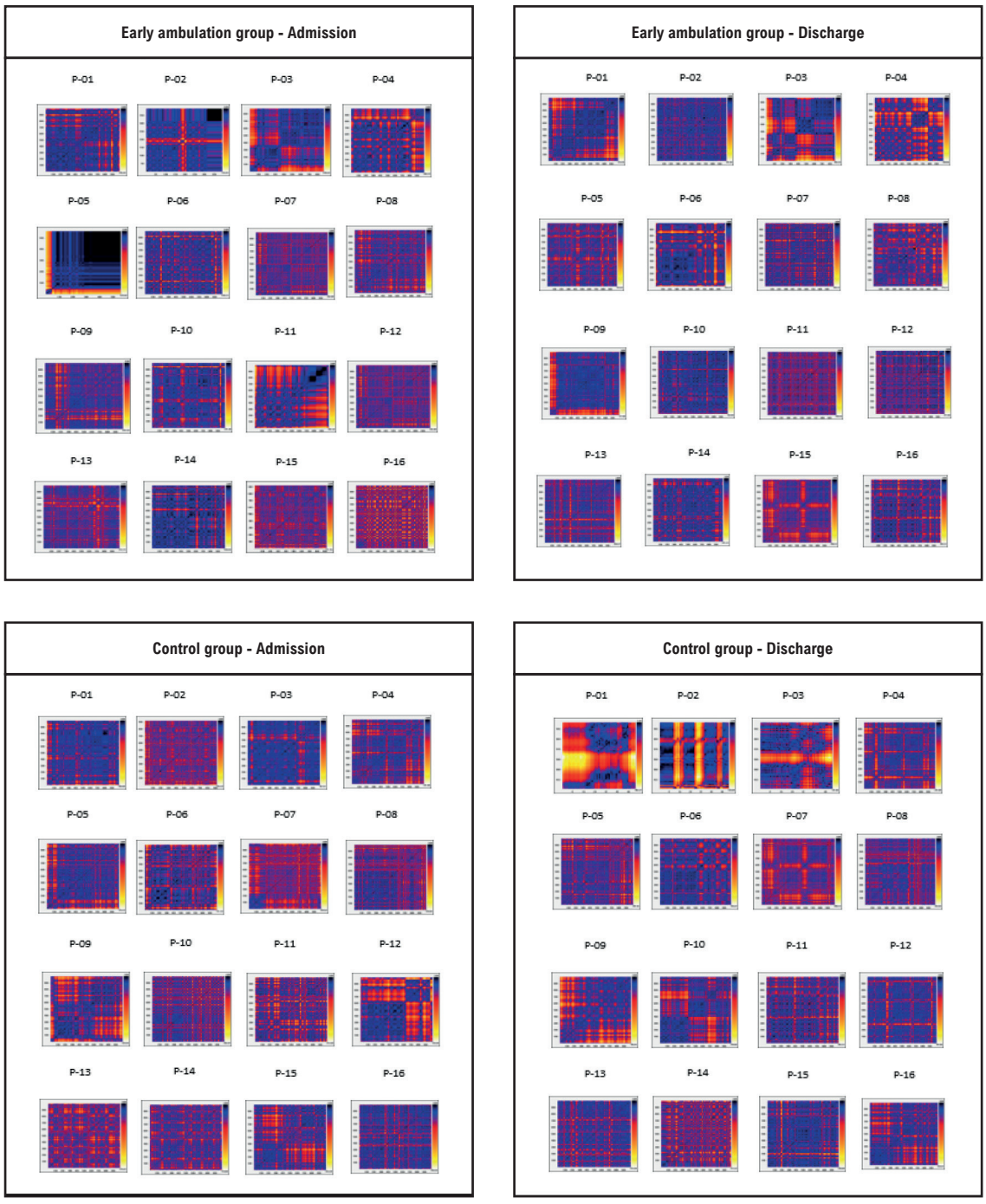

Figure 3 – *Recurrence Plots of participants identified by P_00 admission and discharge. Source: Research*

compared with linear analysis in pathological behaviors, such as tachyarrhythmias.

When analyzing the results of indices for chaos domains, in absolute values, we found no statistically significant differences. However, when analyzing the qualitative aspect of RP (Figure 3), it is possible to notice that the RP of the participants treated with early ambulation show improvement in HRV, as they present more heterogeneous colors and less geometric patterns. When compared with the mathematical models (Figure 2), they show a behavior that

tends to chaos, indicating greater variability, and therefore autonomic improvement. The study conducted by Manata et al.[30] supports our findings, which used RP to compare healthy individuals with individuals with Chronic Obstructive Pulmonary Disease (COPD). The authors concluded that individuals with COPD had lower HRV, as the RP showed more visible squares and a more homogeneous configuration. They further observed higher recurrence points when compared with healthy individuals, which indicates a more recurrent and less dynamic system and less complex autonomic modulation in this population.

Godoy & Gregório,[31] when analyzing the RP of several groups, were able to verify a difference in the variability of these individuals (newborns, adults, renal patients, and individuals with declared brain death), for the quantitative and qualitative analyses of RP. This evidence seems to corroborate our findings, as we observed a positive influence of early ambulation on HRV for the qualitative analysis of RP. However, we did not observe statistical differences in the quantitative analysis.

Takakura et al.[21] analyzed RP in patients who underwent heart transplantation and observed quantitative and qualitative signs of HRV recovery, showing that the heart autonomic re-innervation started gradually after transplantation.

We believe that the small number of interventions of the Early Ambulation Protocol (only 4 interventions) may have contributed to the absence of a statistically significant difference in the quantitative analysis. A larger number of interventions are likely to promote improvement of autonomic modulation in other HRV indices. This can be considered a limiting factor of our study.

This research only used studies that analyzed RP after surgical procedures and/or conditions, and no studies were found that analyzed the acute effects of physical exercise on patients with AMI or Coronary Artery Disease (CAD). This suggests that further research is required to analyze the nonlinear HRV dynamics in relation to different early ambulation protocols.

Conclusion

The Early Ambulation Protocol promotes an improvement in autonomic behavior as evaluated by Heart Rate Variability as well as by Recurrence Graphs, which can then be considered a useful procedure for a better recovery of patients undergoing percutaneous transluminal coronary angioplasty.

Author Contributions

Conception and design of the research: Neri GPO, Gregório ML, Godoy MF, Accioly MF; Acquisition of data: Silveira BO, Melo JL, Neri GPO; Analysis and interpretation of the data: Silveira BO, Melo JL, Gregório ML, Godoy MF, Accioly MF Gregório ML, Godoy MF; Statistical analysis: Gregório ML, Godoy MF, Accioly MF; Writing of the manuscript: Silveira BO, Melo JL, Accioly MF; Critical revision of the manuscript for intellectual content: Silveira BO, Melo JL, Gregório ML, Godoy MF, Accioly MF.

Potential Conflict of Interest

No potential conflict of interest relevant to this article was reported.

Sources of Funding

There were no external funding sources for this study.

Study Association

This article is part of the thesis of master submitted by Gaziella P. O Neri, from Universidade Federal do Triângulo Mineiro.

References

1. Feres F, Costa RA, Siqueira D, Costa Jr JR, Chamié D, Staico R, et al. Diretriz da Sociedade Brasileira de Cardiologia e da Sociedade Brasileira de Cardiologia Intervencionista sobre Intervenção Coronária Percutânea. Arq Bras Cardiol,2017; v.109(1Supl.1):1-81.
2. França EET, Ferrari F, Fernandes P, Cavalcanti R, Duarte A, Martinez BP et al . Fisioterapia em pacientes críticos adultos: recomendações do Departamento de Fisioterapia da Associação de Medicina Intensiva Brasileira. Rev Bras Ter Intensiva. 2012 Mar; 24(1): 6-22. https://doi.org/10.1590/S0103-507X2012000100003.
3. Herdy AH, López-Jiménez F, Terzic CP, Milani M, Stein R, Carvalho T, et al. Diretriz Sul-Americana de Prevenção e Reabilitação Cardiovascular. Arq Bras Cardiol.2014;103(2 Supl 1):1-31.
4. Umeda IIK. Manual de Fisioterapia na Reabilitação Cardiovascular. São Paulo: Manole. p.46-68. ISBN: 9788520424872.
5. Bauernschmitt R, Malberg H, Wessel N, Kopp B, Schirmbeck EU, Lange R. Impairment of cardiovascular autonomic control in patients early after cardiac surgery. Eur J Cardiothorac Surg. 2004 Mar;25(3):320-6. https://doi.org/10.1016/j.ejcts.2003.12.019.
6. Kunz VC, Souza RB, Takahashi ACM, Catai AM, Silva E. The relationship between cardiac autonomic function and clinical and angiographic characteristics in patients with coronary artery disease. Braz J Phys Ther. 2011; 15(6):503–10. https://doi.org/10.1590/S1413-35552011005000020.
7. Wolf MM, Varigos GA, Hunt D, Sloman JG. Sinus arrhythmia in acute myocardial infarction. Med J Austr. 1978;2(2):52-3. https://doi.org/10.5694/j.1326-5377.1925.tb11693.x
8. Kleiger RE, Miller JP, Bigger JT Jr, Moss AJ. Decreased heart rate variability and its association with increased mortality after acute myocardial infarction. Am J Cardiol. 1987;59(4):256-62. https://doi.org/10.1016/0002-9149(87)90795-8.
9. Erdogan A, Coch M, Bilgin M, Parahuleva M, Tillmanns H, Waldecker B, Soydan N. Prognostic value of heart rate variability after acute myocardial infarction in the era of immediate reperfusion. Herzschrittmachertherapie & Elektrophysiologie. 2008;19:161-8. https://doi.org/10.1007/s00399-008-0024-3
10. Beckers F, Verheyden B, Aubert AE. Aging and nonlinear heart rate control in a healthy population. Am J Physiol Heart Circ Physiol. 2006;290(6):H2560-70. https://doi.org/10.1152/ajpheart.00903.2005.

11. Godoy MF. Nonlinear Analysis of Heart Rate Variability: A Comprehensive Review. J Cardiol Ther. 2016;3(3):528-33. https://doi.org/10.17554/j.issn.2309-6861.2016.03.101-4

12. Eckmann, JP, Kamphorst, SO, Ruelle, D. "Recurrence Plots of Dynamical Systems", Europhys Lett. 187;4:973-7. https://doi.org/10.12691/bse-2-1-3.

13. Francesco B, Maria Grazia B, Emanuele G, Valentina F, Sara C, Chiara F, et al. Linear and nonlinear heart rate variability indexes in clinical practice. Computational and mathematical methods in medicine. 2012;(issue special): 1-5. https://doi.org/10.1155/2012/219080.

14. Barbosa P, Santos FV, Neufeld PM, Bernardelli GF, Castro SS, Fonseca JHP, et al.Efeitos da mobilização precoce na resposta cardiovascular e autonômica no pós-operatório de revascularização do miocárdio. ConScientiae Saúde. 2010;9(1):111–8. https://doi.org/10.1590/S0103-507X2012000100011.

15. Shved M, Tsuglevych L, Kyrychok I, Levytska L, Boiko T, Kitsak, Y. Cardioreabilitation peculiarities and correction of violations of sistolic,diasolic function and heart rate variability in patients with acute coronary syndrome and coronary artery revascularization. Galician Med J. 2017;24(4):E201749 doi: 1.21802/gmy.2017.4.9.

16. Quintana DS, Heathers JA, Kemp AH. On the validity of using the Polar RS800 heart rate monitor for heart rate variability research. Eur J Appl Physiol. 2012;112(12):4179-80. https://doi.org/10.1007/s00421-012-2453-2.

17. Santos L, Pillat V, de Godoy MF, Barbosa CL, Barroso J, Macau E. T-RR Filter: Ferramenta computacional gráfica no uso do filtro adaptativo para análise da variabilidade da frequência cardíaca. Proceeding Series of the Brazailian Society of Computacional and Applied Mathematics. 2016;4(1):1133-9. https://doi.org/10.5540/03.2016.004.01.0096.

18. TASK FORCE. Heart rate variability: standards of measurement, physiological interpretation and clinical use. Task Force of the European Society of Cardiology and the North American Society of Pacing and Electrophysiology. Circulation. 1996; 93(5):1043-65. https://doi.org/10.1161/01.CIR.93.5.1043.

19. Hernando D, Garatachea D, Almeida R, Casajus J, Bailon R. Validation of heart rate monitor polar RS800 for heart rate variability analysis during exercise.J Strength Conditioning Res 2018;32(3):716-25. https://doi.org/10.1519/JSC.0000000000001662.

20. Munk, PS, Butt, N, Larsen, AI. High-intensity interval exercise training improves heart rate variability in patients following percutaneous coronary intervention for angina pectoris. International J Int Cardiol.2010. 145(2):312-4. https://doi.org/31214.10.1016/j.ijcard.2009.11.015.

21. Takakura IT, Hoshi RA, Santos MA, Pivatelli FC, Nóbrega JH, Guedes DL et al . Recurrence Plots: a New Tool for Quantification of Cardiac Autonomic Nervous System Recovery after Transplant. Braz. J. Cardiovasc. Surg. 2017 ;32(4):245-52. https://doi.org/10.21470/1678-9741-2016-0035.

22. Ferreira LL, de Souza NM, Bernardo AFB, Vitor ALR, Valenti VE, Vanderlei LCM. Heart rate variability as a resource in physical. Fisioter Mov. 2013;26(1):25-36. https://doi.org/10.1590/S0103-51502013000100003.

23. Vanderlei LC, Pastre CM, Hoshi RA, Carvalho TD, Godoy MF. Basic notions of heart zate variability and its clinical applicability. Rev Bras Cir Cardiovasc. 2009;24(2):205-17. https://doi.org/10.1590/s0102-76382009000200018.

24. Hiss MDBS, Neves, VR, Hiss FC, Silva E, Silva AB, Catai AM. Segurança da intervenção fisioterápica precoce após o infarto agudo do miocárdio. Fisioter. Mov. 2012;25(1):153-63. https://doi.org/10.1590/S0103-51502012000100015.

25. Selig, FA, Tonolli ER, Silva EVCM, Godoy MF. Variabilidade da frequência cardíaca em neonatos prematuros e de termo. Arq. Bras. Cardiol. 2011 June; 96 (6): 443-449. https://doi.org/10.1590/S0066-782X2011005000059.

26. Meyerfeldt U, Wessel N, Schutt H, Selbig D, Schumann A, Voss A, Kurths J, Ziehmann C, Dietz R, Schirdewan A. Heart rate variability before the onset of ventricular tachycardia: differences between slow and fast arrhythmias. Int J Cardiol. 2002;8(2-3):141-51. https://doi.org/10.1016/s0167-5273(02)00139-0.

27. Vanzella L.Bernardo AFB, Carvalho TD, Vanderlei F, Silva AK, Vanderlei LC. Complexidade do sistema nervoso autônomo em indivíduos com DPOC. J Bras Pneumol.2018;44(1):24-30. https://doi.org/10.1590/s1806-7562017000000086.

28. Godoy MF, Gregório ML. Diagnostic Relevance of Recurrence Plots for the Characterization of Health, Disease, or Death in Humans. J Hum Growth Dev. 2019;29(1):39-44. https://doi.org/10.7322/jhgd.157746.

Safety of SF_6 (SonoVue®) Contrast Agent on Pharmacological Stress Echocardiogram

Rogerio Gomes Furtado,[1,2] Daniela do Carmo Rassi,[1,2] Luciano Henrique Melato,[1] Ana Caroline Reinaldo de Oliveira,[1,2] Paula Meneses Nunes,[1] Priscila Elias Baccelli,[1] Sara Camila de Oliveira Santos,[1] Victor Emanuel Santos,[3] Luiz Rassi Junior,[1] Colandy Godoy Nunes[1]

Centro de Diagnóstico por Imagem (CDI),[1] Goiânia, GO – Brazil
Universidade Federal de Goiás,[2] Goiânia, GO – Brazil
Hospital Santa Casa de Misericórdia de Goiânia,[3] Goiânia, GO – Brazil

Abstract

Background: In 2007, the United States Food and Drug Administration mandated safety reviews of commercially available echocardiographic contrast agents (ECA), following reports of death. During the past years, different studies have proven the safety of ECA, but there have been few studies on SonoVue®.

Objectives: To evaluate the safety of SonoVue® during pharmacological stress echocardiography (PSE), by analyzing the incidence of allergic reactions and comparing groups regarding the appearance of arrhythmia, minor side effects and adverse events.

Methods: In this observational, prospective study, 2346 patients underwent PSE, and they were divided into the following 2 groups: group 1 with ECA (n = 1099) and group 2 without ECA (n = 1247). Patients were evaluated during PSE, at 24 hours, and at 30 days. Statistical significance was defined as $p < 0.05$.

Results: Group 1 had fewer minor side effects, such as headache (5/0.5% versus 19/1.5%, p = 0.012) and less reactive hypertension (3/0.3% versus 19/1.5%, p = 0.002); fewer arrhythmias, such as ventricular extrasystoles (180/16.4% versus 247/19.8%, p = 0.032) and paroxysmal supraventricular tachycardia (2/0.2% versus 15/1.2%, p = 0.003); and no adverse events, such as acute myocardial infarction (AMI) or death. In group 2, 1 patient had AMI in < 24 hours (1/01%), and there were 2 deaths in < 30 days (2/0.1%). SonoVue®-related urticaria was seen in 3 (0.3%) patients, without anaphylactic reaction.

Conclusion: SonoVue® demonstrated safety during PSE. No cases of death, AMI, or anaphylactic reaction were observed. There was a lower incidence of minor side effects and arrhythmias in the group that received ECA, as well as a low incidence of mild allergic reactions.

Keywords: Stress Echocardiogram; Echocardiographic Contrast Agent; Sonovue®; Safety.

Introduction

Echocardiography is recognized as a safe, non-invasive, and highly reproducible procedure for analyzing the anatomical and functional structures of the heart. However, up to 30% of exams face technical difficulties due to poor image quality,[1,2] especially in patients who are obese, patients with thoracic deformities, and patients with chronic obstructive pulmonary disease.[3,4]

In 1997, the United States Food and Drug Administration (FDA) approved the use of echocardiographic contrast agents (ECA), with the aim of improving diagnostic accuracy of echocardiography, after reviewed data regarding the safety of ECA.[5] Phase III trials demonstrated their safety, and, consequently, ECA were approved and released for endocardial border delineation.[6,7]

However, in October 2007, the FDA discontinued the use of ECA after 11 deaths that were temporally related to their use.[8] Following review in 2008, the FDA once again approved the use of ECA, albeit with contraindications for patients with known intracardiac shunts or hypersensitivity to perflutren.[9]

The safety of ECA has been documented over the past years in diverse clinical scenarios, such as in patients with pulmonary hypertension, intracardiac shunts, and critical patients. Large studies have led to changes in FDA approval regarding the use of ECA in the described scenarios; moreover, the importance of their use in improving patient outcomes has been documented. Clinical trials have also demonstrated the safety and efficacy of ECA in physical and pharmacological stress echocardiography, as well as their use for evaluation of myocardial perfusion.[10]

Mailing Address: Rogerio Gomes Gomes Furtado •
Centro de Diagnóstico por Imagem (CDI) - Av. Portugal, 1155. Postal Code 74150030, Setor Marista, Goiânia, GO – Brazil
E-mail: rogerio.sbcgo@gmail.com
Manuscript received May 14, 2020, revised manuscript December 11, 2020, accepted January 27, 2021

DOI: https://doi.org/10.36660/abc.20200475

Pharmacological stress echocardiography (PSE) is an established modality for diagnosis of coronary artery disease (CAD), whose safety has been demonstrated in several studies.[11] The use of ECA on PSE has been consolidated over the years, initially, for endocardial border delineation and, subsequently, for evaluation of myocardial perfusion.[10] The use of ECA is indicated when 2 or more segments of the left ventricle (LV) are not adequately visualized.[9,10]

In 2013, the Brazilian National Health Surveillance Agency (ANVISA, acronym in Portuguese) approved the use of SF_6/sulfur hexafluoride (SonoVue®) in Brazil. While its safety has been previously demonstrated, there are few studies in the literature that report its use and the occurrence of adverse events.[12]

Methods

Study design

This observational, prospective, descriptive study was approved by the Research Ethics Committee of the Emergency Hospital of Goiânia (HUGO/protocol number 31442100 on Plataforma Brasil). Patients referred for risk stratification for CAD were evaluated by means of PSE. Patients were included after signing the informed consent form.

During PSE, when 2 or more LV segments were not adequately visualized, SonoVue® infusion was added for better delineation of the endocardial borders.[9,10]

Patients were divided into 2 groups. Group 1 comprised patients who underwent PSE with dobutamine-atropine and SonoVue® ECA, and group 2 comprised patients who underwent PSE with dobutamine-atropine, without any ECA.

Patients with history of allergic reaction to ECA were excluded from this study. Clinical and anthropometric data, risk factors for CAD, echocardiographic data, presence or absence of arrhythmias, adverse events, and allergic reactions within 30 minutes of the exam were obtained.

Patients in group 1 were clinically evaluated regarding signs and symptoms of allergic reaction during the first 30 minutes after the exam in person. After a 24-hour period, patients were evaluated in person or by telephone call.

In order to evaluate adverse events, such as acute myocardial infarction (AMI) and death, at 24 hours and 30 days, the researchers called all patients in both groups by telephone. Patients who did not answer the phone calls (3 calls on different days) and those who did not return to the cardiologists' office or the diagnostic imaging center were excluded from the study.

Echocardiography evaluation

PSE was carried out using EPIQ echocardiography devices (Philips Ultrasound Systems, Andover, MA, USA) . The exams were performed by echocardiographers who had received the same training, in a standardized and uniform manner, in accordance with the recommendations of the American Society of Echocardiography.[13]

Patients initially underwent baseline echocardiography, with acquisition of linear measurements of cardiac structures and valve flows. To evaluate left ventricular ejection fraction (LVEF), the Teichholz or Simpson methods were used, depending on the extent of change in segmental contraction. In some cases, end-systolic diameter was not measured when the Simpson method was used to calculate LVEF.[13,14] Following acquisition of images in the baseline stage (parasternal longitudinal, transversal, apical 4-, 3- and 2-chamber planes), an intravenous infusion of dobutamine was initiated, with an initial dose of 5 μg/kg/min, with dose increments every 3 minutes at 10, 20, 30, and 40 μg/kg/min. Atropine was administered in doses of 0.25 mg, every minute, up to the maximum cumulative dose of 2 mg, in the event that patients did not show echocardiographic signs of myocardial ischemia and had not reached a heart rate of at least 100 bpm at the stage of 20 μg/kg/min.

For acquisition of specific images with ECA, the techniques of pulse-amplitude modulation and ultrasound pulse inversion (fundamental and harmonic) were used, with low mechanical index (< 0.20), associated or unassociated with a flash, to allow for uniform opacification of the endocardial boundary.[10]

A 30-minute monitoring period was standardized after the end of infusion, in order to evaluate the following: adverse effects, signs and symptoms of allergic reaction (group 1), and return of heart rate (HR) to a value below 100 beats per minute (bpm).[11]

During PSE, patients were kept under continuous monitoring (blood pressure, HR, and 12-lead electrocardiogram measurements). Symptoms were registered by directly questioning the patients, at any moment of the study.[14]

PSE was considered effective when the exam achieved 1 of the following objectives: at least 85% of the age-predicted maximal heart rate, calculated using Karvonen's equation (maximal HR: 220 − age),[15] or echocardiographic signs of ischemia (new alterations in LV segmental wall motion).[11]

The criteria for interrupting the exam, which were considered non-diagnostic, were the following: unbearable symptoms, reactive arterial hypertension (systolic blood pressure > 230 mmHg or diastolic blood pressure > 120 mmHg), relative or absolute hypotension (decrease of > 30 mmHg in relation to resting systolic pressure or systolic blood pressure < 80 mmHg), supraventricular arrhythmias (sustained supraventricular tachycardia or atrial fibrillation), and ventricular arrhythmias (non-sustained and sustained ventricular tachycardia).[16]

The safety criteria of the exam were established as the potentially life-threatening complications defined in the meta-analysis published by Geleijnse et al., such as cardiac rupture, AMI, stroke, asystole, ventricular fibrillation, and sustained ventricular tachycardia.[17] Angina, nausea, headache, reactive arterial hypertension, and arterial hypotension (decrease of > 30 mmHg in relation to resting systolic blood pressure, requiring crystalloid replacement) were defined as minor side effects. These events are not life-threatening; they have a short duration, and they are reverted by interrupting the exam, as defined in the safety study by Wilson et al.[18]

Regarding cardiac arrhythmias registered during the exam, the following were defined: paroxysmal supraventricular tachycardia, presence of narrow QRS complexes (< 120 ms), in the absence of a conduction disorder, that were regular and similar to each other; atrial fibrillation, absence of P wave associated with irregular rhythm, narrow QRS complexes, in the absence of a conduction disorder; ventricular extrasystoles, presence of premature ventricular complexes, with a frequency higher than 6 complexes per minute; ventricular bigeminy, the presence of ventricular extrasystoles alternating with normal QRS complexes; non-sustained ventricular tachycardia, the presence of more than 3 premature ventricular contractions, lasting less than 30 seconds, with HR greater than 100 bpm; and sustained ventricular tachycardia, the presence of more than 3 premature ventricular contractions, lasting more than 30 seconds, and HR greater than 100 bpm.[14]

The LV was divided into 17 myocardial segments, in following with the recommendations of the American Society of Echocardiography.[13,15] Qualitative analysis of segmental myocardial wall motion was based on visual evaluation of myocardial thickening and on the degree of wall motion graded on a segmental wall motion index, assigning the following scores to each segment: 1 normal; 2 hypokinesia; 3 akinesia; and 4 dyskinesia. The normal score on this index is 1 (17 points/17 segments). Any value greater than 1 was considered altered segmental wall score. A positive exam for myocardial ischemia was defined as the clear presence of altered segmental myocardial wall motion in 1 or more segments of the LV, during PSE.[11,13,14]

For patients in group 1, the ECA was injected as a bolus, at a dose of 0.5 to 1 ml at rest, during the protocol and the recovery phase. The amount of ECA applied during the PSE was at the discretion of the echocardiographer, with the aim of completely opacifying the endocardial borders during the exam.[9] One ampoule of SonoVue® was used for a maximum number of 2 patients (1:2 ratio), consistently respecting sterility standards, with an interval of fewer than 6 hours between exams.[9]

Allergic reactions to SonoVue® were classified in the following manner:

- **Mild:** sneezing, tingling, urticaria, itching, and costolumbar pain, not requiring medical treatment;
- **Moderate:** sneezing, tingling, urticaria, and itching, requiring antihistamine and/or corticoid use;
- **Severe:** signs and symptoms of severe allergic reaction (anaphylactic shock), requiring immediate treatment with intramuscular epinephrine, inhalation of β-2 adrenergic agonists for bronchospasms, antihistamine, and corticoid drugs.[12]

Statistical analysis

Results were shown as tables and graphs. Categorical variables were shown as frequency and percentage, and continuous variables were shown as median and interquartile range. For comparison of categorical variables between groups, Fisher's test and the chi-square test were used. The Kolmogorov-Smirnov test was used to verify whether there was significant difference in continuous variables that did not show normal distribution between the study groups. This test was used because it was a comparison between both groups, where the tested variables did not show normal distribution; in this situation, it was the most sensitive test to any difference in distribution from which the samples were extracted. For all tests, a 95% confidence interval was applied, and p values less than 0.05 were considered significant. Data were analyzed using the statistics program Statistical Package for Social Sciences 2.1 (SPSS).

To calculate sample size, the safety study by Abdelmoneim et al., which evaluated 26,774 patients, was used as a reference. In that study, there were 94 deaths over 30 days, so the calculation of sample proportion (infinite samples) was estimated at 0.035109 (94/26,774), with an error of 0.25%.[20] In our study, the sample size was calculated at 2150 patients.

Results

This study evaluated 2346 patients, 1099 in group 1 and 1247 in group 2. Clinical follow-up was lost in 37 patients in group 1 (3%) and 73 in group 2 (5%). Thus, the final sample studied included 1062 patients in group 1 and 1174 in group 2.

Patients in group 1 were predominantly male, and they had higher body surface area and body mass indices, as shown in Table 1.

Table 1 – General characteristics of the sample of patients in groups 1 and 2

Variable	With contrast (n = 1099) Median (Q1 – Q3)	Without contrast (n = 1247) Median (Q1 – Q3)	p
Age	65.0 (56.0 – 74.0)	65.0 (57.0 -73.0)	0.460
Weight	84.0 (72.0 – 98.0)	74.0 (64.0 – 85.0)	< 0.001*
Height	167.0 (160.0 -174.0)	164.0 (157.0 – 174.0)	< 0.001*
BSAI	1.90 (1.75 -2.08)	1.80 (1.65-1.95)	< 0.001*
BMI	30.0 (26.0 -35.0)	27.4 (24.4 -31.0)	< 0.001*
Male sex[1]	613 (55.8%)	511 (41.0%)	< 0.001*

*Chi-square and Kolmogorov-Sminorv tests; * significant; Q1 – Q3: interquartile ranges of the median. BMI: body mass index; BSAI: body surface area index.*

An important piece of data in our study is that the use of the ECA made adequate visualization of all LV segments possible in the studied patients, contributing to improved exam quality.

It was also observed that group 1 had a greater number of patients with hypertension, obesity, sedentarism, and higher frequency of prior angioplasty. In group 2, there were more patients who were former tobacco users and patients with family history of CAD. Table 2 shows the distribution of antianginal therapy between groups.

With respect to echocardiography parameters (Table 3), it was observed that group 1 had slightly higher median values, when compared to group 2, for the following variables: aortic root, left atrium, left atrial volume, left ventricular diastolic diameter, interventricular septum, and left ventricular posterior wall.

Regarding analysis of arrhythmias that presented during the exam, group 2 had a higher incidence of isolated ventricular extrasystoles and paroxysmal supraventricular tachycardia. Likewise, in group 2, there was a higher incidence of headache and reactive arterial hypertension during the exam (Table 4).

Adverse events such as AMI and death were observed only in group 2. One patient had AMI fewer than 24 hours after the exam. There were 2 deaths in fewer than 30 days. The first case was an 80-year-old patient with a positive result for myocardial ischemia on PSE (multivessel). The patient progressed to AMI fewer than 24 hours after the exam, requiring hospitalization in an intensive care unit, and he died on the seventh day after the exam. The second case was a death on the seventeenth day after PSE, due to a non-cardiovascular cause. The allergic reactions found in group 1 comprised itching and urticaria. All of these cases occurred in women, in a simultaneous manner. The overall incidence of allergic reactions was low (0.6%). Urticaria was observed in 3 patients (0.3%), with 2 cases of early presentation (under 30 minutes, with 4.8-ml doses) and 1 case of late presentation (after 24 hours, with 2.5-ml doses of ECA), as shown in Figure 1 and Table 5.

Doses of ECA administered during PSE ranged from 1.5 ml to 4.8 ml. The dose of 1.5 ml was administered in 5 patients (0.5%); 2.5 ml in 913 (83.1%); and 4.8 ml in 79 (7.2%).

PSE with ECA was repeated within less than 1 year in 90 patients (8.5%). Of these patients, 1 had urticaria less than 30 minutes after infusion, with an administered dose of 4.8 ml.

Discussion

This cohort included a total number of 2346 patients. Patients were predominantly male in the group that received ECA, and mean age was similar between the groups. These 3 pieces of data are in agreement with the safety study by Tsutsui et al.[19] Our sample size was smaller than that of other safety studies on other existing ECA.[1,20-28] Among these studies, our data were similar to those of the study by Abdelmoneim et al.,[20] where the group that received ECA was predominantly male, with body mass index > 30 kg/m^2.[20] Both groups were similar in terms of risk factors for CAD, but group 2 had a greater number of patients on continuous use of beta-blockers (17.8 versus 27.7 with $p < 0.001$). Patients in group 2 showed a higher incidence of headache and reactive arterial hypertension during PSE, when compared to patients in group 1. Continuous use of beta-blockers, without prior suspension, could justify a higher incidence of these side effects mentioned during PSE with dobutamine, due to higher adrenergic stimulation of alpha receptors and direct block of vasovagal baroreceptors, consequently leading to a higher frequency of reactive arterial hypertension and headache.[19,22]

In our study, there was a greater incidence of paroxysmal supraventricular tachycardia in group 2, where ECA was not used. This piece of data corroborates the safety of ECA in the study population. The appearance of arrhythmias during PSE is related to the presence of ventricular dysfunction, advanced age, previous history of arrhythmia, and alterations in resting segmental wall motion.[17] These risk factors were similar in both study groups; therefore, it is not possible to consider these motives as responsible for this difference in our study.[29] Another explanation could be that a higher dose of dobutamine was used during the exam, given that, in group 2, there was a greater number of patients on continuous use of beta-blockers.[30] We cannot, however, confirm this hypothesis, because, unfortunately, we did not compare the dobutamine doses used between the groups. Data from our study differ from those found in the study by Saikh et al.,[23] which demonstrated a higher incidence of arrhythmias, such as ventricular extrasystole, atrial fibrillation, and non-sustained ventricular tachycardia in the group that received the ECA.[23] In contrast, Abdelmoneim et al.[20] observed that there was a similarity in the occurrence of arrhythmias between their cohorts.[20] Tsutsui et al.[19] found no difference between their 2 study groups regarding the incidence of non-sustained ventricular tachycardia, sustained ventricular tachycardia, or paroxysmal supraventricular tachycardia.[19]

Regarding the outcomes of AMI and death, our data are similar to those of the study conducted by Gabriel et al.,[22] where the outcome of death did not occur in patients in the group that received the ECA (0/0.0% versus 2/0.04%).[22]

Shaikh et al.[23] retrospectively evaluated 2 cohorts, and they did not observe any deaths between the groups.[23] Vancraeynest et al.[30] described, in their study, a case of AMI in the group that received ECA, but a causal relationship was unlikely in this case. Their study evaluated patients referred for diagnostic coronary angiography after undergoing echocardiography with ECA (perfluorocarbon-enhanced dextrose albumin), using a high mechanical index (1.5), with the same imaging plane for 15 minutes and subclinical release of cardiac biomarkers. It was observed that images with low mechanical indices (0.2) were safer.[30]

In the meta-analysis conducted by Khawaja et al.,[31] involving 211,162 patients, the mortality in the group that received ECA versus the group without ECA was 0.34% versus 0.9%, with $p = 0.052$, and that of AMI was 0.15% versus 0.2%, with $p = 0.72$.[31] These findings are similar to those found in the studies by Dolan et al.,[1] Abdelmoneim et al.,[20] and Kunestzky et al.[26] Our study showed a lower incidence of AMI and death when compared to the aforementioned meta-analysis. One of the reasons for this could be the fact that our sample consisted of outpatients who were stable, without acute ischemic syndromes or critical situations.

Table 2 – Distribution of patients by risk factors for coronary artery disease and antianginal therapy in groups 1 and 2

Variables / Risk factors for CAD	Group 1 (n = 1099)	Group 2 (n = 1247)	p
SAH	764 (69.52%)	812 (65.12%)	0.025*
DM	266 (24.20%)	276 (22.13%)	0.220
Previous AMI	93 (8.46%)	96 (7.70%)	0.495
Tobacco use	65 (5.91%)	73 (5.85%)	0.507
Former tobacco use	38 (3.46%)	342 (27.43%)	< 0.001*
DLP	425 (38.67%)	524 (42.02%)	0.109
MRS	30 (2.73%)	23 (1.84%)	0.164
Prior angioplasty	221 (20.11%)	153 (12.27%)	< 0.001*
FHCAD	153 (13.92%)	309 (24.78%)	< 0.001*
Obesity	556 (50.59%)	391 (31.36%)	< 0.001*
Sedentarism	783 (71.25%)	790 (63.35%)	< 0.001*
Chagas disease	8 (0.73%)	39 (3.13%)	< 0.001*
Antianginal therapy			
Beta-blockers	151 (13.74%)	325 (26.06%)	< 0.001*
Nitrates	0 (0.00%)	19 (1.52%)	< 0.001*
Statins	214 (19.47%)	342 (27.43%)	< 0.001*
Antiplatelet agents	198 (18.02%)	255 (20.45%)	0.136

*Fisher's test; * significant. AMI: acute myocardial infarction; CAD: coronary artery disease; DM: diabetes mellitus; DLP: dyslipidemias; FHCAD: family history of coronary artery disease; MRS: myocardial revascularization surgery; SAH: systemic arterial hypertension.*

Table 3 – Hemodynamic, geometric, and functional echocardiographic parameters of groups 1 and 2

Echocardiographic and hemodynamic baseline characteristics	With contrast (n = 1099)	Without contrast (n = 1247)	p
	Median (Q1 – Q3)	Median (Q1 – Q3)	
AoR	32.0 (29.0 – 35.0)	31.0 (28.0 – 34.0)	< 0.001*
LA	37.0 (34.0 - 40.0)	35.0 (31.0 – 38.0)	< 0.001*
LAV	28.0 (23.0 – 30.0)	21.0 (18.0 – 27.0)	< 0.001*
LVDD	47.0 (44.0 – 51.0)	46.0 (43.0 – 50.0)	0.001*
LVSD	29.0 (27.0 – 32.0)	29.0 (26.0 – 32.0)	0.053
LVEF	66.0 (61.0 – 70.0)	65.5 (60.0 – 70.0)	0.001*
IVS	9.0 (8.0 – 10.0)	8.0 (7.0 – 9.0)	< 0.001*
LVPW	9.0 (8.0 – 10.0)	8.0 (7.0 – 9.0)	< 0.001*
RWMSI	1.0 (1.0 – 1.0)	1.0 (1.0 – 1.0)	0.440
SWMSI	1.0 (1.0 – 1.0)	1.0 (1.0 – 1.0)	0.625
SBP	130.0 (120.0 – 140.0)	130.0 (120.0 -130.0)	0.001*
DBP	80.0 (80.0 – 80.0)	80.0 (80.0 – 80.0)	< 0.001*
HR	70.0 (63.0 – 78.0)	70.0 (64.0 – 70.0)	< 0.001*

*Kolmogorov-Sminorv test; * significant; Q1 – Q3: interquartile ranges of the median. AoR: aortic root; bpm: beats per minute; DBP: diastolic blood pressure; HR: heart rate; IVS: interventricular septum; LA: left atrium; LAV: left atrial volume; LVDD: left ventricular diastolic diameter; LVEF: left ventricular ejection fraction; LVPW: left ventricular posterior wall; LVSD: left ventricular systolic diameter; RWMSI: resting wall motion score index; SBP: systolic blood pressure; SWMSI: stress wall motion score index.*

Table 4 – Incidence of arrhythmias, minor side effects, and adverse events induced during PSE in groups 1 and 2

Variables	Group 1 (n = 1099)	Group 2 (n = 1247)	p
Arrhythmias induced during pharmacological stress			
VE	180 (16.4%)	247 (19.8%)	0.032*
SVE	74 (6.7%)	66 (5.3%)	0.162
NSVT	6 (0.5%)	10 (0.8%)	0.617
SVT	0 (0.0%)	1 (0.1%)	1.000
VF	0 (0.0%)	0 (0.0%)	-
PSVT	2 (0.2%)	15 (1.2%)	0.003*
AF	2 (0.2%)	2 (0.2%)	1.000
Bradycardia	1 (0.1%)	0 (0.0%)	0.469
Minor side effects			
Angina	20 (1.8%)	14 (1.1%)	0.170
Headache	5 (0.5%)	19 (1.5%)	0.012*
Nausea	4 (0.4%)	8 (0.6%)	0.397
Reactive AH	3 (0.3%)	19 (1.5%)	0.002*
Arterial hypotension	1 (0.1%)	2 (0.2%)	1.000
Adverse effects	(n=1062)	(n=1174)	
Death within 24 h	0 (0.0%)	0 (0.0%)	-
Death within 30 days	0 (0.0%)	2 (0.17%)	0.276*
AMI within 24 h	0 (0.0%)	1 (0.1%)	0.525
AMI within 30 days	0 (0.0%)	0 (0.00%)	-

*Fisher's test; * significant. AF: atrial fibrillation; AH: arterial hypertension; AMI: acute myocardial infarction; NSVT: non-sustained ventricular tachycardia; PSE: pharmacological stress echocardiogram; PSVT: paroxysmal supraventricular tachycardia; SVE: supraventricular extrasystole; SVT: sustained ventricular tachycardia; VE: ventricular extrasystole; VF: ventricular fibrillation.*

Some studies, for instance, Tsutsui et al.,[19] using Optison® and Definity® as ECA, and Aggeli et al.,[28] using SonoVue®, did not find any events, such as AMI or death, during PSE.

Differently from our sample of outpatients, Anantharam et al.[27] demonstrated the safety of ECA in patients undergoing PSE with suspected stable acute coronary syndrome. Over a 4-year period, 3,704 patients underwent PSE or exercise stress echocardiography; 929 (25%) of these patients had suspected acute coronary syndrome. The ECA used were SonoVue® (46%) and Luminity® (54%), and no deaths occurred in the groups with or without ECA. In this same study, there were no outcomes of AMI in patients who received ECA; on the other hand, 3 patients in the group without ECA had AMI (p = 0.24).[27] Our study showed a low incidence of allergic reactions. These data are similar to those found by Aggeli et al.[28] In their study, 23 (0.44%) patients out of a total of 5250 who received SonoVue® showed itching and urticaria. The condition was reverted with the use of antihistamines, without requiring hospitalization.[28]

Wei et al. retrospectively evaluated 78,383 patients, and they observed that 0.01% of the sample had severe adverse events, considered probably related to Definity®, within the first 30 minutes after administration, distributed equally between men and women. There were 2 cases of allergic reaction such as urticaria and lip edema, but there were no respiratory abnormalities and all patients recovered after use of an antihistamine drug.[21]

In the meta-analysis by Khawaja et al.,[31] which evaluated 110,500 patients, the incidence of severe allergic and anaphylactic reactions immediately after administration of ECA was 0.009% and 0.004%, respectively.[31] In another study conducted by Herzog et al.,[25] the incidence of itching and urticaria was 2 (0.01%), and that of anaphylactic reaction was 1 (0.01%).[25] In the study by Shaikh et al.,[23] anaphylactic reaction was observed in 1 patient (0.03%) after administration of Definity®, without prior exposure to contrast.[23] These very rare and severe allergic reactions are secondary to a type 1 hypersensitivity reaction known as complement activation-related pseudo-allergy or CARPA.[12,32]

According to Muskula et al.,[12] the incidence of allergic reactions with the use of ECA occurs in approximately 0.01% of cases, and these reactions can be avoided by using lower doses with slow infusion.[12] In our study, 83.1% of patients received 2.5 ml, and 7.2% received 4.8 ml of SonoVue®. In our sample, 8.5% of patients repeated PSE with SonoVue®, in under 1 year, and only 1 patient showed urticaria in under 30 minutes, thus making it difficult to determine the dose-response relationship.

Figure 1 – *Example of a patient with allergic reaction/urticaria to use of SonoVue®, with clinical improvement after use of an oral antihistamine drug.*

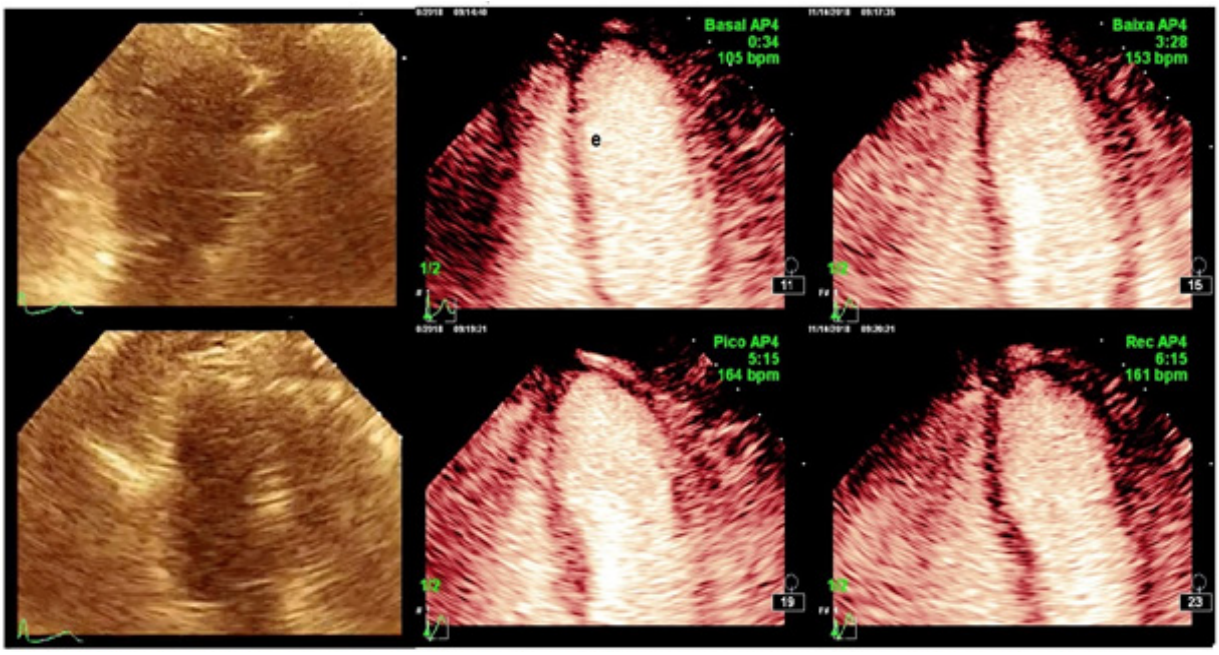

Figure 2 – *Patient with limited acoustic windows, with improved imaged after use of the echocardiographic contrast agent.*

Study limitations

1. This was a prospective, single-center study with outpatients, and it did not include critical patients or patients with acute coronary syndrome

2. The number of patients in the sample was at the lower limit for safety analysis of ECA.

3. Comparisons were not made with other ECA.

Conclusions

SonoVue® demonstrated safety during PSE. No cases of death, AMI, or anaphylactic reaction occurred during the exam or within 24 hours after it was performed. A lower incidence of minor side effects and arrhythmias was observed in the group that underwent PSE with SonoVue® ECA, in comparison with the control group, and there was a low incidence of mild allergic reactions.

Table 5 – Distribution of adverse reactions to echocardiographic contrast agent (SonoVue®) in group I during PSE

Group I (n=1089) Variable	N	%
Allergic reaction	3	0.3
30 min after infusion		
Itching (n=1086)	2	0.2
Sneezing (n=1083)	0	0.0
Urticaria (n=1083)	2	0.2
Wheezing (n=1083)	0	0.0
Anaphylactic reactions (n=1083)	0	0.0
Angioedema (n=1085)	0	0.0
Anaphylactic shock (n=1085)	0	0.0
24 h after infusion		
Itching (n=1081)	1	0.1
Sneezing (n=1081)	1	0.1
Urticaria (n=1082)	1	0.1
Wheezing (n=1082)	0	0.0
Anaphylactic reactions (n=1082)	0	0.0
Angioedema (n=1082)	0	0.0
Anaphylactic shock (n=1082)	0	0.0

N: Número de pacientes; h: horas; min: minutos; EEF: ecocardiograma sob estresse farmacológico.

Author Contributions

Conception and design of the research: Furtado RG; Acquisition of data: Furtado RG, Rassi DC, Melato LH, Oliveira A, Nunes PM, Baccelli P, Santos SCO, Santos VE, Rassi Junior L, Nunes CG; Analysis and interpretation of the data: Furtado RG, Rassi DC, Melato LH, Santos SCO, Santos VE, Rassi Junior L, Nunes CG; Statistical analysis: Furtado RG, Rassi DC; Obtaining financing: Furtado RG, Santos VE, Rassi Junior L, Nunes CG; Writing of the manuscript: Furtado RG, Rassi DC, Melato LH; Critical revision of the manuscript for intellectual content: Furtado RG, Rassi DC, Melato LH.

Potential Conflict of Interest

No potential conflict of interest relevant to this article was reported.

Sources of Funding

There were no external funding sources for this study.

Study Association

This study is not associated with any thesis or dissertation work.

References

1. Dolan MS, Gala SS, Dodla S, Abdelmoneim SS, Xie F, Cloutier D, et al. Safety and efficacy of commercially available ultrasound contrast agents for rest and stress echocardiography. A Multicenter Experience. J Am Coll Cardiol. 2009 Jan 6;53(1):32-8.
2. Mulvagh SL, DeMaria AN, Feinstein SB, Burns PN, Kaul S, Miller JG, et al. Contrast echocardiography: current and future applications. J Am Soc Echocardiogr. 2000 Apr;13(4):331-42.
3. Geleijnse ML, Fioretti PM, Roelandt JR. Methodology, feasibility, safety and diagnostic accuracy of dobutamine stress echocardiography. J Am Coll Cardiol. 1997 Sep;30(3):595-606.
4. Weissman NJ, Cohen MC, Hack TC, Gillam LD, Cohen JL, Kitzman DW. Infusion versus bolus contrast echocardiography: a multicenter, open-label, crossover trial. Am Heart J. 2000 Mar;139(3):399-404.
5. Skyba DM, Camarano G, Goodman NC, Price RJ, Skalak TC, Kaul S. Hemodynamic characteristics, myocardial kinetics and microvascular rheology of FS-069, 2nd gen. echocardiographic contrast agent capable of producing myocardial opacification from a venous injection. J Am Coll Cardiol. 1996 Nov 1;28(5):1292-300.
6. Cohen JL, Cherif J, Segar DS, Gillam LD, Gottdiener JS, Hausnerova E, et al. Improved left ventricular endocardial border delineation and opacification with OPTISON, a new echocardiographic contrast agent. Results of a phase III Multi- center Trial. J Am Coll Cardiol. 1998 Sep;32(3):746-52
7. Kitzman DW, Goldman ME, Gillam LD, Cohen JL, Aurigemma GP, Gottdiener JS. Efficacy and safety of novel ultrasound contrast agent perflutren (Definity) in patients with suboptimal baseline left ventricular echocardiographic images. Am J Cardiol. 2000 Sep 15;86(6):669-74.
8. U.S. FDA prescribing information for Definity approved October 10, 2007. Available at: http://www.fda.gov/cder/foi/label/2007/ 021064s007lbl.pdf. Accessed November 15, 2007.
9. Mathias Jr W, Porter TR, Tsutsui JM, Mattoso AA. Manual de Ecocardiografia Contrastada. Jaypee – Highlights Medical Publishers, ISBN:978-9962-678-82-3. Panamá, Republica do Panamá, 2016.
10. Porter T, Mulvagh S, Abdelmoneim S, Becher H, Belcick JT, Bierig M, et al. Clinical aplications of ultrasonic enhanching agents in echocardiography: 2018 American Society of Echocardiography Guidelines Update. J Am Soc Echocardiogr. 2018 Mar;31(3):241-274.
11. Pellikka PA, Nagueh SF, Elhendy AA, Kuehl CA, Sawada SG; American Society of Echocardiography. American Society of Echocardiography recommendations for performance, interpretation, and application of stress echocardiography. J Am Soc Echocardiogr. 2007;41(9):1021-34.
12. Muskula PR, Main ML. Safety with echocardiographic contrast agents. Circ Cardiovasc Imaging.Circ Cardiovasc Imaging. 2017 Apr;10(4):e005459.
13. Lang RM, BAdano L, Mor-avi V, Afilalo J, Armstrong A, Ernande L, et al. Recommendations for cardiac chamber quantification echocardiography in adults: an update from the American Society of Echocardiography and the European Association Cardiovascular Imaging. J Am Soc Echocardiogr. 2015 Jan;28(1):1-39.e14.
14. Rassi DC, Furtado RG, Turco FP, Melato LH, Oliveira ACR, Dourado CN, et al. Análise da segurança e dos preditores de arritmias durante o ecocardiograma sob estresse com dobutamina em um ambiente não hospitalar. Arq Bras Cardiol:Imagem cardiovasc. 2018;31(3):168-174.
15. KarvonenNJ, KentalaE, MustalaO. The effects of training on heart rate:a "longitudinal" study. Ann Med Exp Biol Fenn. 1957;35(3):307-15.
16. Mathias Jr W, Tsuatsui JM (eds). Ecocardiografia. Barueri(SP): Manole; 2012.
17. Geleijnse M, Krenning B, Nemes A, Van Dalen B, Soliman O, Cate F. Incidence, pathophysiology, and treatment of complications during dobutamine-atropine stress echocardiography. Circulation. 2010;121(15):1756-67.

18. Mathias Jr W, Beneti LP, Santos FC, Duprat R, Beraldo A, Adan Gil M, et al. Segurança e exequiblidade da ecocardiografia com estresse pela dobutamina associada à atropina. Arq Bras Cardiol. 1997 Jul;69(1):31-4.

19. Tsutsui JM, Elhendy A, Xie F, O'Leary E, McGrain AC, Porter TR. Safety of dobutamine stress real time myocardial contrast echocardiography. J Am Coll Cardiol. 2005 Apr 19;45(8):1235-42.

20. Abdelmoneim SS, Mathieu B, Scott CG, Dobble A, Ness AS, Hagen ME, et al. Safety of contrast agent use during stress echocardiography. JACC Cardiovasc Imaging. 2009 Sep;2(9):1048-56.

21. Wei K, Mulvagh SL, Carson L, Davidoff R, Gabriel R, Grimm RA, et al. The safety of definity and optison for ultrasound image enhancement: a retrospective analysis of 78,383 administered contrast doses. J Am Soc Echocardiogr. 2008 Nov;21(11):1202-6.

22. Gabriel RS, Smyth YM, Menon V, Klein AL, Grimm RA, Thomas JD, et al. Safety of ultrasound contrast agents in stress echocardiography. Am J Cardiol. 2008 Nov 1;102(9):1269-72.

23. Shaikh K, Chang SM, Peterson L, Rosendahl-Garcia K, Quinones MA, Nagueh SF, et al. Safety of contrast administration for endocardial enhancement during stress echocardiography compared with noncontrast stress. Am J Cardiol. 2008 Dec 1;102(11):1444-50.

24. Main ML, Ryan AC, Davis TE, Albano MP, Kusnetzky LL, Hibberd M. Acute mortality in hospitalized patients undergoing echocardiography with and without an ultrasound contrast agent (multicenter registry results in 4,300,966 consecutive patients). Am J Cardiol. 2008 Dec 15;102(12):1742-6.

25. Herzog CA. Incidence of adverse events associated with use of perflutren contrast agents for echocardiography. JAMA. 2008 May 7;299(17):2023-5.

26. Kusnetzky LL, Khalid A, Khumri TM, Moe TG, Jones PG, Main ML. Acute mortality in hospitalized patients undergoing echocardiography with and without an ultrasound contrast agent. J Am Coll Cardiol. 2008 Apr 29;51(17):1704-6.

27. Anantharam B, Chahal N, Ramzy I, Garu F, Senior R. Safety of contrast in stress echocardiography in stable patients and in patienys with suspected acute coronary syndrome but negative 12-hour troponin. Am J Cardiol. 2009 Jul 1;104(1):14-8.

28. Aggeli C, Giannopoulos G, Roussakis G, Christoforatou E, Marinos G, Toli C, et al. Safety of myocardial flash- contrast echocardiography in combination with dobutamine stress testing for detection of ischemia in 5250 studies. Heart. 2008 Dec;94(12):1571-7.

29. Camarozano AC, Junior PR, Siqueira-Filho AG, Weitzel LH, Noe R. The effects of beta-blockers on dobutamine-atropine stress echocardiography: early protocol versus standard protocol.Cardiovascular Ultrasound 2006,4:30.

30. Vancraeynest D, Kefer J, Hanet C, Fillee C, Beauloye C, Pasquet A, et al. Release of cardiac bio-markers during high mechanical index contrast-enhanced echocardiography in humans. Eur Heart J. 2007 May;28(10):1236-41.

31. Khawaja OA, Shaikh KA, Al-Mallah MH. Meta-analysis of adverse cardiovascular events associated with echocardiographic contrast agents. Am J Cardiol. 2010 Sep 1;106(5):742-7.

32. Szebeni J. Complement activation-related pseudoallergy: a new class of drug-induced acute immune toxicity. Toxicology. 2005 Dec 15;216(2-3):106-21.

Adiponectin Prevents Restenosis Through Inhibiting Cell Proliferation in a Rat Vein Graft Model

Yang Zhou,[1] Chun Dai,[2] Bing Zhang,[3] Jianjun Ge[1]

Department of Cardiac Surgery, Anhui Provincial Hospital, Anhui Medical University,[1] Hefei, Anhui - China

School of Medicine, Cheeloo College of Medicine, Shandong University,[2] P.R. – China

The First Affiliated Hospital of USTC, Division of Life Sciences and Medicine, University of Science and Technology of China, Hefei,[3] Anhui - China

Abstract

Background: **Coronary artery bypass grafting (CABG) continues to be an effective therapy for coronary artery disease patients, but the vein graft is prone to restenosis or occlude. Adiponectin (ADP) is a plasma hormone protein with the function of regulating cell proliferation.**

Objective: **This study used two different doses of ADP protein in a rat vein graft model to stimulate vein graft change. The aim of our study was to investigate the effect of ADP on vein graft restenosis.**

Methods: **Autologous jugular veins were implanted as carotid interposition grafts through the anastomotic cuff technique in Sprague Dawley rats. Adiponectin (2.5 μg and 7.5 μg) was delivered to the vein bypass grafts in a perivascular fashion, suspended in a 30% Pluronic-F127 gel. No treatment (bypass only) and vehicle loaded Pluronic gel served as controls. Comparisons were made with one-way analysis of variance and a post-hoc test, with $p < 0.05$ considered significant.**

Results: **Cell proliferation (PCNA index) was significantly low in adiponectin-treated versus control and vehicle-gel-treated grafts, both in intima and adventitia, as of day 3 ($p < 0.01$). VCAM-1 and ICAM-1 evaluated by immunohistochemistry significantly down-regulated in the adiponectin-treated vein grafts in the fourth week ($p < 0.01$). Treatment of vein grafts with adiponectin-loaded gels reduced intimal, media, and adventitia thickness when compared with the control and vehicle-gel-treated vein grafts at day 28 ($p < 0.01$).**

Conclusions: **Our studies provide further support for the potential therapeutic role of adiponectin in modulating vascular injury and repair.**

Keywords: **Adiponectin; Cell Proliferation; Hyperplasia.**

Introduction

Coronary artery disease (CAD) is a worldwide disease with an increasing morbidity and mortality.[1] Coronary artery bypass grafting (CABG) continues to be an therapy for advanced stage patients. Saphenous vein grafts provide the most widely used bypass conduit, which make up ~50% of grafts used in CABG for its convenience of harvesting and manipulating, its sufficient length, and its character of not easily being affected by competitive coronary blood flow.[2,3] Despite the advantages in treatments, the grafted vein is prone to restenosis or occlude under the influence of arterial blood pressure, persistent inflammation and associated risks of failure, with a patency rate of 65% - 80% in 5 years after operation.[4-6] Therefore, how to inhibit restenosis in the vein grafts represents a challenge.

Intimal hyperplasia (IH) plays a causal role in grafted vein restenosis, characterized by an excessive accumulation of vascular smooth muscle cells (VSMCs) leading to occlusive disorders.[6-8] In addition, increasing data indicate that the adventitia may also be related to the remodeling of the grafted veins.[9-11] After being injured, adventitial fibroblasts activate and proliferate, followed by adventitia biosynthesizing, and release a variety of cytokines to promote the proliferation of VSMCs. The entire process results in IH and restenosis.[12-15] Many cytokines have proven to be involved in the proliferation of VSMCs, among which VCAM-1 and ICAM-1 can promote cell adhesion and atherosclerotic lesion formation.[16,17]

Adiponectin (ADP), a plasma hormone protein specifically biosynthesized by adipocytes, can exert an effect by binding to adiponectin receptors in fibroblasts.[18,19] ADP can also be used to attenuate endothelial dysfunction.[20] Recent studies have shown that ADP plays important roles in suppressing cell proliferation after damage to the vessel, and decreases cytokines, which also promote cell proliferation.[21,22]

Mailing Address: Bing Zhang e Jianjun Ge •
Department of cardiac surgery, The First Affiliated Hospital of USTC, Lujiang Rd 17, Hefei, Anhui, 230001 - China
E-mail: zkdgjj@ustc.edu.cn
Manuscript received July 11, 2020, revised manuscript December 12, 2020, accepted January 27, 2021

DOI: https://doi.org/10.36660/abc.20200761

Considering these findings, we hypothesize that ADP can prevent vein graft restenosis by inhibiting cell proliferation. ADP was delivered to the external surface of the graft veins with two different concentrations in order to investigate the effect of ADP on vein graft restenosis. The results showed that the ADP significantly decreased intimal, medial, and adventitial thickness of the vein graft. Meanwhile, cell proliferation and cytokine expression (VCAM-1, ICAM-1) also decreased. These results primarily demonstrated the role of ADP in preventing vein graft restenosis and highlighted the potential mechanism.

Methods

Ethical approval for animal experiments was accepted from the Animal Care and Use Committee of the First Affiliated Hospital to the University of Science and Technology of China. Sprague Dawley (SD) rats (male and female, aged 10-12 weeks, body weight of 275-325 g, and N=72) were purchased from the Anhui Lab Animal Research Center and were randomly assigned to the ADP treatment groups (low and high dose groups), vehicle gel treatment group (pluronic-F127 gel), and control group (bypass only). According to previous research, 72 rats were divided into 4 groups, which were then divided into 12 groups at three different points of time[23] (n = 6 per group).

Perivascular drug delivery constructs

The adventitial drug delivery approach used Pluronic F127 gel as a vehicle gel. A total of 2.5μg adiponectin (Abcam) was dissolved in 25 μl of distilled water and resuspended in 300 μl of 30% pluronic-F127 gel for delivery to vein grafts after carotid interposition in a low dose adiponectin treatment group (L-ADP group), while 7.5μg adiponectin was used to coat the graft veins in a high dose adiponectin treatment group (H-ADP group). An equal amount of pluronic-F127 gel was applied to the vehicle gel treatment group (VG group). Only upon application were the pluronic-F 127 gels taken out of a 4℃ environment, which seeks to maintain its liquid form.

Rat autologous vein graft model

SD rats were anesthetized with a 10% chloral hydrate (300 mg/kg) and received heparin (200 U/kg) via caudal vein injection. The left jugular vein was harvested for use as a carotid interposition graft. The bypass was performed by applying the anastomotic cuff model, as previously described.[24] Specifically, 2-mm cuffs were cut from a 20G red arterial puncture needle (BD Company). The carotid artery was isolated up to the branches. The proximal and distal ends of the artery were then placed under suture traction lines and hemoclips to block blood flow before being cut in middle. Both ends of the arteries were then pulled through the cuff. The arteries were then everted and secured to the cuff with 6–0 silk suture. Following an arteriotomy in the left (ipsilateral) common carotid artery, the cuffs were inserted into and secured to the artery with a 6–0 silk suture. The artery was then divided to enable a longitudinal extension of the vein interposition graft. Treatments were applied to the external surface of the graft after unclamping. Both adiponectin treatment groups underwent a perivascular application of 300 μL of ADP gel, the vehicle gel treatment group with 300 μl of pluronic-F127 gel, and the bypass only group with no gel. Additionally, gels were kept on ice until perivascular application and subsequently allowed to solidify at body temperature, as previously described.[25]

Harvest of implanted grafts

Rats were euthanized on the 3rd, 14th, and 28th days after bypass transplantation respectively, 6 rats each time. Following vein grafts patency tested by Doppler ultrasonography, vein graft specimens were harvested and cut into 2 sections. One segment was immediately fixed after perfusion with heparinized saline, followed by 4% formaldehyde for hematoxylin and eosin (H&E), Masson staining and immunohistochemistry assay analyses, while the other was placed at -80℃ for Western blot analysis. Animals were sacrificed by sodium pentobarbital overdose.

Morphometric analysis

After fixation in 4% formaldehyde and processing in 70% ethanol, specimens harvested on the 3rd, 14th and 28th days were paraffin embedded; 3-μm sections were taken throughout the graft, excluding regions immediately adjacent to the anastomotic cuffs. Sections were stained with hematoxylin and Masson kit (Shanghai Gefan Biological, China.), and staining sections were observed by a Leica-DM2000 biological microscope (Leica, Hefei, China). At least five equally spaced sections of the bypass grafts were analyzed for each specimen. Standard morphometric measurements were recorded, including intimal thickness, medial thickness, and adventitial thickness. These data were then calculated by ImageJ (National Institutes of Health, Bethesda, Md).

Immunohistochemistry analysis

Paraffin-embedded tissues (3, 14 and 28-day grafts) were processed, and 3-μm sections were taken throughout the graft, excluding regions immediately adjacent to the anastomotic cuffs. After deparaffinization, the antigen was recovered with a citrate buffer for 20 min at high temperature and pressure, then deactivated with a 3% H_2O_2 endogenous peroxidase for 20 min and block endogenous peroxidase with 5% bovine serum albumin for 10 min. Sections were treated overnight at 4℃ with anti-PCNA monoclonal antibody (D3H8P; Cell Signaling), anti-VCAM1 antibody (ab134047; Abcam, 1:500 dilution), and anti-ICAM1 antibody (ab119871; Abcam, 1:200 dilution). Three separate sections per graft were analyzed for all markers. The slices were washed several times. Biotinylated secondary antibody working solution and horseradish peroxidase conjugated streptavidin working solution were added to the slices, respectively. The slices were washed in PBS (pH 7. 2) for 5 minutes. Diaminobenzidine tetrahydrochloride (DAB) was used to visualize and hematoxylin to counterstain. Lastly, the slices were dehydrated, and then mounted and sealed. All images were acquired by image signal acquisition and analysis system (Leica-DM2000, Hefei, China). PCNA index was used to describe the level of PCNA expression (PCNA index = the numbers of PCNA positive cells / the

numbers of all cells). Average optical density was used to describe the standard of VCAM-1 and ICAM-1 expressions (average optical density = Integral optical density / area).

Western blot assay of PCNA and VCAM-1 protein expression analysis

Total protein was isolated from grafted veins. After electrophoresis and electrotransfer, membranes were blocked with 5% skimmed milk and were incubated at 4℃ with primary antibodies overnight (with anti-PCNA monoclonal antibody D3H8P; Cell Signaling, 1:1000 dilution; anti-VCAM1 antibody ab134047; Abcam, 1:3000 dilution; anti-β-Tubulin antibody GB11017; Servicebio, 1:2000 dilution). After being incubated with secondary antibody (goat anti-mouse IgG-HRP SE131; Solarbio, 1:3000 dilution), the membranes were washed with TBST. The membranes were then exposed on the PVDF film and an ECL coloring solution (PE0010, Solarbio) was added. Separated immunoreactive bands were processed by Odyssey v1.2 software. Gray values were measured based on the internal reference of β-Tubulin.

Statistical analysis

Data were presented as mean ± standard deviation (SD) and were processed by SPSS v.21.0 software (Chicago, IL). Because data followed a normal distribution verified by the Kolmogorov–Smirnov test, comparisons among multiple groups were analyzed by one-way analysis of variance (ANOVA). Comparisons between two groups were analyzed by Fisher's least significant difference (LSD) test. A p-value < 0.05 was considered statistically significant.

Results

The previously described operation method was used to establish the model of autologous jugular vein bypass in rats. After the procedure, the transplanted jugular veins were fully filled, and the blood vessels beat well. Local perivascular delivery of Pluronic-F 127 gel evenly covered the surface of the blood vessel. The incision was closed after the glue solidified. The incision healing and activity status of rats were checked every day after operation. Doppler ultrasound was performed on the day of euthanasia, which showed that the transplanted jugular vein blood did not clearly occlude. In the 28-day control group, the vein grafts were thickened and were slightly stiff, and the surrounding tissue adhesion was relatively obvious. Correspondingly, veins in the high-dose adiponectin group did not expand significantly, and the surrounding tissues were easy to separate (Fig 1).

Adiponectin attenuates vein graft intimal, medial, and adventitial hyperplasia

Morphometric analysis of grafts explanted after bypass (Figure 2A) showed decreased intimal, medial, and adventitial thickness after perivascular delivery of adiponectin. Quantification of the intimal, medial, and adventitial thickness was performed by at least five equally spaced sections along the nonanastomotic vein for each bypass graft. In view of the three time points of day 3, day 14, and day 28, there was no significant difference in the thickness of the intima, media, and adventitia between the control group and the vehicle gel group, which meant the application of Pluronic F-127 gel as the load gel will not affect the pathophysiology of vein grafts. To be specific, the intimal thickness of the vein graft in the H-ADP group diminished significantly on day 14 and day 28 compared with the control group and the vehicle gel group. Similarly, intimal thickness in the L-ADP group evidently decreased more than that in the control group and the vehicle gel group on day 14 and day 28 (Figure 2B, Table 1).

Compared with intimal hyperplasia, the average hyperplasia in the grafted veins occurred earlier; the thickening of the average in the control and the vehicle gel group on day 3 was more obvious than that in the L-ADP and H-ADP groups. Similarly, the thickness of the medial tissue decreased in the high-dose adiponectin groups when compared with the control group and the vehicle gel group on day 14 and day 28. The same tendency also existed in the low-dose adiponectin group on day 14 and day 28 (Figure 2C, Table 1).

The intima-to-media ratios in the L-ADP and H-ADP groups were higher when compared to the control and vehicle gel groups on day 3. After, the intima-to-media ratio was notably lower in the H-ADP group on day 14 and day 28 when compared to the control and vehicle gel groups. Data from the L-ADP group showed a similar tendency at day 14 and day 28 when compared to the control and vehicle gel groups (Figure 2E).

In addition, our study found that the application of adiponectin can also inhibit the adventitia hyperplasia of grafted veins in both of the different dose groups. Adventitia thickness was attenuated by high-dose adiponectin when compared to the control and vehicle gel groups on day 3, day 14, and day 28. The same trend occurred in the low-dose adiponectin treatment groups when compared to the control and vehicle gel groups on day 3, day 14, and day 28 (Figure 2D, Table 1).

Adiponectin decreases cell proliferation after vein grafting

Cell proliferation was quantified by the PCNA index of intima and adventitia (total number of PCNA-positive cells divided by the total number of nucleated cells) at 3 time-points after bypass (Figure 3A, 3B). The cell proliferation between the control and the vehicle group in both intima and adventitia was similar at 3 points of time. High-dose adiponectin-treated veins showed minimal proliferation in intima (26%) and adventitia (10%) three days after bypass as compared to the control and vehicle gel groups. Compared to the control (intima: 36%; adventitia: 36%) and vehicle gel (intima: 37%; adventitia: 37%) groups, proliferation diminished in the L-ADP group both in intima (29%) and adventitia (19%) on the third day. Moreover, proliferation suppression of the H-ADP group was also more obvious in adventitia than that of the L-ADP group on day 3. Proliferation was pronounced in vein grafts on day 14 (intima, 48%; adventitia, 46%) and day 28 (intima, 61%; adventitia, 51%) in the control group, but also on day 14 (intima, 47%; adventitia, 46%) and day 28 (intima, 59%; adventitia, 50%) in the vehicle gel group.

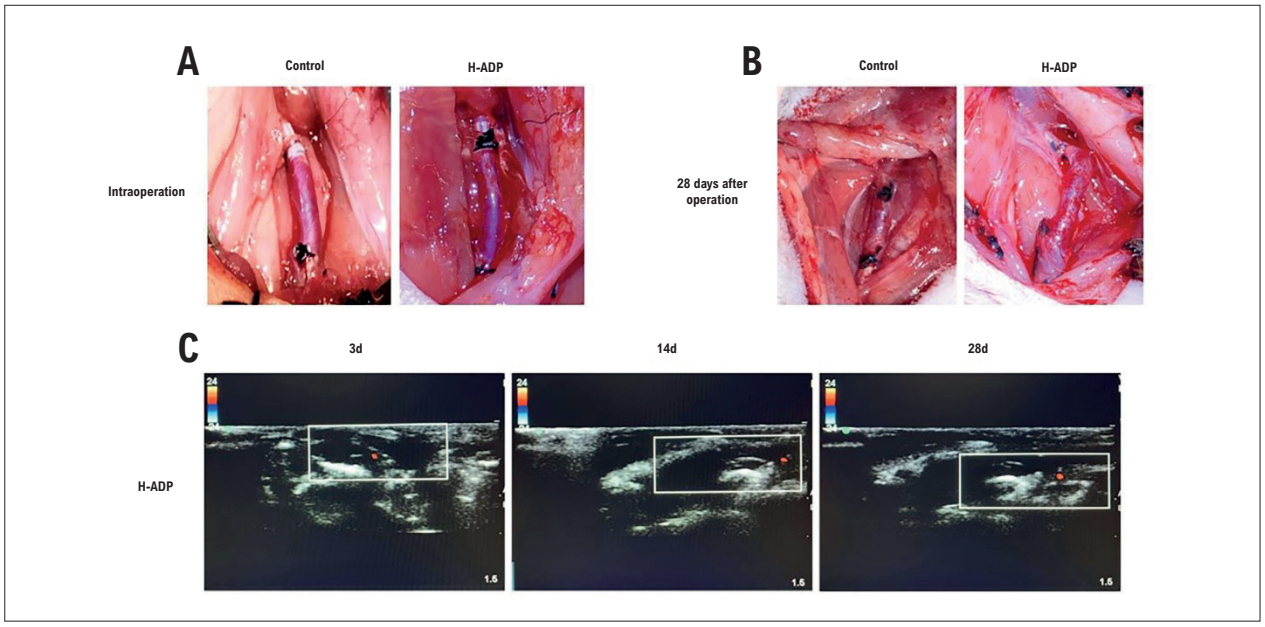

Figure 1 – *Intraoperative and postoperative photographs and Doppler ultrasound photographs. (A) a. Intraoperative photographs of control and high-dose adiponectin groups; (B) postoperative photograph in the fourth week of control and high-dose adiponectin groups; (C) Doppler ultrasound photographs on the day of euthanasia in the control and high-dose adiponectin groups.*

Perivascular application of high-dose adiponectin exhibited 34% proliferation in intima and 20% in adventitia on day 14 when compared to the control and vehicle gel groups. Proliferation in the L-ADP group was visibly lower in both intima (43%) and adventitia (37%) on day 14 when compared to the control and vehicle gel groups. The differences can also be found in intima and adventitia between two different dose groups on day 14. Proliferation inhibition was also evident on day 28 in the L-ADP group, 49% proliferation of intima and 43% of adventitia, which illustrated significant differences when compared to the control and the vehicle gel groups. The expression of PCNA in the H-ADP group showed a similar trend in intima (38%) and adventitia (29%) on day 28. Comparison between two different adiponectin groups also showed notable differences in intima and adventitia on day 28 (Figure 3C, 3D). The expression of PCNA determined by Western blot also demonstrated the same effects of adiponectin (Figure 4A, 4B).

Adiponectin decreases VCAM-1 and ICAM-1 expressions after vein grafting

VCAM-1 was expressed in the early stages, but there was no difference in each group on day 3. Difference was not observed between the control and the vehicle gel group. The expression of VCAM-1 in the high-dose adiponectin treatment group was significantly suppressed in relation to the control and vehicle gel groups on day 14 (0.25 versus 0.31, 0.30) and day 28 (0.30 versus 0.50, 0.50). The expression of VCAM-1 in the L-ADP group was also inhibited in relation to the control and vehicle gel groups on day 14 (0.26) and day 28 (0.40). *In addition*, the difference between the H-ADP and the L-ADP groups was also marked on day 28 (Figure 5A, Figure5C). Results determined by Western blot also illustrated a similar tendency (Figure 4A, Figure 4C).

ICAM-1 expression analyzed by ImageJ was rarely observed in the early stages. The expressions of ICAM-1 showed no prominent difference in the H-ADP group (0.10 versus 0.18 in control group, 0.19 in vehicle gel group) and the L-ADP group (0.10 versus control and vehicle gel group) until day 28 (Figure 5B). No difference could be observed between the two different dose adiponectin groups at the three point in time.

Discussion

Despite advances in CAD therapies, CABG remains the main surgical treatment, and thus restenosis continues to plague the patency of vein grafts.[26] Many experiments have tried to better understand the mechanisms of venous-graft failure and to identify new approaches to reduce vessel injury and to improve healing.[27-29] Our study demonstrated that adiponectin delivered to the external surface of rat vein grafts at the time of implantation through Pluronic-F gel not only reduced intimal hyperplasia on day 28 compared with bypass-only controls, but can also decrease medial and adventitial hyperplasia. Our results suggest that reduced anti-proliferative activity and cytokine expression (VCAM-1, ICAM-1) in the graft wall are likely to be involved in this effect. These results demonstrate the role of ADP in preventing the vein graft restenosis and highlight the potential mechanism.

The complicated remodeling process of vessels results in restenosis of the vein grafts, but the specific mechanism is still unclear. Studies have shown that the process of venous-graft restenosis includes thrombosis, intimal hyperplasia, neointimal formation, and atherosclerosis.[3] After vessel

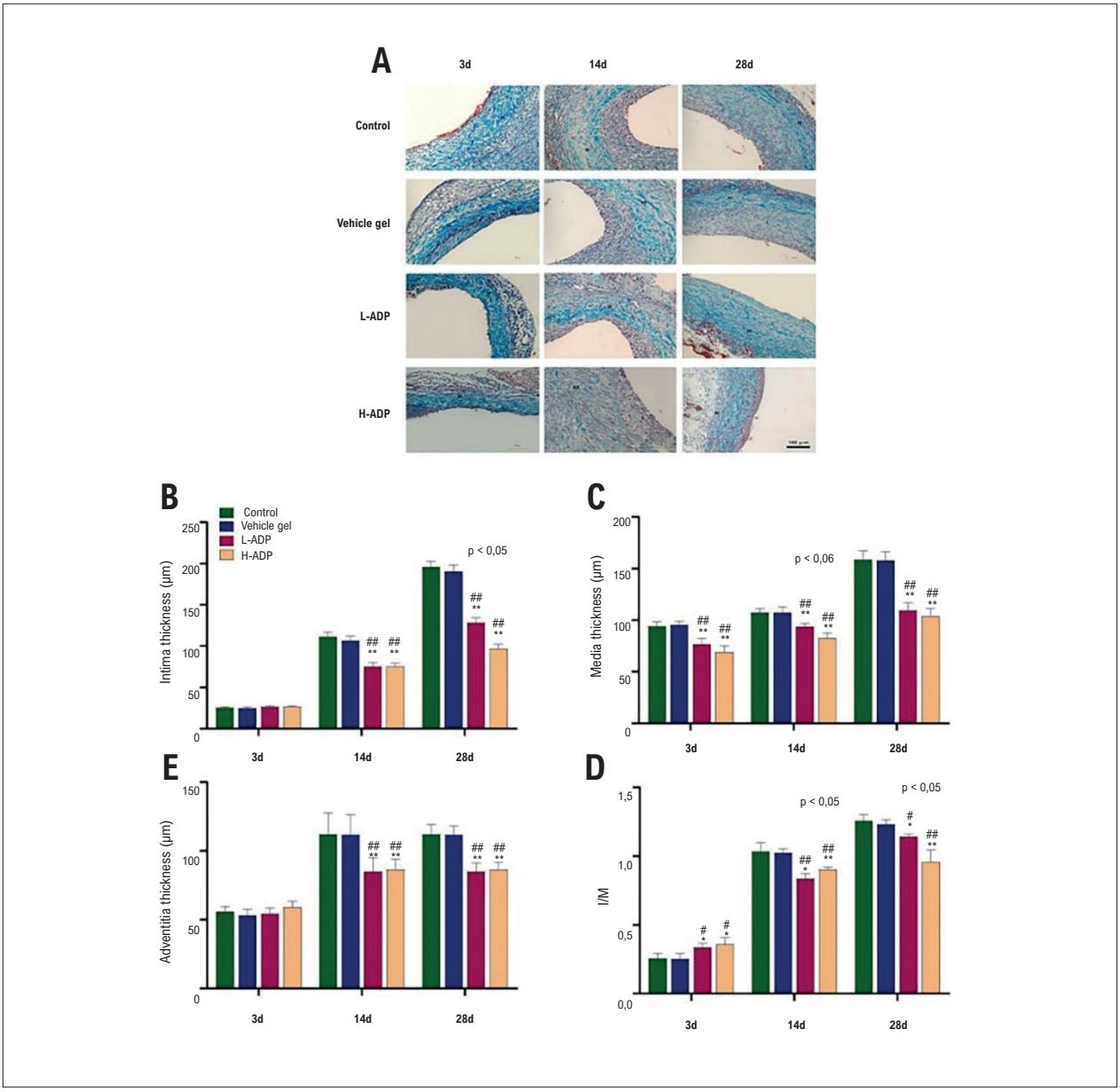

Figure 2 – *Local perivascular delivery of adiponectin attenuates vein graft intimal, medial, and adventitial hyperplasia within rat vein grafts. (A) Light micrographs of Masson-stained sections of grafted veins (200× magnification, bar: 100μm). (B) The change of neointimal thickness; (C) The change of medial thickness; (D) The change of adventitial thickness; (E) intima-to-media (I/M) ratio. Results are presented as mean ± SD. *P < 0.05 versus control group, **P < 0.01 versus control group. #P < 0.05 versus vehicle gel group, ##P < 0.01 versus vehicle gel group. I: intima; M: media.*

transplantation, vascular smooth muscle cell proliferation and migration are affected by changes in endothelial cell dysfunction, inflammation, hemodynamics, among other factors.[11] In addition, the adventitia of the blood vessel is also damaged. The activated adventitial fibroblasts transform into myofibroblasts, and then proliferate and migrate to the media and intima, where they synthesize and release a variety of cytokines to promote smooth muscle cell proliferation and migration.[30-32] Studies have revealed that adiponectin can be bound to adiponectin receptors expressed in adventitial fibroblasts and play a key role. Furthermore, many studies have reported that adiponectin has anti-inflammatory and anti-atherosclerotic effects on the cardiovascular system.[33] However, the effects of ADP on preventing restenosis remain largely unknown. The present study primarily demonstrated the potential efficacy of ADP in inhibiting vein graft hyperplasia.

In this study, adiponectin was applied to the rat autologous vein graft model to stimulate the pathophysiological process of vein grafts after CABG. The thickness of intima in the adiponectin groups was found to be significantly lower than that in the bypass-only group and vehicle-gel treatment group, indicating that adiponectin has an effect on inhibiting intima

Table 1 – The thickness of intima, media, and adventitia in the control, vehicle gel (pluronic-F127 gel), L-ADP (low-ADP dose), and H-ADP (high-ADP dose) groups

Groups	Time(day)	Control N=6	Vehicle gel N=6	L-ADP N=6	H-ADP N=6	Analysis
Intima thickness (μm)	3	25.47±1.02	25.10±1.53	26.55±1.05	26.46±0.71	ANOVA
	14	111.69±5.31	106.62±5.57	75.12±4.94** #	75.46±3.59** ##	ANOVA
	28	196.09±6.78	190.44±7.68	128.30±6.01** ##	96.96±5.45** ##	ANOVA
Media thickness (μm)	3	94.00±4.19	95.47±3.38	76.93±5.30** #	69.03±5.94** #	ANOVA
	14	107.19±3.66	107.41±5.48	93.86±3.17** ##	82.83±4.13** ##	ANOVA
	28	158.83±8.39	157.75±8.75	109.67±7.16** #	104.02±7.12** #	ANOVA
Adventitia thickness (μm)	3	56.09±3.42	53.03±4.59	54.51±3.95	59.21±4.28	ANOVA
	14	112.03±7.08	111.87±6.35	85.04±6.35** ##	86.52±5.20** ##	ANOVA
	28	152.31±3.55	154.49±6.55	95.70±6.05** ##	90.15±4.87** ##	ANOVA

*The values of thickness are presented as mean ± SD (N=6). *: p < 0.05 versus control group, **: p < 0.01 versus control group. #: p < 0.05 versus vehicle gel group, ##: p < 0.01 versus vehicle gel group.*

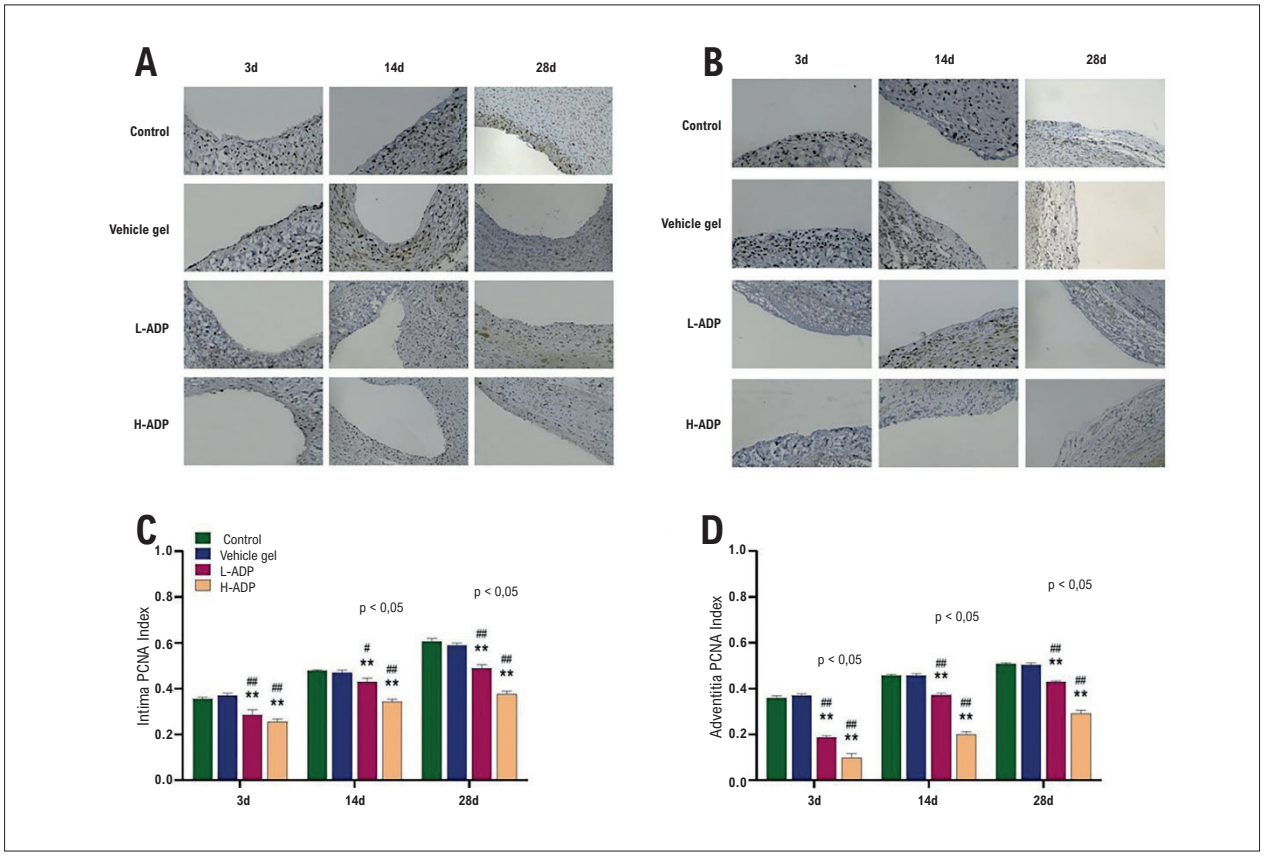

Figure 3 – *Adiponectin decreases cell proliferation. (A) PCNA index of intima determined by immunohistochemistry (200×magnification); (B) PCNA index of adventitia determined by immunohistochemistry (200×magnification); (C) PCNA index of intima; (D) PCNA index of adventitia. Data represent mean ± SD. *p < 0.05 versus control group, **p < 0.01 versus control group. #p < 0.05 versus vehicle gel group, ##p < 0.01 versus vehicle gel group.*

hyperplasia. Moreover, the higher-dose adiponectin was more effective in this study. Interestingly, we found that the PCNA index of intima and adventitia decreased in the adiponectin treated groups as well, demonstrating that adiponectin may well have an inhibitory effect on cell proliferation in the intima and adventitia of grafted veins. This study provides only limited insight into the mechanisms through which ADP reduced vein graft intima in this model. However, comparing our data with that taken in the context of previous studies, it can be concluded that adiponectin was not only able to

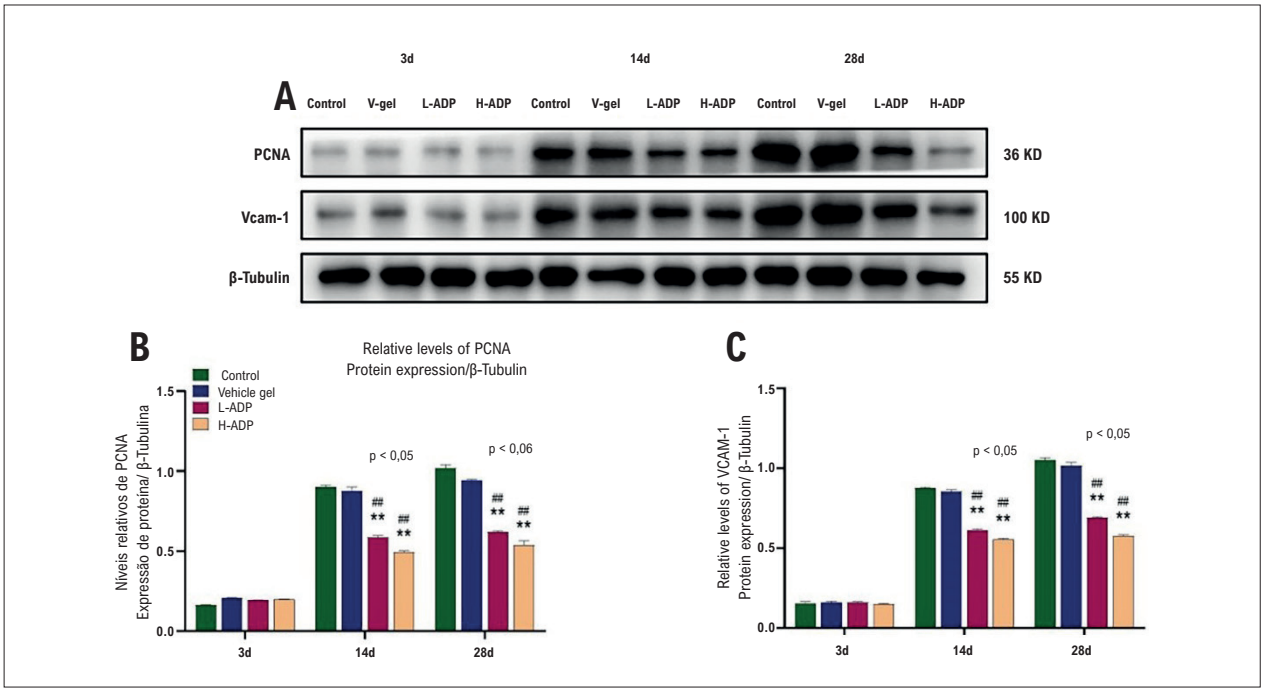

Figure 4 – *Inhibition of PCNA and VCAM-1 expressions by delivery of adiponectin. (A) Expressions of PCNA and VCAM-1 in all groups at three points in time after operation; (B) Expression of PCNA determined by Western blot; (C) Expression of VCAM-1 determined by Western blot. Data represent mean ± SD. *p < 0.05 versus control group, **p < 0.01 versus control group. #p < 0.05 versus vehicle gel group, ##p < 0.01 versus vehicle gel group.*

inhibit intimal hyperplasia, but also to inhibit the proliferation of myofibroblasts and limit its migration to the intima and media.[34,35]

However, the specific mechanism of the interaction between adiponectin and receptors still needs further study. The pharmacokinetics of perivascular delivery of adiponectin also need to be better defined in future studies. Researchers have also shown that thrombosis plays a key role in the early phase of vein graft failure. The vein is subjected to a period of ischemia-reperfusion injury-leading to a reduction in endothelial nitric oxide synthase (eNOS) expressing, damage to endothelial cells and smooth muscle cells (SMCs), and the release of various prothrombotic mediators. Furthermore, the remodeling processes of the vein graft start within days after harvesting and grafting, leading to the formation of intimal hyperplasia.[25] We believe ADP can exert an impact in both the early and intermediate stages. Our study only brings information about the short-term effect. Further research is warranted in order to understand the specific mechanism in the short-term and to know how ADP influences the long-term outcome.

After the endothelium is damaged, an early pathophysiological process of restenosis, the adhesion molecules ICAM-1 and VCAM-1 are released, which lead to adhesion and infiltration of monocytes / macrophages that differentiate and engulf a large amount of ox-LDL, and then form foam cells. In our experiments, we detected the expression of VCAM-1 and ICAM-1 by immunohistochemistry and found that the values of VCAM-1 and ICAM-1 in the adiponectin group were markedly lower than those in the vehicle-gel treatment group and the bypass-only group, which elucidated how the application of adiponectin can downregulate the expression of VCAM-1 and ICAM-1 to promote dysfunction of endothelium.

Conclusion

The present study confirmed that the local perivascular delivery of adiponectin attenuates vein graft hyperplasia in a rat carotid bypass model. This effect appears to be mediated by both decreased cell proliferation and a downregulated expression of VCAM-1 and ICAM-1 within the graft. Although the short-term effects of adiponectin seem promising, the long-term effects and clinical significance of adiponectin in CABG need to be studied in the future. We hope that these studies will eventually be translated into clinical application in the prevention of restenosis and bypass graft failure.

Author Contributions

Conception and design of the research: Zhou Y, Zhang B, Ge J; Acquisition of data: Zhou Y, Dai C; Analysis and interpretation of the data, Statistical analysis and Writing of the manuscript: Zhou Y; Obtaining financing: Ge J; Critical revision of the manuscript for intellectual content: Zhang B, Ge J.

Potential Conflict of Interest

No potential conflict of interest relevant to this article was reported.

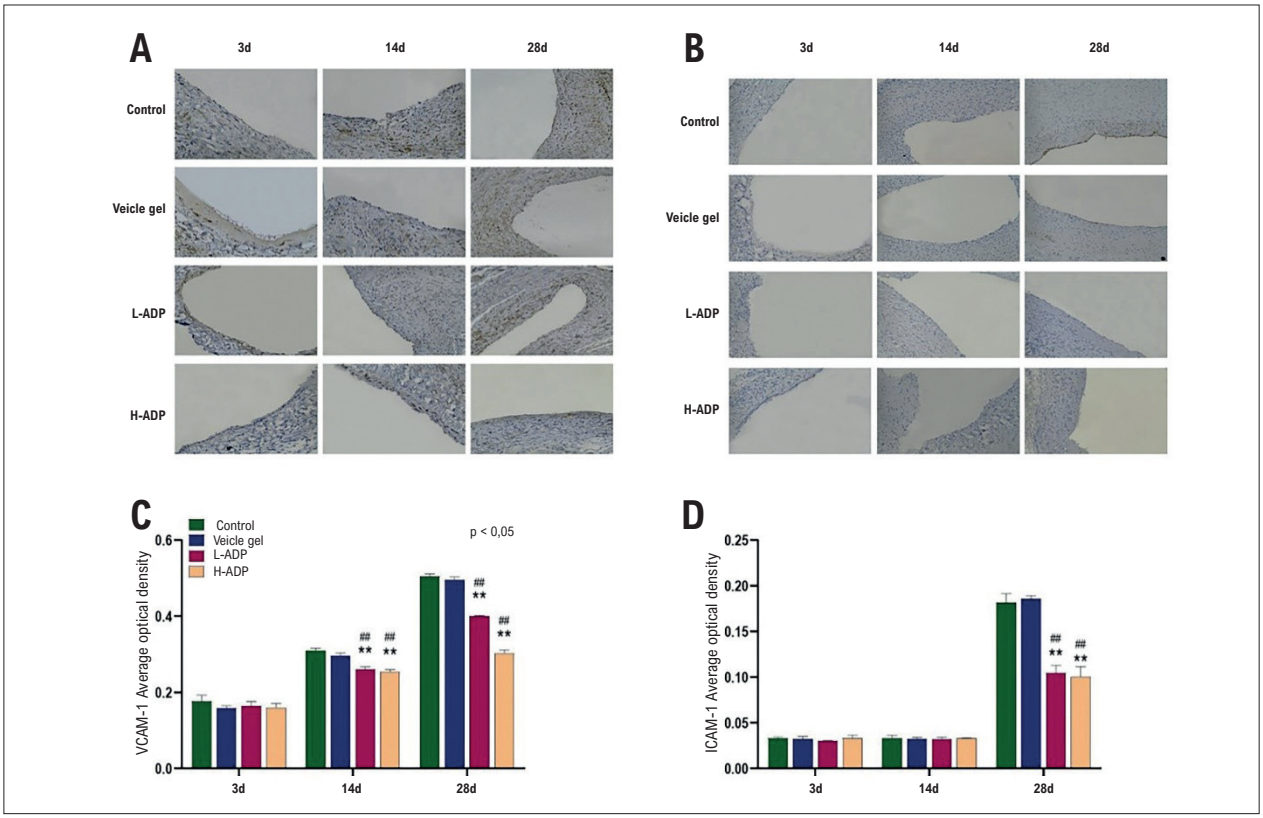

Figure 5 – *Adiponectin decreases cytokine expressions after vein grafting. (A) VCAM-1 expression determined by immunohistochemistry (200×magnification); (B) ICAM-1 expression determined by immunohistochemistry (200×magnification); (C) VCAM-1expression; (D) ICAM-1 expression. Data represent mean ± SD. *p < 0.05 versus control group, **p < 0.01 versus control group. #p < 0.05 versus vehicle gel group, ##p < 0.01 versus vehicle gel group.*

Sources of Funding

This study was partially funded by National Natural Science Foundation of China (grant numbers NSFC 81470530 to J.G).

Study Association

This article is part of the thesis of doctoral submitted by Yang Zhou, from Anhui Medical University.

References

1. Khera AV, Kathiresan S. Genetics of coronary artery disease: discovery, biology and clinical translation. Nat Rev Genet. 2017;18(6):331-44. doi: 10.1038/nrg.2016.160.
2. Sabik III JF. Understanding saphenous vein graft patency. Circulation. 2011;124(3):273-5. doi: 10.1161/CIRCULATIONAHA.111.039842.
3. Blaas I, Heinz K, Würtinger P, Türkcan A, Tepeköylü C, Grimm M, et al. Vein graft thrombi, a niche for smooth muscle cell colonization - a hypothesis to explain the asymmetry of intimal hyperplasia. J Thromb Haemost. 2016;14(5):1095-104. doi: 10.1111/jth.13295.
4. Roubos N, Rosenfeldt FL, Richards SM, Conyers RA, Davis BB. Improved preservation of saphenous vein grafts by the use of glyceryl trinitrate-verapamil solution during harvesting. Circulation. 1995;92(9 Suppl):31-6. doi: 10.1161/01.cir.92.9.31.
5. Sur S, Sugimoto JT, Agrawal DK. Coronary artery bypass graft: why is the saphenous vein prone to intimal hyperplasia? Can J Physiol Pharmacol. 2014;92(7):531-45. doi: 10.1139/cjpp-2013-0445.
6. Wadey K, Lopes J, Bendeck M, George S. Role of smooth muscle cells in coronary artery bypass grafting failure. Cardiovasc Res. 2018;114(4):601-10. doi: 10.1093/cvr/cvy021.
7. Motwani JG, Topol EJ. Aortocoronary saphenous vein graft disease: pathogenesis, predisposition, and prevention. Circulation. 1998;97(9):916-31. doi: 10.1161/01.cir.97.9.916.
8. Jeong K, Kim JH, Murphy JM, Park H, Kim SJ, Rodriguez YAR, et al. Nuclear focal adhesion kinase controls vascular smooth muscle cell proliferation and neointimal hyperplasia through GATA4-mediated cyclin D1 transcription. Circ Res. 2019;125(2):152-66. doi: 10.1161/CIRCRESAHA.118.314344.
9. Rowe GC, Raghuram S, Jang C, Nagy JA, Patten IS, Goyal A, et al. PGC-1 induces SPP1 to activate macrophages and orchestrate functional angiogenesis in skeletal muscle. Circ Res. 2014;115(5):504-17. doi: 10.1161/CIRCRESAHA.115.303829.
10. Taruya A, Tanaka A, Nishiguchi T, Matsuo Y, Ozaki Y, Kashiwagi M, et al. Vasa vasorum restructuring in human atherosclerotic plaque vulnerability: a clinical optical coherence tomography study. J Am Coll Cardiol. 2015;65(23):2469-77. doi: 10.1016/j.jacc.2015.04.020.
11. Tang R, Zhang G, Chen SY. Smooth muscle cell proangiogenic phenotype induced by cyclopentenyl cytosine promotes endothelial cell proliferation and migration. J Biol Chem. 2016;291(52):26913-21. doi: 10.1074/jbc.M116.741967.

12. Meijles DN, Pagano PJ. Nox and inflammation in the vascular adventitia. Hypertension. 2016;67(1):14-9. doi: 10.1161/HYPERTENSIONAHA.115.03622.

13. Malinska A, Podemska Z, Perek B, Jemielity M, Buczkowski P, Grzymislawska M, et al. Preoperative factors predicting saphenous vein graft occlusion in coronary artery bypass grafting: a multivariate analysis. Histochem Cell Biol. 2017;148(4):417-24. doi: 10.1007/s00418-017-1574-4.

14. Li XD, Hong MN, Chen J, Lu YY, Ye MQ, Ma Y, et al. Adventitial fibroblast-derived vascular endothelial growth factor promotes vasa vasorum-associated neointima formation and macrophage recruitment. Cardiovasc Res. 2020;116(3):708-20. doi: 10.1093/cvr/cvz159.

15. Han X, Wu A, Wang J, Chang H, Zhao Y, Zhang Y, et al. Activation and migration of adventitial fibroblasts contributes to vascular remodeling. Anat Rec. 2018;301(7):1216-23. doi: 10.1002/ar.23793.

16. Vogel ME, Idelman G, Konaniah ES, Zucker SD. Bilirubin prevents atherosclerotic lesion formation in low-density lipoprotein receptor-deficient mice by inhibiting endothelial VCAM-1 and ICAM-1 signaling. J Am Heart Assoc. 2017;6(4):e004820. doi: 10.1161/JAHA.116.004820.

17. Olivares-Silva F, Landaeta R, Aránguiz P, Bolivar S, Humeres C, Anfossi R, et al. Heparan sulfate potentiates leukocyte adhesion on cardiac fibroblast by enhancing VCAM-1 and ICAM-1 expression. Biochim Biophys Acta Mol Basis Dis. 2018;1864(3):831-42. doi: 10.1016/j.bbadis.2017.12.002.

18. Vasiliauskaité-Brooks I, Sounier R, Rochaix P, Bellot G, Fortier M, Hoh F, et al. Structural insights into adiponectin receptors suggest ceramidase activity. Nature. 2017;544(7648):120-3. doi: 10.1038/nature21714.

19. Fang H, Judd RL. Adiponectin regulation and function. Compr Physiol. 2018;8(3):1031-63. doi: 10.1002/cphy.c170046.

20. Lu Y, Gao X, Wang R, Sun J, Guo B, Wei R, et al. Adiponectin inhibits proliferation of vascular endothelial cells induced by Ox-LDL by promoting dephosphorylation of Caveolin-1 and depolymerization of eNOS and up-regulating release of NO. Int Immunopharmacol. 2019;73:424-34. doi: 10.1016/j.intimp.2019.05.017.

21. Achari AE, Jain SK. Adiponectin, a therapeutic target for obesity, diabetes, and endothelial dysfunction. Int J Mol Sci. 2017;18(6):1321. doi: 10.3390/ijms18061321.

22. Woodward L, Akoumianakis I, Antoniades C. Unravelling the adiponectin paradox: novel roles of adiponectin in the regulation of cardiovascular disease. Br J Pharmacol. 2017;174(22):4007-20. doi: 10.1111/bph.13619.

23. Meguro T, Nakashima H, Kawada S, Tokunaga K, Ohmoto T. Effect of external stenting and systemic hypertension on intimal hyperplasia in rat vein grafts. Neurosurgery. 2000;46(4):963-9; discussion 969-70. doi: 10.1097/00006123-200004000-00036.

24. Wu B, Werlin EC, Chen M, Mottola G, Chatterjee A, Lance KD, et al. Perivascular delivery of resolvin D1 inhibits neointimal hyperplasia in a rabbit vein graft model. J Vasc Surg. 2018;68(6S):188S-200S.e4. doi: 10.1016/j.jvs.2018.05.206.

25. Wang GJ, Sui XX, Simosa HF, Jain MK, Altieri DC, Conte MS. Regulation of vein graft hyperplasia by survivin, an inhibitor of apoptosis protein. Arterioscler Thromb Vasc Biol. 2005;25(10):2081-7. doi: 10.1161/01.ATV.0000183885.66153.8a.

26. Caliskan E, Souza DR, Böning A, Liakopoulos OJ, Choi YH, Pepper J, et al. Saphenous vein grafts in contemporary coronary artery bypass graft surgery. Nat Rev Cardiol. 2020;17(3):155-69. doi: 10.1038/s41569-019-0249-3.

27. Gaudino M, Antoniades C, Benedetto U, Deb S, Di Franco A, Di Giammarco G, et al. Mechanisms, consequences, and prevention of coronary graft failure. Circulation. 2017;136(18):1749-64. doi: 10.1161/CIRCULATIONAHA.117.027597.

28. Zhang Y, Fang Q, Niu K, Gan Z, Yu Q, Gu T. Time-dependently slow-released multiple-drug eluting external sheath for efficient long-term inhibition of saphenous vein graft failure. J Control Release. 2019;293:172-82. doi: 10.1016/j.jconrel.2018.12.001.

29. Spadaccio C, Antoniades C, Nenna A, Chung C, Will R, Chello M, et al. Preventing treatment failures in coronary artery disease: what can we learn from the biology of in-stent restenosis, vein graft failure, and internal thoracic arteries? Cardiovasc Res. 2020;116(3):505-19. doi: 10.1093/cvr/cvz214.

30. Sartore S, Chiavegato A, Faggin E, Franch R, Puato M, Ausoni S, et al. Contribution of adventitial fibroblasts to neointima formation and vascular remodeling: from innocent bystander to active participant. Circ Res. 2001;89(12):1111-21. doi: 10.1161/hh2401.100844.

31. Coen M, Gabbiani G, Bochaton-Piallat ML. Myofibroblast-mediated adventitial remodeling: an underestimated player in arterial pathology. Arterioscler Thromb Vasc Biol. 2011;31(11):2391-6. doi: 10.1161/ATVBAHA.111.231548.

32. Dutzmann J, Koch A, Weisheit S, Sonnenschein K, Korte L, Haertlé M, et al. Sonic hedgehog-dependent activation of adventitial fibroblasts promotes neointima formation. Cardiovasc Res. 2017;113(13):1653-63. doi: 10.1093/cvr/cvx158.

33. Xiao J, Yang R, Qin X, Zhang Z, Li X, Li L, et al. A role of AMPK and connexin 43 in the suppression of CoCl2-induced apoptosis of spiral modiolar artery smooth muscle cells by adiponectin. Life Sci. 2019;238:116876. doi: 10.1016/j.lfs.2019.116876.

34. Cai XJ, Chen L, Li L, Feng M, Li X, Zhang K, et al. Adiponectin inhibits lipopolysaccharide-induced adventitial fibroblast migration and transition to myofibroblasts via AdipoR1-AMPK-iNOS pathway. Mol Endocrinol. 2010;24(1):218-28. doi: 10.1210/me.2009-0128.

35. Lei H, Wu D, Wang JY, Li L, Zhang CL, Feng H, et al. C1q/tumor necrosis factor-related protein-6 attenuates post-infarct cardiac fibrosis by targeting RhoA/MRTF-A pathway and inhibiting myofibroblast differentiation. Basic Res Cardiol. 2015;110(4):35. doi: 10.1007/s00395-015-0492-7.

Can We Pretreat Vein Grafts with Adiponectin to Improve Their Patency?

Maria Cristina de Oliveira Izar[1] and *Francisco A. H. Fonseca*[2]

Seção de Lípides, Aterosclerose e Biologia Vascular, Divisão de Cardiologia, Escola Paulista de Medicina, Universidade Federal de São Paulo,[1] *São Paulo, SP – Brazil*

Escola Paulista de Medicina da Universidade Federal de São Paulo – Cardiologia,[2] *Santana de Parnaiba, SP – Brazil*

Short Editorial related to the article: Adiponectin Prevents Restenosis Through Inhibiting Cell Proliferation in a Rat Vein Graft Model

Saphenous vein graft remains an option for patients with multivessel coronary artery disease,[1,2] mainly in individuals with type 2 diabetes.[3] Although artery bypass should offer better patency rates than venous grafts, in many situations, complete revascularization cannot be achieved using solely arterial grafts. Venous graft failure has been associated with cardiovascular outcomes, including mortality.[4,5] Therefore, there is a need to improve vein graft patency. The mechanisms involved in graft failure include intimal hyperplasia, smooth muscle cell proliferation, and endothelial dysfunction, among others.[6,7] There have been some attempts to improve the preservation of saphenous vein grafts before implantation.[8]

In the experimental study by Zhou et al.[9] the authors used autologous jugular veins implanted as carotid interposition grafts in Sprague Dawley rats. Two groups received adiponectin (2.5 μg and 7.5 μg) applied externally to the vein bypass grafts, suspended in a 30% Pluronic-F127 gel. The other two groups (controls) received vehicle or no treatment (bypass only).[9] At day 3, cell proliferation was significantly lower in adiponectin-treated versus control and vehicle-gel-treated grafts, both in intima and adventitia, whereas expression of VCAM-1 and ICAM-1 was significantly down-regulated in the adiponectin-treated vein grafts in week four. In addition, the treatment of vein grafts with adiponectin-loaded gels reduced intimal, media, and adventitia thickness when compared with the control and vehicle-gel-treated vein grafts at day 28.[9]

Adiponectin, an adipokine secreted by adipocytes, is a well-known homeostatic factor that regulates glucose levels, lipid metabolism, and insulin sensitivity through its anti-inflammatory, anti-fibrotic, and antioxidant effects. These effects are mediated by its interaction with two receptors: AdipoR1 and AdipoR2. Initially described as being expressed in skeletal muscle and the liver,[10] respectively, they were identified in the myocardium, macrophages, brain, endothelial cells, lymphocytes, adipose tissue, and pancreatic beta-cells.[11] Adiponectin is one of the hormones with the highest plasma concentrations, and the adiponectin pathway can play a crucial role in the mechanisms to treat type 2 diabetes mellitus and other diseases affected by insulin resistance like cancers or cardiovascular diseases.[12] A study by Marino et al.[13] showed that adiponectin was associated with thin-cap fibro atheroma in stable angina, seen by virtual histology.[13] Recently, Chu et al.[14] and Gatto et al.[15] demonstrated that atorvastatin could inhibit intimal hyperplasia in the rat vein graft model by inhibiting the p38 MAPK pathway. The results by Zhou et al.[9] expand the possibilities of treating vein grafts, using the adiponectin pathway as a therapeutic target to improve its patency. However, the precise mechanisms need elucidation, and further long-term studies in humans are necessary to confirm if they translate into longer vein graft patency, and consequently, better outcomes.

Keywords

Coronary Artery Disease; Saphenous Vein; Adiponectin/therapeutic use; Capillary Permeability; Rats.

Mailing Address: Maria Cristina de Oliveira Izar •
Rua Loefgren, 1350. Postal Code 04040-001, Vila Clementino, São Paulo, SP - Brazil
Email: mcoizar@terra.com.br; mcoizar@cardiol.br

DOI: https://doi.org/10.36660/abc.20210902

References

1. Yusuf S, Zucker D, Peduzzi P, Fisher D, Takaro T, Kennedy JW, et al. Effect of coronary artery bypass graft surgery on survival: overview of 10-year results from randomised trials by the Coronary Artery Bypass Graft Surgery Trialists Collaboration. Lancet.1994;344(8922):563-70.
2. Davis KB, Chaitman B, Ryan T, Bittner V, Kennedy JW. Comparison of 15-year survival for men and women after initial medical or surgical treatment for coronary artery disease. J Am Coll Cardiol. 1995;25(5):1000–9.
3. Dangas GD, Farkouh ME, Sleeper LA, Yang M, Schoos MM, Macaya C, et al.et al, FREEDOM Investigators. Long-term outcome of PCI versus CABG in insulin and non-insulin-treated diabetic patients: results from the FREEDOM trial. J Am Coll Cardiol. 2014;64(12):1189–97.
4. Campeau L, Enjalbert M, Lesperance J, Bourassa MG, Kwiterovich P Jr,Wacholder S, et al. The relation of risk factors to the development of atherosclerosis in saphenous-vein bypass grafts and the progression of disease in the native circulation. A study 10 years after aortocoronary bypass surgery. N Engl J Med. 1984;311(21):1329–32.
5. Greenland P, Knoll MD, Stamler J, Neaton JD, Dyer AR, Garside DB, et al. Major risk factors as antecedents of fatal and nonfatal coronary heart disease events. JAMA. 2003;290(7):891–7.
6. Sur S, Sugimoto JT, Agrawal DK. Coronary artery bypass graft: why is the saphenous vein prone to intimal hyperplasia? Can J Physiol Pharmacol. 2014;92(7):531-45. doi: 10.1139/cjpp-2013-0445.
7. Wadey K, Lopes J, Bendeck M, George S. Role of smooth muscle cells in coronary artery bypass grafting failure. Cardiovasc Res. 2018;114(4):601-10.
8. Roubos N, Rosenfeldt FL, Richards SM,Conyers RA, Davis BB. Improved preservation of saphenous vein grafts by the use of glyceryl trinitrate-verapamil solution during harvesting. Circulation. 1995;92(9 Suppl):31-6.
9. Zhou Y, Dai C, Zhang B, Ge J. Adiponectin prevents restenosis through inhibiting cell proliferation in a rat vein graft model. Arq Bras Cardiol. 2021; 117(6):1179-1188.
10. Yamauchi T, Kamon J, Ito Y, Tsuchida A, Yokomizo T, Kita S, et al. Cloning of adiponectin receptors that mediate antidiabetic metabolic effects. Nature. 2003;423(6941):762–9.
11. Yamauchi T, Iwabu M, Okada-Iwabu M, Kadowaki T. Adiponectin receptors: A review of their structure, function and how they work. Best Pract Res Clin Endocrinol Metab. 2014;28(1):15–23.
12. Nguyen TMD. Adiponectin: Role in Physiology and Pathophysiology. Int J Prev Med. 2020;11:136.
13. Marino BCA, Buljubasic N, Akkerhuis M, Cheng JM,Garcia HM, Regar E, et al. Adiponectin in Relation to Coronary Plaque Characteristics on Radiofrequency Intravascular Ultrasound and Cardiovascular Outcome. Arq Bras Cardiol. 2018 Sep;111(3):345-53.
14. Chu T, Huang M, Zhao Z,Ling F, Cao J,Ge J. Atorvastatin reduces accumulation of vascular smooth muscle cells to inhibit intimal hyperplasia via p38 MAPK pathway inhibition. Arq Bras Cardiol. 2020; 115(4):630-6.
15. Gatto M, Pagan LU, Mota GAF. Influence of atorvastatin on intimal hyperplasia in the experimental model. Arq Bras Cardiol 2020; 115(4):637-8.

Crossroads between Estrogen Loss, Obesity, and Heart Failure with Preserved Ejection Fraction

Allan Kardec Nogueira de Alencar,[1] Hao Wang,[2,6] Gláucia Maria Moraes de Oliveira,[3] Xuming Sun,[2] Gisele Zapata-Sudo,[4,5] Leanne Groban[2,6]

Faculdade de Medicina de Petrópolis,[1] Petrópolis, RJ - Brazil

Wake Forest School of Medicine - Departments of Anesthesiology,[2] Winston-Salem, North Carolina – United States of America

Universidade Federal do Rio de Janeiro - Departamento de Clínica Médica, Faculdade de Medicina,[3] Rio de Janeiro, RJ - Brazil

Universidade Federal do Rio de Janeiro - Instituto de Ciências Biomédicas,[4] Rio de Janeiro, RJ - Brazil

Universidade Federal do Rio de Janeiro - Instituto de Cardiologia Edson Saad, Faculdade de Medicina,[5] Rio de Janeiro, RJ - Brazil

Wake Forest School of Medicine - Internal Medicine-Section of Molecular Medicine,[6] Winston-Salem, North Carolina - United States of America

Abstract

The prevalence of obesity and heart failure with preserved ejection fraction (HFpEF) increases significantly in postmenopausal women. Although obesity is a risk factor for left ventricular diastolic dysfunction (LVDD), the mechanisms that link the cessation of ovarian hormone production, and particularly estrogens, to the development of obesity, LVDD, and HFpEF in aging females are unclear. Clinical, and epidemiologic studies show that postmenopausal women with abdominal obesity (defined by waist circumference) are at greater risk for developing HFpEF than men or women without abdominal obesity. The study presents a review of clinical data that support a mechanistic link between estrogen loss plus obesity and left ventricular remodeling with LVDD. It also seeks to discuss potential cell and molecular mechanisms for estrogen-mediated protection against adverse adipocyte cell types, tissue depots, function, and metabolism that may contribute to LVDD and HFpEF.

Introduction

The prevalence of obesity is steadily increasing worldwide.[1] Because obesity is associated with high mortality and the development of comorbid conditions, including diabetes mellitus and cardiovascular disease (CVD), it is one of the most difficult public health issues facing our society. This cluster of obesity-related comorbidities, whether directly or indirectly (e.g., side effect from anthracycline-formulated chemotherapy)[2] often culminates in heart failure (HF).[3-6]

While obesity, defined as having a body mass index (BMI) > 30 kg/m^2, is an independent predictor of incident HF in the general population, evidence shows that even being overweight (BMI 25-29 kg/m^2) carries an increased risk of HF.[7-10]

Several studies show that measures of central adiposity, such as waist circumference (WC), are superior to measures of global adiposity, such as weight and BMI, in estimating the risk of CVD.[11-16] WC is independently associated with left ventricular diastolic dysfunction (LVDD), defined by echocardiographic parameters.[17] Both LVDD and obesity are common factors that contribute to a heart failure with preserved ejection fraction (HFpEF) phenotype, and appear to be causally linked.[17-19] Indeed, HF patients can have different phenotypes according to the morpho-functional characteristics of the disease.[20] Briefly, HF patients are classified according to LV function; those with LV ejection fractions less than or equal to 40% fall into the category of heart failure with reduced ejection fraction (HFrEF), and patients with LV ejection fractions equal to or greater than 50% are deemed to have HFpEF. According to the American College of Cardiology and American Heart Association guidelines,[21] there is also an intermediate or borderline group of patients who have ejection fractions between 41% and 49%, sometimes referred to as HFmEF. Moreover, a subset of patients with ejection fractions greater than 40% with HFpEF who previously had HFrEF is considered to be clinically distinct from those with persistently preserved or reduced ejection fractions. For purposes of this review, we have focused only on HFpEF, and, specifically, features of the "fat, female, and fatigued" obese HFpEF phenotype.[21]

For a narrative of the literature of all the clinical phenotypes of HFpEF, we refer the reader to the review by Silverman.[20] Regardless of the biological phenotype, HFpEF is a heterogeneous clinical syndrome, including cardiomyocyte, extracellular matrix, vascular, and comorbidity-related pathophysiological mechanisms.[22] It is characterized by reduced end-diastolic volume, left ventricular hypertrophy, and increased left atrial volume and left ventricular filling pressure. These pathophysiological abnormalities are associated with increased left ventricular stiffness, decreased left ventricular relaxation, cardiomyocyte hypertrophy, myocardial interstitial fibrosis, and reduced intramyocardial capillaries.[23-26]

Another important factor involved in the HFpEF phenotype is sex. HFpEF disproportionally affects more women (sex ratio of about 2:1) then men.[27,28] The higher prevalence of HFpEF in elderly women[29] appears related to the loss of ovarian hormones, primarily estrogens, that occur after the menopause.

Keywords

Estrogens; Obesity; Heart Failure; Stroke Volume; Menopause; Adiposity; Overweight; Echocardiography/methods; Body Mass Index.

Mailing Address: Allan Kardec Nogueira de Alencar •
Faculdade de Medicina de Petrópolis, School Clinic, Av. Barão do Rio Branco, Centro. Postal Code 25680-120, Petrópolis, RJ, Brazil.
E-mail: allankdc@gmail.com
Manuscript received July 31, 2020, revised manuscript December 16, 2020, acceptd January 27, 2021

DOI: https://doi.org/10.36660/abc.20200855

Accordingly, in this review, we will explore pre-clinical and clinical data about the relationships between sex, "fatness", including mechanisms of fat-induced cardiac impairment, specifically LVDD and HFpEF, and the cardioprotective effects of estrogen on fat metabolism in women.

Link between "fatness", sex, and HFpEF: clinical evidence

HF is a major problem that is increasing in scope. Despite recent therapeutic advances, morbidity and mortality after the onset of HF still remain substantial.[30] Consequently, prevention of HF through the identification of the preclinical phases of the disease and the management of risk factors is a priority. Considering that 50 percent of all HF patients have HFpEF,[31] the complex pathophysiology of this disease is still not fully understood, with no specific therapy available to improve patient outcomes. In this context, several studies have evaluated obesity as a risk factor for LV remodeling and subsequent HFpEF.[32-34] In these studies, obesity has been consistently associated with LV stiffness and diastolic dysfunction, particularly in women.[17,35]

A community-based clinical study of 377 randomly selected participants older than 16 years of age assessed the independent contribution of indices of adiposity to variations in early-to-late (atrial) transmitral velocity (E/A), as determined by echocardiography. The main goal was to clarify why some previous studies failed to establish a contribution of obesity to LV diastolic function, while others demonstrated a relatively minor contribution. For each study participant, the independent relationship between adiposity and diastolic (E/A) or systolic (LV ejection fraction; LVEF) chamber functions were determined using multivariate linear regression analysis with adjustments for age, gender, conventional systolic or diastolic blood pressure measurements, and either LV mass index or relative wall thickness (calculated from echocardiography). Excessive central adiposity (WC), but not elevated BMI, was independently and inversely correlated with E/A; the investigators emphasized that WC might represent a progressive preclinical condition that contributes to obesity-induced diastolic HF.[36] WC was second only to age and equivalent to blood pressure in the magnitude of effect on E/A. Findings from this study also suggested that, at a population level, LV mass and geometry play little or no role in the pathogenesis of obesity-induced LV diastolic abnormalities.[36] Interestingly, there was no relationship between WC and LVEF (systolic dysfunction), confirming the findings of other researchers that identified WC as a risk factor for HFpEF.[7,9,17,37-43] Finally, it is relevant to comment that the data reported by these authors were restricted to women as they have recruited a limited proportion of male participants.[36] Additional data from the clinical study performed by Canepa et al.,[17] in which the sample, from both genders, is part of the Baltimore Longitudinal Study of Aging (BLSA) propose that a possible pathophysiologic explanation for the association of central adiposity with worse cardiovascular outcomes is its relationship with LVDD. They found that central adiposity was strongly associated with LV dysfunction, particularly with impaired LV relaxation. The researchers also found that the effect of central adiposity on LVDD was independent of general adiposity and, surprisingly, this was more pronounced in women than in men. The gender-specific effect of central fat accumulation on LVDD was then graded using various echocardiographic parameters. The study confirmed their previous reports showing a negative correlation between the indices of adiposity and the E/A ratio; however, the authors also found that E/A alone was not enough to discriminate between subjects with normal or abnormal diastolic function and that mitral valve inflow velocities were also significantly influenced by the increase in preload, a condition frequently encountered in obese subjects. When these issues were normalized by combining tissue Doppler measures of mitral annular velocity, or e' and dynamic (E/A) parameters, it was found that the E/e' ratio was positively correlated with WC. Thus, this epidemiological study provided further evidence of the link between central obesity (WC) and the prevalence and development of LVDD, and that this link is influenced by sex.[17]

One limitation of cross-sectional studies is that they offer a snapshot of a single moment in time, and thus fail to capture changes that occur over time. The complex relationships between aging, sex, adiposity, and ventricular mechanisms were evaluated in a large longitudinal study conducted over a period of 4 years in 1,402 subjects, 45 years of age and older, who were randomly selected from a community-based population.[35] It was found that weight gain during a 4-year period was associated with significant increases in LV diastolic stiffness in both men and women, but that it was more pronounced in women, indicating a sex difference in the biology of age-related ventricular stiffening. Furthermore, evaluating central obesity in women may help to identify a group at higher risk for incident HFpEF who might benefit from preventive treatment.[35] Finally, the results of this longitudinal study confirmed the findings of cross-sectional investigations regarding the positive relationship between WC and echocardiographic measures of diastolic dysfunction (e.g., E/e' ratio).

How changes in fat tissue depot might influence the link between obesity and impairments in cardiac function and remodeling, particularly among women, are important to consider. While female sex hormones are believed to cause fat to be stored in the buttocks, thighs, and hips of women, which may be essential for normal reproduction purposes, menopause-related changes in body fat distribution may partially explain the increased risk of cardiovascular and metabolic disease during the postmenopausal years.[44-46] In 2011, Wehr et al.,[47] published results from a longitudinal study of gender-specific differences in the relationship between the lipid accumulation product, which is calculated from WC, and cardiovascular mortality, as well as the presence of type 2 diabetes. The study included 2,279 men and 875 postmenopausal women, with a median follow-up of 77 years. Lipid accumulation product levels were independently associated with congestive HF mortality in all postmenopausal women and with all-cause mortality in diabetic postmenopausal women, but not in men. These data not only support the concept that fat redistribution after estrogen loss may contribute to cardiovascular disease progression, but also endorse an inexpensive and simple risk biomarker, namely, lipid accumulation product, which could identify postmenopausal women at higher cardiovascular risk.[47]

Treatment modalities for weight loss: an evidence-based approach to measure outcomes in patients with HFpEF

Given clinical evidence for crosstalk between the heart and "fatness", with respect to female sex-specific HFpEF, weight reduction or maintenance of ideal body weight is one preventive approach to mitigate age- and estrogen-loss related changes in ventricular structure and function. Essential treatments for weight reduction include changes in eating habits to reduced-calorie and low-fat diets, increased physical activity or exercise, and other behavioral modification strategies, such as self-monitoring (e.g., daily record keeping of food intake and exercise), stimulus control (e.g., avoiding triggers that prompt eating), and problem solving (e.g., identifying barriers and ways to overcome them). Additionally, bariatric surgery is another effective strategy to treat severely obese patients. Thus, it is important to review the literature addressing the effects of different weight loss strategies on the cardiovascular outcomes in patients with LVDD and HFpEF.

Observational studies suggest that overweight or mildly-to-moderately obese patients with HFpEF survive longer than those who are normal-weight.[18,48] However, Kitzman et al.[49] recently reported that 20 weeks of caloric restriction combined with aerobic exercise training among obese older patients with HFpEF reduced their body weight with additive improvements in exercise capacity, defined by peak $V0_2$. Even so, only caloric restriction resulted in decreases in LV mass and relative wall thickness, along with an inkling for improvements in diastolic function, as per the increase in E/A observed in this treatment arm, without effecting resting cardiac function, depicted by ejection fraction or Doppler-derived cardiac output.[49] It was further reported that no changes in magnetic resonance imaging (MRI) measures of epicardial or pericardial fat were observed across treatments, but that there were significant reductions in thigh and abdominal subcutaneous and visceral fat depots in the diet only group.[49] While these findings favor a role for weight reduction strategies, along with exercise, to improve the detriments in exercise capacity and maximal oxygen consumption associated with HFpEF among obese patients, they also support the concept that extra-cardiac mechanisms are uniquely involved in the pathogenesis of HFpEF.[50,51]

Another weight reduction strategy that is conducive to evaluating the link between "fatness", LVDD, and HFpEF is bariatric surgery. Indeed, morbidly obese patients who commonly present hemodynamic and cardiac morphometric characteristics, such as elevations in cardiac preload and afterload and increases in LV chamber and wall dimensions, which contribute to myocardial stiffness and impairments in myocardial relaxation.[52] Multiple clinical studies[52-55] and one systemic review with a meta-analysis[56] reported the benefits of bariatric surgery with subsequent weight loss on echocardiographic and MRI measures of LV structure, including substantial reductions in LV wall thickness and mass and diastolic function. Along with upgrades in diastolic function, others found that extensive weight loss after bariatric surgery also led to favorable changes in muscle metabolism[57] and characteristics of arterial elasticity.[58,59]

Link between cardiac-specific regional adiposity, LVDD, and HFpEF

In addition to peripheral and total body fat linked to LVDD, the potential role of cardiac-specific regional adiposity (e.g. pericardial and epicardial fat depots) in the disease process should not be ignored.[60] Pericardial and epicardial fat, commonly found in obese and overweight patients, are considered ectopic adipose depots that can induce a lipotoxic state in close proximity to cardiac muscle and coronary arteries.[61,62] Moreover, we know that metabolic syndrome, a common condition among obese and overweight patient,[63] is associated with increased adipose tissue volume around the heart,[60] particularly the accumulation of epicardial fat,[64] which is significantly linked to adverse cardiovascular events,[65-69] including HFpEF.[61,70,71] The direct correlation between these local fat depots and LVDD can be explained, in part, by paracrine processes, whereby proinflammatory cytokines and other damaging mediators (e.g. TNF-α and IL-6),[72] collectively called adipokines, are released from the local adipose repositories.[61,72-74]

Distinguishing between the two fat depots and their respective link to LVDD may be important both anatomically and biochemically. For instance, epicardial fat is located between the outer wall of the heart muscle and the visceral layer of pericardium,[64] and its proximity to the myocardium is significant in that both tissue layers share the same blood microcirculation, the coronary arteries.[64] Potential interactions can be elicited when dysfunctional adipocytes from cardiac fat depots release proinflammatory adipokines into the microcirculation,[37] which in turn can interact with cardiomyocytes and cardiac fibroblasts. These cells independently respond to adipokines, which contribute to the pathologic process of myocardial fibrosis,[75] thereby leading to myocardial remodeling, via low grade inflammation and fibrotic processes, which can intensify LV hypertrophy, wall stiffness, and LVDD progression.[76-79] Pericardial fat, which can be more specifically referred to as *para*-cardial fat or intrathoracic fat,[80] is that fat which is deposited outside the parietal pericardium. This fat depot originates from primitive thoracic mesenchyme and is supplied by noncoronary sources. While increases in paracardial fat volume in HFpEF have been reported to induce a mechanical compressive-like load on the myocardium, which impairs LV filling,[81] paracrine processes have also been noted. Excessive pericardial adiposity contains high levels of proinflammatory mediators that, when released from adipocytes, promote a collagen turnover, thus leading to myocardial stiffness, impaired lusitropism and subsequent LVDD.[82] Indeed, Konishi et al.,[61] reported that a high volume of pericardial fat was significantly correlated with Doppler-derived increases in filling pressure, or E/e', in HFpEF patients. Moreover, studies have documented a strong potential for epicardial adiposity to be associated with poor prognosis in obese or overweight patients with LVDD and HFpEF.[71,83-85]

Given the link between local cardiac fat depots and adverse cardiovascular health, weight reduction strategies should be strongly considered among the armamentarium in the management of the obese LVDD patient. Interestingly, in obese

postmenopausal women with HFpEF, Brinkley et al.,[86] showed that caloric restriction, aerobic exercise, or combination therapy significantly reduced body weight and pericardial fat, and the changes in pericardial fat were inversely correlated with cardiorespiratory fitness defined by VO_2max. Certainly, future therapies targeting low-grade inflammatory processes arising from epi- and pericardial fat depots could also limit the progression of LVDD.

Link between estrogen and fat-induced cardiovascular risk

The high predilection of HFpEF among older women compared to older men with HF is well accepted.[27,28] The role that differences in adipocyte distribution among men and woman might have with respect to this sex-specific differential in HF prevalence is new and still coming together. Indeed, women have more body fat than men, but in contrast to the adverse metabolic consequences of central obesity that is typical of men, the pear-shaped, or gluteal-femoral body fat subcutaneous distribution of many women is associated with lower cardiometabolic risk.[87,88] However, with advancing age there is a general shift and expansion of fat from the subcutaneous to visceral compartment.[87-89] In aging males this means expansion of abdominal visceral adiposity, while in aging females this involves a redistribution of fat from the subcutaneous gluteal-femoral compartment to the visceral-abdominal compartment.[87-89] In both cases, cardiovascular disease risk increases with age-related abdominal compartment expansion of visceral fat.[89,90]

As outlined in the introduction, loss of gonadal hormones in older women seems to represent a component associated with increased risk for developing HFpEF. Since women are less likely to develop CVD before menopause,[91] the production of ovarian estrogen appears to protect against HF.[92,93] Consistently, there are several reports confirming the beneficial effects of estrogen in the cardiovascular system.[94-96]

To understand the specific role of gonadal hormones in the expansion of age-related visceral fatness in women and, in turn, its potential influence on diastolic function, a brief review of gonadal hormones, particularly the estrogens and their receptors, is first warranted. The three naturally occurring estrogens in women are estrone (E1), estradiol (E2), and estriol (E3). A fourth form of estrogen, estetrol (E4), is produced only during pregnancy. All these different estrogen forms are synthesized from androgens.[97] For simplicity, we will use the term estrogen, to include all forms.

Estrogen binds to multiple receptors, including classical nuclear estrogen receptors (ERs), ERα, and ERβ, and a G protein-coupled receptor, GPER.[98] The ERs signal not only through a "classical" regulation of gene transcription, but also by activating a "non-nuclear" signaling pathway.[94,99] Accumulating findings have been well described and reviewed in the literature, concerning the roles triggered by ERs in maintaining the homeostasis of the cardiovascular system.[99-101]

Estrogen directly regulates adiposity distributions through estrogen receptors. In the premenopausal state, subcutaneous fat has relatively more estrogen and progesterone receptors than androgen receptors, whereas visceral fat has higher levels of androgen receptors.[102] With menopause, the fall of estrogen leads to estrogen receptors on subcutaneous fat to be inactivated, while the androgen receptors on visceral fat become relatively activated, thereby contributing to the inverse relationship between estrogen levels and visceral fat.[103,104] Likewise, in estrogen deficient rodent models induced by ovariectomy, the observed increase in body weight is mainly due to gains in visceral fat.[105] Estrogenic protection can further be seen upon the systemic administration of estrogen in OVX models whereby the body fat distribution mirrors that of gonad-intact counterparts.[106]

The specific roles may offset the classical steroid receptors ERα and ERβ in the context of fat one to another. In a recent study by Zidon et al.,[107] gonad intact ERα KO mice were found to be 25% heavier with reduced energy expenditure compared to age-matched gonad intact wild-type and ERβ KO mice.[107] Furthermore, following OVX, αKO mice did not increase body weight or exhibit more pronounced insulin resistance, whereas WT and βKO mice did, suggesting that the loss of signaling through ERα facilitates OVX-induced metabolic dysfunction. These new data further suggest that following estrogen deficiency, ERβ may mediate protective metabolic benefits.[107] This contradicts previous preclinical reports showing that the two classical ERs on adipose tissue regulate fat reciprocally.[108-110] Despite this discrepancy, the linkage between polymorphisms in the structure of both classical ERs and increased CV risk among postmenopausal women corroborate the important role of ER isoforms in the regulation of adiposity, metabolic derangement, and cardiovascular risk.[111-113]

Fat-derived adipokines and roles in cardiovascular disease risk

The main role of brown fat, mainly located around the neck and large blood vessels of the thorax, is to generate heat by "uncoupling" the respiratory chain of oxidative phosphorylation within mitochondria.[114] White visceral fat (abdominal fat) is mainly involved in a complex and multidirectional network of autocrine, paracrine, and endocrine signaling that crosstalk between organs and tissues. It is the white fat that mainly participates in the pathogenesis of metabolic diseases, such as type 2 diabetes mellitus, insulin resistance, hypertension, coronary heart disease, stroke, and HF.[17,115,116] It is currently well accepted that adipose tissue is an active endocrine organ that secretes heterogeneous bioactive factors called adipokines,[115] including cytokines and chemokines, vasoactive and coagulation factors, regulators of lipoprotein metabolism, and proteins, such as adiponectin and leptin.[115]

In obesity, enlargement of adipose tissue mass has been linked to a dysregulation of adipokine secretion and the related tissue inflammation, which represents a critical pathogenic link between obesity and the development of cardiometabolic diseases.[117] In obese individuals, adipose tissue is infiltrated with activated macrophages and several other types of inflammatory cells, leading to an augmented production of proinflammatory adipokines, such as TNF-α, IL-6, monocyte chemoattractant protein (MCP)-1, resistin, leptin, lipocalin-2, adipocyte fatty acid binding protein (A-FABP), and plasminogen activator inhibitor-1.[116]

These inflammatory factors are key components of the "adipo-cardiovascular axis" that mediates crosstalk between adipose tissue and the CV system.

Among the various adipose depots, perivascular adipose tissue is an important contributor to vascular inflammation because of its proximity to the blood vessel wall and its pronounced proinflammatory properties. Proinflammatory cytokines/adipokines released from other major adipose tissue depots, such as subcutaneous and abdominal fat, may further contribute to vascular inflammation by virtue of their endocrine actions.[116] These findings explain, in part, why WC may be considered a surrogate biomarker of CVD risk.

Adiponectin is one of the most abundant adipokines secreted by adipocytes, accounting for 0.01% of the total plasma protein content in humans.[118] The production of adiponectin from white adipocytes, which exerts beneficial effects on insulin sensitivity and cardiovascular function, is markedly reduced in obese individuals.[116,119,120] Epidemiological studies show that low circulating adiponectin levels, particularly the high molecular weight form, is a risk factor for type 2 diabetes, hypertension, atherosclerosis, and myocardial infarction.[116]

Adiponectin and adiponectin receptors

The relationship between obesity and LVDD may be linked to adiponectin and adiponectin receptors. The full-length adiponectin consists of 247 amino acid residues, assembled into an *N*-terminal hypervariable region followed by a conserved collagenous domain of 22 Gly-Xaa-Yaa repeats and a *C*-terminal C1q-like globular domain.[119] In human and mouse plasma, adiponectin is present in three major oligomeric forms.[119,121,122] The monomeric form has never been detected under native conditions. The basic unit of oligomeric adiponectin is a homotrimer called low-molecular-weight (LMW) adiponectin.[119,123,124] Two subunits of the adiponectin trimer are linked by a disulfide bond via cysteine residues in the collagen-like domain, which forms a hexamer termed middle-molecular-weight (MMW) adiponectin. This hexamer provides the building block for the formation of the bouquet-like high-molecular-weight (HMW) adiponectin comprised of 12-18 hexamers.

Post-translational modifications to the adiponectin protein are required for the intracellular assembly of the HMW oligomeric complex in adipocytes.[125] Different oligomeric forms of adiponectin act on different targets and possess distinct biological functions.[119]

The two main adiponectin receptors (AdipoRs), AdipoR1 and AdipoR2, are structurally and functionally distinct from classic G-protein-coupled receptors.[126] AdipoR1 is expressed ubiquitously, whereas AdipoR2 is expressed most abundantly in the liver.[126] Both AdipoR1 and AdipoR2 are expressed in cardiac cells,[127] but the exact roles of these two receptors in the antioxidative/nitrative stress and anti-inflammatory actions in cardiomyocytes remain unclear.

Although adipocytes are the major contributors to plasma adiponectin, adiponectin is also expressed in cardiomyocytes,[127] and cardiomyocyte-derived adiponectin is biologically active in protecting cells against ischemic injury via paracrine/autocrine activation of cardiac AdipoRs in mice.[128] In patients with dilated cardiomyopathy, cardiac adiponectin expression is downregulated.[129]

Adiponectin and LVDD

In addition to AdipoRs, T-cadherin has also been suggested as a potential receptor for adiponectin,[130] and it is highly expressed in the heart, smooth muscle, and endothelium, representing the main target of adiponectin in the cardiovascular system.[131,132] T-cadherin is anchored at the cell surface by glycosyl phosphatidylinositol, and it plays an indispensable role in adiponectin-induced cardioprotection in mice,[133] acting as a physiological adiponectin-binding receptor that enables the association of this adipokine with cardiac tissue.[133]

As low levels of adiponectin have been linked to obesity-related cardiometabolic complications, its role in the maintenance of cardiac health should not be ignored.[120,134,135] Preclinical data show that adiponectin can attenuate or prevent the progression of LVDD to HFpEF.[120,136,137] In a mouse model of aldosterone-induced HFpEF, Sam et al.[137] showed that a lack of adiponectin was associated with increased systolic blood pressure, LV remodeling, diastolic dysfunction, and pulmonary congestion, while the chronic hyperadiponectinemia in transgenic mice overexpressing adiponectin, reported by Tanaka et al.,[120] ameliorated aldosterone-induced LV hypertrophy, diastolic dysfunction, and lung congestion, regardless of changes in blood pressure. The early filling-to-early mitral annular descent ratio, or E/e', which was increased in the aldosterone-induced HFpEF mice and indicative of elevated filling pressures,[137] which was significantly attenuated in adiponectin transgenic mice. Tanaka et al.,[120] also found that adiponectin overexpression decreased myocardial oxidative stress and calcium handling by preserving protein kinase A (PKA)-dependent phosphorylation of phospholamban. Moreover, adiponectin replacement in adiponectin knock-out mice, attenuated transmitral Doppler indices of pseudonormalization, indicative of impaired LV compliance.[120] Taken together, these preclinical findings suggest that adiponectin may have a therapeutic potential in the management of LVDD and HFpEF, via direct actions on the heart.

Our observation that circulating adiponectin was not associated with LV fractional shortening is consistent with existing literature, which suggests that adiponectin acts primarily as an inhibitor of cardiac hypertrophy.

Clinical studies also support an association between adiponectin and cardiac function and structure.[129,138] In a community-based cohort study, McManus et al.[139] showed that relatively higher plasma levels of adiponectin associated with reduced LV mass, suggesting a cardioprotective effect. There are additional clinical data addressing the cardioprotective roles of adiponectin on the heart.[140-142] For instance, Francisco et al.[143] comprehensively reviewed the relevance of adiponectin signaling for the prevention of obesity related diastolic dysfunction with an emphasis on its role in limiting myocardial hypertrophy, cardiac fibrosis, nitrative and oxidative stress, atherosclerosis, and inflammation.

As there are several studies showing adiponectin's modulatory role in the maintenance of diastolic function, it is worth mentioning that other investigators report no relationship to fat-associated LVDD. Sawada et al.[144] found that while plasma adiponectin levels significantly decreased with increased visceral adiposity in the general population, the association between adiponectin and diastolic function was not independent of fat. In other words, decreased circulating levels of adiponectin did not appear to have a central role in the association between visceral adiposity and LVDD. As this work was performed in a population with normal or grade 1 LVDD, subjects with more than moderate LVDD were not included. These authors suggested that a larger-scale study, including patients with moderate or severe LVDD are needed to confirm findings.

Sex differences, adiponectin, and cardiac function

Whether there are sex differences in the effects of adiponectin on cardiac function and structure is not clear. Fontes-Carvalho et al.[145] reported data from a population-base study involving individuals aged 45 years and older on associations of leptin and adiponectin levels and LV diastolic function. These investigators found significant sex differences for both leptin and adiponectin levels and their relationships with diastolic function. Relatively higher levels of leptin were associated with worse diastolic function, particularly among women, and this was regardless of age and hypertension. Interestingly, adiponectin did not correlate with diastolic function parameters.[145] Even so, it is plausible to postulate a sex-specific effect for adiponectin on changes in myocardial structure and function, as women have significantly higher systemic adiponectin levels.[146] In two small studies involving patients undergoing coronary angiography[147] or with HF,[142] decreased adiponectin levels were associated with worse diastolic function. Figure 1 summarizes the main mechanisms involved in estrogen loss and obesity in the development of LVDD and HFpEF.

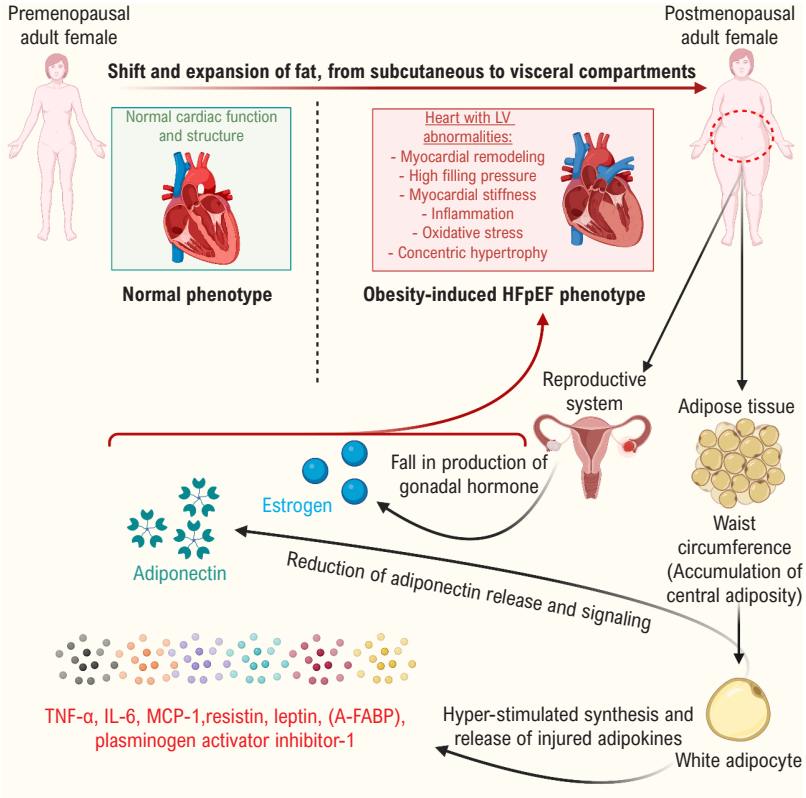

Figure 1 – *A schematic diagram showing the involvement of estrogen loss and obesity in HFpEF. An expansion and a shift of subcutaneous to visceral fat occurs in women after menopause. Abdominal obesity, defined by increased waist circumference, is a major risk factor for the development of HFpEF, which may involve an uptick in the synthesis and release of adipokines, including TNF-α, IL-6, MCP-1, resistin, leptin, lipocalin-2, and plasminogen activator inhibitor-1. These adipokines play critical roles in cardiac inflammation, oxidative stress, and impaired metabolism. On the other hand, the production of adiponectin from white adipocytes, which exerts beneficial effects on insulin sensitivity and cardiovascular function, is markedly reduced in obese individuals. Abnormalities in adipokines, in addition to estrogen loss, might participate in the development of HFpEF by inducing cardiac inflammation and oxidative stress, and finally leading to concentric cardiac hypertrophy, remodeling, stiffness, and diastolic dysfunction. HFpEF, heart failure with preserved ejection fraction; TNF-α, tumor necrosis factor alpha; IL-6, interleukin 6; MCP- 1, monocyte chemoattractant protein; A-FABP, adipocyte fatty acid binding protein.*

Conclusion

In summary, estrogen plays a major role in the regulation of body weight and body fat, and that role may also protect the premenopausal heart from LV dysfunction. Compared with age-matched men, postmenopausal women display increased ventricular and arterial stiffness, and are more likely to develop LVDD and subsequent HFpEF. The lower estrogen levels after menopause are involved in changes in body fat distribution and content, a factor that increases the incidence of CVD. This review collected the recent evidence and clarified the molecular routes by which estrogen triggers these effects and provides new directions for future research in this exciting area of sex-specific cardiac aging and diastolic dysfunction, which is a harbinger for HFpEF.

Author Contributions

Conception and design of the research: Alencar AKN, Wang H, Sun X, Groban L; Acquisition of dat and Writing of the manuscript: Alencar AKN, Wang H, Oliveira GMM, Sun X, Groban L; Analysis and interpretation of the data: Alencar AKN, Wang H, Oliveira GMM, Sun X, Zapata-Sudo G, Groban L; Obtaining financing: Alencar AKN, Zapata-Sudo G, Groban L; Critical revision of the manuscript for intellectual content: Alencar AKN, Oliveira GMM, Groban L.

Potential Conflict of Interest

No potential conflict of interest relevant to this article was reported.

Sources of Funding

This study was funded by National Institute on Aging of the National Institute of Health to Leanne Groban (AG033727; AG061588) and partially funded by Conselho Nacional de Desenvolvimento Científico e Tecnológico (CNPq), Coordenação de Aperfeiçoamento de Pessoal de Nível Superior (CAPES), and Fundação Carlos Chagas Filho de Amparo à Pesquisa do Estado do Rio de Janeiro (FAPERJ) to Gisele Zapata-Sudo and Allan Kardec Nogueira de Alencar.

Study Association

This study is not associated with any thesis or dissertation work.

Ethics approval and consent to participate

This article does not contain any studies with human participants or animals performed by any of the authors.

References

1. Collaborators GBDO, Afshin A, Forouzanfar MH, Reitsma MB, Sur P, Estep K, et al. Health Effects of Overweight and Obesity in 195 Countries over 25 Years. N Engl J Med. 2017;377(1):13-27.
2. Guenancia C, Lefebvre A, Cardinale D, Yu AF, Ladoire S, Ghiringhelli F, et al. Obesity As a Risk Factor for Anthracyclines and Trastuzumab Cardiotoxicity in Breast Cancer: A Systematic Review and Meta-Analysis. J Clin Oncol. 2016;34(26):3157-65.
3. Alpert MA, Lavie CJ, Agrawal H, Aggarwal KB, Kumar SA. Obesity and heart failure: epidemiology, pathophysiology, clinical manifestations, and management. Translat Res. 2014;164(4):345-56.
4. Lee HJ, Kim HL, Lim WH, Seo JB, Kim SH, Zo JH, et al. Subclinical alterations in left ventricular structure and function according to obesity and metabolic health status. PloS one. 2019;14(9):e0222118.
5. Russo C, Sera F, Jin Z, Palmieri V, Homma S, Rundek T, et al. Abdominal adiposity, general obesity, and subclinical systolic dysfunction in the elderly: A population-based cohort study. Eur Heart J Fail.2016;18(5):537-44.
6. Yang H, Huynh QL, Venn AJ, Dwyer T, Marwick TH. Associations of childhood and adult obesity with left ventricular structure and function. Int J Obes. 2017;41(4):560-8.
7. Russo C, Jin Z, Homma S, Rundek T, Elkind MS, Sacco RL, et al. Effect of obesity and overweight on left ventricular diastolic function: a community-based study in an elderly cohort. J Am Coll Cardiol. 2011;57(12):1368-74.
8. Rayner JJ, Banerjee R, Holloway CJ, Lewis AJM, Peterzan MA, Francis JM, et al. The relative contribution of metabolic and structural abnormalities to diastolic dysfunction in obesity. Int J Obes (Lond). 2018;42(3):441-7.
9. Lee SL, Daimon M, Di Tullio MR, Homma S, Nakao T, Kawata T, et al. Relationship of Left Ventricular Diastolic Function to Obesity and Overweight in a Japanese Population With Preserved Left Ventricular Ejection Fraction. Circ J. 2016;80(9):1951-6.
10. Pandey A, Patel KV, Vaduganathan M, Sarma S, Haykowsky MJ, Berry JD, et al. Physical Activity, Fitness, and Obesity in Heart Failure With Preserved Ejection Fraction. JACC Heart Fail. 2018;6(12):975-82.
11. Bigaard J, Frederiksen K, Tjonneland A, Thomsen BL, Overvad K, Heitmann BL, et al. Waist circumference and body composition in relation to all-cause mortality in middle-aged men and women. Int J Obes. 2005;29(7):778-84.
12. Ashwell M, Hsieh SD. Six reasons why the waist-to-height ratio is a rapid and effective global indicator for health risks of obesity and how its use could simplify the international public health message on obesity. Int Nat Food Sci Nutr. 2005;56(5):303-7.
13. Ho SY, Lam TH, Janus ED, Hong Kong Cardiovascular Risk Factor Prevalence Study Steering C. Waist to stature ratio is more strongly associated with cardiovascular risk factors than other simple anthropometric indices. Ann Epidemiol. 2003;13(10):683-91.
14. Janssen I, Katzmarzyk PT, Ross R. Waist circumference and not body mass index explains obesity-related health risk. Am J Clin Nutr. 2004;79(3):379-84.
15. Wei M, Gaskill SP, Haffner SM, Stern MP. Waist circumference as the best predictor of noninsulin dependent diabetes mellitus (NIDDM) compared to body mass index, waist/hip ratio and other anthropometric measurements in Mexican Americans--a 7-year prospective study. Obes Res. 1997;5(1):16-23.
16. Welborn TA, Dhaliwal SS. Preferred clinical measures of central obesity for predicting mortality. Eur J Clin Nutr. 2007;61(12):1373-9.
17. Canepa M, Strait JB, Abramov D, Milaneschi Y, AlGhatrif M, Moni M, et al. Contribution of central adiposity to left ventricular diastolic function (from the Baltimore Longitudinal Study of Aging). Am J Cardiol. 2012;109(8):1171-8.
18. Haass M, Kitzman DW, Anand IS, Miller A, Zile MR, Massie BM, et al. Body mass index and adverse cardiovascular outcomes in heart failure patients with preserved ejection fraction: results from the Irbesartan in Heart Failure with Preserved Ejection Fraction (I-PRESERVE) trial. Circ Heart Fail. 2011;4(3):324-31.

19. Ho JE, Lyass A, Lee DS, Vasan RS, Kannel WB, Larson MG, et al. Predictors of new-onset heart failure: differences in preserved versus reduced ejection fraction. Circ Heart Fail. 2013;6(2):279-86.

20. Silverman DN, Shah SJ. Treatment of Heart Failure With Preserved Ejection Fraction (HFpEF): the Phenotype-Guided Approach. Curr Treat Options Cardiovasc Med. 2019;21(4):20.

21. Lam CSP, Chandramouli C. Fat, Female, Fatigued: Features of the Obese HFpEF Phenotype. JACC Heart Fail. 2018;6(8):710-3.

22. Lewis GA, Schelbert EB, Williams SG, Cunnington C, Ahmed F, McDonagh TA, et al. Biological Phenotypes of Heart Failure With Preserved Ejection Fraction. J Am Coll Cardiol. 2017;70(17):2186-200.

23. Mohammed SF, Borlaug BA, Roger VL, Mirzoyev SA, Rodeheffer RJ, Chirinos JA, et al. Comorbidity and ventricular and vascular structure and function in heart failure with preserved ejection fraction: a community-based study. Circ Heart Fail. 2012;5(6):710-9.

24. Lam CS, Roger VL, Rodeheffer RJ, Bursi F, Borlaug BA, Ommen SR, et al. Cardiac structure and ventricular-vascular function in persons with heart failure and preserved ejection fraction from Olmsted County, Minnesota. Circulation. 2007;115(15):1982-90.

25. Zile MR, Gottdiener JS, Hetzel SJ, McMurray JJ, Komajda M, McKelvie R, et al. Prevalence and significance of alterations in cardiac structure and function in patients with heart failure and a preserved ejection fraction. Circulation. 2011;124(23):2491-501.

26. Zile MR, Baicu CF, Gaasch WH. Diastolic heart failure--abnormalities in active relaxation and passive stiffness of the left ventricle. N Engl J Med. 2004;350(19):1953-9.

27. Maslov PZ, Kim JK, Argulian E, Ahmadi A, Narula N, Singh M, et al. Is Cardiac Diastolic Dysfunction a Part of Post-Menopausal Syndrome? JACC Heart Fail. 2019;7(3):192-203.

28. Pandey A, Omar W, Ayers C, LaMonte M, Klein L, Allen NB, et al. Sex and Race Differences in Lifetime Risk of Heart Failure With Preserved Ejection Fraction and Heart Failure With Reduced Ejection Fraction. Circulation. 2018;137(17):1814-23.

29. Upadhya B, Kitzman DW. Heart Failure with Preserved Ejection Fraction in Older Adults. Heart Fail Clin. 2017;13(3):485-502.

30. Benjamin EJ, Blaha MJ, Chiuve SE, Cushman M, Das SR, Deo R, et al. Heart Disease and Stroke Statistics-2017 Update: A Report From the American Heart Association. Circulation. 2017;135(10):e146-e603.

31. Fonarow GC, Stough WG, Abraham WT, Albert NM, Gheorghiade M, Greenberg BH, et al. Characteristics, treatments, and outcomes of patients with preserved systolic function hospitalized for heart failure: a report from the OPTIMIZE-HF Registry. J Am Coll Cardiol. 2007;50(8):768-77.

32. Alpert MA, Karthikeyan K, Abdullah O, Ghadban R. Obesity and Cardiac Remodeling in Adults: Mechanisms and Clinical Implications. Prog Cardiovasc Dis. 2018;61(2):114-23.

33. Ferron AJT, Francisqueti FV, Minatel IO, Silva C, Bazan SGZ, Kitawara KAH, et al. Association between Cardiac Remodeling and Metabolic Alteration in an Experimental Model of Obesity Induced by Western Diet. Nutrients. 2018;10(11).

34. Antonini-Canterin F, Di Nora C, Poli S, Sparacino L, Cosei I, Ravasel A, et al. Obesity, Cardiac Remodeling, and Metabolic Profile: Validation of a New Simple Index beyond Body Mass Index. J Cardiovasc Echogr. 2018;28(1):18-25.

35. Wohlfahrt P, Redfield MM, Lopez-Jimenez F, Melenovsky V, Kane GC, Rodeheffer RJ, et al. Impact of general and central adiposity on ventricular-arterial aging in women and men. JACC Heart failure. 2014;2(5):489-99.

36. Libhaber CD, Norton GR, Majane OH, Libhaber E, Essop MR, Brooksbank R, et al. Contribution of central and general adiposity to abnormal left ventricular diastolic function in a community sample with a high prevalence of obesity. Am J Cardiol. 2009;104(11):1527-33.

37. Fuster JJ, Ouchi N, Gokce N, Walsh K. Obesity-Induced Changes in Adipose Tissue Microenvironment and Their Impact on Cardiovascular Disease. Circ Res. 2016;118(11):1786-807.

38. Schiattarella GG, Altamirano F, Tong D, French KM, Villalobos E, Kim SY, et al. Nitrosative stress drives heart failure with preserved ejection fraction. Nature. 2019;568(7752):351-6.

39. Chirinos JA, Zamani P. The Nitrate-Nitrite-NO Pathway and Its Implications for Heart Failure and Preserved Ejection Fraction. Curr Heart Fail Rep. 2016;13(1):47-59.

40. Alvarez P, Briasoulis A. Immune Modulation in Heart Failure: the Promise of Novel Biologics. Current treatment. Options Cardiovasc Med. 2018 2018;20(3):26.

41. Hulsmans M, Sager HB, Roh JD, Valero-Munoz M, Houstis NE, Iwamoto Y, et al. Cardiac macrophages promote diastolic dysfunction. J Exper Med.. 2018;215(2):423-40.

42. Van Tassell BW, Trankle CR, Canada JM, Carbone S, Buckley L, Kadariya D, et al. IL-1 Blockade in Patients With Heart Failure With Preserved Ejection Fraction. Circ Heart Fail. 2018;11(8):e005036.

43. Van Tassell BW, Buckley LF, Carbone S, Trankle CR, Canada JM, Dixon DL, et al. Interleukin-1 blockade in heart failure with preserved ejection fraction: rationale and design of the Diastolic Heart Failure Anakinra Response Trial 2 (D-HART2). Clin Cardiol. 2017;40(9):626-32.

44. Garaulet M, Perez-Llamas F, Baraza JC, Garcia-Prieto MD, Fardy PS, Tebar FJ, et al. Body fat distribution in pre-and post-menopausal women: metabolic and anthropometric variables. J Nutr Health Aging. 2002;6(2):123-6.

45. Zamboni M, Armellini F, Milani MP, De Marchi M, Todesco T, Robbi R, et al. Body fat distribution in pre- and post-menopausal women: metabolic and anthropometric variables and their inter-relationships. Int In and related metabolic disorders : journal of the International Association for the Study of Obesity. Int J Obes.1992;16(7):495-504.

46. Toth MJ, Tchernof A, Sites CK, Poehlman ET. Menopause-related changes in body fat distribution. Ann NY Acad Sci. 2000;904:502-6.

47. Wehr E, Pilz S, Boehm BO, Marz W, Obermayer-Pietsch B. The lipid accumulation product is associated with increased mortality in normal weight postmenopausal women. Obesity. 2011;19(9):1873-80.

48. Joyce E, Lala A, Stevens SR, Cooper LB, AbouEzzeddine OF, Groarke JD, et al. Prevalence, Profile, and Prognosis of Severe Obesity in Contemporary Hospitalized Heart Failure Trial Populations. JACC Heart failure. 2016;4(12):923-31.

49. Kitzman DW, Brubaker P, Morgan T, Haykowsky M, Hundley G, Kraus WE, et al. Effect of Caloric Restriction or Aerobic Exercise Training on Peak Oxygen Consumption and Quality of Life in Obese Older Patients With Heart Failure With Preserved Ejection Fraction: A Randomized Clinical Trial. JAMA. 2016;315(1):36-46.

50. Kitzman DW, Brubaker PH, Herrington DM, Morgan TM, Stewart KP, Hundley WG, et al. Effect of endurance exercise training on endothelial function and arterial stiffness in older patients with heart failure and preserved ejection fraction: a randomized, controlled, single-blind trial. J Am Coll Cardiol. 2013;62(7):584-92.

51. Haykowsky MJ, Brubaker PH, Stewart KP, Morgan TM, Eggebeen J, Kitzman DW. Effect of endurance training on the determinants of peak exercise oxygen consumption in elderly patients with stable compensated heart failure and preserved ejection fraction. J Am Coll Cardiol. 2012;60(2):120-8.

52. Shin SH, Lee YJ, Heo YS, Park SD, Kwon SW, Woo SI, et al. Beneficial Effects of Bariatric Surgery on Cardiac Structure and Function in Obesity. Obes Surg. 2017;27(3):620-5.

53. Aggarwal R, Harling L, Efthimiou E, Darzi A, Athanasiou T, Ashrafian H. The Effects of Bariatric Surgery on Cardiac Structure and Function: a Systematic Review of Cardiac Imaging Outcomes. Obes Surg. 2016;26(5):1030-40.

54. Karason K, Wallentin I, Larsson B, Sjostrom L. Effects of obesity and weight loss on left ventricular mass and relative wall thickness: survey and intervention study. BMJ. 1997;315(7113):912-6.

55. Jhaveri RR, Pond KK, Hauser TH, Kissinger KV, Goepfert L, Schneider B, et al. Cardiac remodeling after substantial weight loss: a prospective cardiac magnetic resonance study after bariatric surgery. Surg Obes Relat Dis. 2009;5(6):648-52.

56. Cuspidi C, Rescaldani M, Tadic M, Sala C, Grassi G. Effects of bariatric surgery on cardiac structure and function: a systematic review and meta-analysis. Am J Hypertens. 2014;27(2):146-56.

57. Leichman JG, Wilson EB, Scarborough T, Aguilar D, Miller CC, 3rd, Yu S, et al. Dramatic reversal of derangements in muscle metabolism and left ventricular function after bariatric surgery. Am J Med. 2008;121(11):966-73.

58. Ikonomidis I, Mazarakis A, Papadopoulos C, Patsouras N, Kalfarentzos F, Lekakis J, et al. Weight loss after bariatric surgery improves aortic elastic properties and left ventricular function in individuals with morbid obesity: a 3-year follow-up study. J Hypert.2007;25(2):439-47.

59. Iancu ME, Copaescu C, Serban M, Ginghina C. Favorable changes in arterial elasticity, left ventricular mass, and diastolic function after significant weight loss following laparoscopic sleeve gastrectomy in obese individuals. Obes Surg. 2014;24(3):364-70.

60. Nyman K, Graner M, Pentikainen MO, Lundbom J, Hakkarainen A, Siren R, et al. Cardiac steatosis and left ventricular function in men with metabolic syndrome. J Cardiovasc Magn Reson. 2013;15:103.

61. Konishi M, Sugiyama S, Sugamura K, Nozaki T, Matsubara J, Akiyama E, et al. Accumulation of pericardial fat correlates with left ventricular diastolic dysfunction in patients with normal ejection fraction. J Cardiol. 2012;59(3):344-51.

62. Iacobellis G, Ribaudo MC, Assael F, Vecci E, Tiberti C, Zappaterreno A, et al. Echocardiographic epicardial adipose tissue is related to anthropometric and clinical parameters of metabolic syndrome: a new indicator of cardiovascular risk. J Clin Endocrinol Metab. 2003;88(11):5163-8.

63. Morelli NR, Scavuzzi BM, Miglioranza L, Lozovoy MAB, Simao ANC, Dichi I. Metabolic syndrome components are associated with oxidative stress in overweight and obese patients. Arch Endocrinol Metab. 2018;62(3):309-18.

64. Iacobellis G. Epicardial and pericardial fat: close, but very different. Obesity. 2009;17(4):625; author reply 6-7.

65. Ding J, Hsu FC, Harris TB, Liu Y, Kritchevsky SB, Szklo M, et al. The association of pericardial fat with incident coronary heart disease: the Multi-Ethnic Study of Atherosclerosis (MESA). Am J Clin Nutr. 2009;90(3):499-504.

66. Tamarappoo B, Dey D, Shmilovich H, Nakazato R, Gransar H, Cheng VY, et al. Increased pericardial fat volume measured from noncontrast CT predicts myocardial ischemia by SPECT. JACC Cardiovasc Imag. 2010;3(11):1104-12.

67. Aslanabadi N, Salehi R, Javadrashid A, Tarzamni M, Khodadad B, Enamzadeh E, et al. Epicardial and pericardial fat volume correlate with the severity of coronary artery stenosis. J Cardiovasc Thorac Res. 2014;6(4):235-9.

68. Cheng VY, Dey D, Tamarappoo B, Nakazato R, Gransar H, Miranda-Peats R, et al. Pericardial fat burden on ECG-gated noncontrast CT in asymptomatic patients who subsequently experience adverse cardiovascular events. JACC Cardiovasc Imag 2010;3(4):352-60.

69. Mahabadi AA, Berg MH, Lehmann N, Kalsch H, Bauer M, Kara K, et al. Association of epicardial fat with cardiovascular risk factors and incident myocardial infarction in the general population: the Heinz Nixdorf Recall Study. J Am Coll Cardiol. 2013;61(13):1388-95.

70. Alonso-Gomez AM, Tojal Sierra L, Fortuny Frau E, Goicolea Guemez L, Aboitiz Uribarri A, Portillo MP, et al. Diastolic dysfunction and exercise capacity in patients with metabolic syndrome and overweight/obesity. Int J Cardiol Heart Vasc. 2019;22:67-72.

71. Haykowsky MJ, Nicklas BJ, Brubaker PH, Hundley WG, Brinkley TE, Upadhya B, et al. Regional Adipose Distribution and its Relationship to Exercise Intolerance in Older Obese Patients Who Have Heart Failure With Preserved Ejection Fraction. JACC Heart failure. 2018;6(8):640-9.

72. Mazurek T, Zhang L, Zalewski A, Mannion JD, Diehl JT, Arafat H, et al. Human epicardial adipose tissue is a source of inflammatory mediators. Circulation. 2003;108(20):2460-6.

73. Sacks HS, Fain JN. Human epicardial adipose tissue: a review. Am Heart J. 2007;153(6):907-17.

74. Iacobellis G, Corradi D, Sharma AM. Epicardial adipose tissue: anatomic, biomolecular and clinical relationships with the heart. Nature clinical practice Cardiovasc Med. 2005;2(10):536-43.

75. Schram K, Sweeney G. Implications of myocardial matrix remodeling by adipokines in obesity-related heart failure. Trends Cardiovasc Med. 2008;18(6):199-205.

76. Packer M. Epicardial Adipose Tissue May Mediate Deleterious Effects of Obesity and Inflammation on the Myocardium. JJ Am Coll Cardiol. 2018;71(20):2360-72.

77. Patel VB, Basu R, Oudit GY. ACE2/Ang 1-7 axis: A critical regulator of epicardial adipose tissue inflammation and cardiac dysfunction in obesity. Adipocyte. 2016;5(3):306-11.

78. Patel VB, Mori J, McLean BA, Basu R, Das SK, Ramprasath T, et al. ACE2 Deficiency Worsens Epicardial Adipose Tissue Inflammation and Cardiac Dysfunction in Response to Diet-Induced Obesity. Diabetes. 2016;65(1):85-95.

79. Wu CK, Tsai HY, Su MM, Wu YF, Hwang JJ, Lin JL, et al. Evolutional change in epicardial fat and its correlation with myocardial diffuse fibrosis in heart failure patients. J Clin Lipidol. 2017;11(6):1421-31.

80. Lee JJ, Yin X, Hoffmann U, Fox CS, Benjamin EJ. Relation of Pericardial Fat, Intrathoracic Fat, and Abdominal Visceral Fat With Incident Atrial Fibrillation (from the Framingham Heart Study). Am J Cardiol. 2016;118(10):1486-92.

81. Fox CS, Gona P, Hoffmann U, Porter SA, Salton CJ, Massaro JM, et al. Pericardial fat, intrathoracic fat, and measures of left ventricular structure and function: the Framingham Heart Study. Circulation. 2009;119(12):1586-91.

82. Mak GJ, Ledwidge MT, Watson CJ, Phelan DM, Dawkins IR, Murphy NF, et al. Natural history of markers of collagen turnover in patients with early diastolic dysfunction and impact of eplerenone. J Am Coll Cardiol. 2009;54(18):1674-82.

83. van Woerden G, Gorter TM, Westenbrink BD, Willems TP, van Veldhuisen DJ, Rienstra M. Epicardial fat in heart failure patients with mid-range and preserved ejection fraction. Eur J Heart Fail. 2018;20(11):1559-66.

84. Obokata M, Reddy YNV, Pislaru SV, Melenovsky V, Borlaug BA. Evidence Supporting the Existence of a Distinct Obese Phenotype of Heart Failure With Preserved Ejection Fraction. Circulation. 2017;136(1):6-19.

85. Cavalcante JL, Tamarappoo BK, Hachamovitch R, Kwon DH, Alraies MC, Halliburton S, et al. Association of epicardial fat, hypertension, subclinical coronary artery disease, and metabolic syndrome with left ventricular diastolic dysfunction. Am J Cardiol. 2012;110(12):1793-8.

86. Brinkley TE, Ding J, Carr JJ, Nicklas BJ. Pericardial fat loss in postmenopausal women under conditions of equal energy deficit. Med Sci Sports Exerc. 2011;43(5):808-14.

87. Karastergiou K, Smith SR, Greenberg AS, Fried SK. Sex differences in human adipose tissues - the biology of pear shape. Biol Sex Differ. 2012;3(1):13.

88. Manolopoulos KN, Karpe F, Frayn KN. Gluteofemoral body fat as a determinant of metabolic health. Int J Obes (Lond). 2010;34(6):949-59.

89. Frank AP, de Souza Santos R, Palmer BF, Clegg DJ. Determinants of body fat distribution in humans may provide insight about obesity-related health risks. J Lipid Res. 2019;60(10):1710-9.

90. Mancuso P, Bouchard B. The Impact of Aging on Adipose Function and Adipokine Synthesis. Front Endocrinol (Lausanne). 2019;10:137.

91. Lobo RA, Davis SR, De Villiers TJ, Gompel A, Henderson VW, Hodis HN, et al. Prevention of diseases after menopause. Climacteric. 2014;17(5):540-56.

92. Redfield MM, Jacobsen SJ, Borlaug BA, Rodeheffer RJ, Kass DA. Age- and gender-related ventricular-vascular stiffening: a community-based study. Circulation. 2005;112(15):2254-62.

93. Regitz-Zagrosek V, Oertelt-Prigione S, Seeland U, Hetzer R. Sex and gender differences in myocardial hypertrophy and heart failure. Circ J. 2010;74(7):1265-73.

94. Gorodeski GI. Update on cardiovascular disease in post-menopausal women. Best Pract Res Clin Obstet Gynaecol. 2002;16(3):329-55.

95. Mendelsohn ME, Karas RH. The protective effects of estrogen on the cardiovascular system. N Engl J Med. 1999;340(23):1801-11.

96. Turgeon JL, McDonnell DP, Martin KA, Wise PM. Hormone therapy: physiological complexity belies therapeutic simplicity. Science. 2004;304(5675):1269-73.

97. Watson CS, Jeng YJ, Kochukov MY. Nongenomic actions of estradiol compared with estrone and estriol in pituitary tumor cell signaling and proliferation. FASEB J. 2008;22(9):3328-36.

98. Haas E, Bhattacharya I, Brailoiu E, Damjanovic M, Brailoiu GC, Gao X, et al. Regulatory role of G protein-coupled estrogen receptor for vascular function and obesity. Circ Res. 2009;104(3):288-91.

99. Ueda K, Adachi Y, Liu P, Fukuma N, Takimoto E. Regulatory Actions of Estrogen Receptor Signaling in the Cardiovascular System. Front Endocrinol (Lausanne). 2019;10:909.

100. Iorga A, Cunningham CM, Moazeni S, Ruffenach G, Umar S, Eghbali M. The protective role of estrogen and estrogen receptors in cardiovascular disease and the controversial use of estrogen therapy. Biol Sex Differ. 2017;8(1):33.

101. Dworatzek E, Mahmoodzadeh S. Targeted basic research to highlight the role of estrogen and estrogen receptors in the cardiovascular system. Pharmacol Res. 2017;119:27-35.

102. Mayes JS, Watson GH. Direct effects of sex steroid hormones on adipose tissues and obesity. Obes Rev. 2004;5(4):197-216.

103. Bouchard C, Despres JP, Mauriege P. Genetic and nongenetic determinants of regional fat distribution. Endocr Rev. 1993;14(1):72-93.

104. Brown LM, Clegg DJ. Central effects of estradiol in the regulation of food intake, body weight, and adiposity. J Steroid Biochem Mol Biol. 2010;122(1-3):65-73.

105. Clegg DJ, Brown LM, Woods SC, Benoit SC. Gonadal hormones determine sensitivity to central leptin and insulin. Diabetes. 2006;55(4):978-87.

106. Stubbins RE, Holcomb VB, Hong J, Nunez NP. Estrogen modulates abdominal adiposity and protects female mice from obesity and impaired glucose tolerance. Eur J Nutr. 2012;51(7):861-70.

107. Zidon TM, Padilla J, Fritsche KL, Welly RJ, McCabe LT, Stricklin OE, et al. Effects of ERbeta and ERalpha on OVX-induced changes in adiposity and insulin resistance. J Endocrinol. 2020;245(1):165-78.

108. Crandall DL, Busler DE, Novak TJ, Weber RV, Kral JG. Identification of estrogen receptor beta RNA in human breast and abdominal subcutaneous adipose tissue. Biochem Biophys Res Comm. 1998;248(3):523-6.

109. Matelski H, Greene R, Huberman M, Lokich J, Zipoli T. Randomized trial of estrogen vs. tamoxifen therapy for advanced breast cancer. Am J Clin Oncol. 1985;8(2):128-33.

110. Kuiper GG, Enmark E, Pelto-Huikko M, Nilsson S, Gustafsson JA. Cloning of a novel receptor expressed in rat prostate and ovary. Proc Nat Acad Sci USA. 1996;93(12):5925-30.

111. Rexrode KM, Ridker PM, Hegener HH, Buring JE, Manson JE, Zee RY. Polymorphisms and haplotypes of the estrogen receptor-beta gene (ESR2) and cardiovascular disease in men and women. Clin Chem. 2007;53(10):1749-56.

112. Lo JC, Zhao X, Scuteri A, Brockwell S, Sowers MR. The association of genetic polymorphisms in sex hormone biosynthesis and action with insulin sensitivity and diabetes mellitus in women at midlife. Am J Med. 2006;119(9 Suppl 1):S69-78.

113. Schuit SC, Oei HH, Witteman JC, Geurts van Kessel CH, van Meurs JB, Nijhuis RL, et al. Estrogen receptor alpha gene polymorphisms and risk of myocardial infarction. JAMA. 2004;291(24):2969-77.

114. Trayhurn P. Hypoxia and adipocyte physiology: implications for adipose tissue dysfunction in obesity. Ann Rev Nutr. 2014;34:207-36.

115. Romacho T, Elsen M, Rohrborn D, Eckel J. Adipose tissue and its role in organ crosstalk. Acta Physiol. 2014;210(4):733-53.

116. Xu A, Vanhoutte PM. Adiponectin and adipocyte fatty acid binding protein in the pathogenesis of cardiovascular disease. Am J Physiol Heart Circ Physiol. 2012;302(6):H1231-40.

117. Lehr S, Hartwig S, Lamers D, Famulla S, Muller S, Hanisch FG, et al. Identification and validation of novel adipokines released from primary human adipocytes. Mol Cell Proteom. MCP. 2012;11(1):M111 010504.

118. Arita Y, Kihara S, Ouchi N, Takahashi M, Maeda K, Miyagawa J, et al. Paradoxical decrease of an adipose-specific protein, adiponectin, in obesity. Biochem Biophys Res Comm. 1999;257(1):79-83.

119. Zhu W, Cheng KK, Vanhoutte PM, Lam KS, Xu A. Vascular effects of adiponectin: molecular mechanisms and potential therapeutic intervention. Clin Sci. 2008;114(5):361-74.

120. Tanaka K, Wilson RM, Essick EE, Duffen JL, Scherer PE, Ouchi N, et al. Effects of adiponectin on calcium-handling proteins in heart failure with preserved ejection fraction. Circ Heart Fail. 2014;7(6):976-85.

121. Tsao TS, Murrey HE, Hug C, Lee DH, Lodish HF. Oligomerization state-dependent activation of NF-kappa B signaling pathway by adipocyte complement-related protein of 30 kDa (Acrp30). J Biol Chem. 2002;277(33):29359-62.

122. Xu A, Chan KW, Hoo RL, Wang Y, Tan KC, Zhang J, et al. Testosterone selectively reduces the high molecular weight form of adiponectin by inhibiting its secretion from adipocytes. J Biol Chem. 2005;280(18):18073-80.

123. Pajvani UB, Du X, Combs TP, Berg AH, Rajala MW, Schulthess T, et al. Structure-function studies of the adipocyte-secreted hormone Acrp30/adiponectin. Implications fpr metabolic regulation and bioactivity. J Biol Chem.. 2003;278(11):9073-85.

124. Tsao TS, Tomas E, Murrey HE, Hug C, Lee DH, Ruderman NB, et al. Role of disulfide bonds in Acrp30/adiponectin structure and signaling specificity. Different oligomers activate different signal transduction pathways. J Biol Chem. 2003;278(50):50810-7.

125. Richards AA, Stephens T, Charlton HK, Jones A, Macdonald GA, Prins JB, et al. Adiponectin multimerization is dependent on conserved lysines in the collagenous domain: evidence for regulation of multimerization by alterations in posttranslational modifications. Mol Endocrinol. 2006;20(7):1673-87.

126. Yamauchi T, Kamon J, Ito Y, Tsuchida A, Yokomizo T, Kita S, et al. Cloning of adiponectin receptors that mediate antidiabetic metabolic effects. Nature. 2003;423(6941):762-9.

127. Ding G, Qin Q, He N, Francis-David SC, Hou J, Liu J, et al. Adiponectin and its receptors are expressed in adult ventricular cardiomyocytes and upregulated by activation of peroxisome proliferator-activated receptor gamma.J Mol Cell Cardiol. 2007;43(1):73-84.

128. Wang Y, Lau WB, Gao E, Tao L, Yuan Y, Li R, et al. Cardiomyocyte-derived adiponectin is biologically active in protecting against myocardial ischemia-reperfusion injury. Am J Physiol Endocrinol Metab. 2010;298(3):E663-70.

129. Skurk C, Wittchen F, Suckau L, Witt H, Noutsias M, Fechner H, et al. Description of a local cardiac adiponectin system and its deregulation in dilated cardiomyopathy. Eur Heart J. 2008;29(9):1168-80.

130. Hug C, Wang J, Ahmad NS, Bogan JS, Tsao TS, Lodish HF. T-cadherin is a receptor for hexameric and high-molecular-weight forms of Acrp30/adiponectin. Proc Nat Acad Sci USA. 2004;101(28):10308-13.

131. Ivanov D, Philippova M, Antropova J, Gubaeva F, Iljinskaya O, Tararak E, et al. Expression of cell adhesion molecule T-cadherin in the human vasculature. Histochem Cell Biol. 2001;115(3):231-42.

132. Doyle DD, Goings GE, Upshaw-Earley J, Page E, Ranscht B, Palfrey HC. T-cadherin is a major glycophosphoinositol-anchored protein associated with noncaveolar detergent-insoluble domains of the cardiac sarcolemma. J Biol Chem.. 1998;273(12):6937-43.

133. Denzel MS, Scimia MC, Zumstein PM, Walsh K, Ruiz-Lozano P, Ranscht B. T-cadherin is critical for adiponectin-mediated cardioprotection in mice. J Clin Invest. 2010;120(12):4342-52.

134. Pou KM, Massaro JM, Hoffmann U, Vasan RS, Maurovich-Horvat P, Larson MG, et al. Visceral and subcutaneous adipose tissue volumes are cross-sectionally related to markers of inflammation and oxidative stress: the Framingham Heart Study. Circulation. 2007;116(11):1234-41.

135. Ouchi N, Shibata R, Walsh K. Cardioprotection by adiponectin. Trends Cardiovasc Med. 2006;16(5):141-6.

136. Shibata R, Ouchi N, Ito M, Kihara S, Shiojima I, Pimentel DR, et al. Adiponectin-mediated modulation of hypertrophic signals in the heart. Nature Med. 2004;10(12):1384-9.

137. Sam F, Duhaney TA, Sato K, Wilson RM, Ohashi K, Sono-Romanelli S, et al. Adiponectin deficiency, diastolic dysfunction, and diastolic heart failure. Endocrinology. 2010;151(1):322-31.

138. Hui X, Lam KS, Vanhoutte PM, Xu A. Adiponectin and cardiovascular health: an update. Br J Pharmacol. 2012;165(3):574-90.

139. McManus DD, Lyass A, Ingelsson E, Massaro JM, Meigs JB, Aragam J, et al. Relations of circulating resistin and adiponectin and cardiac structure and function: the Framingham Offspring Study. Obesity. 2012;20(9):1882-6.

140. Hong SJ, Park CG, Seo HS, Oh DJ, Ro YM. Associations among plasma adiponectin, hypertension, left ventricular diastolic function and left ventricular mass index. Blood Press. 2004;13(4):236-42.

141. Norvik JV, Schirmer H, Ytrehus K, Jenssen TG, Zykova SN, Eggen AE, et al. Low adiponectin is associated with diastolic dysfunction in women: a cross-sectional study from the Tromso Study. BMC Cardiovasc Disord. 2017;17(1):79.

142. Negi SI, Jeong EM, Shukrullah I, Raicu M, Dudley SC, Jr. Association of low plasma adiponectin with early diastolic dysfunction. Congest Heart Fail. 2012;18(4):187-91.

143. Francisco C, Neves JS, Falcao-Pires I, Leite-Moreira A. Can Adiponectin Help us to Target Diastolic Dysfunction? Cardiovasc Dugs Ther. 2016;30(6):635-44.

144. Sawada N, Daimon M, Kawata T, Nakao T, Kimura K, Nakanishi K, et al. The Significance of the Effect of Visceral Adiposity on Left Ventricular Diastolic Function in the General Population. Scientific Rep. 2019;9(1):4435.

145. Fontes-Carvalho R, Pimenta J, Bettencourt P, Leite-Moreira A, Azevedo A. Association between plasma leptin and adiponectin levels and diastolic function in the general population. Exper Opin Ther Targets. 2015;19(10):1283-91.

146. Han SH, Quon MJ, Kim JA, Koh KK. Adiponectin and cardiovascular disease: response to therapeutic interventions. J Am Coll Cardiol 2007;49(5):531-8.

147. Fukuta H, Ohte N, Wakami K, Goto T, Tani T, Kimura G. Relation of plasma levels of adiponectin to left ventricular diastolic dysfunction in patients undergoing cardiac catheterization for coronary artery disease. Am J Cardiol. 2011;108(8):1081-5.

A Case Report of Valvular Heart Disease Complicated with a Blood Cyst in Right Atrium. Review of the Literature

Shu Jiang,[1] *Xiao-Cong Wang,*[1] *Yan-Li Zhang,*[1] *Wei Yu,*[1] *Li-Ping Pei,*[1] *Yan Ma*[1]

Jilin University First Hospital,[1] *Changchun – China*

Introduction

Blood cysts in the heart are often recognized as benign. They usually do not cause clinical symptoms and are often found in infants younger than two months of age.[1] In most cases, blood cysts are attached to cardiac valves or their supporting structures.[2] Cardiac blood cysts in adults are extremely rare, especially in the chambers of the heart. Here, we report a case of valvular heart disease complicated with a blood cyst in the right atrium. Transthoracic echocardiography, contrast echocardiography and esophageal echocardiography were used to examine the patient.

Case report

The patient was a 64-year-old woman with palpitations and shortness of breath after exercise for four months. In the previous two weeks, the symptoms had worsened. Local hospitals recommended referral to superior hospitals, and then she was referenced to our hospital for treatment. She had a history of hypertension for seven years, smoking for 30 years and hysteromyoma surgery more than 20 years ago. She had no history of diabetes and denied tuberculosis, hepatitis and other infectious diseases. The patient did not have a clear record of medication. At admission, her vital signs were stable. The electrocardiogram showed atrial fibrillation. Systolic murmurs could be heard in the auscultation area of the mitral valve. There were no murmurs in other valve auscultation areas.

Transthoracic echocardiography showed bilateral enlarged atria, mild mitral stenosis and severe insufficiency, with normal left ventricular systolic function (LVEF=52%). In addition, a circular anechoic lesion was approximately 30x41 mm in size in the right atrium, which did not cause tricuspid valve obstruction (Figure 1A).

A GE Vivid E9 ultrasound diagnostic device with an M5sC probe was used for a contrast echocardiography examination. SonoVue (1 ml) was slowly injected through the median cubital vein over 1 minute. The scintillation artifact was triggered approximately 2 minutes after injection of the contrast agent. The microbubbles in the myocardium were quickly destroyed when a high MI pulse was emitted. Then the filling process of the contrast agent in the myocardium and tumors was observed in a low-MI state. Contrast perfusion imaging showed a cystic structure with a septum of approximately 36x42 mm in the right atrium and the absence of perfusion in the mass (Figure 1B, C).

Intraoperative transesophageal echocardiography revealed a circular echo in the right atrium, with spontaneous echocardiographic contrast and septation, which we considered to be a blood cyst. (Figure 1D).

The patient underwent right atrial mass excision, mitral valve replacement and tricuspid valvuloplasty. The mass was located in the right atrium connected to the oval fossa, near the orifice of the inferior vena cava, by a pedicle approximately 5 mm in diameter. It was around 40 x 40 mm in size (Figure 2A, B). The capsule was intact, tough and purple-black. The atrial septal tissue attached to the tumor and pedicle was completely removed. Mitral valve replacement and tricuspid valvuloplasty were performed.

Macroscopic examination showed that the right atrial mass was round with a volume of 45x35x27 mm, had a complete capsule, and a narrowed pedicle on the surface. The mass section was unilocular, the cystic wall was 1-2 mm thick, the inner lining was smooth, and the content was mainly coagula. Light microscopic examination of paraffin-embedded sections showed fibrocystic wall-like tissue, interstitial fibrous tissue hyperplasia, hyaline degeneration and mucinous degeneration in the right atrium mass, and massive coagulation tissue, which accorded with the cyst changes (Figure 3A, B). The valve tissue examined showed hyaline degeneration and mucinous degeneration with scattered infiltration of chronic inflammatory cells (Figure 3C).

The patient recovered well after the operation. No abnormal mass was found in the right atrium by echocardiography. In addition, her mitral valve prosthesis and tricuspid valve function were normal.

Discussion

Elsasser first reported blood cysts in 1844.[3] They are usually of congenital origin and are found within a few months after birth, then disappear spontaneously with time. They mostly occur in cardiac valves, such as mitral valves, tricuspid, aortic, and pulmonary valves. Sometimes they exist in the left atrium and right atrium.[4,5] Blood cysts in adults are extremely rare, especially in the heart cavity. There are several hypotheses about the causes of hemocyst formation: 1. During the development of valves, blood cysts are formed because the blood is squeezed and gets stuck in the gap that later closes. 2. Possible heteroplastic changes in primary pericardial mesothelial tissue. 3. Sakakibara et al.[6] suggested that a sudden blockage of

Keywords

Blood Cysts; Cysts/surgery; Heart Valve Diseases; Heart Atria/physiology; Atrial Function; Echocardiography/methods

Mailing Address: Xiao-Cong Wang •
Jilin University First Hospital - The First Hospital of Jilin University, 1 Xin Min Street, Changchun,Jilin Changchun 130021 – China
E-mail: 247266443@qq.com
Manuscript received January 26, 2021, revised manuscript May 20, 2021, accepted June 16, 2021

DOI: https://doi.org/10.36660/abc.20210063

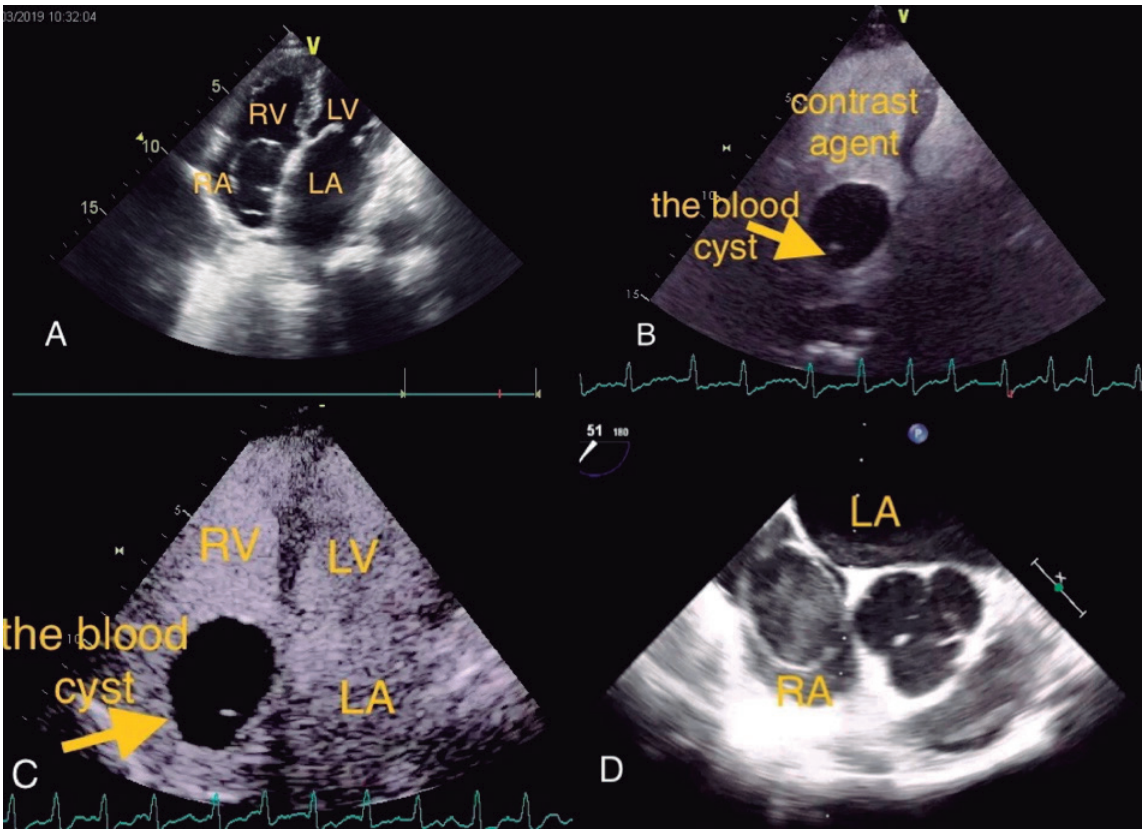

Figure 1 – *A) Transthoracic echocardiography showed a circular anechoic lesion in the right atrium. B, C) Contrast perfusion imaging showed a cystic structure with a septum and the absence of perfusion in the mass. D) Intraoperative transesophageal echocardiography revealed a circular echo in the right atrium, with spontaneous echocardiographic contrast and septation. RV: right ventricle; LV left ventricle; RA: right atrium; LA: left atrium.*

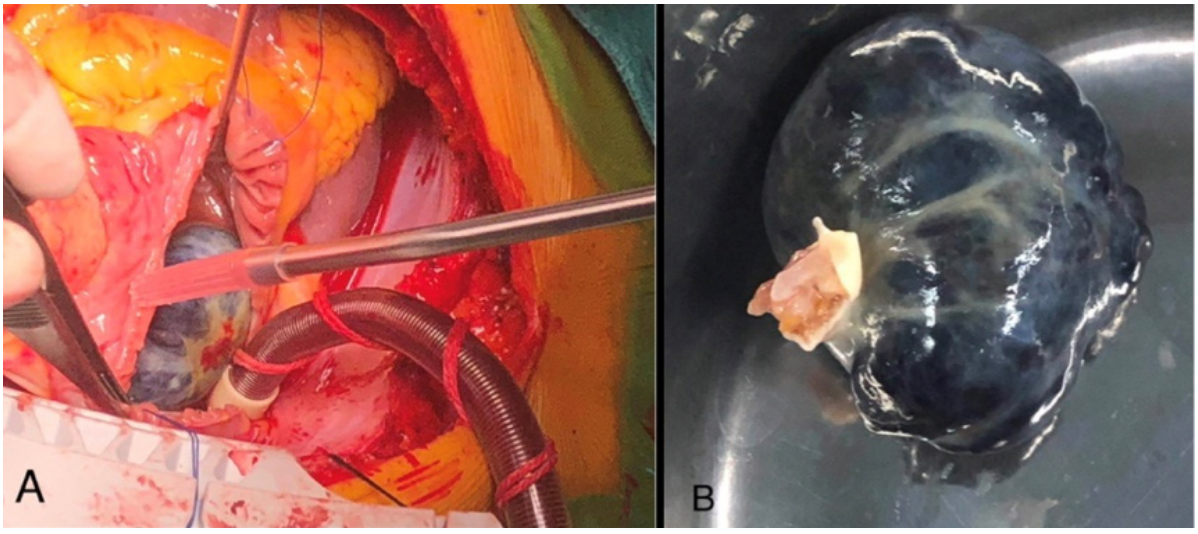

Figure 2 – *A, B) Surgical findings. The tumor was located in the right atrium connected to the oval fossa, near the orifice of the inferior vena cava, by a pedicle approximately 5 mm in diameter.*

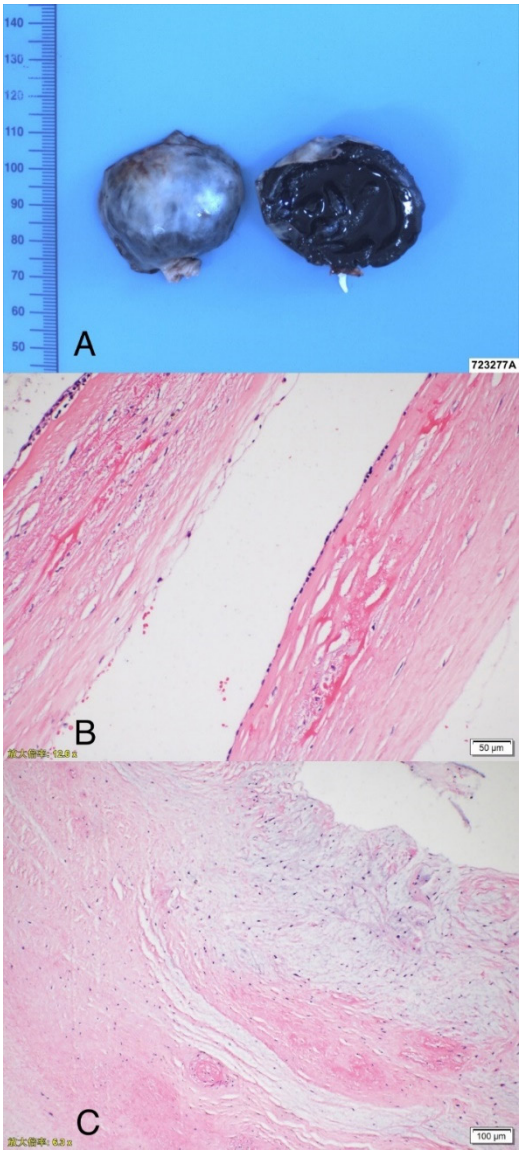

Figure 3 – *A, B) Pathology findings. The mass was filled with fibrocystic wall-like tissue, interstitial fibrous tissue hyperplasia, hyaline degeneration and mucinous degeneration in the right atrium mass, and massive coagulation tissue. C: The valve tissue examined showed hyaline degeneration and mucinous degeneration with scattered infiltration of chronic inflammatory cells.*

circulation causes blood cysts in the atrium or ventricle. They believed that hypoxia, inflammation and bleeding tendencies might be responsible for developing endocardial hematoma into hemocysts. 4. Blood cysts only represent dilated blood vessels. 5. Mucinous degeneration.[7] However, there is still no consensus on the cause of blood cysts.[4,8,9] The current patient had mitral insufficiency. Pathological examination of the valve showed hyaline degeneration and mucinous degeneration. It is presumed that this was related to the formation of blood cysts.

Cardiac tumors are mostly benign and myxomatous. They can occur at any age. Myxoma usually occurs on the endocardial surface of the cardiac cavity, 60% -80% of the time in the left atrium. The pedicle attaches to the oval fossa of the atrial septum and has a certain range of motion with the cardiac cycle.

However, myxoma is usually a round or oval strong-echo mass with regular inside echoes. If there is necrosis in the center, it may be an anechoic area.

Left ventricular contrast echocardiography of myxoma shows that the contrast medium is sparse but enhanced in the lesion. Its intensity is lower than that of adjacent myocardial tissue, which is not consistent with this case.

The echocardiographic manifestations of cardiac echinococcosis are cystic space-occupying lesions in the heart. The distribution of cysts in the heart is mainly related to the myocardial blood supply. Therefore, the most common site is the ventricular wall myocardium, which has the most blood supply of the heart, followed by the atrial wall, and the cardiac cavity is less often involved.[10] However, the patient did not have a clear history of contact with cattle or sheep or an unclean diet, so that diagnosis was not supported.

From 1958 to 2020, there were only ten articles about blood cysts in the right atrium confirmed by pathology. Our review of the English-language literature revealed ten other entries since 1996, describing a total of 10 patients with details of these blood cysts in the right atrium (Table 1). The symptoms of reported blood cysts vary. Four patients were asymptomatic.[11-14] Other patients had symptoms. The common symptoms were dyspnea and chest discomfort, one case of chronic grief, and one case of headache. The attachment site has also been different. Six cysts were attached to the atrial septum,[11,13-17] 2 to the oval fossa,[12,18] 1 to the tricuspid valve,[19] and 1 to the coronary sinus valve.[20] Calcification was found in 5 of the blood cysts.[12,14-16,18] After surgery, most patients recovered,[11-15,18,20] 2 patients did not have an explained prognosis,[16,19] and 1 patient died.[17]

At present, there is no uniform standard for the treatment of blood cysts. Therefore, patients with symptoms can be followed up regularly. It is reported that hemocysts may cause left ventricular outflow tract obstruction, valve dysfunction, ventricular dysfunction, embolic stroke, pulmonary embolism and coronary artery obstruction.[8] Therefore, for patients with symptoms, early surgical treatment should be carried out.

Conclusion

Echocardiography has become the first choice for diagnosing blood cysts because it can let us observe the size, shape, structure, function and valvular development of the heart, and it is noninvasive and safe. Furthermore, contrast-enhanced echocardiography is helpful in the diagnosis of blood cysts because it can show whether there is a contrast medium filling in the mass. In addition, intraoperative transesophageal echocardiography can be used to locate the cardiac mass and thereby help with the operation.

Acknowledgments

The authors would like to thank the patient and her family for allowing the use and publishing of her medical records in this case report.

Table 1 – Clinical summary of Blood cysts cases found in English literature since 1958

Patient	First author	Year	Gender	Age	Tumor size	Attachment	Blood cyst with calcium	Symptom	History	Prognosis
1	H Niinam[15]	1996	F	59	20x20mm	atrial septum between the fossa ovalis and tricuspid valve annulus	yes	periodic episodes of substernal pressure and dry cough	none	recovery
2	Hiroyuki Tanaka[11]	2003	M	52	40x30mm	atrial septum between the fossa ovalis and tricuspid valve	no	none	gastric cancer	recovery
3	Gernot Seebacher[18]	2006	F	65	44x20mm	fossa ovalis of atrial septum	yes	dyspnea, angina, and tachycardia	none	recovery
4	Kaoru Otsuka[12]	2007	M	56	30x20mm	fossa ovalis of the atrial septum	yes	none	none	recovery
5	Tomasa Centella[16]	2015	Unknown	62	28x28mm	atrial septum	yes	headache	elevated ferritin unrelated to the hemochromatosis gene, a hiatal hernia, mild esophagitis, and renal sinus cysts	unknown
6	Hiroyuki Otsuka[13]	2016	F	85	30x30mm, 25x25mm	atrial septum between the fossa ovalis and the tricuspid valve	no	none	sick sinus syndrome	recovery
7	Hilary Bews[19]	2018	F	62	45x54mm	tricuspid valve	no	chronic back pain	none	unknown
8	Feridoun Sabzi[20]	2019	M	76	unknown	coronary sinus valve	unknown	dyspnea	none	recovery
9	Behnam Shakerian[14]	2019	M	73	16x10mm	atrial septum	yes	none	none	recovery
10	A Angelov[17]	2012	F	28	60x65mm	atrial septum	no	chest discomfort, shortness of breath, and fever	none	death

Author Contributions

Conception and design of the research and Writing of the manuscript: Jiang S; Acquisition of data: Yu W; Analysis and interpretation of the data: Li-Ping P, Yan M; Critical revision of the manuscript for intellectual content: Xiao-Cong W, Yan-Li Z.

Potential Conflict of Interest

No potential conflict of interest relevant to this article was reported.

Sources of Funding

There were no external funding sources for this study.

Study Association

This study is not associated with any thesis or dissertation work.

Ethics approval and consent to participate

This article does not contain any studies with human participants or animals performed by any of the authors.

References

1. Sharma S, Strauss R, Swanson JS. Giant blood cyst of the mitral valve. Asian Cardiovasc Thorac Ann; 2000;8(3):278-9.
2. Kuhn A, Schreiber C, Weirich G, Vogt M.Intracardiacbloodcyst: rare finding in a complex congenital heart lesion. Eur Heart J. 2012;33(2):229.
3. Elsasser C. Bericht uber die Ereignisse in der gebaranstalt des Catherinen Hospital im Jahre 1844. Med Correspondenzblatt.1844;14(2):297.
4. Dencker M, Jexmark T, Hansen F, Tyden PC, Roijer A, Luhrs C. Bileaflet blood cysts on the mitral valve in an adult. J Am Soc Echocardiogr. 2009;22(9): 1085.e5-1085.e8.
5. Zimmerman KG, Paplanus SH, Dong S, Nagle RB. Congenital blood cysts of heart valves. Human Pathol. 1983;14(8):699–703.
6. Sakakibara S, Katsuhara K, Iida Y, Nishida H. Pulmonary subvalvular tumor. Dis Chest 1967;51(6):637–42.
7. Ozmen G, Demir M, Arı H, Aktas I. A rare association: concomitant presence of mitral valve blood cyst with atrial septal aneurysm and cor triatriatum dexter. Anatol J Cardiol. 2015; 15(6):502-3.
8. Minneci C, Casolo G, Popoff G, Sulla A, Comin CE, Pedemonti E. A rare case of left ventricular outflow obstruction. Eur J Echocardiogr. 2004;5(1):72-5
9. Xie SW, Lu OL, Picard MH. Blood cyst of the mitral valve: detection by transthoracic and transesophageal echocardiography. J Am Soc Echocardiogr 1992;5(5):547-50.
10. Djoshibaev S, Kudaiberdiev T, Maralov A, Shabralier S, Djooshiv K, Halikov UM, et al. Surgical treatment of isolated cardiac echinococciasis: report of five cases. Anadolu Kardiyol Derg 2003;3(2):137-43.
11. Hiroyuki T, Mio E , Takashi N, Narisawa T, Mori T, Masuda M, et al. Atrial Blood Cyst With Ischemic Heart Disease. Circ J. 2003;67(1): 91–2.
12. Ptsuka K, Tonari LA, Limori A, Shimomura H, Ko T, Kitaura Y, et al. Right atrial blood cyst with total occlusion of the right coronary artery. Heart Vessels .2007;22(3):208–10 .
13. Hiroyuki O , Kouichi A ,Toshifumi F,Takasya T, Shojima T, Takagi K, et al. Double Right Atrial Blood Cysts. Ann Thorac Surg.2016;101(5):147–9 .
14. Behnam S, Mohammad J. Right Atrium Blood Cyst and Calcified Kernel in an Adult. Clin Med Insights Case Rep. 2019 Sep 29;12:117954-6198740807
15. H Niinami , S Ishihara, S Hara Tanaka S,Yamaguti E,Takase S. Blood cyst with a calcium stone originating from the right atrial septum. Cardiovasc Surg. 1996;4(2):260-2.
16. Centella T, Moya JL, Munoz M, Reguero EM. Giant Endocardial Blood Cyst in the Right Atrium Echocardiographic and Magnetic Resonance Imaging Features. Circulation. 2008;117(12):3250-1.
17. A Angelov, Y Yotov, K Kalchev,et al. Right atrium giant blood cyst in a young female with acute pericarditis, complicated with fatal cardiac tamponade. Int J Cardiol. 2013;163(2):31-32.
18. Seebacher G, Binder T, Frank H, Wolner E, Mohl W. Cystic Formation of the Foramen Ovale Mimicking a Right Atrial Myxoma.Ann Thorac Surg .2006;82(6)::2296–8.
19. Bewstt H, Strzelzyk J, Luqman Z, Jassal D. Multimodality imaging of a right atrial blood cyst. Eur Heart J. 2017;38(48):3603.
20. Sabzi F, Heydari A, Asadmobini A, Heidari MB. Right Atrial Blood Cyst with Stones Suspended from the Coronary Sinus. Sultan Qaboos Univ Med J. 2019,9(2):161-3.

Echocardiographic Findings in Patients with COVID-19 with and without Previous Cardiovascular Disease

Silvio Henrique Barberato,[1,2] Rafael Borsoi,[3] Fabio Roston,[4] Hudson Laerte Machado Miranda,[5] Pedro Patriota,[6] Maria Estefania Otto,[7,8] Adenalva Lima de Souza Beck,[7,9] Anderson da Costa Armstrong,[6] João Marcos Bemfica Barbosa Ferreira,[10] Ana Cristina Camarozano,[11] Letícia Braga Paciello da Silva,[12] Marcos Valério Coimbra Resende,[12] Marcelo Luiz Campos Vieira,[12] Miguel Morita Fernandes-Silva[1,3]

Quanta Diagnóstico – Ecocardiografia,[1] Curitiba, PR – Brazil
CardioEco Centro de Diagnóstico Cardiovascular,[2] Curitiba, PR – Brazil
Hospital de Clínicas da Universidade Federal do Paraná,[3] Curitiba, PR – Brazil
Hospital Universitário da Universidade Estadual de Londrina,[4] Londrina, PR – Brazil
Hospital Samel,[5] Manaus, AM – Brazil
Hospital Universitário da Universidade Federal do Vale do São Francisco,[6] Petrolina, PE – Brazil
Instituto de Cardiologia do Distrito Federal (ICDF),[7] Brasília, DF – Brazil
Hospital Sirio Libanês,[8] Brasília, DF – Brazil
Hospital Santa Lúcia de Brasília,[9] Brasília, DF – Brazil
Universidade do Estado do Amazonas,[10] Manaus, AM – Brazil
Hospital Nossa Senhora das Graças,[11] Curitiba, PR – Brazil
Hospital Samaritano,[12] São Paulo, SP – Brazil

Introduction

Coronavirus disease-2019 (COVID-19) caused by the severe acute respiratory syndrome coronavirus 2 (SARS-Cov-2) may result in severe respiratory distress and acute cardiac injury. Impaired cardiac function and/or prior cardiovascular disease (CVD) in patients with COVID-19 are associated with worse prognosis.[1] Transthoracic echocardiography (TTE) has a central role in the management of patients, as it provides a crucial assessment of abnormalities in cardiac function and structure that impact on their prognosis and treatment.[2] Studies have reported varied rates of left ventricular (LV) and right ventricular (RV) dysfunction, but it is unclear how often cardiac dysfunction result directly from COVID-19.[3-6] We described the prevalence of the main abnormal echocardiographic findings in hospitalized patients with COVID-19 with and without previous cardiovascular disease (CVD) through a real-world, multicenter collaborative study (Brazilian Echocardiography Registry during COVID-19 pandemic, or ECOVID).

Methods

ECOVID is a prospective multicenter observational study of hospitalized patients with COVID-19 in Brazil that started on April 4th, 2020, by collecting clinical and echocardiographic data in all five macro-regions of the country. Full description of the study methods was detailed in the Supplemental Material. Briefly, consecutive hospitalized patients (> 18 years old) with confirmed or highly probable COVID-19 were included. At each participant center, clinical data was obtained from medical charts and patient interview by cardiologists, and echocardiographic measures were locally obtained. The results were registered using an online case report form. Most echocardiographic scans used a focused protocol aiming to mitigate the risk to the healthcare professional.[7] Imaging acquisition and interpretation were performed by certified physicians according to international guidelines.[8,9] Specifically, LV systolic dysfunction was defined by LV ejection fraction (LVEF) below 50% (mild between 40-49%; moderate between 30-39%, and severe <30%). LV diastolic dysfunction, RV systolic dysfunction and pulmonary artery systolic pressure (PASP) were defined and classified according to guidelines (please see Supplemental material). The echocardiographic findings were summarized according to the history of previous CVD, as defined by previous obstruction ≥50% in any major coronary artery demonstrated by coronary computed tomography angiography or coronary angiography, coronary revascularization, myocardial infarction, heart failure or atrial fibrillation. This study was approved by the ethics committee of the coordinating center (# 4.033.139) and the local ethics committees from each respective site.

Statistical analysis

Continuous variables were presented as mean ± standard deviation. The Gaussian distribution of the data was analyzed by looking at the shape of the distribution, skewness, kurtosis, and using the Kolmogorov-Smirnov test. Categorical data were expressed as counts and percentages. Clinical, demographic and echocardiographic parameters were compared between the individuals with and without history of previous CVD using unpaired Student's *t* test or Chi-squared test, accordingly. We

Keywords

Acute Respiratory Syndrome/complications SARS-CoV2/complications; Coronavirus-19/complications; Pandemics; Cardiac Function; Cardiovascular Diseases/complications; Heart Failure, Echocardiography/méthods; Mortality; Comorbidity.

Mailing Address: Silvio Henrique Barberato •
CardioEco Centro de Diagnóstico Cardiovascular - Avenida República Argentina, 1336, conj 215. Postal Code 80620-010, Curitiba, PR - Brazil
E-mail: silviohb@cardiol.br
Manuscript received December 08, 2020, revised manuscript June 09, 2021, accepted June 16, 2021

DOI: https://doi.org/10.36660/abc.20201300

considered statistically significant p-values<0.05. Statistical analyses were performed using Stata version 15.1 (Stata Corp, College Station, TX).

Results

We included 223 hospitalized patients admitted between April 4th and September 9th, 2020, aged 61.4 ± 15.3 years old (range19 to 94), 59% men, 83% with RT-PCR-confirmed COVID-19, 17% with highly probable COVID-19. The main clinical indications for referral for echocardiography were suspected heart failure (50%), suspected acute coronary syndrome (chest pain, electrocardiogram abnormalities and troponin elevation) (20%), hemodynamic instability (18%), suspected myocarditis (16%), suspected pulmonary embolism (6%), clinically relevant arrhythmias (5%), and others (such as suspected pericardial effusion, endocarditis, syncope, and cardioembolic source of brain stroke) (5%).

Table 1 summarizes the demographics, clinical characteristics and comorbidities of the population. Patients without previous CVD were younger and had lower prevalence of cardiovascular risk factors, such as hypertension, diabetes and smoking, and were less likely to have chronic obstructive pulmonary disease and chronic kidney disease, when compared with patients with previous CVD (Table 1). COVID-19-related symptoms and supportive measures were similar between patients without and with previous CVD (Supplemental table 1).

Table 2 shows the main echocardiographic findings in hospitalized patients with COVID-19 according to a history of previous CVD. As expected, patients without CVD were less likely to have echocardiographic findings suggesting abnormal LV structure and/or function, including LV hypertrophy (27 vs 52%, p<0.001), LV systolic dysfunction (13 vs. 34%, p<0.001), regional wall motion abnormalities (8 vs. 24%, p<0.001) and grade II or III LV diastolic dysfunction (11 vs. 26%, p=0.011). On the other hand, only 52% of patients without previous CVD had a normal echocardiogram (Figure 1). RV systolic dysfunction (17 vs. 22%, p=0.40) and pulmonary hypertension (24 vs. 38%, p=0.06) were relatively common and they were similar between patients without and with previous CVD. RV systolic dysfunction was also common in patients without previous pulmonary disease (15 vs. 20% for patients without and with previous CVD, respectively, p=0.45). Pericardial effusion and moderate-to-severe valve regurgitation were uncommon. Of note, in patients without previous CVD and presumably new LV systolic dysfunction (n=21), 48% of them displayed regional wall motion abnormalities. No patient had evidence of wall motion abnormalities suggestive of stress-induced cardiomyopathy. Echocardiography results changed clinical management in 25% of the cases, mostly triggering the initiation of therapy for heart failure or anticoagulation or referral to catheterization.

Discussion

In this multicenter registry, we found that clinically relevant abnormalities in cardiac function or structure

Table 1 – Demographics and comorbidities in hospitalized patients with COVID-19 according to a history of previous cardiovascular disease

	All patients	No previous CVD	Previous CVD	p value
	n=223	n=173	n=50	
Age, years	61.4± 15.3	59 ± 15	68 ± 14	<0.001
Male, n (%)	132 (59.2%)	103 (59.5%)	29 (58.0%)	0.85
BMI, Kg/m^2	27.6± 5.0	27.6 ± 5.3	27.5 ± 3.6	0.83
Obesity, n (%)	60 (26.9%)	49 (28.3%)	11 (22.0%)	0.37
Hypertension, n (%)	115 (51.6%)	78 (45.1%)	37 (74.0%)	<0.001
Diabetes mellitus, n (%)	77 (34.5%)	47 (27.2%)	30 (60.0%)	<0.001
Smoking, n (%)	30 (13.5%)	17 (9.8 %)	13 (26.0%)	0.003
Previous CAD, n (%)	30 (13.5%)		30 (60.0%)	ND
Previous HF, n (%)	16 (7.2%)		16 (32.0%)	ND
Previous AF, n (%)	9 (4.0%)		9 (18.0%)	ND
Pulmonary disease, n (%)	24 (10.8%)	14 (8.1 %)	10 (20.0%)	0.017
Chronic Kidney disease, n (%)	28 (12.6%)	17 (9.8 %)	11 (22.0%)	0.022
Dialysis, n (%)	3 (1.3%)	3 (1.7 %)	0 (0.0 %)	0.35
Cerebrovascular disease, n (%)	7 (3.1%)	4 (2.3 %)	3 (6.0 %)	0.19
Cancer, n (%)	5 (2.2%)	2 (1.2 %)	3 (6.0 %)	0.042

CVD: cardiovascular disease; BMI: body mass index; CAD: coronary artery disease; HF: Heart failure; AF: atrial fibrillation; COPD: Chronic obstructive pulmonary disease.

Table 2 – Echocardiographic findings in hospitalized patients with COVID-19 according to a history of previous cardiovascular disease

Parameter	All patients	No previous CVD	Previous CVD	p value
	n=223	n=173	n=50	
LV hypertrophy, n(%)	73 (32.7%)	47 (27.2%)	26 (52.0%)	<0.001
LV dilation, n(%)	31 (14.0%)	13 (7.6%)	18 (36.0%)	<0.001
LV systolic dysfunction, n(%)				0.005
None	183 (82.1%)	150 (86.7%)	33 (66.0%)	
Mild	10 (4.5%)	7 (4.0%)	3 (6.0%)	
Moderate	14 (6.3%)	8 (4.6%)	6 (12.0%)	
Severe	16 (7.2%)	8 (4.6%)	8 (16.0%)	
LV diastolic dysfunction, n(%)				<0.001
None	88 (42.5%)	82 (49.7%)	6 (14.3%)	
Mild	90 (43.5%)	65 (39.4%)	25 (59.5%)	
Moderate	27 (13.0%)	17 (10.3%)	10 (23.8%)	
Severe	2 (1.0%)	1 (0.6%)	1 (2.4%)	
Unknown	16 (7.2%)	8 (4.6%)	8 (16.0%)	
LV regional wall abnormality, n(%)	25 (11.2%)	13 (7.5%)	12 (24.0%)	0.001
RV dysfunction, n(%)				0.20
None	183 (82.1%)	144 (83.2%)	39 (78.0%)	
Mild	21 (9.4%)	17 (9.8%)	4 (8.0%)	
Moderate	9 (4.0%)	7 (4.0%)	2 (4.0%)	
Severe	10 (4.5%)	5 (2.9%)	5 (10.0%)	
Pulmonary hypertension				0.06
None	160 (72.4%)	129 (75.4%)	31 (62.0%)	
Mild	36 (16.3%)	28 (16.4%)	8 (16.0%)	
Moderate	21 (9.5%)	12 (7.0%)	9 (18.0%)	
Severe	4 (1.8%)	2 (1.2%)	2 (4.0%)	
Moderate-to-severe valve regurgitation, n(%)				
Aortic	2 (0.9%)	1 (0.6%)	1 (2.0%)	0.34
Mitral	10 (4.5%)	6 (3.5%)	4 (8.2%)	0.16
Tricuspid	8 (3.6%)	4 (2.3%)	4 (8.2%)	0.05
Pericardial effusion, n(%)	5 (2.2%)	5 (2.9%)	0 (0.0%)	0.22

CVD: cardiovascular disease; LV: left ventricular; RV: right ventricular.

were relatively common among hospitalized patients with COVID-19, even in those without previous CVD, with roughly half showing at least one abnormal finding. Moreover, 1 in 8 patients without previous CVD had at least one severe echocardiographic abnormality.

Previous studies describing echocardiographic findings in patients with COVID-19 have been considerable heterogeneous. The prevalence of LV systolic dysfunction, RV dysfunction and RV dilation have ranged from 5.4[10] to 37.4%,[4] 3.6,[11] to 33%,[12] and 0,12 to 46.9%,[13] respectively. This wide variation may be related to referral bias, different TTE protocols, inaccurate definitions of echocardiographic abnormalities, and differences in population characteristics, such as the proportion of patients with previous CVD. Aiming to mitigate referral bias, Szekely et al.[5] systematically performed TTE in 100 consecutive patients hospitalized for COVID-19, 43% of which had prior CVD. They found that the most frequent abnormality was RV dysfunction/dilation while only a minority of patients (10%) had LV systolic dysfunction.[5]

Our study sheds light on the importance of previous CVD on the prevalence of echocardiographic findings of patients hospitalized with COVID-19. While RV dysfunction was common and apparently unrelated to the prevalence of previous CVD, LV systolic and diastolic dysfunction were more common in patients with previous CVD, likely in part due to pre-existing cardiovascular conditions. Noteworthy, thirteen percent of patients without CVD had LV systolic dysfunction, which may reflect a COVID-19-related *"de novo"*

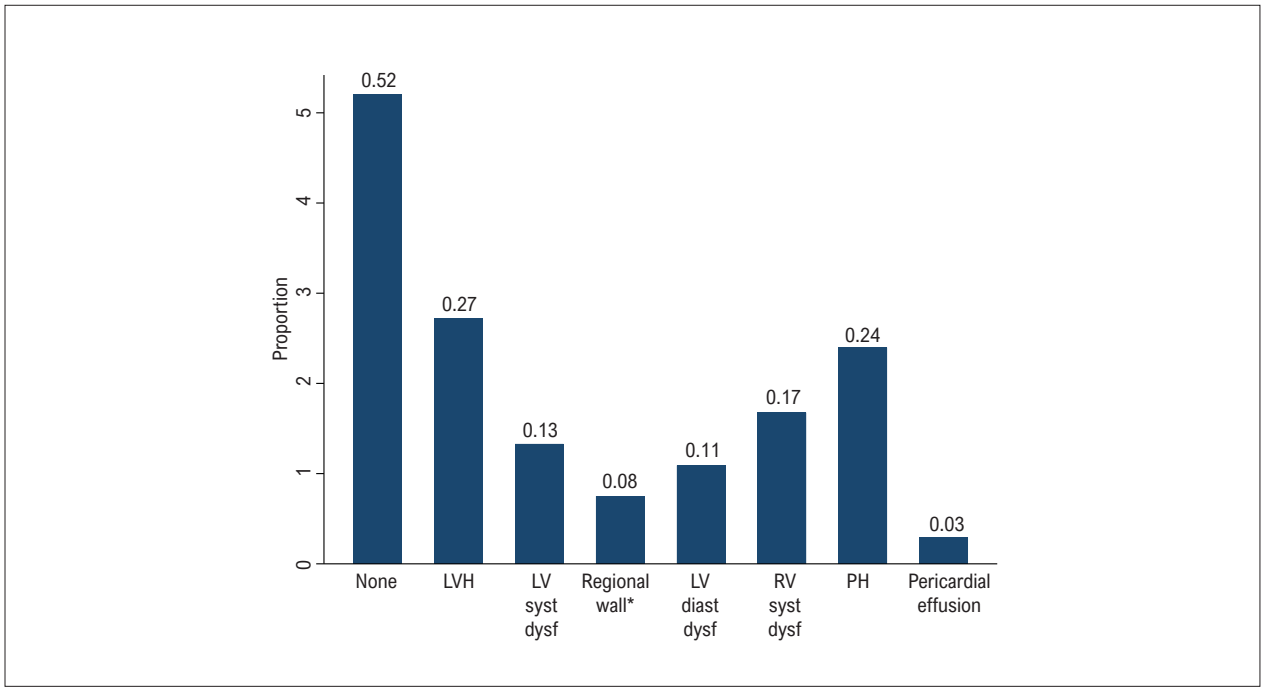

Figure 1 – *Echocardiographic findings in patients hospitalized for COVID-19 without previous cardiovascular disease. LVH: left ventricular hypertrophy; LV: left ventricle; RV: right ventricle; PH: pulmonary hypertension. *Refers to LV regional wall motion abnormality. †LV diastolic dysfunction includes only moderate or severe LV diastolic dysfunction.*

LV impairment. On the other hand, pulmonary hypertension and RV systolic dysfunction are more likely to result from a myriad of phenomena that affects the lungs, such as hypoxia, inflammation, acute respiratory distress syndrome, pulmonary microvascular thrombosis, pulmonary thromboembolism and mechanical ventilation.

As major efforts by the scientific community aim to mitigate the severe health consequences of the COVID-19 pandemic, it becomes challenging to balance the use of echocardiography to provide high quality of medical care without excessively increasing the risk of cross-infection between healthcare professionals and patients. Our results help understand which cardiac function parameters are most frequently abnormal in hospitalized patients with COVID-19, according to the history of previous CVD through a real-world national registry. It is important to emphasize that the presence of cardiac dysfunction is independently associated with worse prognosis in patients with severe COVID-19.[14] TTE evaluation should be considered in patients with COVID-19 and suspected cardiovascular complications to characterize the underlying cardiac substrate, for risk stratification, and to potentially guide management strategies.[14] On the other hand, its indications should be based in critical consideration of the benefits to patient, contamination risk for healthcare personnel and use of the limited personal protective equipment.

Our study has limitations that deserve attention. First, the echocardiographic measures were performed by local investigators without final assessment by a core lab. Nevertheless, all echocardiograms were performed by experienced physicians, who followed the procedures according to international guidelines. Second, abnormal findings may have been overestimated due to referral bias, as the echocardiograms were performed at the discretion of the attending physician. Third, serum biomarkers of myocardial injury were unavailable in this study. Finally, although we described the TTE findings in patients without previous CVD, we still cannot rule out whether these cardiac abnormalities were pre-existing, and these results should be interpreted with caution.

Conclusions

Among hospitalized patients with COVID-19 submitted to an echocardiogram, RV and LV systolic dysfunction were found in almost one out of five patients, but the latter was less common in those without previous CVD. Only half of the patients without previous CVD had a normal TTE.

Acknowledgments

We would like to thank the following colleagues who provided help in carrying out this research: Francisco de Assis Carvalho Santana; Fernando Melo Netto, Simone Ferreira Leite, Bianca Corrêa Rocha de Mello, Dassis Cajuba, Filipe Lima de Menezes, Nathalia Caetano Lobo, Vanessa Guimarães Esmanhoto Andrioli, Pedro Gabriel Melo de Barros e Silva.

Author Contributions

Conception and design of the research and Obtaining financing: Barberato SH, Borsoi R; Acquisition of data: Borsoi R, Roston F, Miranda HLM, Patriota P, Otto ME, Beck ALS, Armstrong AC, Ferreira JMBB, Camarozano AC, Silva LBP, Resende MVC, Vieira MLC; Analysis and interpretation of the data: Barberato SH, Borsoi R, Fernandes-Silva MM; Statistical analysis: Barberato SH, Borsoi R, Fernandes-Silva MM; Writing of the manuscript: Barberato SH; Critical revision of the manuscript for intellectual content: Barberato SH, Fernandes-Silva MM.

Potential Conflict of Interest

No potential conflict of interest relevant to this article was reported.

Sources of Funding

There were no external funding sources for this study.

Study Association

This study is not associated with any thesis or dissertation work.

References

1. Costa IBSD, Bittar CS, Rizk SI, Araújo Filho AE, Santos KAQ, Machado TIV, et al. The Heart and COVID-19: What Cardiologists Need to Know. Arq Bras Cardiol. 2020;114(5):805-16.
2. Costa IBSD, Rochitte CE, Campos CM, Barberato SH, Oliveira GMM, Lopes MACQ, et al. Cardiovascular Imaging and Interventional Procedures in Patients with Novel Coronavirus Infection. Arq Bras Cardiol. 2020;115(1):111-26.
3. Sud K, Vogel B, Bohra C, Garg V, Talebi S, Lerakis S, et al. Echocardiographic Findings in Patients with COVID-19 with Significant Myocardial Injury. J Am Soc Echocardiogr. 2020;3(8):1054-5.
4. Dweck MR, Bularga A, Hahn RT, Bing R, Lee KK, Chapman AR, et al. Global evaluation of echocardiography in patients with COVID-19. Eur Heart J Cardiovasc Imaging. 2020;21(9):949-58.
5. Szekely Y, Lichter Y, Taieb P, Banai A, Hochstadt A, Merdler I, et al. The Spectrum of Cardiac Manifestations in Coronavirus Disease 2019 (COVID-19) - a Systematic Echocardiographic Study. Circulation. 2020,142(4):342-53.
6. Jain SS, Liu Q, Raikhelkar J, Fried J, Elias P, Poterucha TJ, et al. Indications for and Findings on Transthoracic Echocardiography in COVID-19. J Am Soc Echocardiogr. 2020;33(10):1278-84.
7. Kirkpatrick JN, Mitchell C, Taub C, Kort S, Hung J, Swaminathan M. ASE Statement on Protection of Patients and Echocardiography Service Providers During the 2019 Novel Coronavirus Outbreak: Endorsed by the American College of Cardiology. J Am Soc Echocardiogr. 2020;33(6):648-53.
8. Lang RM, Badano LP, Mor-Avi V, Afilalo J, Armstrong A, Ernande L, et al. Recommendations for cardiac chamber quantification by echocardiography in adults: an update from the American Society of Echocardiography and the European Association of Cardiovascular Imaging. J Am Soc Echocardiogr. 2015;28(1):1-39.e14.
9. Douglas PS, Carabello BA, Lang RM, Lopez L, Pellikka PA, Picard MH, et al. 2019 ACC/AHA/ASE Key Data Elements and Definitions for Transthoracic Echocardiography: A Report of the American College of Cardiology/American Heart Association Task Force on Clinical Data Standards (Writing Committee to Develop Cardiovascular Endpoints Data Standards) and the American Society of Echocardiography. J Am Coll Cardiol. 2019;74(3):403-69.
10. Deng Q, Hu B, Zhang Y, Wang H, Zhou X, Hu W, et al. Suspected myocardial injury in patients with COVID-19: Evidence from front-line clinical observation in Wuhan, China. Int J Cardiol. 2020;311:116-21.
11. Li Y, Li H, Zhu S, Xie Y, Wang B, He L, et al. Prognostic Value of Right Ventricular Longitudinal Strain in Patients With COVID-19. JACC Cardiovasc Imaging. 2020;13(11):2287-99.
12. van den Heuvel FMA, Vos JL, Koop Y, van Dijk APJ, Duijnhouwer AL, de Mast Q, et al. Cardiac function in relation to myocardial injury in hospitalised patients with COVID-19. Neth Heart J. 2020;28(7-8):410-7.
13. Rath D, Petersen-Uribe Á, Avdiu A, Witzel K, Jaeger P, Zdanyte M, et al. Impaired cardiac function is associated with mortality in patients with acute COVID-19 infection. Clin Res Cardiol. 2020;109(12):1491-9.
14. Giustino G, Croft LB, Stefanini GG, Bragato R, Silbiger JJ, Vicenzi M, et al. Characterization of Myocardial Injury in Patients With COVID-19. J Am Coll Cardiol. 2020;76(18):2043-55.

*Supplemental Materials

For additional information, please click here.

Coherent Map for Atypical Atrial Flutter – A Step Forward for the Understanding of the Arrhythmia Mechanism

Pedro A. Sousa,[1] Sérgio Barra,[2,3] Mariana Pereira,[1] Luís Elvas[1]

Pacing & Electrophysiology Unit, Cardiology Department, Centro Hospitalar e Universitário de Coimbra, Coimbra, Portugal,[1] Coimbra – Portugal
Hospital da Luz Arrábida V - Cardiology Department,[2] Vila Nova de Gaia – Portugal
Royal Papworth Hospital NHS Foundation Trust – Cardiology Department,[3] Cambridge - United Kingdom

Case Presentation

An 86-year-old woman with a previous history of paroxysmal atrial fibrillation was referred for atypical atrial flutter (AFL) ablation. She had never been submitted to catheter ablation before. The transthoracic echocardiogram revealed a left ventricular ejection fraction of 65%, a mildly dilated left atrium (42mm) and moderate mitral regurgitation. The baseline 12-lead ECG exhibited positive F waves in V1 and the lower limb leads, isoelectric F waves in DI and negative F wave in aVL. (Figure 1A) Given the earlier concentric activation in the coronary sinus (CS), with a tachycardia cycle length (TCL) of 330ms, (Figure 1B) a right atrial (RA) activation map, performed with the PentaRay® catheter, was initially analyzed using the HD Coloring tool (CARTO® 3V7, Biosense Webster, CA, USA). It revealed an earlier activation in the interatrial septum with only 1/3 of the TCL (Figure 2). A subsequent left atrial (LA) activation map revealed a large area of scar with likely conduction block in almost all of the anterior wall, represented as a white line by the lower threshold Extended Early Meets Late (EEML) feature, and several areas with early local activation time (LAT) points – in the left atrial appendage (LAA), the anterior aspect of the mitral valve (MV) and the roof near the anterior segment of the right superior pulmonary vein (RSPV). It also showed two zones of re-entry as established by the Early Meets Late (EML) feature (Figure 3A and S-3 A). These maps suggested a probable circuit around the right pulmonary veins but did not explain the color activation in the LAA and MV. A new mapping algorithm – Coherent (CARTO® 3V7, Biosense Webster) – unveiled the circuit (Figure 3B and S-3 B). What is the mechanism of this atypical AFL?

Discussion

This case highlights some interesting features.

First, taking into consideration the concentric activation in the CS (Figure 1B), the mapping was initially performed in the RA with the HD Coloring software. The bipolar map revealed normal electrograms, defined as voltage above 0.3mV, in most of the chamber (Figure S-2 A and S-2 B). A RA high-density activation map revealed earliest LAT points in the interatrial septum (Figure 2). The propagation wave at this point was consistent with a focal source, but since the unipolar signal had an initial "r" deflection and only 1/3 of the TCL was comprised in this chamber, an exclusively RA circuit was ruled out (Supplemental Video 1).

An LA bipolar map was subsequently performed, revealing a diseased LA, with extensive dense scarring in the anterior wall, as defined by a voltage below 0.1mV, and some patchy scar areas in the posterior wall (Figure S-2 A and S-2 B). The high-density activation map performed with the HD Coloring software (Figure 3A and S-3 A), comprising all of the TCL, displayed multiple areas of early activation (in the LAA, the anterior aspect of the MV and the roof near the anterior segment of the RSPV). Two areas of re-entry, as defined by the EML feature, were also observed – one from the LAA to the MV and another in the roof. Both the EML and EEML depend on the mapped tachycardia cycle (which in our case corresponded to the TCL) and they are established taking into consideration the LAT difference between adjacent points.[1,2] In this case, since the difference between LAT points was greater than 25% of the TCL (82ms = 0.25 * 330ms), a white line was displayed from the MV to the RSPV (sparing only a small portion in the anterior wall, near the RSPV) and also in the posterior wall near the RSPV, suggesting probable lines of conduction block.

The propagation map of the LA (Supplemental Video 2) suggested a circuit around the right pulmonary veins, with the propagation wave moving through the interrupted white line. However, it did not explain the color activation in the LAA and MV. Even after combining both maps (Figure S-1), several questions remained unexplained:

1) How could there be a propagation wave in the anterior wall given the presence of extensive scar?

2) How was there a simultaneous activation of different areas of the LA?

3) Do the two areas of reentry – in the posterior roof and from the LAA to the MV- correspond to two independent circuits or one circuit with passive conduction to the other area?

4) In case of independent circuits, where are they located and how can the wavefront propagate through the anterior aspect of the MV if, according to the EEML, this appears blocked (as shown by the uninterrupted white line)?

Keywords

Atrial Flutter/etiology; Conduction; Arrhytmias,Cardiac; HC Coloring; Coherent Mapping; Electrophysiologic Techniques Cardiac/methods

Mailing Address: Pedro A. Sousa •
Pacing & Electrophysiology Unit, Cardiology Department, Centro Hospitalar e Universitário de Coimbra, Coimbra, Portugal - Praceta Mota Pinto Coimbra 3004 – Portugal
E-mail: peter_senado2002@yahoo.com
Mnuscript received December 08, 2020, revised manuscript April 20, 2021, accepted May 12, 2021

DOI: https://doi.org/10.36660/abc.20201311

Figure 1 – *Twelve-lead electrocardiogram (A) and intracardiac tracings obtained during AFL (B) and during radiofrequency applications (C and D).*

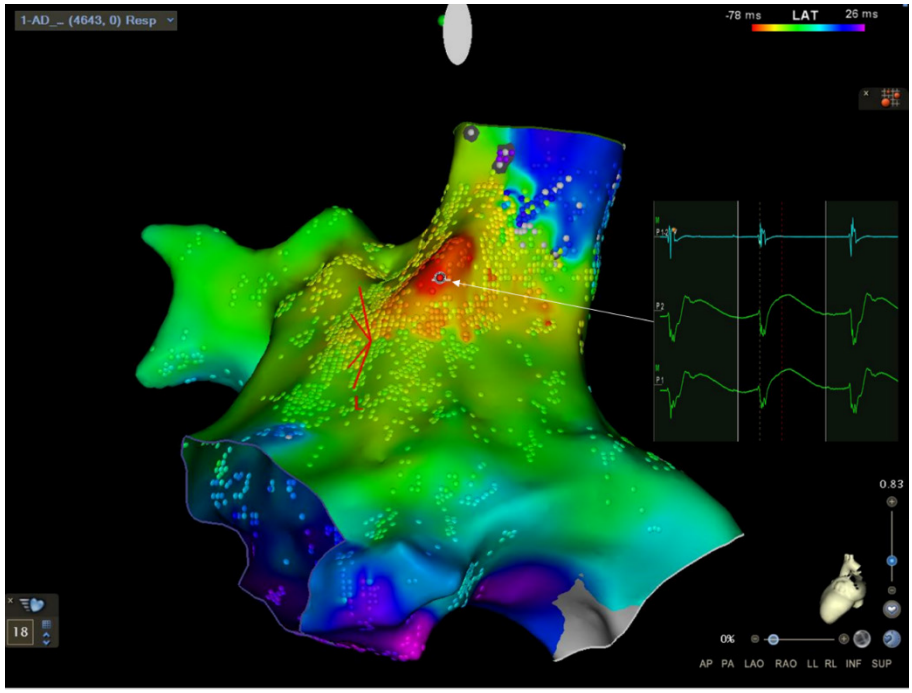

Figure 2 – *High-density activation map of the RA acquired during AFL with a TCL of 330ms. The map was performed with the HD Coloring software, included 4,643 points, with 32% of the TCL and displayed a centrifugal high septal activation (red indicates the areas with earliest LAT, while orange, yellow, green, blue and purple indicate progressively delayed activation). Unipolar electrograms showed an initial "r" deflection. AFL: atrial flutter; RA: right atrium; TCL: tachycardia cycle length.*

Research Letter

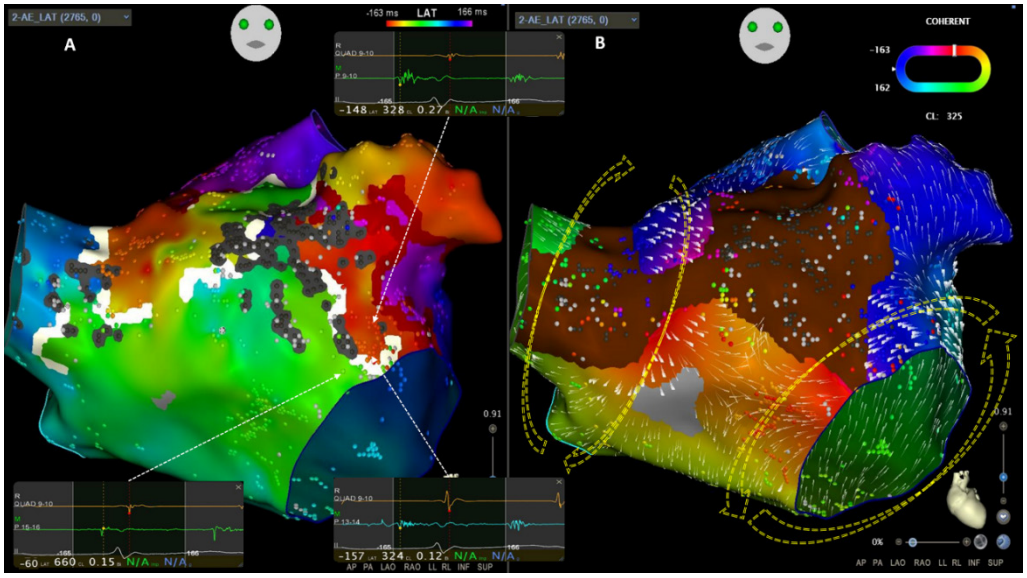

Figure 3 – *Left atrial activation maps performed with the PentaRay® catheter including 2,765 points and 330ms of the tachycardia cycle length. Map A was performed with the HD Coloring software (EML and EEML set at 75% and 25%, respectively), with bipolar scar settings at 0.03mV and a scar area size of 1 displayed as grey tags. The activation map revealed three distinct areas of early LAT points – in the roof, near the anterior MV and in the LAA – and two zones of probable re-entry as defined by a difference between adjacent points superior to 75% of the TCL (the EML threshold) - in the roof and between the LAA and MV, respectively. There was a probable line of conduction block (displayed as a white line) from the MV until almost the RSPV, since the difference between adjacent LAT points on both sides of the line were greater than 25% of the mapped tachycardia cycle. Map B was performed with the Coherent mapping algorithm, revealing a SNO (slow or no conduction) zone (displayed as brown) from the RSPV to the anterior aspect of the mitral valve and also towards the LAA. With the velocity vector set at 17 (slow velocity is represented by thicker vectors), we observed conduction through the anterior wall near the RSPV - a clockwise circuit (dashed yellow arrow) around the right pulmonary veins. Coherent also revealed a small area of slow conduction (fractionated electrograms as depicted in Map A) near the mitral valve suggestive of a second circuit - a counterclockwise propagation wave around the MV (dashed yellow arrow). EML: early meets late; EEML: extended early meets late; LAT: local activation time; MV: mitral valve; LAA: left atrial appendage; TCL: tachycardia cycle length; RSPV: right superior pulmonary vein.*

As previously reported,[2] in the HD Coloring feature each LAT requires a voltage of only ≥ 0.03mV to be integrated into the activation map. This is the reason why we could see an activation wavefront in the anterior wall, despite the presence of extensive scar (bipolar electrogram voltage below 0.1mV). Entrainment could in theory provide valuable information (like excluding an 8-digit atrial flutter with a common isthmus), but in our center this is typically performed only if other methods fail to explain the circuit, given the small risk of terminating the arrhythmia or its degeneration into atrial fibrillation.[3] Ripple mapping can also be useful in these cases, since it overcomes some limitations of the LAT maps, such as the incorrect annotation of the electrograms and the fact that it is not influenced by the window of interest.[4]

Recently, a novel mapping algorithm – Coherent (CARTO® 3V7, Biosense Webster) was developed to address some of the limitations associated with the current activation mapping. Briefly, the Coherent mapping algorithm takes into account the LAT value, the conduction vector and the probability of non-conductivity and displays the most likely arrhythmia mechanism.[3] It introduces some new features: 1) The presence of the vectors and their corresponding direction and velocity and 2) A "slow or no conduction" (SNO) zone displayed with a brown color, representing an area where there is slow conduction or no conduction.

The analysis with this new mapping algorithm (Figure 3B and S-3 B) allowed us to overcome some of the limitations of conventional activation mapping, even with the HD coloring feature: 1) The difficulty in discriminating between active and passive activation – in our case, although the window of interest was defined as equal to the TCL, the posterior wall and the LAA were activated with such delay that its activation continued into the next cycle and consequently were displayed with a red color, explaining why they seemed to be simultaneously activated; 2) Each LAT receives one single time annotation regardless of its fractionation or duration, which can mislead the operators and even the software itself. In the present case, by annotating the fractionated electrograms in the lateral mitral valve as very early LAT, a white line of conduction block was displayed, which hindered the interpretation of the wavefront activation map. By analyzing the vectors' directions and their velocity (slow velocity if represented by thicker vectors) we observed conduction through the anwterior wall near the RSPV – a clockwise circuit (dashed yellow arrow in Figure 3B) around the right pulmonary veins. However, Coherent mapping also revealed a small area of slow conduction near the mitral valve, suggestive of a second circuit – a counterclockwise mitral flutter. This circuit corresponded to the area of fractionated electrograms and could have gone unnoticed as a white line, suggesting that a block had been placed by HD Coloring (Figure 3A) for the reason mentioned above (each LAT receives one

single time annotation regardless of its fractionation or duration) (Figure 3B, S-3 B and Supplemental Video 3).

To confirm our hypothesis of a double loop AFL, the final step was the choice of location for the application of radiofrequency (RF) energy. We initially closed the gap near the RSPV with immediate elongation of the TCL (Figure 1C). After delivery of RF energy in the anterior aspect of the mitral valve, the AFL was successfully terminated (Figure 1D and Figure 4). Bidirectional block along the ablation line was confirmed with differential pacing maneuvers and with repeat activation mapping while pacing from the LAA (Supplemental Video 4). Also, no further arrhythmia was subsequently inducible. After 5 months of follow-up, the patient remains free from any sustained arrhythmia.

This case highlights some of the new features of the Coherent mapping algorithm and its usefulness, particularly in patients with extensive scar, fractionated electrograms and areas of very slow conduction. By displaying the "best fit" activation wavefront, Coherent mapping overcame the limitations related with the presence of very slow conduction and the incorrect annotation of fractionated electrograms with incorrect consequent display of conduction block, unveiling a double loop atrial flutter, and allowing us to successfully treat the patient.

Author Contributions

Conception and design of the research and Analysis and interpretation of the data: Sousa PA; Acquisition of data: Sousa PA, Pereira M; Writing of the manuscript: Sousa PA, Barra S; Critical revision of the manuscript for intellectual content: Barra S, Elvas L.

Potential Conflict of Interest

No potential conflict of interest relevant to this article was reported.

Sources of Funding

There were no external funding sources for this study.

Study Association

This study is not associated with any thesis or dissertation work.

Ethics approval and consent to participate

This article does not contain any studies with human participants or animals performed by any of the authors.

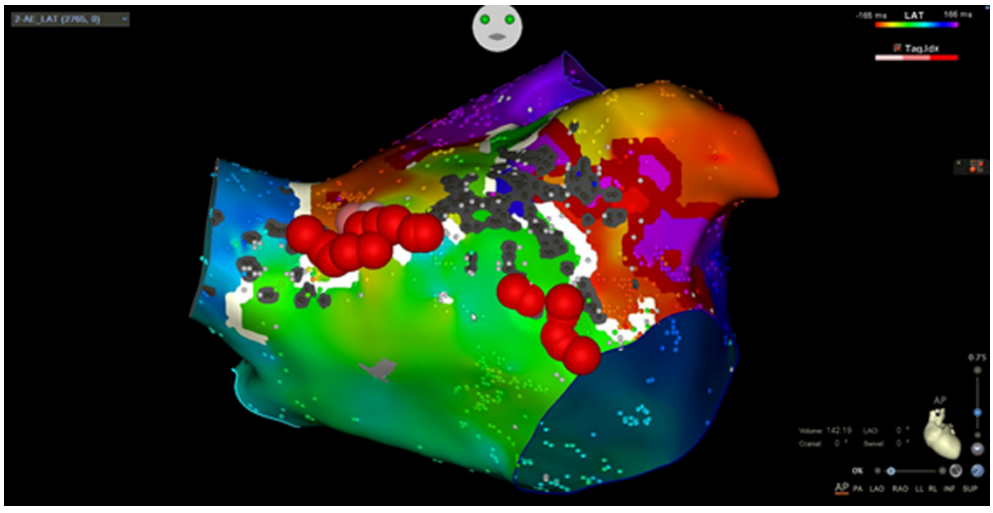

Figure 4 – *Location of the sites of radiofrequency delivery, corresponding to the places of slow conduction, which allowed the double loop atrial flutter termination.*

References

1. Sousa PA, Barra S, António N,Gonçalves L. HD Coloring for assessment of block along an ablation line. J Cardiovasc Electrophysiol. 2019;30(9):1692-3.
2. Sousa, PA, Barra S, Elvas L, Gonçalves L. HD Coloring for Atypical Flutter after Mitral Valve Repair: What's the mechanism? J Cardiovasc Electrophysiol 2020; 31(1): 252-5.
3. Anter E, Duytschaever M, Shen C,Strisciuglio T, Leshem E, Valdes FM, et al.. Activation Mapping With Integration of Vector and Velocity Information Improves the Ability to Identify the Mechanism and Location of Complex Scar-Related Atrial Tachycardias. Circ Arrhythm Electrophysiol. 2018;11(8): e006536.
4. Luther V, Cortez-Dias, N, Carpinteiro L, Sousa J, Balasubramaniam R, Agarwal S, et al. J Cardiovasc Electrophysiol. 2017;28(11):1285-94.

*Supplemental Materials

For supplement figures, please click here.

See the Supplemental Video 1, please click here.

See the Supplemental Video 2, please click here.

See the Supplemental Video 3, please click here.

See the Supplemental Video 4, please click here.

Safety Margin for Plasma Hyperviscosity in Cardiovascular Disease Patients after COVID-19 Vaccination for Thrombosis Prevention

Rujittika Mungmunpuntipantip[1] *and Viroj Wiwanitkit*[1]

Dr DY Patil, Universidade de Pune,[1] *Pune - India*

Dear Editor,

We read the article entitled "Vaccinating Patients with Heart Disease Against COVID-19: The Reasons for Priority" with great interest.[1] COVID-19 vaccination is accepted as the best way for preventing the disease, but data on its safety are still warranted. An important problem found after COVID-19 vaccination is the rheological change causing intravascular clotting and thrombotic complications.[2] Changes in blood viscosity after COVID-19 vaccination have been confirmed. A vaccine can induced rapid production of antibody, which is a protein that can increase plasma viscosity by an estimated 2.4 centipoise (cP) from normal values in healthy person.[3,4] The problem might occur if changes in plasma viscosity reach levels above 5 cP, considered a hyperviscosity state.[5]

For any person receiving the COVID-19 vaccine, there may be a safety margin for the hyperviscosity problem. This safety margin would be difference between baseline plasma viscosity to the hyperviscosity level. The concern on the safety margin for the hyperviscosity problem should be discussed for a person with underlying heart disease. It is observed that a person with hyperlipidemia or cardiovascular disease has higher plasma viscosity than a healthy person.[6,7]

In this paper,[1] the authors tried to estimate the safety margin for plasma hyperviscosity for healthy people and for those with different underlying heart diseases who will be vaccinated against COVID-19. The estimated safety margin values are shown in Table 1; the safety margins differed not only between healthy individuals and cardiovascular disease patients, but also between different cardiovascular diseases. A person with unstable angina seems to have the highest risk. Patients with some specific underlying diseases might have lower safety margin values, which may imply a higher risk for developing a thrombotic disease. As a recommendation, special attention should be given to cardiovascular patients at high risk of hyperviscosity, and pre-vaccination monitoring of plasma viscosity might be useful.

Table 1 - Estimated safety margin for plasma hyperviscosity after COVID-19 vaccination in healthy individuals and patients with cardiovascular diseases

Groups	Background viscosity * value (cP)	Estimated safety margin** (cP)
Healthy person	1.40	1.1
Patient with dyslipidemia	1.44	1.06
Patient with stable angina	1.42	1.08
Patient with unstable angina	1.66	0.84
Patient with myocardial infarction	1.53	0.97

**Background viscosity values are derived from previous studies.[3,6,7] ** safety margin for hyperviscosity can be estimated by "hyperviscosity cutoff value – baseline plasma viscosity - expected increase in plasma viscosity after vaccination. cP: centipoise.*

Keywords

Viscosity; Patients; Margins of Excision.

Mailing Address: Rujittika Mungmunpuntipantip •
Private Academic Consultant, Bangkok - Thailand
Email:rujittika@gmail.com

DOI: https://doi.org/10.36660/abc.20210555

Letter to the Editor

References

1. Martins WA, Oliveira GMM, Brandão AA, Mourilhe-Rocha R, Mesquita ET, Saraiva JFK, Bacal F, et al. Vaccinating Patients with Heart Disease Against COVID-19: The Reasons for Priority. Arq Bras Cardiol. 2021;116(2):213-8. doi: 10.36660/abc.20210012.
2. Merchant HA. COVID Vaccines and Thrombotic Events: EMA Issued Warning to Patients and Healthcare Professionals. J Pharm Policy Pract. 2021;14(1):32. doi: 10.1186/s40545-021-00315-w.
3. Joob B, Wiwanitkit V. Expected Viscosity After COVID-19 Vaccination, Hyperviscosity and Previous COVID-19. Clin Appl Thromb Hemost. 2021;27:10760296211020833. doi: 10.1177/10760296211020833.
4. Dalakas MC. High-Dose Intravenous Immunoglobulin and Serum Viscosity: Risk of Precipitating Thromboembolic Events. Neurology. 1994;44(2):223-6. doi: 10.1212/wnl.44.2.223.
5. Mehta J, Singhal S. Hyperviscosity Syndrome in Plasma Cell Dyscrasias. Semin Thromb Hemost. 2003;29(5):467-71. doi: 10.1055/s-2003-44554.
6. Irace C, Carallo C, Scavelli F, Esposito T, De Franceschi MS, Tripolino C, et al. Influence of Blood Lipids on Plasma and Blood Viscosity. Clin Hemorheol Microcirc. 2014;57(3):267-74. doi: 10.3233/CH-131705.
7. Fuchs J, Weinberger I, Rotenberg Z, Erdberg A, Davidson E, Joshua H, et al. Plasma Viscosity in Ischemic Heart Disease. Am Heart J. 1984;108(3):435-9. doi: 10.1016/0002-8703(84)90405-8.